2008

Analysis of jointed plain concrete pavement systems with nondestructive test results using artificial neural networks

Mustafa Birkan Bayrak
Iowa State University

Analysis of jointed plain concrete pavement systems with nondestructive test results using artificial neural networks

by

Mustafa Birkan Bayrak

A dissertation submitted to the graduate faculty

in partial fulfillment of the requirements for the degree of

DOCTOR OF PHILOSOPHY

Major: Civil Engineering (Geotechnical Engineering)

Program of Study Committee:
Halil Ceylan, Major Professor
Vern Schaefer
Kejin Wang
Omar Smadi
Igor Beresnev
Thomas Rudolphi

Iowa State University

Ames, Iowa

2008

To the memories of my father-in-law Dr. Ali Anil (1955-2006).

To my wife, family, relatives, and friends.

ACKNOWLEDGEMENTS

I would like to express my sincere appreciation to my advisor, Dr. Halil Ceylan, for his guidance and invaluable advice throughtout my graduate years at the Iowa State University.

Sincere appreciation must also be expressed to my Ph.D. committee members, Dr. Vern Schaefer, Dr. Omar Smadi, Dr. Kejin Wang, Dr. Igor Beresnev, and Dr. Thomas Rudolphi for their contribution and helpful advice. Their review and comments were very helpful and always constructive.

I cannot express enough thanks to Dr. James Alleman and Dr. Reginald Souleyrette for their help, support and guidance which made it possible for me to accomplish this endeavor.

I would like to also gratefully acknowledge the Iowa Department of Transportation (IA-DOT) for sponsoring this study.

Finally, and most importantly, I would like to acknowledge and thank my wife Nergis Ani Anil-Bayrak, my father Saban Bayrak, my father-in-law Dr. Ali Anil, my mother Melahat Bayrak, my mother-in-law Yasemin Anil, my brother Serkan Bayrak, my aunt Ipek Bayrak, my nephew Berke Bayrak, my niece Ecrin Bayrak, my sister-in-law Bihter Anil, and my intended brother-in-law Cengiz Gulbahar for their love, understanding, and support during my time at the Iowa State University.

TABLE OF CONTENTS

LIST OF FIGURES

LIST OF TABLES

ABSTRACT

The primary goal of this research was to show that artificial neural network (ANN) models could be developed to perform rapid and accurate predictions of jointed plain concrete pavement system (JPCP) parameters which will enable pavement engineers to incorporate the state-of-the-art finite element (FE) solutions into routine practical design. The ISLAB2000 finite element program has been used as an advanced structural model for solving the responses of the concrete pavement systems and generating a large knowledge database.

Totally, fifty-six ANN-based backcalculation and forward calculation models were developed as part of this research for the analysis of JPCP systems under traffic and temperature loading combinations to predict the concrete pavement parameters and critical pavement responses. In this research, BCM stands for the ANN-based backcalculation model and FCM stands for the ANN-based forward calculation model. BCM-E_{PCC}, BCM-k_S, BCM-TELTD, FCM-RRS, and FCM-σ_{MAX} models were developed for the prediction of elastic modulus of Portland cement concrete (PCC) layer (E_{PCC}), coefficient of subgrade reaction (k_S) of the pavement foundation, total effective linear temperature difference (TELTD) between top and bottom of the PCC layer, radius of relative stiffness (RRS) of the pavement system, and maximum tensile stresses at the bottom of the Portland cement concrete layer (σ_{MAX}), respectively. These ANN-based models gave average errors less than 1 % for synthetic database. In order to develop more robust networks that can tolerate the noisy or inaccurate pavement deflection patterns collected from the Falling Weight Deflectometer (FWD) field tests, several network architectures were also trained with varying levels of noise in them.

One of the most important advantages of the presented ANN approach is that the use of the ANN-based models resulted in a drastic reduction in computation time. Rapid prediction ability of the ANN-based models (capable of analyzing 100,000 FWD deflection profiles in one second) provides a tremendous advantage to the pavement engineers by allowing them to

nondestructively assess the condition of the transportation infrastructure in real time while the FWD testing takes place in the field. In the developed approach, there is also no need a seed moduli or iteration process of the solution in order to predict the JPCP system parameters. The prediction of temperature difference (TELTD) in PCC layer which causes the slab curling and warping in concrete pavements is another tremendous advantage of the developed approach over the other methods since no other method does not take into account this parameter in the analyses. Finally, it can be concluded that ANN-based analysis models can provide pavement engineers and designers with state-of-the-art solutions, without the need for a high degree of expertise in the input and output of the problem, to rapidly analyze a large number of concrete pavement deflection basins needed for project specific and network level pavement testing and evaluation.

CHAPTER 1. GENERAL INTRODUCTION

INTRODUCTION

Concrete pavements are constructed of Portland cement concrete. The first concrete pavement was built in Bellofontaine, Ohio in 1893 and the second concrete pavement was constructed in Detroit, Michigan in 1908 (Fitch 1996). Concrete pavements are placed either directly on the prepared subgrade or on a single layer of granular or stabilized material. Closely spaced contraction joints are constructed in jointed plain concrete pavements and dowels or aggregate interlocks may be used for load transfer across the joints. Joint spacing between 15 to 30 ft have been used depending on the type of aggregate, climate, and prior experience. Due to the amount of transportation infrastructure, rehabilitation is one of the most important issues in pavement management.

Evaluating the structural condition of existing, in-service pavements is a part of the routine maintenance and rehabilitation activities undertaken by most Department of Transportations (DOTs). In the field, the pavement deflection profiles (or basins) gathered from the nondestructive falling weight deflectometer test data are typically used to evaluate pavement structural conditions. The deflection-testing program is being conducted periodically to obtain the load-response characteristics of the pavement structure and subgrade. This kind of evaluation requires the use of backcalculation and forward calculation type structural analysis to determine pavement layer stiffness and critical pavement responses and is used to estimate pavement remaining life.

Falling weight deflectometer testing have become the main nondestructive testing (NDT) techniques to structurally evaluate the in-service highway pavements over the last twenty years. Falling weight deflectometer testing is often preferred over destructive testing methods because FWD testing is faster than destructive tests and do not entail the removal of pavement materials. In addition, the testing apparatus is easily transportable. Pavement properties are backcalculated from the observed dynamic response of the pavement surface

to an impulse load (the falling weight). The FWD can either be mounted in a vehicle or on a trailer and is equipped with a weight and several velocity transducer sensors. To perform a test, the vehicle is stopped and the loading plate (weight) is positioned over the desired location. The sensors are then lowered to the pavement surface and the weight is dropped. The advantage of an impact load response measuring device over a steady state deflection measuring device is that it is quicker, the impact load can be easily varied and it more accurately simulates the transient loading of traffic. Sensors located at specific radial distances monitor the deflection history. The deflections measured at radial distances away from load form the deflection basin. In order to calculate the pavement structural capacity correctly the deflection basins should be measured and analyzed accurately.

To evaluate the structural condition of in-service pavements and to characterize the layer properties as inputs into available numerical or analytical programs, backcalculation of pavement layer properties and forward calculation of critical pavement responses are very useful tools. Most backcalculation procedures estimate pavement properties by matching measured and calculated pavement surface deflection basins. On the other hand, there is no need this step in the developed ANN-based approach in this research. Although there are numerous methods for evaluating the structural capacity of pavements from deflection basin data, there is no standard or universally accepted procedure that presently exists (PCS/Law Engineering 1993).

The time spent on analyzing the deflection data composes the most of the work required to interpret the results. Can the routine in-service pavement evaluation be more rapid and accurate in the field during the FWD testing? The purpose of this research is to investigate the pavement layer properties and critical pavement responses in-depth under traffic and environmental loading conditions more rapidly to provide practical techniques to pavement engineers for analyzing the jointed Portland cement concrete pavements in project specific and network level project testing and evaluations.

The comparison / validation of the developed ANN-based model predictions with the actual results is unfortunately a challenging problem. It is not easy to compare the ANN-based

model predictions with the actual results even though some laboratory or in-situ test results are available for the JPCP system parameters predicted. For example, one of the JPCP system parameters that is backcalculated in the presented research is coefficient of subgrade reaction (k_S). In order to measure the k_S value in the field, static plate loading tests are conducted on top of the subgrade before the pavement is constructed. The k_S value is affected from the environmental conditions significantly due to the freeze-thaw effects. Therefore, subgrade stiffness is a not constant value and changes with the season due to the climatic conditions throughout the year. As a result, there should be a FWD test and plate loading test conducted at the same time and location on the same pavement section to compare the developed ANN-based model predictions and field test results. Most probably, the seasonal and climatic environmental conditions are not the same for the times that plate loading test and FWD test are conducted, and there might be several years between these two tests. Therefore, it is not possible every time to compare these two different values.

Another JPCP system parameter is elastic moduli of the PCC layer (E_{PCC}). In order to validate the proposed models, several PCC cores might be taken from the same concrete slabs that FWD test is conducted. Very different elastic moduli values might be measured even in the laboratory tests for a same pavement section. In addition, it should be also noted that elastic modulus from the laboratory tests is a parameter solely related to the material property. However, the backcalculated E_{PCC} value is no more a unique property for material and it becomes a parameter depends not only on material property but also on the structural model and boundary conditions employed in the backcalculation (Guo and Marsey 2001).

The other two JPCP system parameters that are predicted in this research are radius of relative stiffness (RRS) and maximum tensile stress at the bottom of the PCC layer. These two parameters can not be measured in the field or in the laboratory but they can be calculated by other parameters. The radius of relative stiffness value is a fictitious parameter which is a function of elastic modulus of PCC layer, thickness of the PCC layer, coefficient of subgrade reaction and Poisson's ratio ($RRS = [(E_{PCC}.h_{PCC}^3)/(12.k_S.(1-\nu^2)]^{0.25}$). Also, stress values can not be measured in the field; they are calculated from the measured strain values.

Therefore, the comparison of these two pavement parameters with actual field or laboratory test results is not possible.

The parameter whose validation is the most difficult is the equivalent effect of total amount of curling and warping in terms of temperature difference between the top and bottom of the concrete slabs (TELTD) in JPCP systems. In order to validate this parameter, several measurements should be taken on the same pavement section in several days since five different parameters contribute to the total amount of curling and warping in concrete slabs. Transient temperature gradient, transient moisture gradient, permanent built-in temperature gradient, permanent drying shrinkage, and permanent creep values should be measured and FWD test should be conducted in both mid-slab (center) and corner of the concrete slab to compare the actual field results with the ANN-based model predictions. Unfortunately, there is not an available method today that can measure these five curling and warping parameters separately. Since there were not such data available, the ANN-based model predictions were compared with the Crovetti's (2002) data (FWD tests and transient temperature gradient measurements available) and typical ranges for TELTD parameter.

Due to the all of these reasons, the backcalculated and forward calculated concrete pavement parameters were compared with the available methods, techniques and softwares already validated over the years such as statistical regression analysis, closed-form solutions, ISLAB2000, DIPLOMAT, KENSLABS finite element programs, EverCALC 5.0, BAKFAA, EverFE 2.24 pavement backcalculation programs, and typical ranges for each JPCP parameter.

THESIS OBJECTIVES

In order to evaluate the jointed plain concrete pavements, it is essential to have a good understanding of the behavior of the PCC pavements under loading from a structural perspective. The combined effect of the traffic and environmental loading conditions should be taken into account together in the evaluation process which is a very complicated non-linear problem. The existing methods are not adequate to solve this complex problem properly. The research presented in this dissertation therefore mainly focuses on the development and performance of ANN-based models based on ISLAB2000 solutions for the analysis of jointed plain concrete pavements under different traffic and temperature loadings. One of the major objectives of this research is to develop a rapid and accurate technique to backcalculate the pavement layer and foundation properties and forward calculate the critical pavement responses from the FWD deflection basin data by using the advantages of the artificial neural networks which can capture the very complex relationships between the dependant and independent input variables.

It is also well known that environmental conditions have a huge influence on the in-service pavement conditions and on the remaining life of pavements. For example, slab curling and warping in concrete pavements due to temperature and moisture differentials throughout the thickness of a slab affect the nondestructive testing results which are conducted to measure the pavement surface deflections. These erroneous measurements may divert the pavement engineers to inaccurate predictions of pavement and foundation properties and critical pavement responses. That's why curling and warping effects should be taken into account in the evaluation process of concrete pavements. A second objective of this research is to predict the equivalent effect of total amount of curling and warping in terms of temperature difference between the top and bottom of the concrete slab in JPCP systems. Such an approach that takes into accounts both the traffic and environmental loading is invaluable since there is not an existing method which analyzes these effects together in JPCP systems.

PROBLEM DESCRIPTION

There are more than 3,000,000 miles rural highways and more than 900,000 miles urban highways in United States according to Federal Highway Administration (FHWA) statistics. Due to the amount of transportation infrastructure, rehabilitation is one of the most important issues in pavement management. To facilitate managing this demanding task and to efficiently allocate resources, US Department of Transportation pavement evaluation engineers and technicians are relying more and more on nondestructive testing techniques to asses the structural integrity of the existing highways and to provide the data base needed for improving design and construction techniques of new generation of pavements and pavement overlays.

The falling weight deflectometer tests are commonly used to assess the structural integrity of highway/airport pavements in a nondestructive manner. There are many advantages to using FWD tests, in lieu of, or supplement traditional destructive tests for pavement structural evaluation. Most important, is the capability to quickly gather data at several locations while keeping a runway, taxiway, or apron operational during these 2-minute to 3-minute tests. Without FWD, structural data must be obtained from numerous cores, borings, and excavation pits on an existing highway/airport pavement. This can be very disruptive to highway/airport operations. FWD tests are economical to perform and data can be collected at up to 250 locations per day using a single FWD machine. The FWD equipment measures pavement surface deflections from an applied dynamic load that simulates a moving wheel. The deflection data that are collected with the FWD equipment can provide both qualitative and quantitative data about the overall condition of a pavement system at the time of testing.

To evaluate the structural condition of in-service concrete pavements and to characterize the layer properties as inputs into available numerical or analytical programs, backcalculation of pavement properties and forward calculation of critical pavement responses from FWD test data is a useful tool. Such a methodology will enable pavement engineers to easily and quickly incorporate the needed sophistication in structural analysis, such as from finite element modeling with proper characterization of pavement layers, into routine practical

mechanistic-based analysis and design. The number and thickness of the pavement layers, and the strength and behavioral characteristics of the pavement materials are the structural design variables. Pavement layer stiffness parameters at the time of testing of the in-service pavements are used to decide what type of rehabilitation and maintenance should be performed on the pavement and critical pavement responses are used to estimate the pavement remaining life. Furthermore, the adequacy of maintenance during its service life and the quality of construction workmanship affect the performance of pavement systems under service conditions.

RESEARCH APPROACH

Today, a variety of finite element programs are available for the analysis and design of pavement systems. The two main categories of FE programs are those: (1) programs specifically designed for the analysis of pavement systems, and (2) general-purpose programs. Finite element programs which can incorporate the environmental effects in the analysis allow the user to analyze pavement systems subjected to various traffic and temperature loading combinations. The ISLAB2000 finite element program (Tabatabaie and Barenberg 1978; Khazanovich 1994; Khazanovich et al. 2000) has been chosen as an advanced structural model for solving the responses of the concrete pavement systems and generating a large knowledge database to provide a better understanding of the deflection response of concrete pavements subjected to traffic and temperature loadings. ISLAB2000 has been extensively tested and validated over the years by comparing its predictions with available theoretical solutions and results from experimental studies.

ISLAB2000 finite element runs were generated by modeling slab-on-grade concrete pavement systems in order to train the ANN-based models. A single slab layer resting on a Winkler foundation was analyzed in all cases. 4-noded 12 DOF thin plate element and 2-noded spring element were employed in the ISLAB2000 analyses for PCC layer and subgrade, respectively (see Figure 1.1).

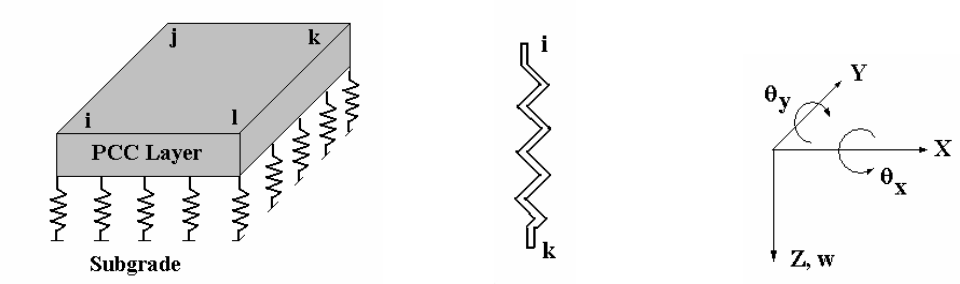

(a) Plate element (b) Spring element

Figure 1.1. Finite elements employed in ISLAB2000 analysis

Concrete pavements analyzed in the backcalculation of elastic modulus of PCC layer (E_{PCC}), coefficient of subgrade reaction (k_S) and forward calculation of radius of relative stiffness (RRS) and maximum tensile stress at the bottom of the PCC layer (σ_{MAX}) were represented by a six-slab assembly, each slab having dimensions of 20 ft by 20 ft. On the other hand, concrete pavements analyzed in the backcalculation of total effective linear temperature difference (TELTD) models were represented by a six-slab assembly, each slab having dimensions of 15 ft by 15 ft.

The ISLAB2000 solutions were compared with the Westergaards's closed-form solutions and DIPLOMAT and KENSLABS finite element program solutions for thirty-six different pavement configurations by varying E_{PCC}, h_{PCC}, and k_S. A very good agreement was obtained from different finite element programs solutions for thirty-six different pavement configurations. Among these programs, ISLAB2000 finite element program was chosen as the main structural analysis program since ISLAB2000 is the main structural model in the new Mechanistic-Empirical Pavement Design Guide (MEPDG). The finite element model solutions could not be compared with the actual pavement deflection measurements since there were not any available actual elastic modulus for PCC layer, coefficient of subgrade reaction and FWD test results for a specific pavement test section available in this research.

In the second part of the research, backpropagation type artificial neural network models were trained with the ISLAB2000 solution knowledge database to develop models that can predict the pavement layer properties and critical pavement responses. The developed ANN-based models have proved to be very effective in analyzing jointed plain Portland cement concrete pavements and provided an opportunity for pavement engineers to incorporate current sophisticated methodology into practical pavement testing and evaluation. The adoption and use of ANN modeling techniques in the recently released Mechanistic-Empirical Pavement Design Guide (NCHRP project 1-37A: Development of the 2002 Guide for the Design of New and Rehabilitated Pavement Structures: Phase II) has especially placed the emphasis on the successful use of artificial neural networks in geomechanical and pavement systems.

RESEARCH SCOPE

Developed ANN-based backcalculation and forward calculation analysis models can provide pavement engineers and designers with state-of-the-art solutions, without the need for a high degree of expertise in the input and output of the problem, to rapidly analyze a large number of concrete pavement deflection basins needed for project specific and network level pavement testing and evaluation.

This research study is devoted mainly to the development of evaluation procedures applicable to existing jointed plain Portland cement concrete pavements with slabs of variable thickness, elastic moduli, foundation properties, and temperature difference between the top and bottom of the slab. A brief information about the artificial neural networks was also given in the research. A more comprehensive description and analysis of ANNs is beyond the scope of this research. In addition, a sensitivity study was conducted to determine the most appreciate architecture for predicting the concrete pavement parameters and also developed ANN-model predictions were compared with the other available method results and theoretical solutions.

THESIS ORGANIZATION

CHAPTER ONE: Statement of thesis objectives, description of the problem, description of research approach, and description of research scope.

CHAPTER TWO: Artificial neural networks.

CHAPTER THREE: Sensitivy study for finite slab sizes, dimensional analysis.

CHAPTER FOUR: First journal paper: Use of artificial neural networks in transportation infrastructure systems: 1987 – 2007.

CHAPTER FIVE: Second journal paper: Use of neural networks to develop robust backcalculation and forward calculation models for concrete pavement systems.

CHAPTER SIX: Third journal paper: Backcalculation of total effective linear temperature difference (TELTD) in jointed plain concrete pavement systems.

CHAPTER SEVEN: Rehabilitation design applications.

CHAPTER EIGHT: Summary and conclusions on evaluations of jointed plain concrete pavement systems and recommendations for further research.

REFERENCES

Fitch, M. 1996. Bellefontaine, Ohio: Home of America's Oldest Concrete Pavement. Summer 1996, pp.4-6; Ohio T2 Center, Ohio State University.

Huang, Y.H. 2004. Pavement Analysis and Design. Pearson Prentice Hall, NJ.

Khazanovich, L. 1994. Structural Analysis of Multi-Layered Concrete Pavement Systems. Ph.D. dissertation, University of Illinois, Illinois, USA.

Khazanovich, L., Yu, H.T., Rao, S., Galasova, K., Shats, E., and Jones, R. 2000. ISLAB2000 - Finite Element Analysis Program for Rigid and Composite Pavements User's Guide, ERES Consultants, A Division of Applied Research Associates, Champaign, Illinois.

NCHRP Report. 2003. Guide for Mechanistic-Empirical Design of New and Rehabilitated Pavement Structures, Appendix QQ: Structural Response Models for Rigid Pavements.

PCS/Law Engineering. 1993. SHRP's Layer Moduli Back-Calculation Procedure: Software Selection, SHRP-P651, Washington, DC: Strategic Highway Research Program, National Academy of Science.

Tabatabaie, A.M., and Barenberg, E.J. 1978. Finite Element Analysis of Jointed or Cracked Concrete Pavements. In Transportation Research Record: No. 671, TRB, pp. 11-18.

CHAPTER 2. ARTIFICIAL NEURAL NETWORKS

BACKGROUND ON ARTIFICIAL NEURAL NETWORKS

Over the past two decades, there has been an increased interest in the use of artificial neural networks (ANNs) in civil engineering fields such as structural engineering, environmental and water resources engineering, traffic engineering, geotechnical engineering as well as pavement engineering. ANNs represent a class of robust, non-linear models applicable for solving a wide variety of problems. ANNs have been found to be very useful tools for solving pavement engineering problems, which deal with highly nonlinear functional approximations.

Pavement engineering covers a wide area which includes both highway and airport pavements and involves disciplines including pavement analysis and design, pavement evaluation, pavement performance prediction, and pavement maintenance, rehabilitation, and management issues.

Artificial neural networks are information processing computational tools in which highly interconnected processing neurons work in harmony to analyze and solve complex problems in a nontraditional manner. This power of the ANNs, emulating the biological nervous system, lies in the tremendous number of interconnections between the neurons or processing elements as they provide notable advantages in learning and generalizing from examples, producing meaningful and cost effective solutions to various problems even when input data contain errors or are incomplete, adapting solutions over time to compensate for changing circumstances and processing information quite rapidly and often in real time.

Figure 2.1 displays a typical structure of ANNs that consists of a number of neurons that are usually arranged in layers: an input layer, hidden layers, and an output layer. One of the most important issues in the development of an ANN model is the architecture. Determination of the input and output variables, number of hidden layers, and number of hidden neurons in

each hidden layers is crucial in the development part of the ANN models. The architecture of the ANN models has significant effects on the success of the developed models. Usually, a neural network with too few hidden neurons is unable to learn sufficiently from the training data set, whereas a neural network with too many hidden neurons will allow the network to memorize the training set instead of generalizing the acquired knowledge for unseen patterns (Lawrence and Fredricson 1993). Haykin (1994) recommends using two hidden layers.

Backpropagation ANNs are very powerful and versatile networks that can be taught a mapping from one data space to another using a representative set of patterns/examples to be learned. The term "backpropagation network" actually refers to a multi-layered, feed-forward neural network trained using an error backpropagation algorithm. The learning process performed by this algorithm is called "backpropagation learning" which is mainly an "error minimization technique" (Haykin, 1999; Hecht-Nielsen, 1990; Rumelhart, et al., 1986). In the development of backpropagation ANN models, the connection weights and node biases are initially selected at random.

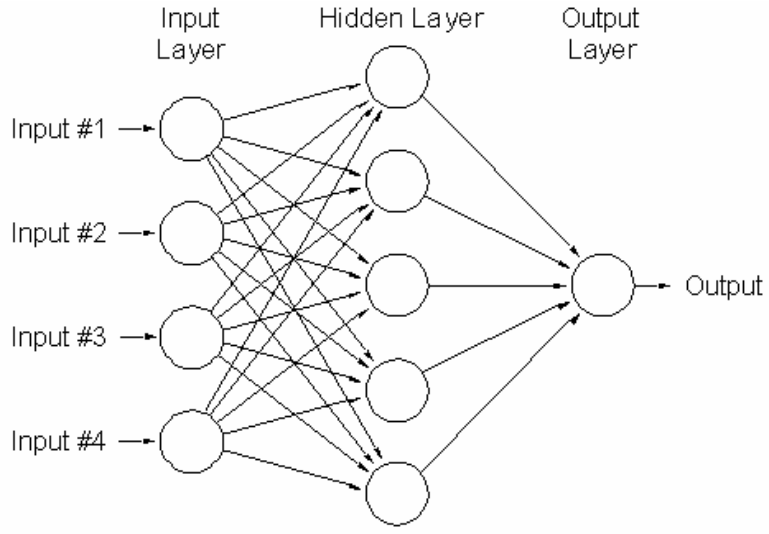

Figure 2.1. Schematic view of typical ANN architecture

Inputs from the mapping examples are propagated forward through each layer of the network to emerge as outputs. The errors between those outputs and the correct answers are then

propagated backwards through the network and the connection weights and node biases are individually adjusted to reduce the error. After many examples (training patterns) are propagated through the network many times, the mapping function is learned with some specified error tolerance. This is called supervised learning because the network has adjusted functional mapping using the correct answers. Backpropagation ANNs excel at data modeling with their superior function approximation (Haykin, 1999).

A neuron is an information-processing unit that is fundamental to the operation of a neural network. A neural network consists of many neurons which each one is an independent processing element. Each neuron has its own inputs and output. A typical neuron is shown in figure below.

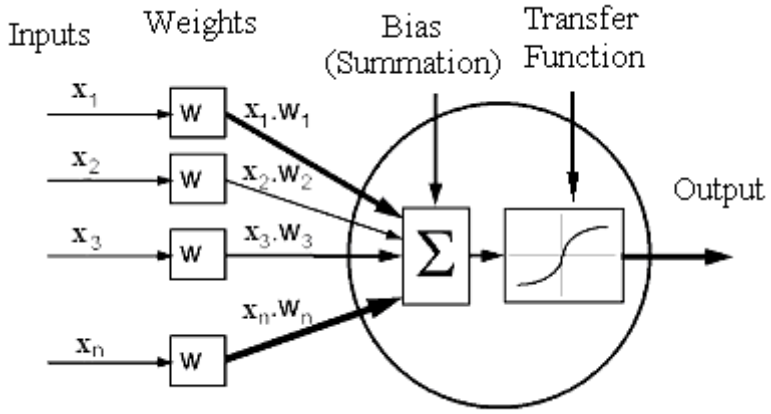

Figure 2.2. An artificial neuron
(http://www.warwick.ac.uk/atc/tig/whatwedo/projects/PBN/neuralnetworks.php)

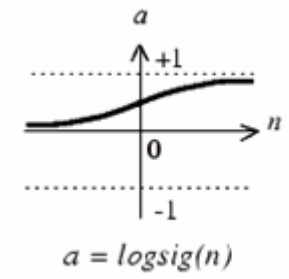

$$log\,sig(n) = \frac{1}{1+e^{(-n)}}$$

(a) Log-Sigmoid activation transfer function

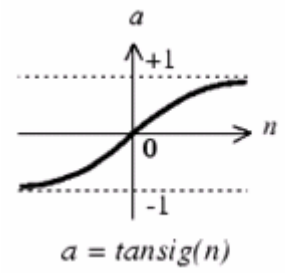

$$tan\,sig(n) = \frac{1}{1+e^{(-2n)}} - 1$$

(b) Tan-Sigmoid activation transfer function

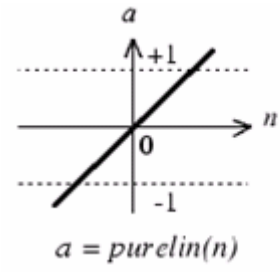

$$purelin(n) = n$$

(a) Linear activation transfer function

Figure 2.3. Activation transfer functions: (a) Log-Sigmoid, (b) Tan-Sigmoid, (c) Linear

ARTIFICIAL NEURAL NETWORK PROGRAM: BACKPROP 3.5

The artificial neural network used in this research is Backprop (BP) 3.5 Fortran code written by Roger W. Meier. This program trains a standard backpropagation-style artificial neural network using the Generalized Delta Rule with a momentum term added with gradient descent learning algorithm. The hidden neurons have a sigmoidal activation function and the output neurons use either sigmoidal or linear activation. The training data set can be presented to the network sequentially or randomly. The remaining testing data set are used to monitor training progress. Every 10 passes (might be changed by the user) through the data set, the target and computed outputs of the testing data set are output to a "results" file, the mean-squared errors for the training and testing data set are output to a "progress" file, and the current values of the interconnection weights are output to a "weights" file. All of the files are sequential ASCII files. The progress file grows with each additional output record. The results and weights files are simply overwritten each time they are accessed. This keeps them from growing too large. This program allows networks to be trained incrementally. If an existing training weights file is located, it will be used as the starting point for additional network training (Meier BP 3.5 Fortran code).

The network training inputs in BP 3.5:

- Number of training data set,
- Number of testing data set,
- Number of iterations (epochs),
- Frequency of training progress printouts,
- Training data set, randomly or sequentially?
- Normalization of target data?
- Linear or sigmoidal activation function in output neurons?
- + / - range of initial random numbers?
- Initial random number stream?
- Learning rate?
- Momentum factor?

The network architecture inputs in BP 3.5:

- Number of layers in hidden layers,
- Number of neurons in input layer,
- Number of neurons in hidden layers,
- Number of neurons in output layer.

Limitations of the BP 3.5 compared to MATLAB ANN toolbox:

- Maximum 2 hidden layers in BP 3.5,
  - May be more than one hidden layer in MATLAB.
- Only one learning algorithm in BP 3.5,
  - Traingd, traingda, traingdx, trainrp, traincgf, traincgp, trainscg, trainoss, trainbfg, trainlm etc. in MATLAB.
- Only one activation function in hidden neurons in BP 3.5 (Logsig),
  - Logsig, Tansig, Purelin in MATLAB.
- Only two activation function in output neurons in BP 3.5 (Logsig and Purelin),
  - Logsig, Tansig, Purelin in MATLAB.
- Constant learning rate in BP 3.5,
  - May be variable in MATLAB.
- There is not a Graphical User Interface (GUI) in BP 3.5,
  - There is a GUI in MATLAB ANN Toolbox.

Additional MATLAB ANN Toolbox training parameters:

- Minimum performance gradient,
- Ratio to increase learning rate,
- Ratio to decrease learning rate,
- Increment to weight change,
- Decrement to weight change,
- Initial weight change,
- Maximum weight change,
- Maximum time to train in seconds.

The Comparison of Backprop 3.5 and MATLAB ANN Toolbox Trainings

In order to investigate the effect of different learning algorithms, the same elastic modulus of PCC layer (E_{PCC}) data set was trained with different learning algorithms by using MATLAB ANN Toolbox. The default values were used for the training suggested by MATLAB. As seen from the training and testing progress curves for this specific data set, the trends in the curves are very sensitive to the learning algorithms used in the training.

In addition to this data set, also another k_S dataset was trained again with different learning algorithms in MATLAB ANN Toolbox. Similarly, different training and testing progress curves was obtained from that data set, as well. For all trainings 5-20-1 (D_0, D_{12}, D_{24}, D_{36}, and h_{PCC}) and 6-20-1 (D_0, D_{12}, D_{24}, D_{36}, D_{48}, and D_{60}) ANN architectures were used in the analyses for E_{PCC} and k_S models, respectively. 250 and 50 patterns were used for the training and testing data set, respectively, for both E_{PCC} and k_S models.

In order to investigate the effects of learning rate (LR), momentum factor (MF), and also initial random weight and bias numbers, several sensitivity studies were conducted by using both Backprop 3.5 and MATLAB ANN Toolbox using the same E_{PCC} and k_S data sets. The average absolute error values, R^2 values, training data set mean-squared-error (MSE) values, and testing data set MSE values were compared for each developed ANN model. The results of these sensitivity analyses showed that the success of the ANN model is highly related with the ANN architecture parameters (learning rate, momentum factor, etc.). The initial random weight and bias numbers also affect the training and testing progress curves and consequently average absolute error value.

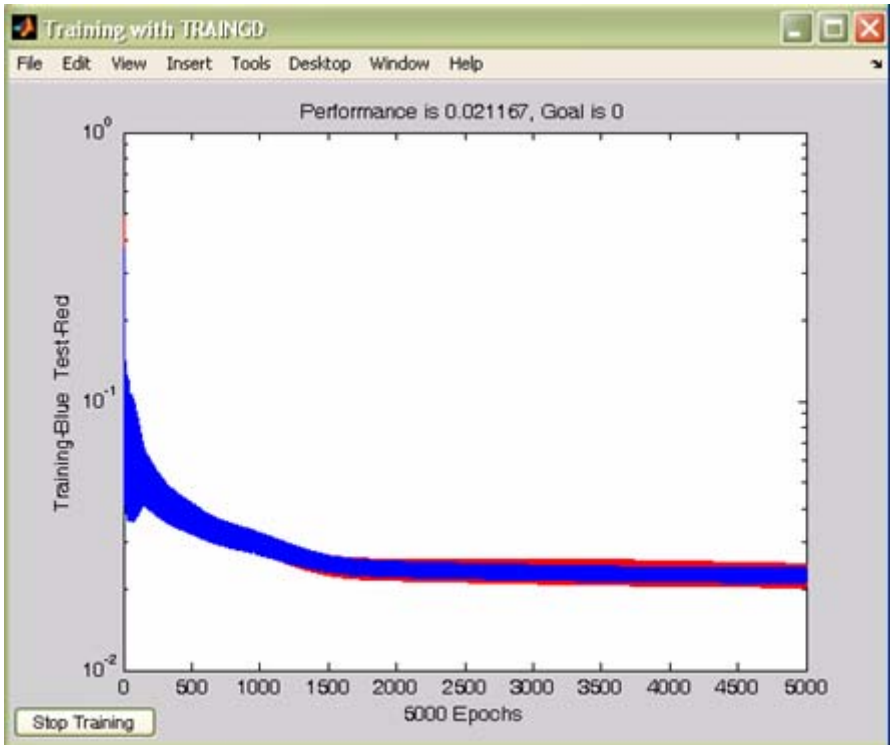

Figure 2.4.Training and testing progress curves for E_{PCC} data set with Traingd algorithm

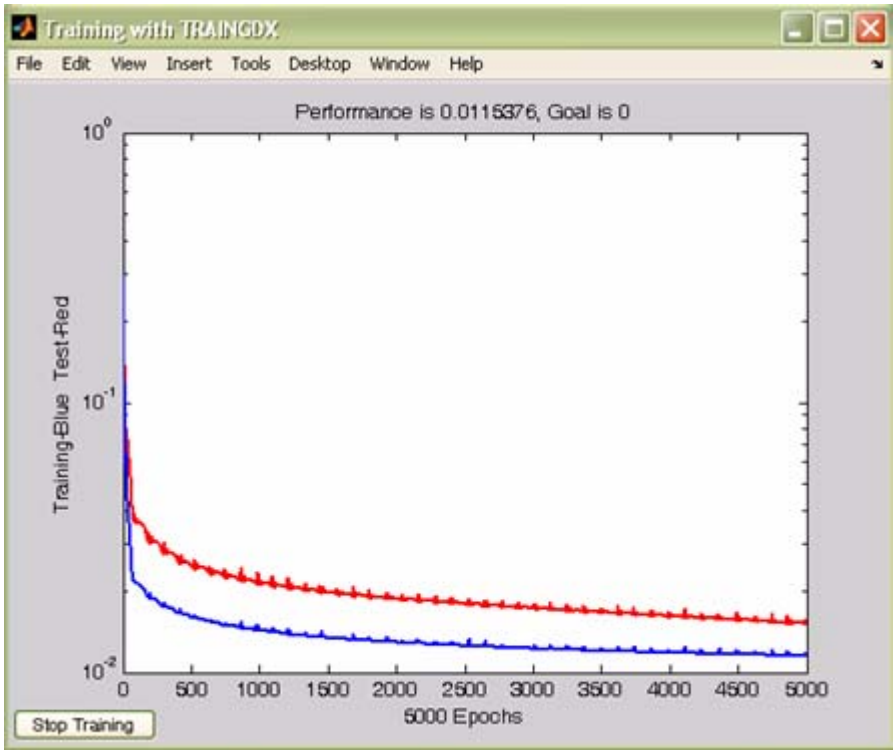

Figure 2.5.Training and testing progress curves for E_{PCC} data set with Traingdx algorithm

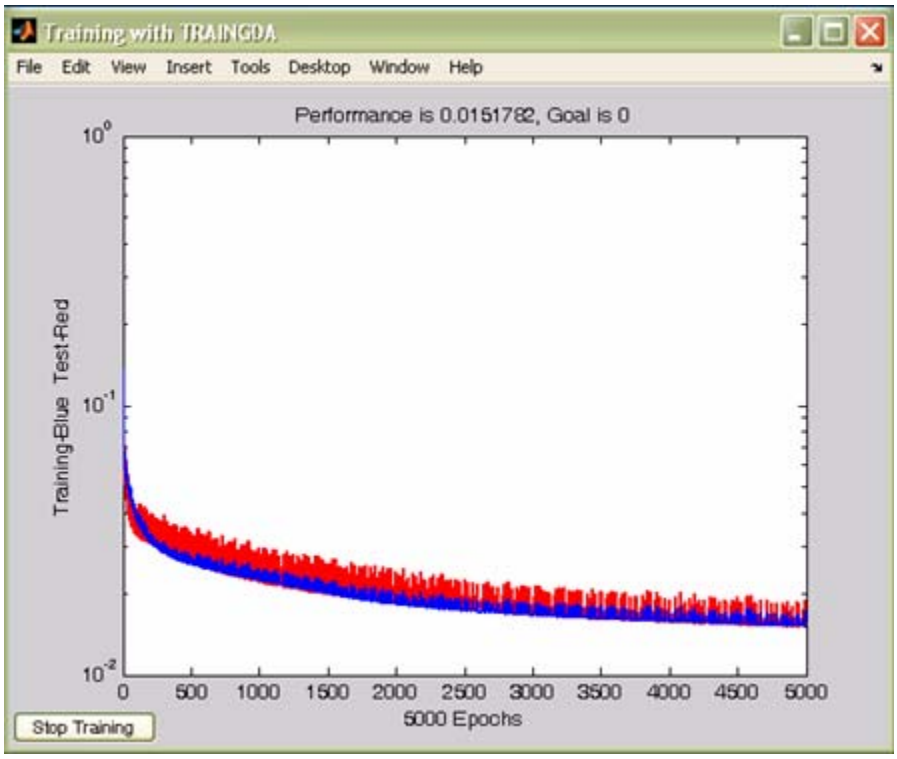

Figure 2.6.Training and testing progress curves for E_{PCC} data set with Traingda algorithm

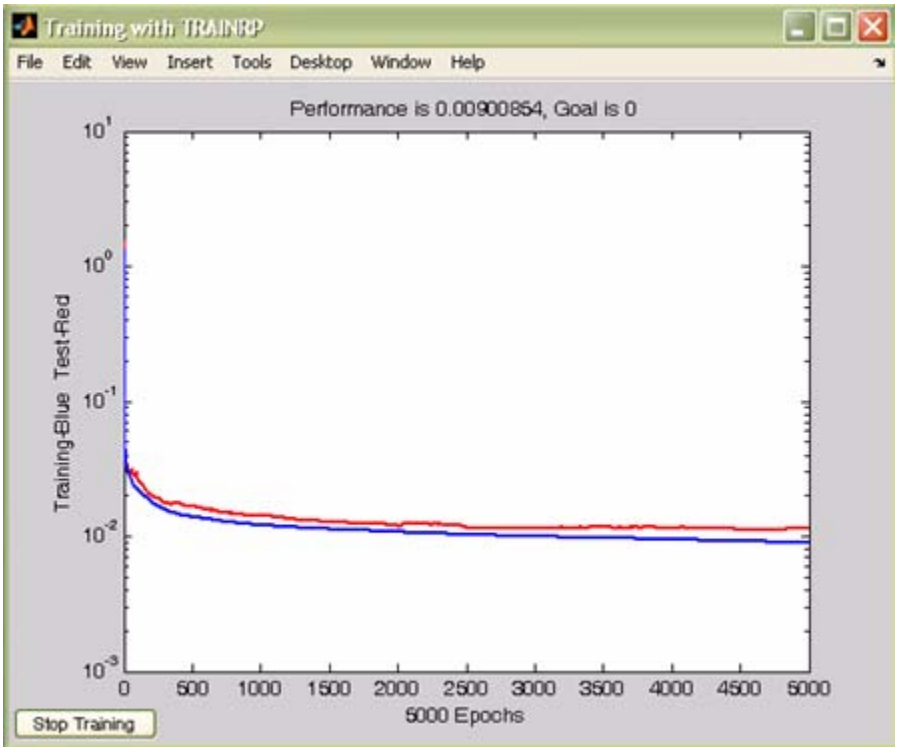

Figure 2.7.Training and testing progress curves for E_{PCC} data set with Trainrp algorithm

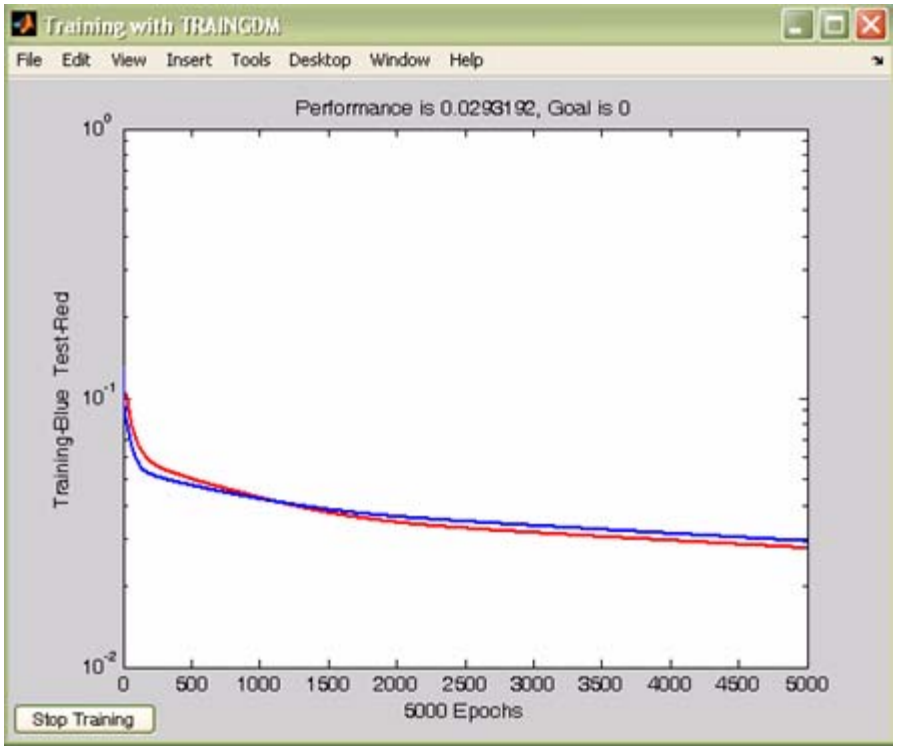

Figure 2.8.Training and testing progress curves for E_{PCC} data set with Traingdm algorithm

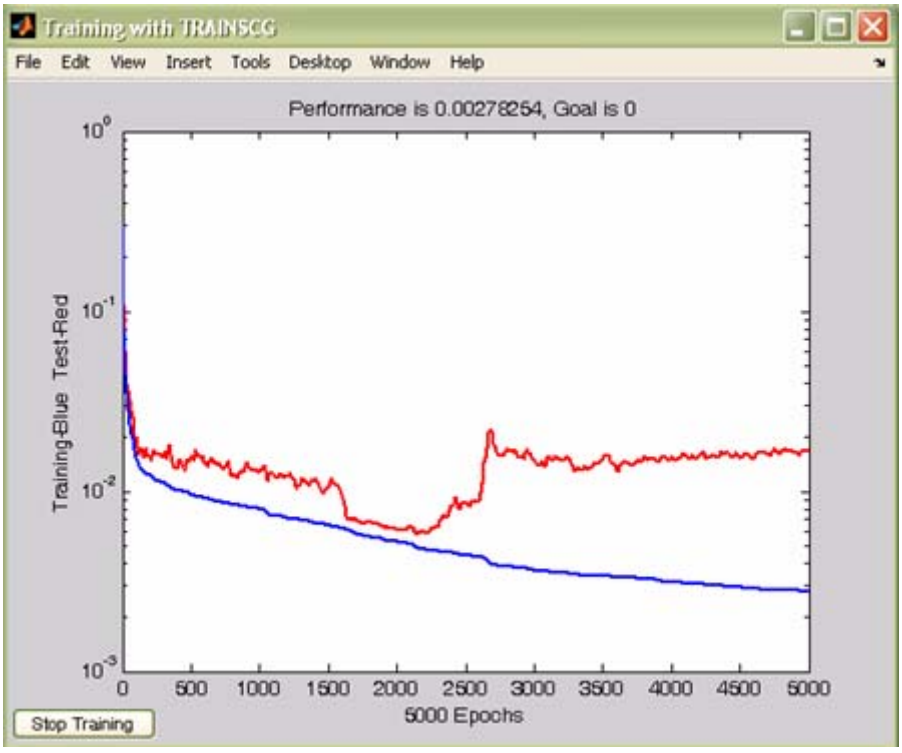

Figure 2.9.Training and testing progress curves for E_{PCC} data set with Trainscg algorithm

Sensitivity study for learning rate and momentum factor (E_{PCC} data set):

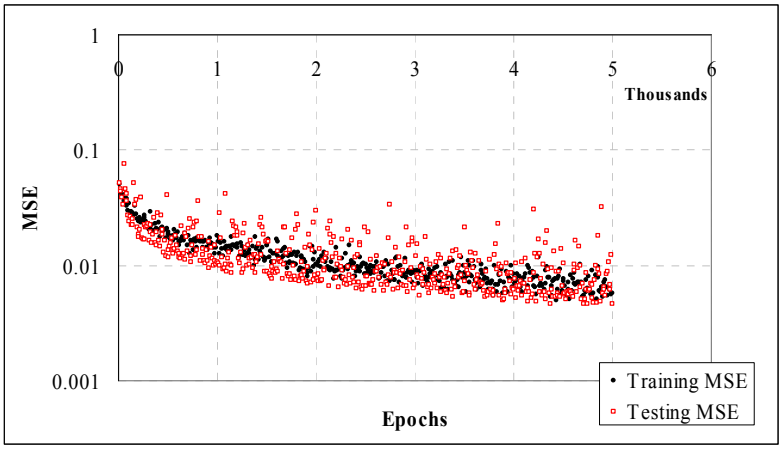

Figure 2.10.Training and testing progress curves for E_{PCC} with BP 3.5 (LR=0.1, MF=0.9)

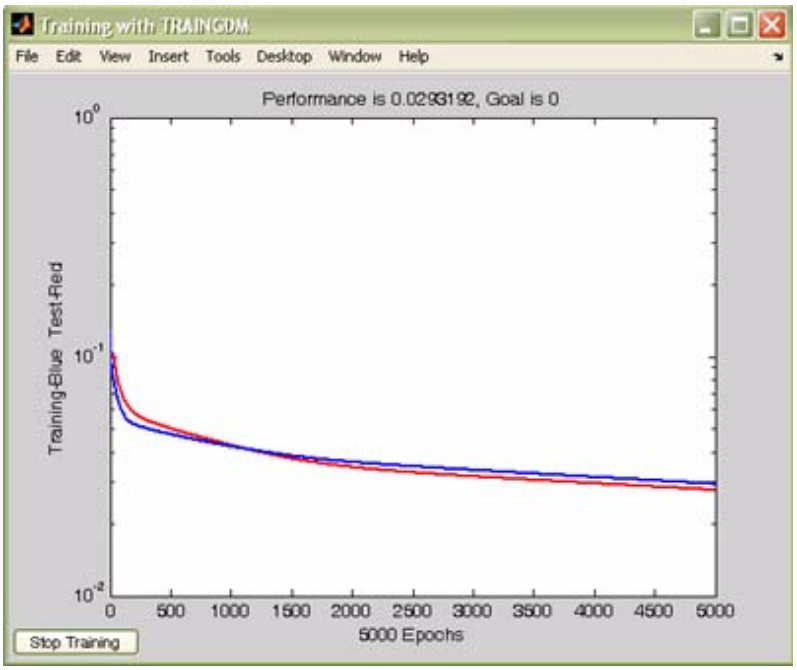

Figure 2.11. Training and testing progress curves for E_{PCC} with MATLAB (LR=0.1, MF=0.9)

Table 2.1. Comparison of the results for E_{PCC} (LR=0.1, MF=0.9)

Learning Rate = 0.1	**Momentum Factor = 0.9**	
	Backprop 3.5	**MATLAB - ANN**
AAE (%) =	11.9	39.1
R^2 =	0.91	0.51
TRN - MSE =	5.7×10^{-3}	29.3×10^{-3}
TST - MSE =	4.7×10^{-3}	27.6×10^{-3}

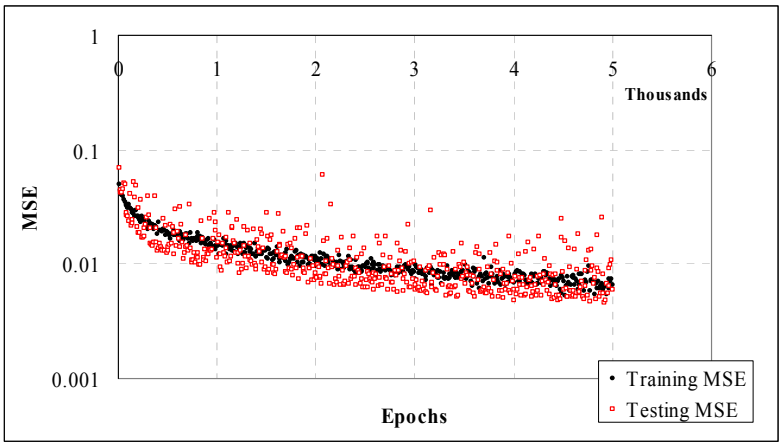

Figure 2.12.Training and testing progress curves for E_{PCC} with BP 3.5 (LR=0.3, MF=0.7)

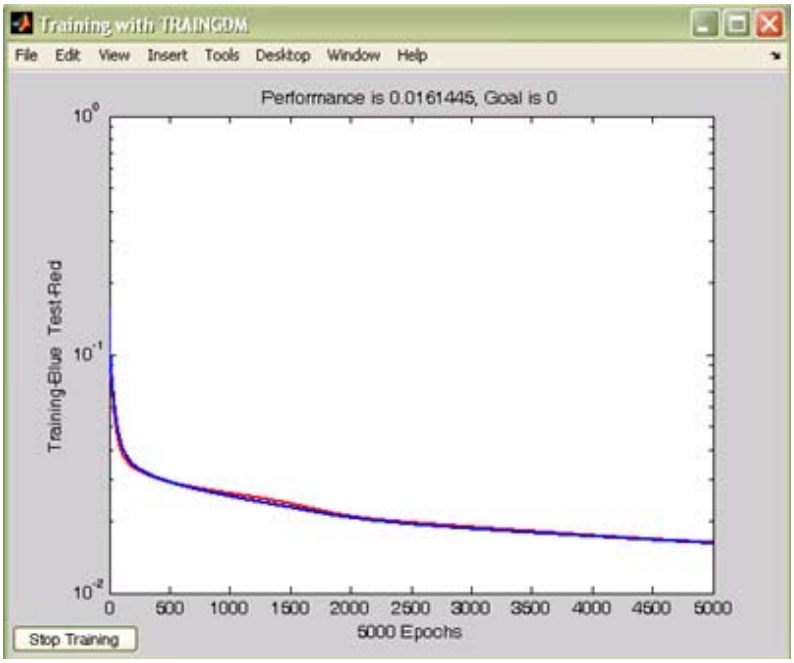

Figure 2.13. Training and testing progress curves for E_{PCC} with MATLAB (LR=0.3, MF=0.7)

Table 2.2. Comparison of the results for E_{PCC} (LR=0.3, MF=0.7)

Learning Rate = 0.3	**Momentum Factor = 0.7**	
	Backprop 3.5	**MATLAB - ANN**
AAE (%) =	13.4	26.5
R^2 =	0.90	0.70
TRN - MSE =	6.6×10^{-3}	16.1×10^{-3}
TST - MSE =	6.0×10^{-3}	16.2×10^{-3}

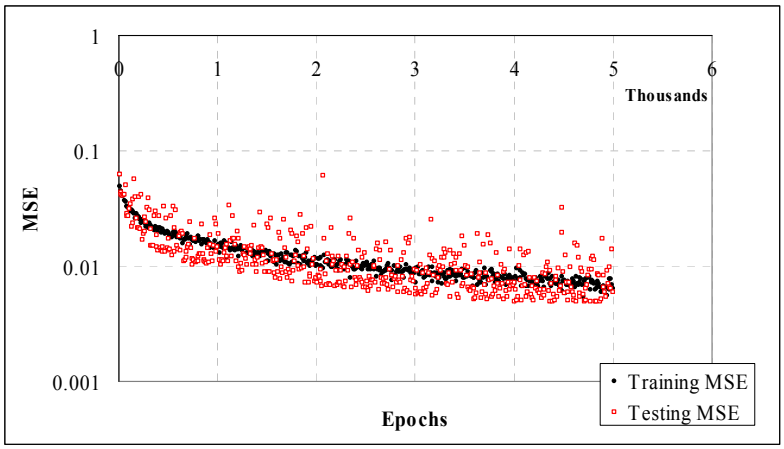

Figure 2.14.Training and testing progress curves for E_{PCC} with BP 3.5 (LR=0.5, MF=0.5)

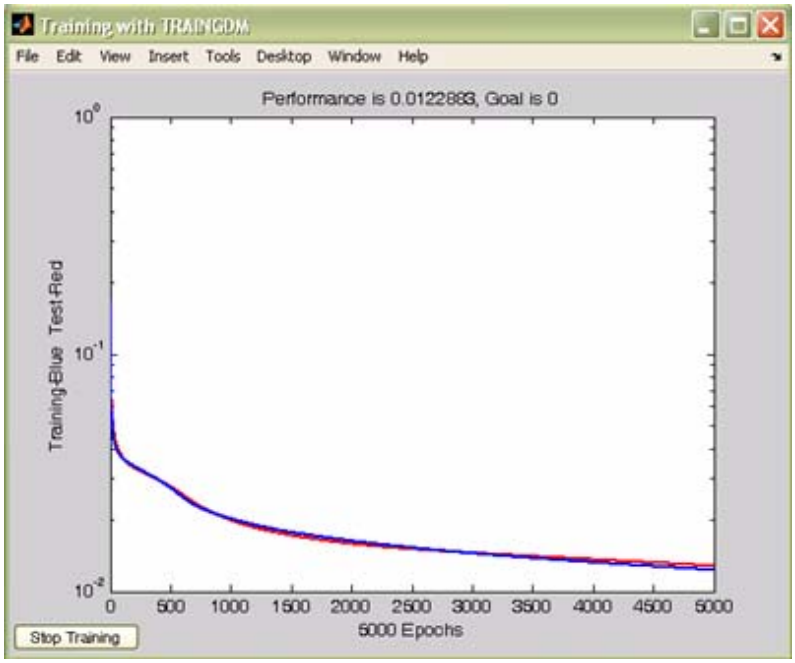

Figure 2.15. Training and testing progress curves for E_{PCC} with MATLAB (LR=0.5, MF=0.5)

Table 2.3. Comparison of the results for E_{PCC} (LR=0.5, MF=0.5)

Learning Rate = 0.5	**Momentum Factor = 0.5**	
	Backprop 3.5	**MATLAB - ANN**
AAE (%) =	13.1	21.4
R^2 =	0.88	0.77
TRN - MSE =	6.4×10^{-3}	12.3×10^{-3}
TST - MSE =	5.9×10^{-3}	12.8×10^{-3}

Sensitivity study for initial random numbers for weights and node biases (E_{PCC} data set):

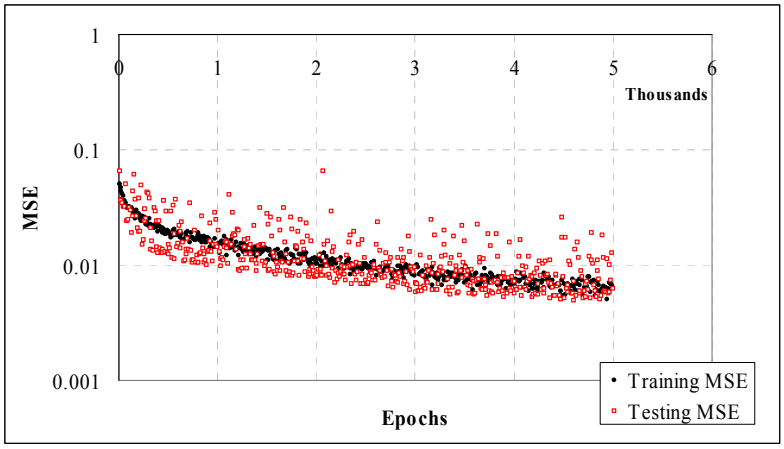

Figure 2.16.Training and testing progress curves for E_{PCC} with BP 3.5 (Random # 1)

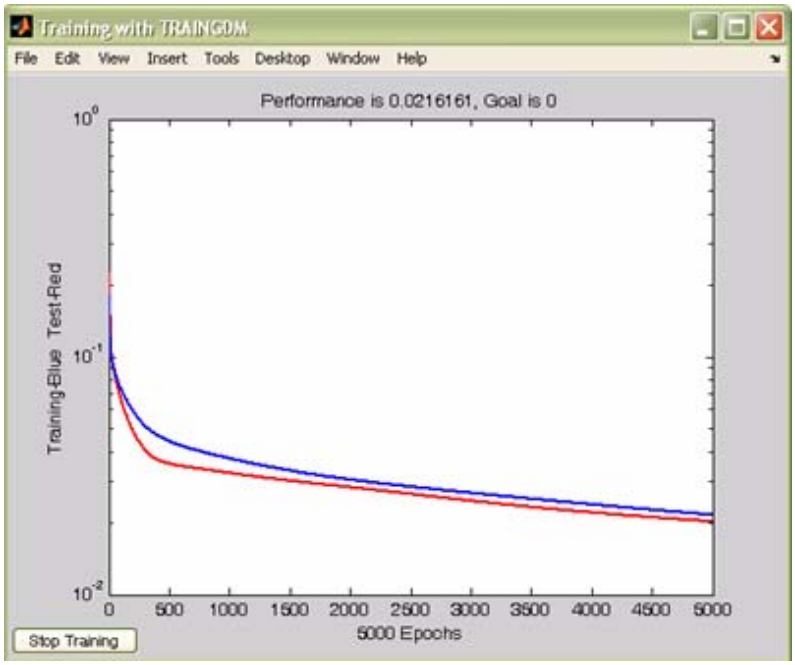

Figure 2.17. Training and testing progress curves for E_{PCC} with MATLAB (Random # 1)

Table 2.4. Comparison of the results for E_{PCC} (Random # 1)

Initial random connection numbers: # 1		
	Backprop 3.5	**MATLAB - ANN**
AAE (%) =	14.4	29.9
R^2 =	0.90	0.65
TRN - MSE =	6.3×10^{-3}	21.6×10^{-3}
TST - MSE =	6.2×10^{-3}	20.2×10^{-3}

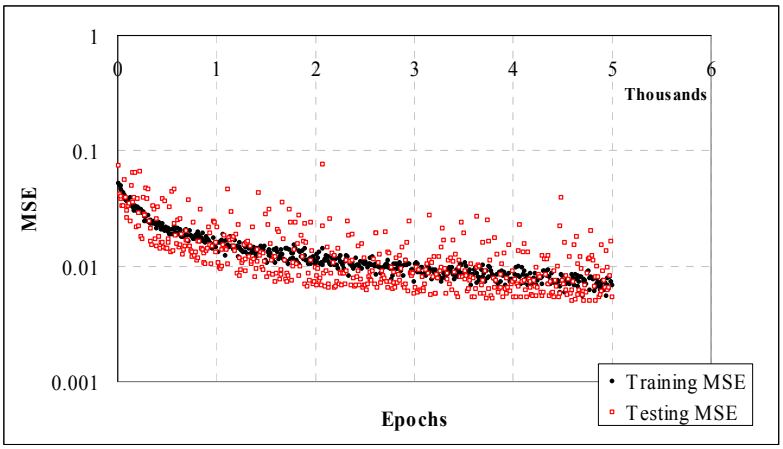

Figure 2.18.Training and testing progress curves for E_{PCC} with BP 3.5 (Random # 2)

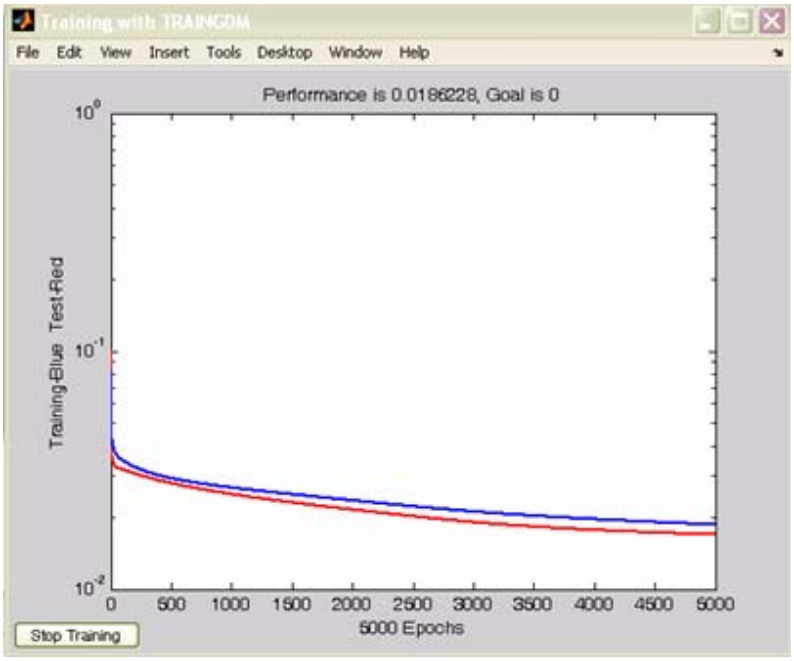

Figure 2.19. Training and testing progress curves for E_{PCC} with MATLAB (Random # 2)

Table 2.5. Comparison of the results for E_{PCC} (Random # 2)

Initial random connection numbers: # 2		
	Backprop 3.5	**MATLAB - ANN**
AAE (%) =	13.5	27.5
R^2 =	0.90	0.69
TRN - MSE =	6.8×10^{-3}	18.6×10^{-3}
TST - MSE =	5.4×10^{-3}	16.9×10^{-3}

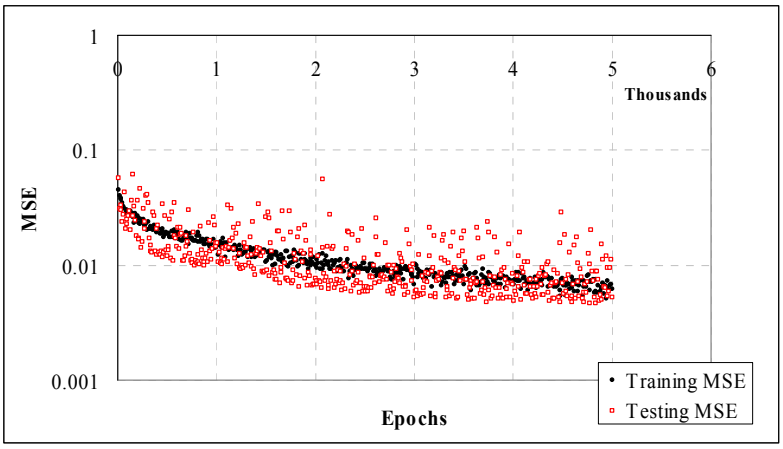

Figure 2.20.Training and testing progress curves for E_{PCC} with BP 3.5 (Random # 3)

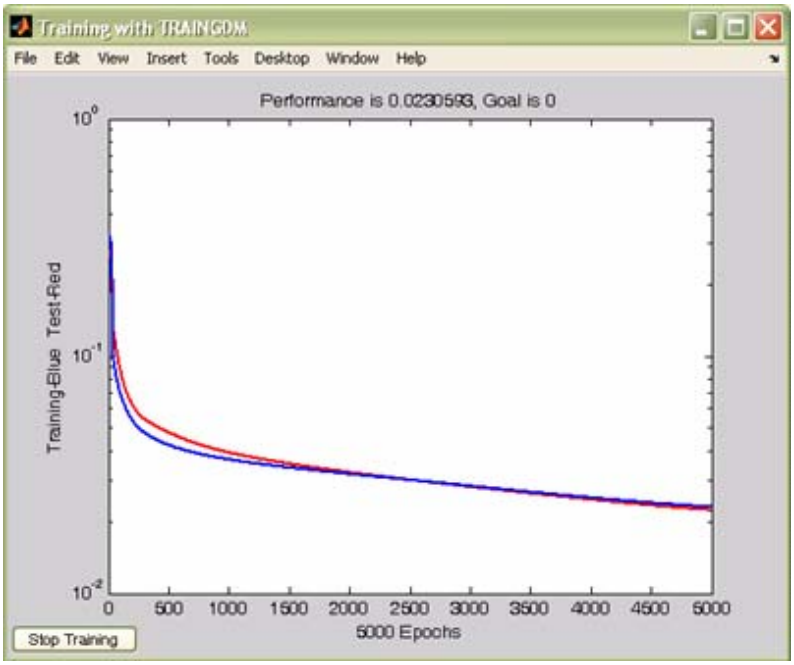

Figure 2.21. Training and testing progress curves for E_{PCC} with MATLAB (Random # 3)

Table 2.6. Comparison of the results for E_{PCC} (Random # 3)

Initial random connection numbers: # 3		
	Backprop 3.5	**MATLAB - ANN**
AAE (%) =	12.7	31.4
R^2 =	0.91	0.61
TRN - MSE =	6.2×10^{-3}	23.1×10^{-3}
TST - MSE =	5.3×10^{-3}	22.4×10^{-3}

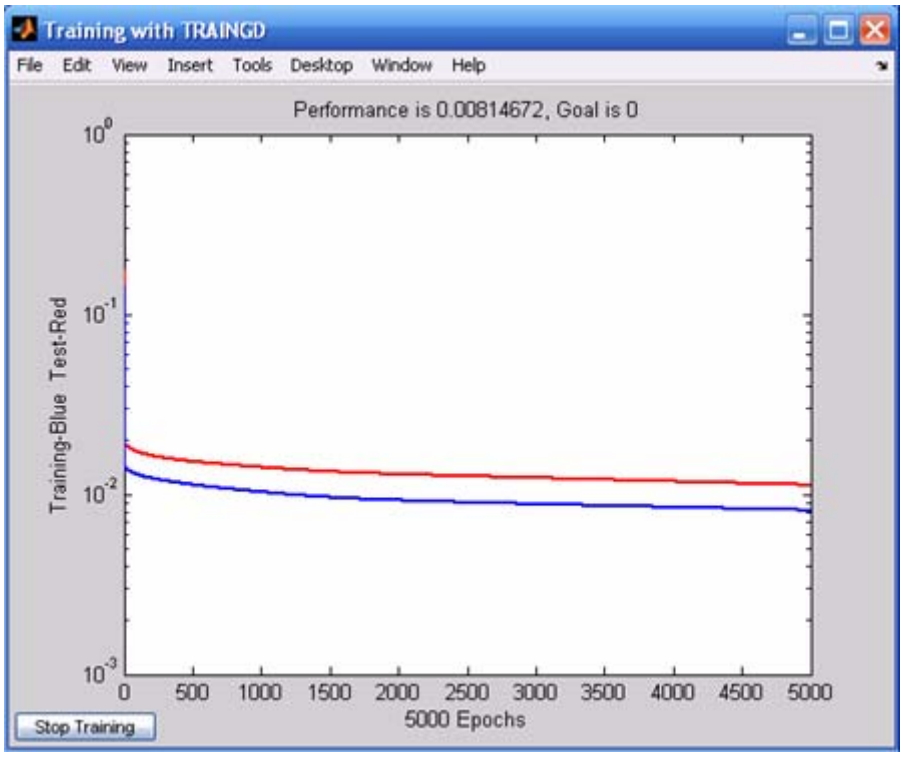

Figure 2.22.Training and testing progress curves for k_S data set with Traingd algorithm

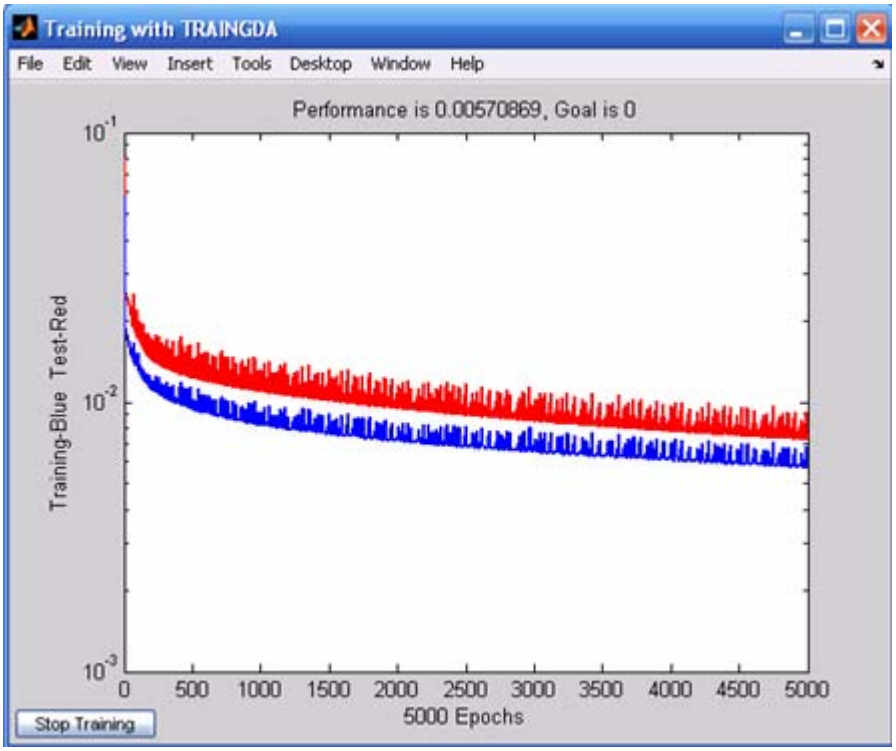

Figure 2.23.Training and testing progress curves for k_S data set with Traingda algorithm

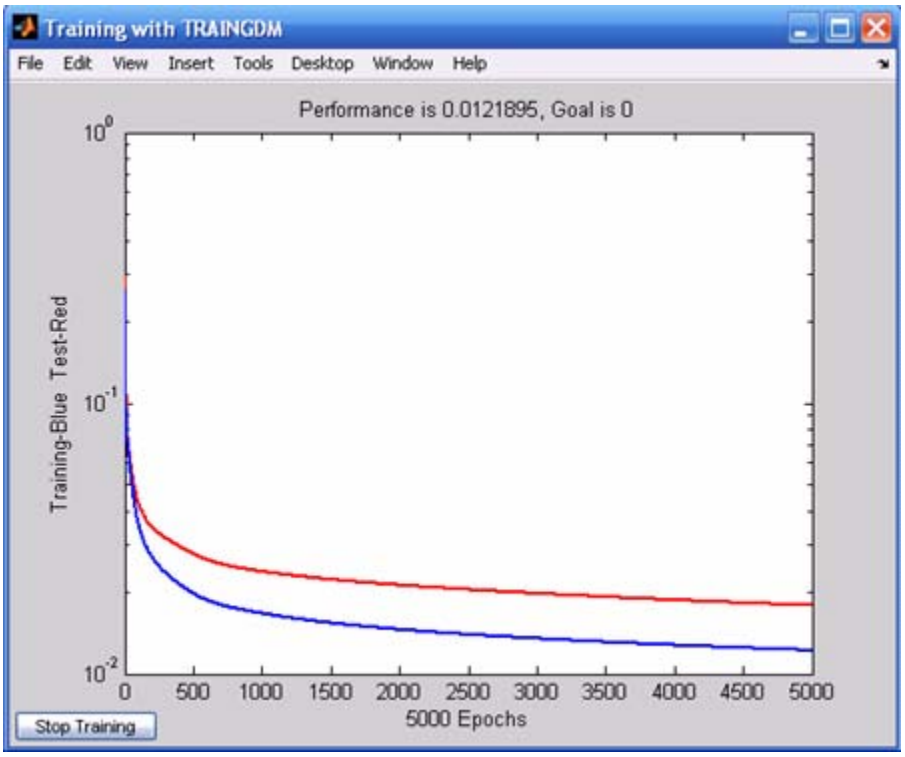

Figure 2.24.Training and testing progress curves for k_S data set with Traingdm algorithm

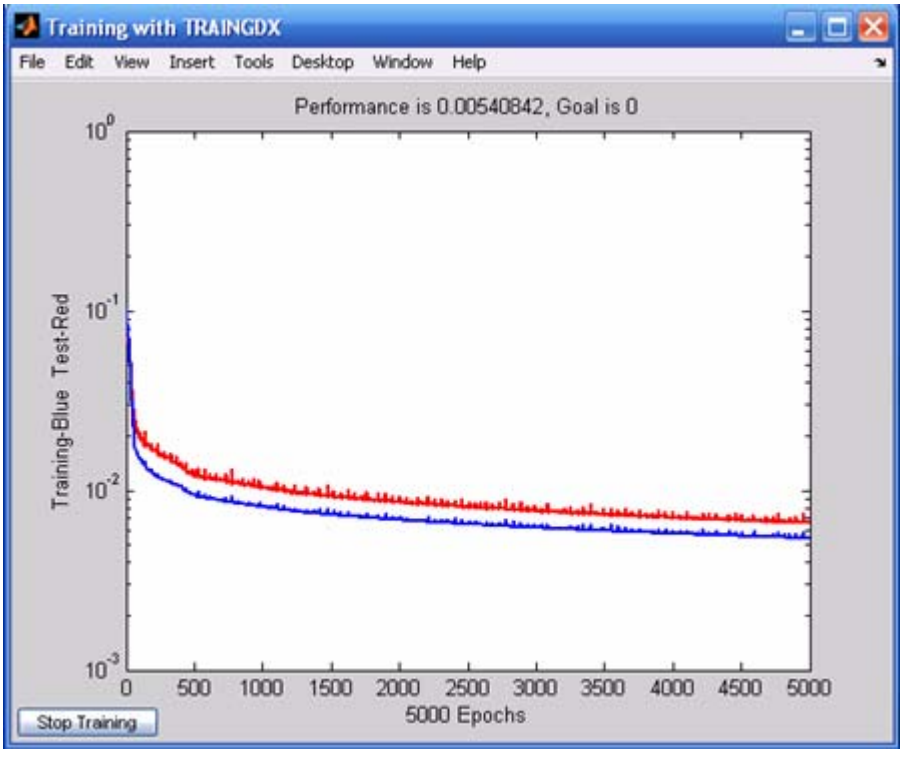

Figure 2.25.Training and testing progress curves for k_S data set with Traingdx algorithm

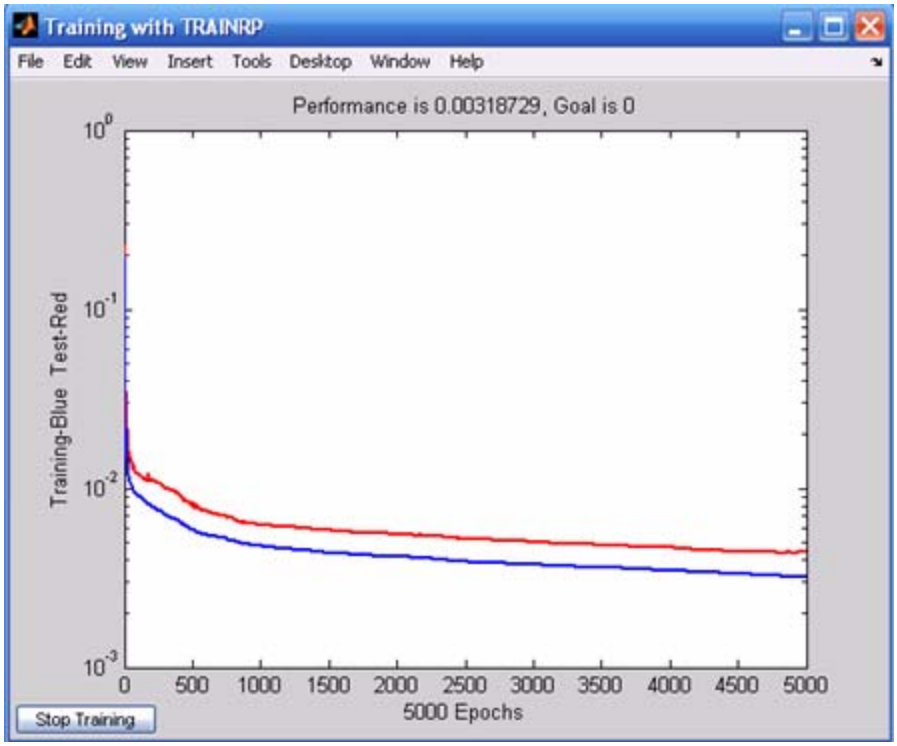

Figure 2.26.Training and testing progress curves for k_S data set with Trainrp algorithm

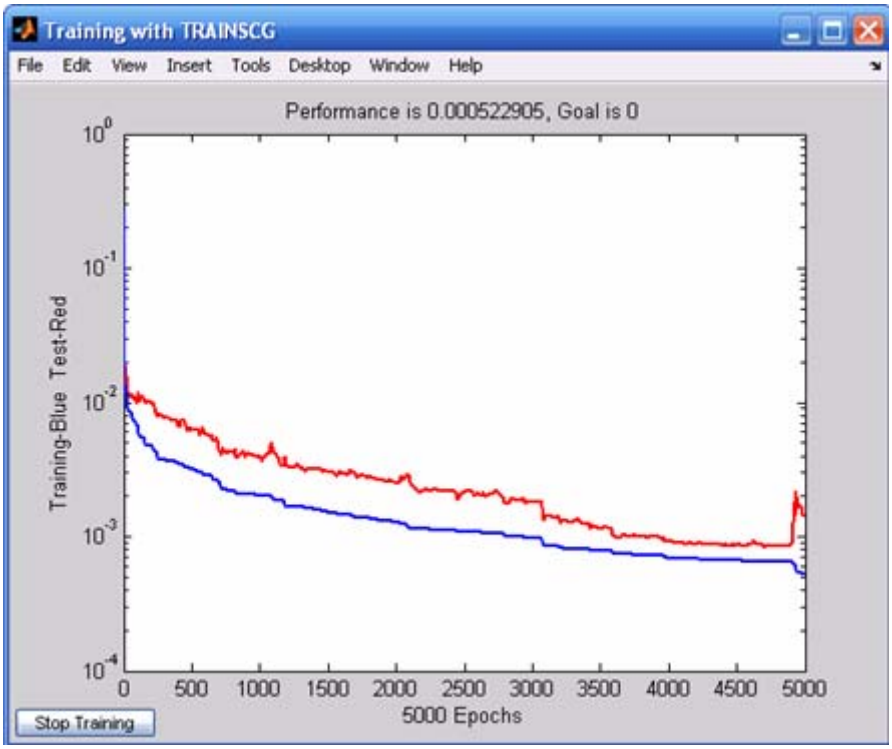

Figure 2.27.Training and testing progress curves for k_S data set with Trainscg algorithm

Sensitivity study for learning rate and momentum factor (k_S data set):

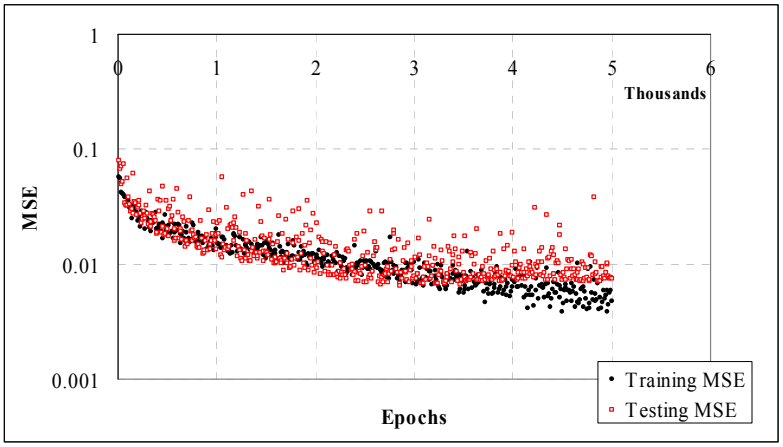

Figure 2.28.Training and testing progress curves for k_S with BP 3.5 (LR=0.1, MF=0.9)

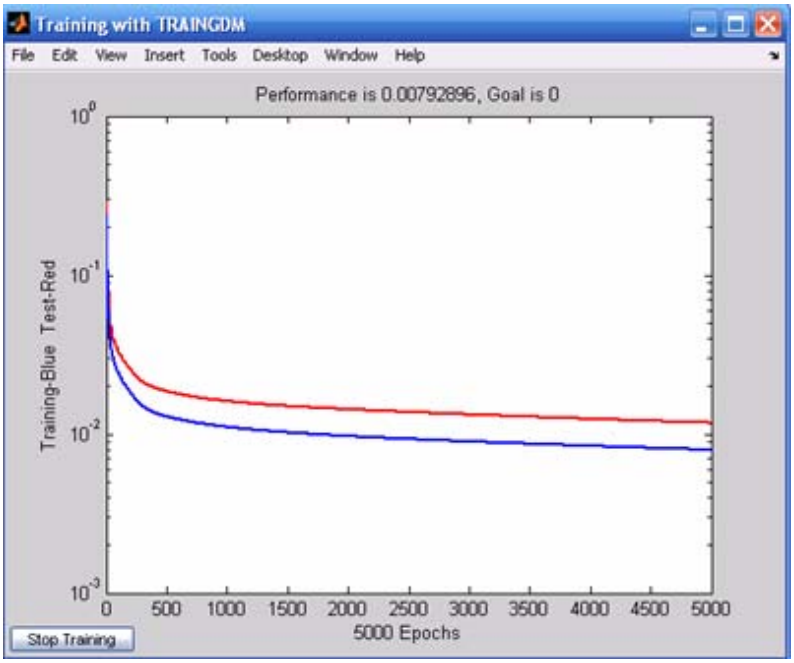

Figure 2.29. Training and testing progress curves for k_S with MATLAB (LR=0.1, MF=0.9)

Table 2.7. Comparison of the results for k_S (LR=0.1, MF=0.9)

Learning Rate = 0.1	**Momentum Factor = 0.9**	
	Backprop 3.5	**MATLAB - ANN**
AAE (%) =	21.1	30.1
R^2 =	0.89	0.81
TRN - MSE =	4.8×10^{-3}	7.9×10^{-3}
TST - MSE =	7.5×10^{-3}	11.7×10^{-3}

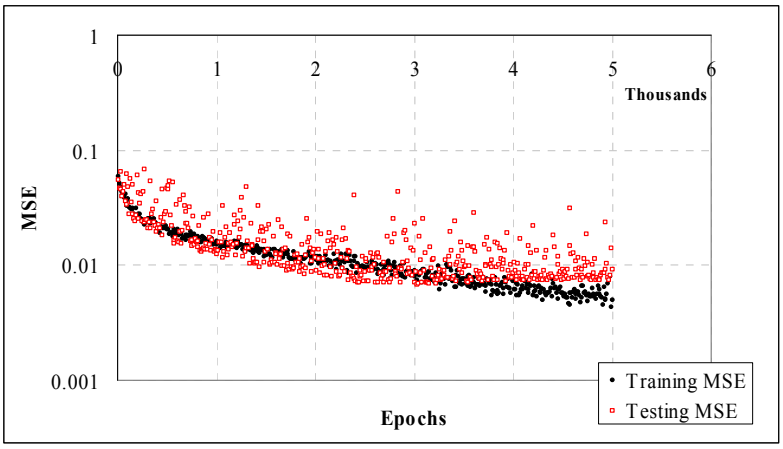

Figure 2.30.Training and testing progress curves for k_S with BP 3.5 (LR=0.3, MF=0.7)

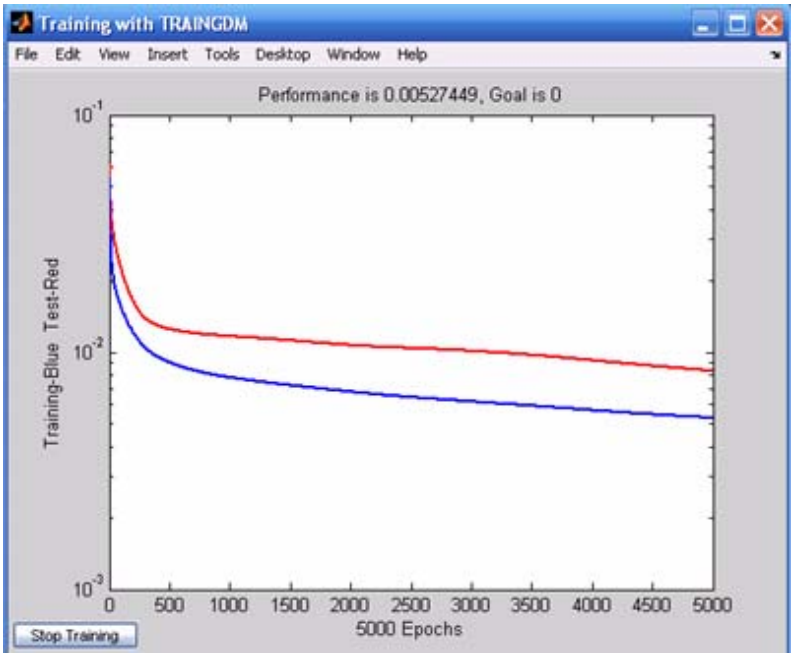

Figure 2.31. Training and testing progress curves for k_S with MATLAB (LR=0.3, MF=0.7)

Table 2.8. Comparison of the results for k_S (LR=0.3, MF=0.7)

Learning Rate = 0.3	**Momentum Factor = 0.7**	
	Backprop 3.5	**MATLAB - ANN**
AAE (%) =	22.9	21.5
R^2 =	0.87	0.87
TRN - MSE =	5.0×10^{-3}	5.3×10^{-3}
TST - MSE =	9.2×10^{-3}	8.3×10^{-3}

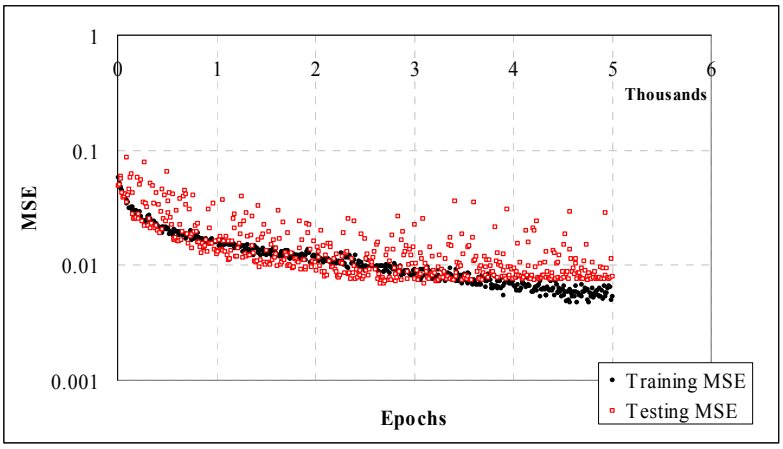

Figure 2.32.Training and testing progress curves for k_S with BP 3.5 (LR=0.5, MF=0.5)

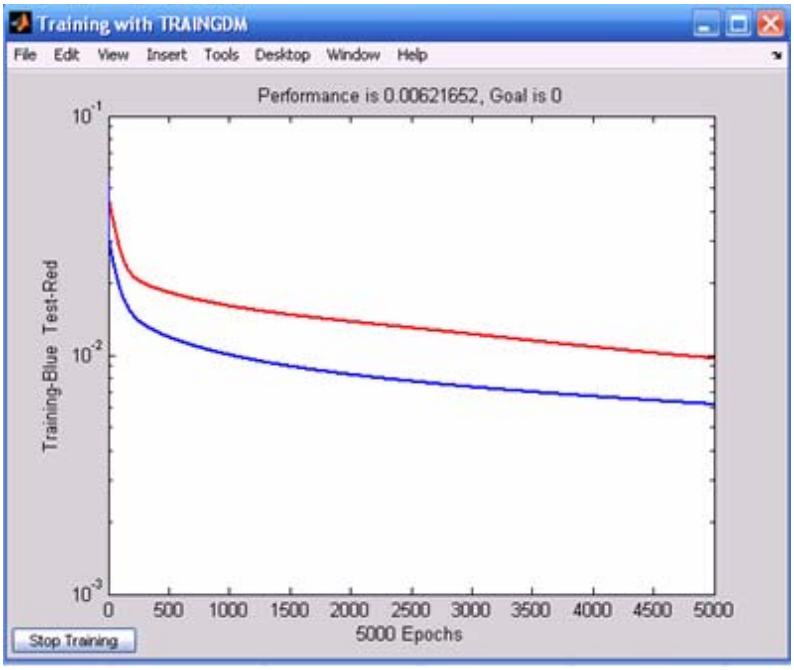

Figure 2.33. Training and testing progress curves for k_S with MATLAB (LR=0.5, MF=0.5)

Table 2.9. Comparison of the results for k_S (LR=0.5, MF=0.5)

Learning Rate = 0.5	**Momentum Factor = 0.5**	
	Backprop 3.5	**MATLAB - ANN**
AAE (%) =	20.7	21.4
R^2 =	0.88	0.84
TRN - MSE =	5.3×10^{-3}	6.2×10^{-3}
TST - MSE =	8.0×10^{-3}	8.7×10^{-3}

Sensitivity study for initial random numbers for weights and node biases (k_S data set):

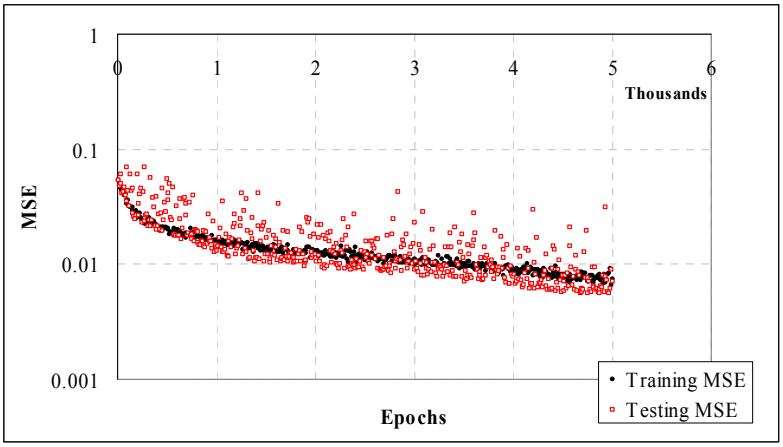

Figure 2.34.Training and testing progress curves for k_S with BP 3.5 (Random # 1)

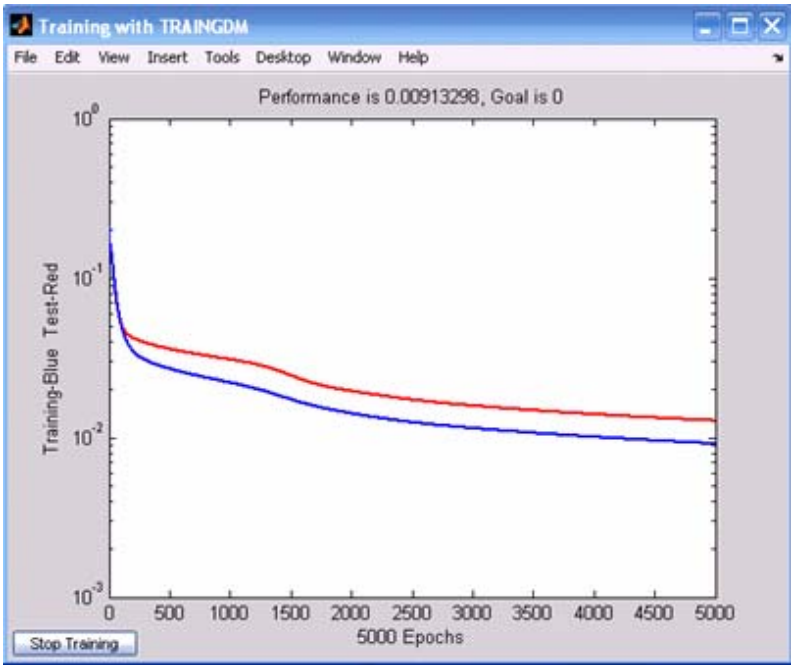

Figure 2.35. Training and testing progress curves for k_S with MATLAB (Random # 1)

Table 2.10. Comparison of the results for k_S (Random # 1)

Initial random connection numbers: # 1		
	Backprop 3.5	**MATLAB - ANN**
AAE (%) =	27.2	28.2
R^2 =	0.92	0.79
TRN - MSE =	7.3×10^{-3}	9.13×10^{-3}
TST - MSE =	7.1×10^{-3}	12.7×10^{-3}

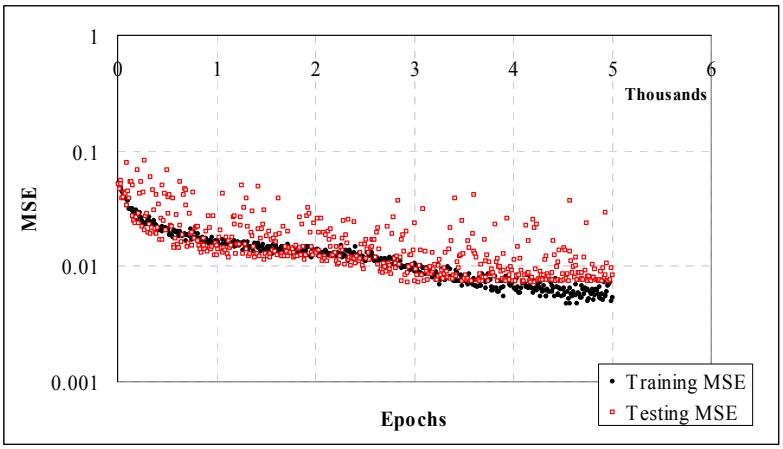

Figure 2.36.Training and testing progress curves for k_S with BP 3.5 (Random # 2)

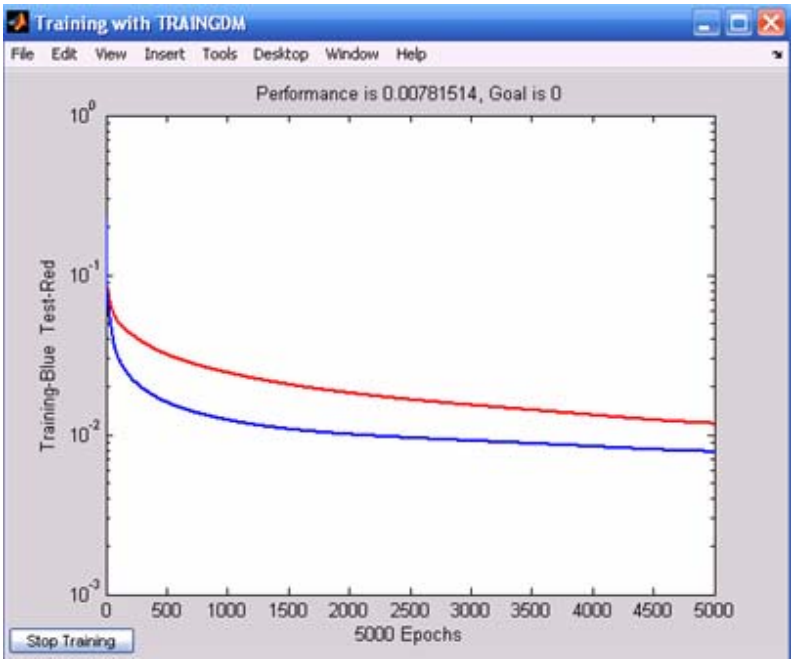

Figure 2.37. Training and testing progress curves for k_S with MATLAB (Random # 1)

Table 2.11. Comparison of the results for k_S (Random # 1)

Initial random connection numbers: # 2		
	Backprop 3.5	**MATLAB - ANN**
AAE (%) =	24.5	28.7
R^2 =	0.87	0.82
TRN - MSE =	5.3×10^{-3}	7.8×10^{-3}
TST - MSE =	8.3×10^{-3}	10.1×10^{-3}

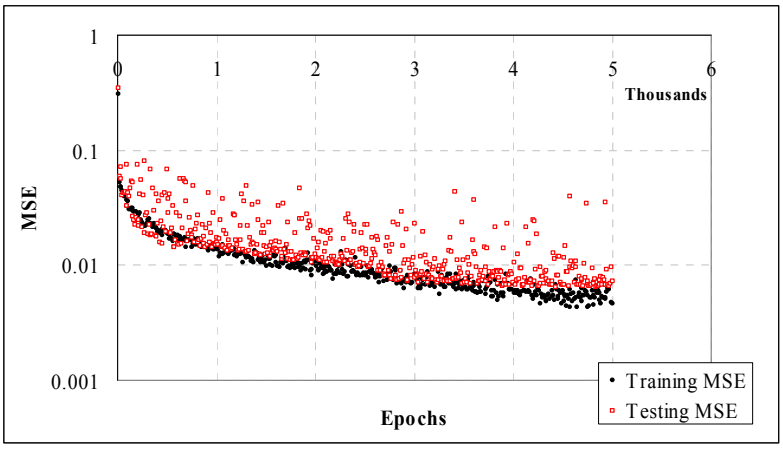

Figure 2.38.Training and testing progress curves for k_S with BP 3.5 (Random # 3)

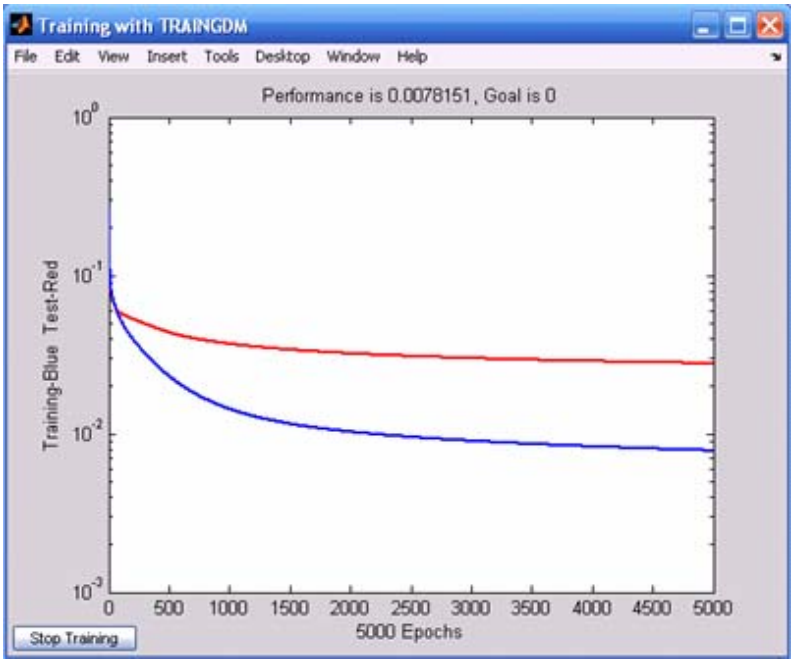

Figure 2.39. Training and testing progress curves for k_S with MATLAB (Random # 3)

Table 2.12. Comparison of the results for k_S (Random # 3)

Initial random connection numbers: # 3		
	Backprop 3.5	**MATLAB - ANN**
AAE (%) =	27.2	27.7
R^2 =	0.92	0.79
TRN - MSE =	7.3×10^{-3}	7.8×10^{-3}
TST - MSE =	7.1×10^{-3}	11.9×10^{-3}

REFERENCES

Backprop 3.5. Meier, R. Artificial neural network Fortran code.

Haykin, S. 1994. Neural Networks: A Comprehensive Foundation. Macmillan Publishing, New York.

Haykin, S. 1999. Neural networks: A comprehensive foundation. Prentice-Hall, Inc., NJ, USA.

Hecht-Nielsen, R. 1990. Neurocomputing, Addison-Wesley, Reading, MA.

Lawrence, J. and Fredricson, J. 1993. BrainMaker user's guide and Reference Manual 7th Edition, California Scientific Software, Nevada City, CA.

MATLAB 7.0 software program, The MathWorks.

Rumelhart, D.E., Hinton, G.E., and Williams, R.J. 1986. Learning integral representation by error propagation, in Rumelhart, D.E. et al., eds., Parallel Distributed Processing, MIT Press, Cambridge, MA, pp. 318-362.

CHAPTER 3. ANALYSIS OF FINITE-SIZED CONCRETE PAVEMENTS

SENSITIVITY STUDY FOR FINITE SLAB SIZES

In order to investigate the effect of slab sizes on the pavement surface deflection basins, a sensitivity study was conducted in ISLAB200 finite element program with three different size six-slab assembly configuration, 12ft x 12ft, 16ft x 16ft, and 20ft x 20ft. One hundred different pavement structures were created by varying E_{PCC} (3 to 12 million psi), h_{PCC} (6 to 15 in.), and k_S (100 to 700 psi/in.). Deflection basins were extracted for the mid-slab locations for 100 different pavement configurations and D_0 and D_{60} deflections were compared to each other for three slab sizes. D_0 and D_{60} deflections show very good agreement for three different slab sizes. The differences between D_{60} deflections for different slab sizes were slightly higher than the D_0 deflections since D_{60} deflections are closer to the slab joints than D_0 deflections.

Crovetti (1994) proposed to use some adjustment factors that can be applied to pavement surface deflections and radius of relative stiffness values based on the length and width of the concrete slabs. The method that Crovetti proposed can be summarized as below:

- Estimate radius of relative stiffness of the pavement-foundation system, RRS_{est}
- Calculate L / RRS_{est} $L = (Length.Width)^{0.5}$
- Calculate adjustment factors for deflections (AF_D) and radius of relative stiffness (AF_{RRS})
- $D_{adjusted} = D_{measured} \times AF_D$
- $RRS_{adjusted} = RRS_{estimated} \times AF_{RRS}$
- Backcalculate E_{PCC} and k_S by using $D_{adjusted}$ and $RRS_{adjusted}$

$$AF_{RRS} = 1 - 0.89434\, exp\left[-0.61662 \left(\frac{L}{RRS_{est}} \right)^{1.04831} \right] \tag{3.1}$$

$$AF_D = 1 - 15085\,exp\left[-0.71878\left(\frac{L}{RRS_{est}}\right)^{0.80151}\right] \quad \text{(for mid-slab deflections)} \qquad (3.2)$$

$$AF_{D(edge)} = 1 - 1.35481\,exp\left[-0.32629\left(\frac{L}{RRS_{adj}}\right)^{1.39066}\right] \quad \text{(for edge deflections)} \qquad (3.3)$$

$$AF_{D(corner)} = 1 - 0.94382\,exp\left[-0.16667\left(\frac{L}{RRS_{adj}}\right)^{2.37506}\right] \quad \text{(for corner deflections)} \qquad (3.4)$$

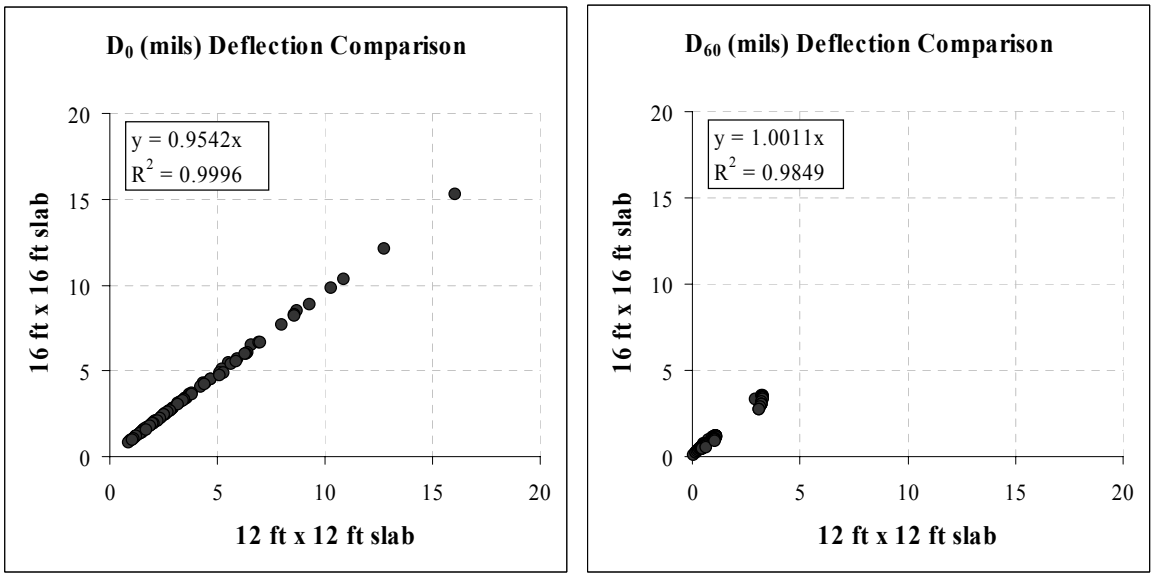

Figure 3.1. Comparisons of the D_0 and D_{60} deflections for 16ft x 16ft vs. 12ft x 12ft

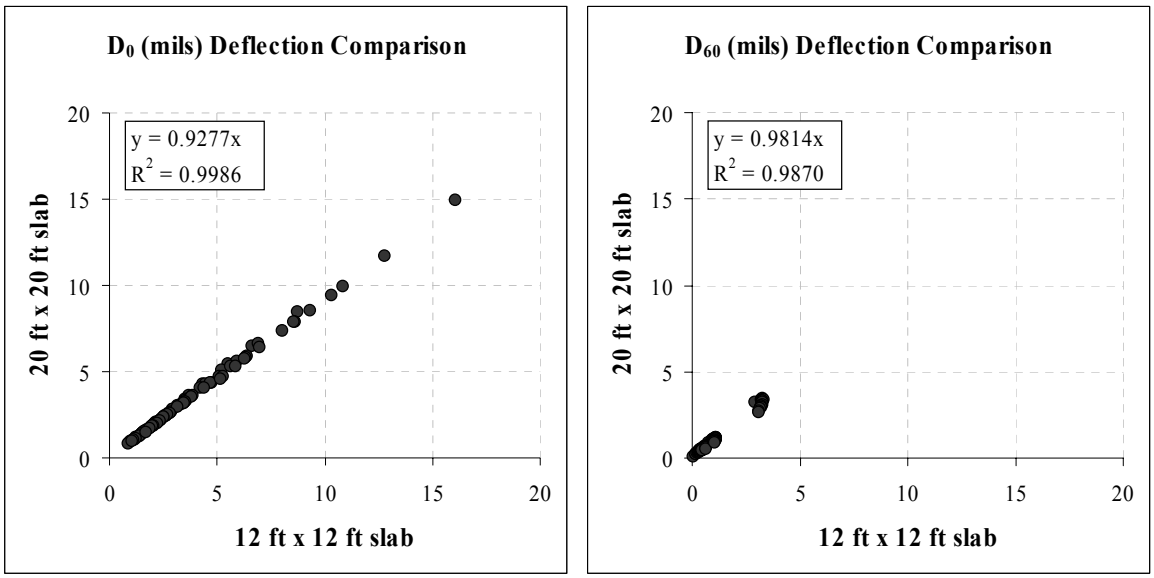

Figure 3.2. Comparisons of the D_0 and D_{60} deflections for 20ft x 20ft vs. 12ft x 12ft

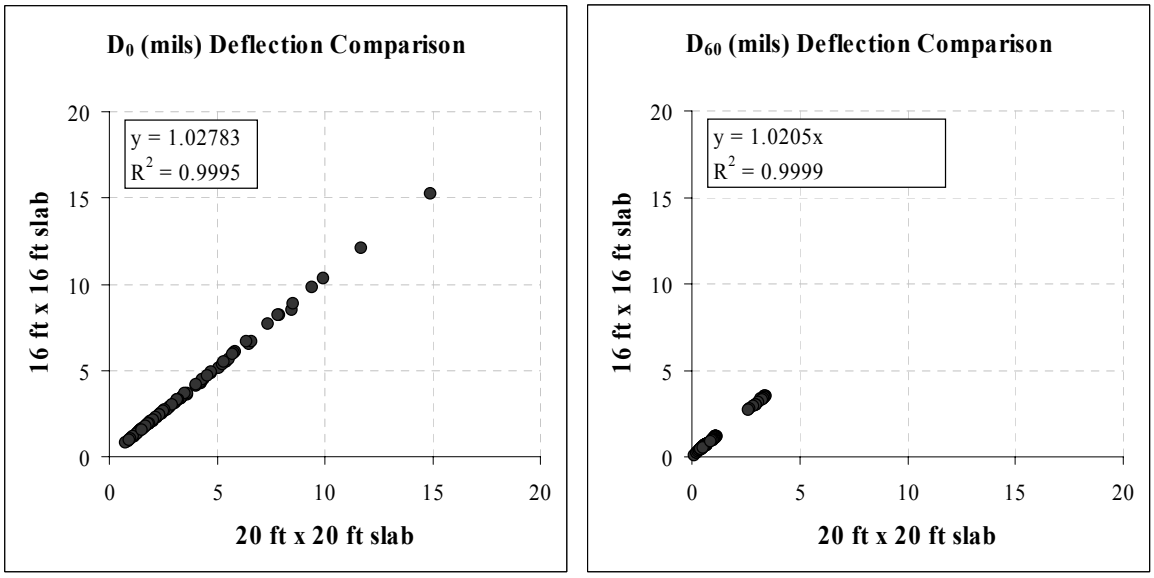

Figure 3.3. Comparisons of the D_0 and D_{60} deflections for 16ft x 16ft vs. 20ft x 20ft

DIMENSIONAL ANALYSIS

There are two significant concrete pavement parameters that govern the shape and maximum amount of the deflections and behavior of the concrete slabs, coefficient of subgrade reaction, k_S, and radius of relative stiffness, RRS. The variation of maximum deflections in mid-slab with varying subgrade stiffness and radius of relative stiffness was shown in figure below. This figure shows that there is only one unique deflection basin for a specific combination of k_S and RRS.

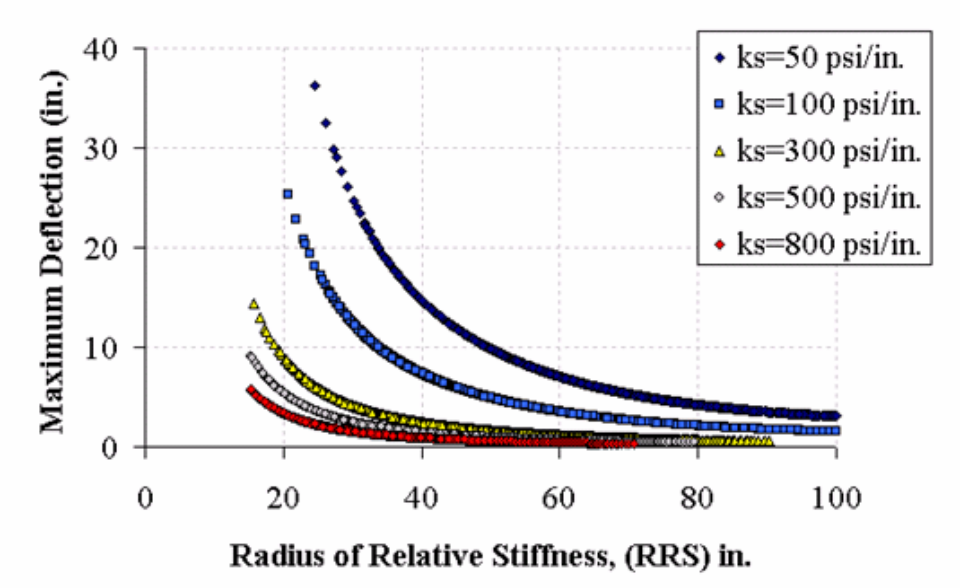

Figure 3.4. The variation of maximum deflections with coeeficient of subgrade reaction and radius of relative stiffness.

Based on reviewing the previous studies on the dimensional analysis to evaluate pavement systems (Ioannides and Salsilli-Murua 1989; Ioannides et al 1989; Ioannides 1990), the following dimensionless parameters were identified as applicable. They were essentially determined to be controlling parameters for a constant Poisson's ratio of 0.15 and unit weight of 0.087 lbs/in^3. A more general and rigorous examination of the nondimensional response would involve both unit weight and Poisson's ratio, but unfortunately it is not feasible at this time (Ioannides and Salsilli-Murua 1989).

$$D_0^* = \frac{D_0 . k_S . RRS^2}{P} = \frac{[L].\left[\frac{F.L^{-2}}{L}\right].[L^2]}{[F]} \tag{3.5}$$

$$\frac{W}{RRS} = \frac{[L]}{[L]} \tag{3.6}$$

$$\frac{L}{RRS} = \frac{[L]}{[L]} \tag{3.7}$$

$$\frac{h}{RRS} = \frac{[L]}{[L]} \tag{3.8}$$

$$\frac{a}{RRS} = \frac{[L]}{[L]} \tag{3.9}$$

$$\frac{AGG}{k_S . RRS} = \frac{[FL^{-2}]}{\left[\frac{FL^{-2}}{L}\right].[L]} \tag{3.10}$$

$$\frac{E_{PCC} . h^2}{P} = \frac{[FL^{-2}].[L^2]}{[F]} \tag{3.11}$$

$$\frac{k_S . h^3}{P} = \frac{\left[\frac{F.L^{-2}}{L}\right].[L^3]}{[F]} \tag{3.12}$$

$$\frac{\sigma_{MAX} . h^2}{P} = \frac{[F.L^{-2}].[L^2]}{[F]} \tag{3.13}$$

$$TELTD.\alpha = [T].[L.L^{-1}.T^{-1}] \tag{3.14}$$

where;

D = slab deflection [L],

W = slab width [L],

L = slab length [L],

h = slab thickness [L],

a = radius of the applied load [L],

P = applied load [L],

AGG = aggregate interlock factor [FL^{-2}],

k_S = coefficient of subgrade reaction [FL^{-3}],

RRS = radius of relative stiffness [L],

E_{PCC} = elastic modulus of the PCC layer [FL^{-2}],

σ_{MAX} = critical tensile stress at the bottom of the PCC layer [FL^{-2}],

TELTD = total effective linear temperature difference [T],

α = coefficient of thermal expansion [$L.L^{-1}.T^{-1}$].

Note that primary dimension for force is represented by [F], length is represented by [L], and temperature is represented by [T].

The ANN-based model input parameters can be rearranged as shown below. In this research, this method was not applied because the coefficient of subgrade reaction of the pavement foundation and radius of relative stiffness of pavement-foundation system should be known earlier in order to convert the dimensional parameters to nondimensional parameters, but these parameters are actually the outputs of the developed models in this research. Therefore, dimensional analysis was not applied in this research.

$$D_0^* - D_{36}^*, \frac{h}{RRS}, \frac{W}{RRS}, \frac{L}{RRS} = \frac{E_{PCC}.h^2}{P} \tag{3.15}$$

$$D_0^* - D_{60}^*, \frac{W}{RRS}, \frac{L}{RRS} = \frac{k_S.h^3}{P} \tag{3.16}$$

$$D_0^* - D_{36}^*, \frac{h}{RRS}, \frac{W}{RRS}, \frac{L}{RRS} = \frac{\sigma_{MAX}.h^2}{P} \tag{3.17}$$

$$D_0^* - D_{60}^*, \frac{h}{RRS}, \frac{W}{RRS}, \frac{L}{RRS} = TELTD.\alpha \tag{3.18}$$

REFERENCES

Crovetti, J.A. 1994. Design and evaluation of jointed concrete pavement systems incorporating free draining base layers, Ph.D. Dissertation, Urbana, Illionois.

Ioannides, A. M. 1990. Dimensional Analysis in NDT Rigid Pavement Evaluation. Journal of Transportation Engineering, Vol.116, No. 1, pp.23-36.

Ioannides, A.M., Barenberg, E.J., and Lary, J.A. 1989. Interpretation of falling weight deflectometer results using principals of dimensional analysis. Proceedings, 4th International Conference on Concrete Pavement Design and Rehabilitation, Purdue University, pp.231-247.

Ioannides, A.M. and Salsilli-Murua, R.A. 1989. Temperature curling in rigid pavements:an application of dimensional analysis. Transportation Research Record, No.1227, Transportation Research Board, Natioanal Research Council, Washington, D.C., pp.1-11.

CHAPTER 4. USE OF ARTIFICIAL NEURAL NETWORKS IN TRANSPORTATION INFRASTRUCTURE SYSTEMS: 1987-2007

A paper to be submitted to *The International Journal of Pavement Engineering*

Mustafa Birkan Bayrak and Halil Ceylan

ABSTRACT

The use of artificial neural networks (ANNs) has increased tremendously in several areas of engineering over the last two decades. This paper reviews a significant number of research publications which specifically deals with applications of ANNs in pavement engineering, transportation infrastructure systems between 1987 and 2007. These studies have been briefly summarized in this paper in six different categorizations: (1) predictions of pavement performance and pavement condition, (2) pavement management and maintenance strategies, (3) pavement distress forecasting, (4) structural evaluation of pavement systems, (5) image analysis and classification, and (6) pavement material modeling. This paper provides an overview of the state of the practice in using ANNs for solving diverse pavement engineering problems often in real time.

Key Words: Artificial Neural Network, Pavement Engineering, Pavement Performance and Condition, Pavement Management and Maintenance, Pavement Analysis and Design, Image Analysis and Classification, Pavement Material Modeling.

INTRODUCTION

Over the past two decades, there has been an increased interest in the use of artificial neural networks (ANNs) in civil engineering fields such as structural engineering, environmental and water resources engineering, traffic engineering, geotechnical engineering as well as pavement engineering. ANNs represent a class of robust, non-linear models applicable for solving a wide variety of problems. ANNs have been found to be very useful tools for

solving pavement engineering problems, which deal with highly nonlinear functional approximations.

Pavement engineering covers a wide area which includes both highway and airport pavements and involves disciplines including pavement analysis and design, pavement evaluation, pavement performance prediction, and pavement maintenance, rehabilitation, and management issues. The ANN-related studies reviewed in this paper focus on three pavement types of flexible, rigid, and composite pavements.

Neural networks are information processing computational tools in which highly interconnected processing neurons work in harmony to analyze and solve complex problems in a nontraditional manner. This power of the ANNs, emulating the biological nervous system, lies in the tremendous number of interconnections between the neurons or processing elements as they provide notable advantages in learning and generalizing from examples, producing meaningful and cost effective solutions to various problems even when input data contain errors or are incomplete, adapting solutions over time to compensate for changing circumstances and processing information quite rapidly and often in real time.

The adoption and use of ANN modeling techniques in the recently released Mechanistic-Empirical Pavement Design Guide (NCHRP project 1-37A: Development of the 2002 Guide for the Design of New and Rehabilitated Pavement Structures: Phase II) has especially placed the emphasis on the successful use of neural nets in geomechanical and pavement systems. Yet, many practitioners still have a lack of understanding and even skepticism towards the use of ANNs and other computational intelligence tools. These obstacles can be overcome by providing the engineering practitioners with a better understanding through necessary background information and documentation of successful ANN applications in pavement and transportation infrastructure systems engineering.

This paper presents an overview of artificial neural network techniques and applications used in pavement engineering between 1987 and 2007 classified in six major categories: (1)

predictions of pavement performance and pavement condition, (2) pavement management and maintenance strategies, (3) pavement distress forecasting, (4) structural evaluation of pavement systems, (5) image analysis and classification, and (6) pavement material modeling. Although similar articles focusing on the use of ANNs in civil and transportation engineering applications have been published previously (Dougherity 1995, Transportation Research Circular 1999, Adeli 2001, Sundin and Braban-Ledoux 2001), these publications did not specifically concentrate on pavement, transportation infrastructure engineering. The aim of this paper is to fill the gap in this area and present an up to date comprehensive review on the use of artificial neural networks in pavement and transportation infrastructure systems engineering area.

OVERVIEW OF ARTIFICIAL NEURAL NETWORKS

Imitating the biological nervous system, artificial neural networks are information processing computational tools capable of solving nonlinear relations in a specific problem. Similar to the human brain, ANNs have the flexibility to learn from examples by means of massively interconnected processing units, namely neurons. Neural network architectures, arranged in layers, involve synaptic connections amid neurons which receive signals and transmit them to the other neurons via activation functions. Each connection has its own connection weight and learning is the process of adjusting the connection weights between neurons to minimize the error between the predicted and given values. In the learning process, node biases are also adjusted in addition to the connection weights. Since interconnected neurons have the flexibility to adjust the weights, neural networks have powerful capacities in analyzing complex problems. ANNs, inspired by the neuronal architecture and operation of the human brain, contribute to our understanding of several complex, non-linear pavement engineering problems with various pavement materials and pavement foundation variables. Figure 4.1 displays a typical structure of ANNs that consists of a number of neurons that are usually arranged in layers: an input layer, hidden layers, and an output layer.

There are several different types of artificial neural networks such as back-propagation neural networks (BPNN), radial basis function networks (RBFNN), probabilistic neural

networks (PNN), and generalized regression neural networks (GRNN). Computing abilities of neural networks have been proven in the fields of prediction and estimation, pattern recognition, and optimization (Adeli and Hung 1995; Golden 1996; Mehrotra et al. 1997; Adeli and Park 1998; Haykin 1999). The best-known example of a neural network training algorithm is *back-propagation* (Rumelhart et al. 1986; Haykin 1994; Fausett 1994; Patterson 1996) which is based on a gradient-descent optimization technique. The back-propagation neural networks have been described in many sources (Hegazy et al. 1994; Adeli and Hung 1995; Mehrotra et al. 1997; Topping and Bahreininejad 1997; Haykin 1999). A more comprehensive description of ANNs is beyond the scope of this paper.

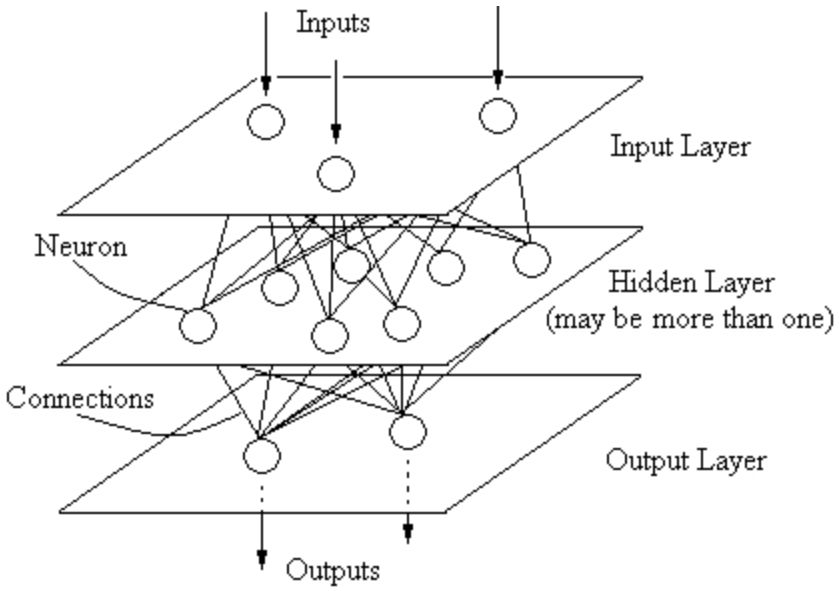

Figure 4.1. A general schematic view of the artificial neural networks

Advantages and Limitations of Artificial Neural Networks

ANNs provide an analytical alternative to conventional techniques which are often limited by strict assumptions of normality, linearity, variable independence, etc. Because an ANN can capture many kinds of relationships, it allows the user to quickly and relatively easily model a phenomenon which otherwise may have been very difficult. Neural networks offer a number of advantages, including requiring less formal statistical training, ability to implicitly detect complex nonlinear relationships between dependent and independent variables, ability

to detect all possible interactions between predictor variables, and the availability of multiple training algorithms.

Despite their good performance in many situations, ANNs suffer from a number of shortcomings. For example, artificial neural networks cannot explain results. In problems where explaining rules may be critical, neural networks are not the tool of choice. They are the tool of choice when acting on the results is more important than understanding them. Even though neural networks cannot produce explicit rules, sensitivity analysis does enable them to explain which inputs are more important than others. This analysis can be performed inside the network, by using the errors generated from back propagation, or it can be performed externally by poking the network with specific inputs. Secondly, ANNs usually converge on some solution for any given training set. Unfortunately, there is no guarantee that this solution provides the best model (global minimum) of the data. Therefore, the test set must be utilized to determine when a model provides good enough performance to be used on unknown data. In conclusion, even there are some limitations of ANNs, the advantages of neural networks appear to outweigh these limitations.

CATEGORY 1: PREDICTION OF PAVEMENT PERFORMANCE AND PAVEMENT CONDITION

This section summarizes a large number of research publications related to the use of ANNs in pavement performance and pavement condition predictions. Performance and condition of the pavements are generally presented by an index such as the international roughness index (IRI), pavement condition rating (PCR) and visual condition index (VCI). Artificial neural networks have been found to be very powerful and versatile computational tools for determining and predicting the condition and performance of the existing pavement systems.

Attoh-Okine (1994) used back-propagation type ANNs to develop a pavement roughness progression model. To generate synthetic pavement roughness data, an empirical simulation model was utilized in this study. Then, the neural network model was trained with the simulated training data which included several factors affecting pavement roughness such as

pavement structural deformation, incremental traffic loadings, extent of cracking and thickness of surface layer, incremental variation of rut depth, surface defects such as patching and potholes, and environmental and other non-traffic-related variables such as age of the pavement structure. In addition, the results obtained from the neural network trainings were compared with the actual results. According to the findings, when the pavement condition database considered was large enough, the ANN prediction results were found to be more satisfactory. However, since the simulated data set was used in the study, it was concluded that the model might not perform well with other data sets as for the simulated data set.

An ANN system for the condition rating of rigid pavements was developed and implemented by Eldin and Senouci (1995a). Oregon State DOT condition rating scheme based on the cracking and rutting indices was used for the ANN development. A backpropagation neural network with one hidden layer was used in this study. Fifteen inputs corresponding to 15 distresses used in the study were rutting, lane joint, shoulder joint, transverse cracking (low, medium, and high severity), longitudinal cracking (low, medium, and high severity), patching (low, medium, and high severity), and punchout (low, medium, and high severity). The output of the model was condition index ranging between 0.1 and 0.5. The proposed ANN model showed good generalization capability and unlike the Oregon State DOT condition rating model, the ANN model also showed a good fault-tolerance capability. When noise was introduced to the model, the network was still able to accurately identify the condition ratings. The developed ANN system was proposed to be incorporated as a module into the pavement management system (PMS) of the Oregon DOT.

Eldin and Senouci (1995b) also developed another neural network system for the determination of condition rating for rigid pavements. In this study, the backpropagation algorithm was applied to model the condition rating scheme adopted by the Oregon State DOT. The pavement condition rating was computed based on the ODOT`s cracking and rutting indices. The neural network model had 22 input nodes which were rutting, transverse joint, lane joint, shoulder joint, transverse crack (low, medium, and high severity), severity of

the longitudinal cracks (low, medium, and high), severity of the corner cracks (low, medium, and high), severity of the corner breaking (low, medium, and high), patch severity (low, medium, and high), and punchout severity (low, medium, and high). The output layer consisted of the pavement condition index. A hypothesis test was also conducted to verify the fault-tolerance and generalization properties of the developed system. The authors concluded that the ANN model showed a good fault-tolerance and generalization capability.

In another study, Eldin and Senouci (1995c) presented a feed-forward ANN used for the condition rating of flexible pavements. The purpose of this study was to prepare an ANN model that could give outputs similar to the ODOT`s model. The pavement condition rating model was based on cracking and rutting indices, alligator cracks, transverse cracks, block cracks, patching, bleeding, and rutting distresses. The performance of the ANN model was investigated by introducing different levels of noise and the performance of the ANN model were compared with the expert opinions and the results of ODOT`s model. Results reported by ODOT indicated that the neural network outperformed the ODOT`s model in estimating the condition ratings.

An ANN model was presented as an alternative to regression models for predicting skid resistance on flexible pavements containing no overlays for assessing future rehabilitation needs by Owusu-Ababio (1995). Connecticut DOT pavement performance study results were used in the study. Four input variables that are pavement age, location, accumulated average annual daily traffic, and posted speed limit and one output variable that is skid number were used in the analyses. The results of the ANN model and regression models were compared. The R^2 values of ANN model were consistently higher than regression models as shown in Table 4.1.

Wang (1995) investigated the feasibility of using a specially designed and programmable neural net chip, Ni1000, in a PC to conduct pavement surface processing. A total of 6 crack types on AC surface were proposed to be identified: 1) fatigue cracking, 2) block cracking, 3) edge cracking, 4) wheel/non-wheel path longitudinal cracking, 5) reflective cracking, and

6) transverse cracking. Based on the feasibility study, Wang concluded that the neural net chip was capable of providing real-time processing for pavement surface distress survey.

Table 4.1. Comparison of NN and MLR (Multiple Linear Regression) models (Owusu-Ababio 1995)

Data Set Type	Model Type	R^2 value
Training Data Set	NN	0.87
	MLR	0.63
Testing Data Set	NN	0.89
	MLR	0.71

Artificial neural networks were used to predict the area of indexed cracks in flexible pavements based on modified structural number, incremental traffic loadings, and environmental mechanisms (Attoh-Okine 1996). Annual equivalent standard axle load per year, age of pavement since the last resurfacing activity, ravel area, potholing, rut depth, patching, environmental factors, and thickness were the input variables to predict the cracking index which was the output of the proposed model. According to the results of the analyses, the author concluded that the neural network approach in flexible pavements was accurate enough in predicting cracking index giving information about the performance and condition of the pavement. In addition, it was emphasized that the adaptive neural network approach can be used as a sensitivity analysis tool to identify the most significant variables needed to predict cracking index.

Banan and Hjelmstad (1996) demonstrated a study to re-examine the American Association of State Highway Officials (AASHO) road test data using the Monte Carlo hierarchical adaptive random partitioning (MC-HARP) neural network model developed by the authors. The input variables in the neural network model were the surface, base, and subbase thicknesses (D_1, D_2, and D_3), the axle load (L), and the logarithm of accumulated single-axle load applications (log W). The output variable was the present serviceability index (PSI). Two MC-HARP neural networks with linear and AASHO subdomain approximations were built. The network exhibited the trends of decrease of PSI with increasing W and increase of PSI with increasing thicknesses or decreasing axle load. Based on the analysis, the authors

concluded that a local approximation like an MC-HARP neural network can model the pavement performance data for the entire input domain better than a global approximation like the AASHO formula.

To model the performance of non-overlaid thick asphalt pavements having a thickness of more than 152.4 mm (6 in.), Owusu-Ababio (1998) presented an ANN study. The database used for this study was developed through a survey of the Wisconsin DOT district offices and selected city governments. The pavement condition was represented by the pavement distress index (PDI) which ranged from 0 to 100. In this range, 0 represented the best condition while 100 represented the worst condition. The input parameters utilized in this study were the pavement surface thickness, pavement age, traffic level (ESAL, Equivalent 18-kip single axle load, per day), base thickness, and roadbed condition. To compare the performance of the ANN model with traditional statistical tools, multiple linear regression (MLR) models were also developed. According to this comparison, the ANN model outperformed the MLR model in terms of the standard error and the coefficient of multiple determination (R^2) value.

In another study, Owusu-Ababio (1998) investigated the effect of the neural network architecture on flexible pavement cracking prediction. Backpropagation neural network (BPNN) algorithms consisting of one, two, and three hidden layers were used in the analyses in which the Connecticut DOT database was used to investigate and compare the pavement cracking prediction performance. Pavement surface thickness, pavement surface age, and equivalent single axle load (ESAL) were used as input parameters, and total cracking (ft/100ft) was used as the pavement condition indicator which was the only output variable ofthe proposed model. The author concluded that one hidden layer BPNN may be sufficient in achieving satisfactory results for successfully predicting the cracking in flexible pavements.

Van der Gryp et al. (1998) introduced a one-hidden layer feed-forward neural network model to estimate the overall pavement condition based on the visual condition index (VCI) that

ranges from 0 to 10, where 0 indicates the worst surface condition (severe cracking, corner breaking, rutting, pumping, etc.), and 10 indicates excellent pavement surface condition where no distresses exist. Although VCI is a well-defined analytical criterion, it contains some weighting factors whose values are determined according to the subjective appreciation of an expert panel based on the importance of one distress type compared with the other. The analysis was based on the severity and extent of various types of distresses including failure, surface cracks, longitudinal cracks, transverse cracks, patching, potholes, bleeding, and pumping. The reported simulations made it difficult to conclude on the effectiveness of the ANN.

To estimate the pavement condition rating (PCR) index, George et al. (1998) developed an ANN model. A PCR index value of 0 indicates worst condition and 100 represents the best condition. The entire data set used in this study was extracted from the Mississippi DOT database which included three different families of pavements: flexible, jointed plain concrete and composite pavements. The ANN results were compared with the results of the classic regression and Bayesian regression models. Based on the results of the analysis, the ANN outperformed the other two models in terms of higher correlation coefficient.

In another study, Attoh-Okine (1999) used real pavement condition and traffic data to investigate the effect of learning rate and momentum term (in backpropagation algorithm neural network) on flexible pavement performance prediction. In this study, rutting, faulting, transverse cracking, block cracking, and equivalent axle loads were used as input variables to predict the international roughness index (IRI). Kansas DOT pavement condition data (1993) was used to investigate the effect of learning rate and momentum term on backpropagation algorithm. Based on the analysis results, the author suggested that a learning rate (η) of around 0.2 to 0.5 and a momentum (α) factor of around 0.4 to 0.5 seem to provide the appropriate combination for the pavement performance prediction. Figure 4.2 depicts the predicted versus the given IRI values for the model with a learning rate of 0.3 and a momentum factor of 0.5.

Shekharan (2000) demonstrated the use of ANNs for prediction of pavement conditions for five different types of pavements: original flexible, overlaid flexible, composite, jointed plain, and continuously reinforced concrete pavements (CRCP). Pavement condition rating (PCR), a composite index derived by combining the distresses and roughness measurements and formulated for Mississippi DOT, was utilized in this study to represent the pavement condition. Pavement structure, pavement history represented by pavement age in years, traffic volume by cumulative equivalent 18-kip single axle loads (ESALs) were the input parameters used in the neural network approach in which a genetic adaptive neural network training (GANNT) algorithm was employed. Based on the findings, the neural network results were compared with the regression model results and it was concluded that ANNs gave better results than the regression models owing to the mapping ability of ANNs. It was also indicated in the study that artificial neural networks could take into account any functional form of equation.

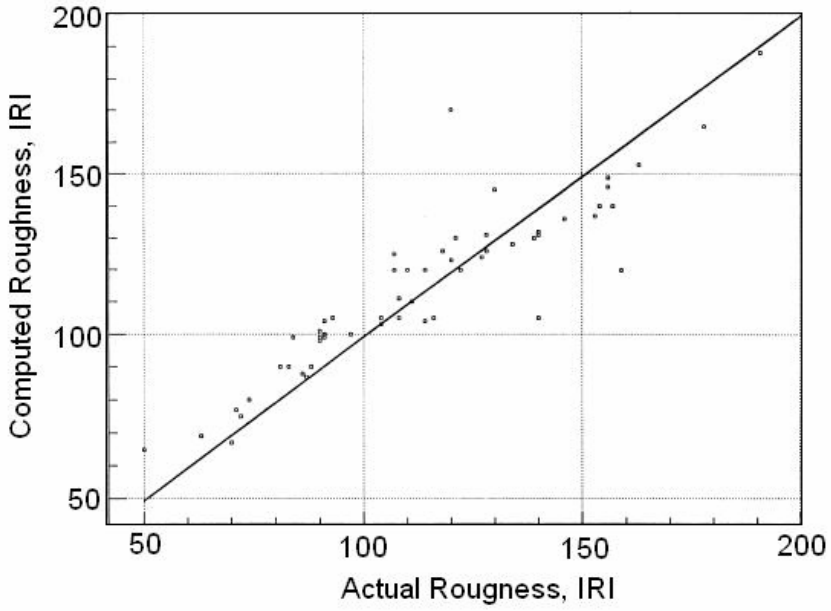

Figure 4.2. Plot of the computed vs. actual roughness (Attoh-Okine 1999)

The use of the ANN self-organizing maps for the grouping of pavement condition variables in developing pavement performance models to evaluate pavement conditions on the basis of

pavement distresses was introduced by Attoh-Okine (2001). The variables (distresses) considered in this study were average annual daily traffic (AADT), the load converted into standard equivalent single-axle load (ESAL) taken annually, age of pavement since resurfacing, alligator cracking, wide cracking (cracking 3 mm or more wide in the pavement), index cracking, raveling, potholing, rut depth, patching, thickness, and environmental factors including information regarding to wet, freeze, thaw, and dry conditions of the local subsoil. Two types of grouping were conducted in the study. The first grouping was "the variable grouping" used to group the distresses based on the severity of roughness later being used to develop the performance model. The second grouping was "the data grouping" used in the determination of the coefficients of the roughness equation. Based on the results of the analyses, self-organized maps were proven to be an effective technique to group pavement condition variables. It was also stated in this study that these grouped variables and data may be later utilized to develop the pavement performance equation for prediction and evaluation purposes.

Lin et al. (2003) presented the results of the analyses of the relationship between the IRI and pavement distresses. The authors used a 14-6-6-1 backpropagation type ANN architecture. The input variables used in the network were road level, rutting on the left wheel path, rutting on the right wheel path, alligator cracking, cracking, digging/patching, mild potholes, severe potholes, patching, bleeding, corrugation, stripping, mild man-holes, and severe man-holes. The output layer consisted of only one variable, international roughness index (IRI). Hundred records of training data and 25 records of testing data were used in the ANN model. The correlation coefficients for the training data set and the testing data set were 0.84 and 0.94, respectively. The authors concluded that it was successful network architecture in predicting the IRI from the above mentioned 14 variables. Severe potholes, digging/patching, and rutting had been found to be the most important input parameters in sensitivity analyses.

In order to estimate the load related shallow crack depths and surface-initiated fatigue cracks in asphalt pavements based on crack-surface geometry and pavement and traffic characteristics, Mei et al. (2004) developed an ANN model. The variables used in model

development were annual average daily traffic, truck percentage, age, number of lanes, crack depth (d), crack width (w), slope one (S_1), slope two (S_2), and actual crack depth (D, output).Based on the analysis results given in Figure 4.3, the authors concluded that the complex relationship between depths, surface geometrical properties of cracks and other pavement and traffic parameters was modeled successfully by ANN model.

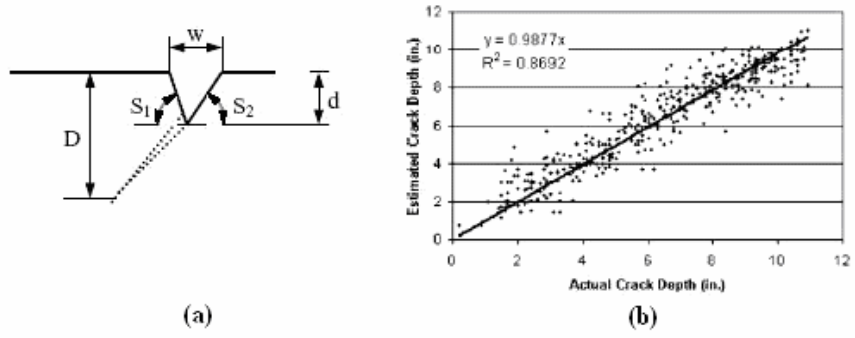

Figure 4.3. (a) Crack opening geometry (b) Goodness of fit for the testing data set (Mei et al. 2004)

In another study, Choi et al. (2004) trained a backpropagation neural network algorithm to predict the performance of flexible pavement systems using the Long Term Pavement Performance (LTPP) database. The objective of this study was to develop a pavement performance model for prediction of roughness and to apply a sensitivity analysis to identify the relative significance of the material and construction variables on pavement performance. The total asphalt layer thickness, F_{200} (the percent fines passing the no. 200 sieve), the asphalt content, the structural number (SN) and CESAL (the cumulative equivalent single axle loading) variables were utilized as input variables and IRI was used as output variable in the proposed model. The authors concluded that the proposed neural network model could be effectively used to develop the pavement prediction model required for performance-related specification (PRS) implementation by quantifying the complex and nonlinear relationship between the selected material and construction variables.

Discussion: Prediction of Pavement Performance and Pavement Condition

Summarized research publications show that artificial neural networks can be successfully utilized as alternative methods to the traditional methods to predict the pavement

performance and current pavement condition. Most of the studies in this section used backpropagation algorithms with one or two hidden layers in the ANN architecture. The validation of the proposed models was generally made with the statistical methods, expert opinions, and actual results. One shortcoming of some proposed models is that there are too many input parameters in some models which make them inapplicable. The usefulness of the models can be increased significantly as the number of the input parameters used in the proposed models is kept as few as possible.

CATEGORY 2:PAVEMENT MANAGEMENT AND MAINTENANCE STRATEGIES

In the field of pavement engineering, pavement management and maintenance issues must be considered very seriously in the selection of an economical treatment for rehabilitation of a deteriorated pavement section. To preserve or improve pavement condition, there are many maintenance and rehabilitation treatments that have to be chosen carefully due to financial problems. Therefore, the engineering judgment and experience on deciding the maintenance and repair actions have significant importance. There are several articles summarized in this section in which the artificial neural networks were utilized as a computational tool to decide which maintenance and rehabilitation actions should be performed on deteriorated pavement sections.

Hayek et al. (1987) compared two different techniques, rule-based system and artificial neural networks, for selecting and recommending routing and sealing (R&S) treatments. There were about 40 different variables and factors such as width of cracks, crack type, pavement serviceability, pavement structure and age, raveling, flushing, and rutting influencing the R&S decisions. ANNs were regarded as alternative solutions that required substantially less time and effort for development. The output of the ANN model was a data set ranging between 0 and 10; 10 being the highest desirability of the R&S treatment, whereas 0 meant that there was no need for any R&S treatment. Even though ANN technology was seen as a powerful and efficient alternative technique to the rule-based

system, the authors concluded that actually more benefits can be obtained by combining both technologies.

The feasibility of using ANNs for priority assessment of highway pavement maintenance needs was investigated by Fwa and Chan (1991). Ability of backpropagation neural networks was tested separately with three different priority-setting schemes: Linear relations, non-linear relations, and an assessment by a pavement engineer. The results of the neural network approach were compared with the aggregated condition index approach. Fwa and Chan (1991) concluded that the use of neural networks had several significant advantages over the aggregated condition index.

In another study, Taha et al. (1995) developed a model that was a combination of genetic algorithm and backpropagation neural network for selecting the optimal maintenance strategy for flexible pavements. The factors affecting the maintenance strategy selection were identified as distress type, severity of distress, density of distress, riding comfort index (RCI), traffic volume, climate, and crack type. The different pavement maintenance strategies available were “do nothing”, “crack seal coating”, “route and seal”, “cold-mix patching”, “hot-mix patching”, “hot-mix recycled patching”, and “reconstruction”. Taha et al. (1995) indicated that the ANN performances can be improved by applying genetic algorithms.

A neural network study which is a part of an automatic procedure for preliminary screening and identifying roadway sections for pavement preservation at the Arizona DOT (ADOT) was presented by Flintsch et al. (1996). Maintenance needs in the pavement sections were identified according to the cracking and roughness severity over the past three years’ rutting, patching, skid resistance, structural number, flushing, maintenance costs, daily traffic volumes, and rate index. To determine whether the maintenance was needed or not for a given road section, the output layer of the ANN consisted of one neuron representing the decision. The pavement section was recommended for maintenance if the output value was larger than 0.5 and the section was not recommended for maintenance if the output value was

less than 0.5. The database was extracted from the several projects in ADOT from 1990 to 1996. According to the results of the analysis, the ANN learned 100 percent of the training data set and 76 percent of the testing data set.

Artificial neural networks and knowledge-based expert systems for choosing proper rehabilitation schemes of deteriorated pavement sections were combined by Goh (1997). The knowledge-based expert system gave the list of the recommended repair schemes and the associated costs of the repair schemes. On the other hand, a feed forward ANN fed the knowledge-based expert system with the list of the recommended repair schemes. The input layer contained six input parameters such as the type and the extent of distress and the classification of the road type and output layer had nine different possibilities: “50-mm asphalt overlay”, “25-mm asphalt overlay”, “25-mm asphalt and partial reconstruction”, “50-mm asphalt and partial reconstruction”, “clean and refill cracks”, “patch”, “reseal”, “full reconstruction”, and “do nothing”. The effectiveness of the ANN was not clearly demonstrated in this study.

Alsugair and Al-Qudrah (1998) reported results from an artificial neural network study which focused on determining the appropriate maintenance and repair (M&R) actions. The pavement condition data used in this study were obtained from the comprehensive visual inspection data from Riyadh road network in Saudi Arabia. In order to collect data on the surface distresses and the corresponding severity levels and quantities, the Pavement Condition Index (PCI) procedure was used in this study. Five M&R actions were recognized: “thin overlay”, “thick overlay”, “strengthening and overlay”, “localized maintenance” (crack seal, skin patch, partial depth-patch, full depth-patch, pothole filling, apply heat and roll sand, apply surface seal emulsion, apply rejuvenation, apply aggregate seal coat), and “do nothing”. In conclusion, the study showed that the ANN model was able to achieve high reliability rates. The network architectures presented in the study for implementation are shown in Table 4.2.

Table 4.2. Selected architectures for networks (Alsugair and Al-Qudrah 1998)

Network	PCI Rating	Reliability Level (%)	Layer's Node		
			Input	Hidden	Output
1	PCI ≤ 70	100.0	12	28	5
2	70 ≤ PCI ≤ 85	96.2	12	22	5
3	PCI > 85	91.3	12	34	5

A genetic adaptive neural network training (GANNT) algorithm with single hidden layer to predict the optimum maintenance strategy based on realistic (noisy) data for the rehabilitation of a deteriorated pavement section was used by Abdelrahim and George (2000). In the proposed model, the input vector represented the factors affecting the maintenance strategy selection while the output vector represented the appropriate maintenance strategy. The different maintenance strategies considered for flexible pavements in this study were “do nothing”, “surface seal coat”, “crack seal + 1 inch overlay”, “milling + 1.5 inch overlay”, “2 inches overlay (with full depth patching of cracked area)”, and “reconstruction”. Based on the study findings, it was concluded that neural networks provide an efficient and optimum solution for such complex problems with the added advantage of faster implementation and easier updating than other traditional techniques.

Finally, Bosurgi and Trifiro (2005) defined a procedure to make use of the available economic resources in the best way possible for resurfacing interventions on flexible pavements by using artificial neural networks and genetic algorithms. In this study, neural networks were utilized to define both a Sideway Force Coefficient prediction model and an accident prediction model. In the second part of the proposed model, authors used genetic algorithm using the results of the neural networks designed in order to resolve the optimization problem. Authors concluded that the procedure represents an efficient approach to obtain one of optimal solutions in a very big space of possible solutions in sufficiently short periods of time.

Discussion: Pavement Management and Maintenance Strategies

Due to the nature of the problem, it is not very easy everytime to reach an optimum management and maintenance decision for a specific pavement section since there might be more than one reasonable solution. The applicability of the solution is strongly related with the financial opportunities and an erroneous approach might cause millions of dollars to be spent unnecessarily. An optimum solution requires substantially less time and effort; therefore, the pavement management and maintenance strategies should be determined very carefully.

Generally, the outcomes of the developed ANN models in this section are not a single output as in the previous section. ANN models were developed to select the one of the several possible solutions which is generally an expert opinion or pavement engineer decision for a specific problem. Therefore, mostly it is not possible to compare the ANN model results with other techniques every time in this section. The success of the developed ANN models is generally checked by the success rate of the testing data set. What seems from the ANN studies for the pavement maintenance and rehabilitation treatments is that the combination of the ANN approach with other approaches such as genetic algorithms and knowledge-based expert systems improves the success rate of the developed models significantly.

CATEGORY 3: PAVEMENT DISTRESS FORECASTING

Several ANN models that can predict the current condition of the pavement sections were developed. Having an artificial neural network model that can accurately forecast the condition of a pavement system at some future time is also invaluable and cost effective. In this section, papers relating to the use of ANNs for forecasting the pavement condition in future time are summarized.

To develop models for forecasting the infrastructure condition of the pavement sections, Schwartz (1993) developed an artificial neural network. The future condition was forecasted as a function of time, current and historical condition, loading, inventory materials, and other

data elements. Finally, the neural network and non-linear regression forecasting techniques were evaluated in terms of their abilities to predict the simulated future PCI as a function of the appropriate predictor variables. The authors concluded that the major advantage of using ANNs over current forecasting models at that time is that there was no need to specify the form of the non-linearity in advance.

In order to predict roughness distress level probability at some future time for flexible pavements, Huang and Moore (1997) used ANN models. The pavement structural characteristics, traffic, and climatic conditions were included in the historical pavement condition data and in the specific project-levels of the database. A backpropagation neural network with one hidden layer was employed in the study. Based on the analysis, the ANN models were found to be generally much better predictors of the roughness distress level probability than the traditional multiple regressions developed for comparison purposes in this study.

Roberts and Attoh-Okine (1998) compared two artificial neural networks using pavement performance predictions. The results of two different ANN types, dot product ANN (using backpropagation algorithm) and quadratic function ANN, were compared by using the same data taken from the Kansas DOT database. The quadratic function ANN was a generalized adaptive feed-forward neural network that combined supervised and self-organizing learning. Both the dot product ANN model and quadratic function ANN model were trained to predict the IRI for three types of asphalt pavements: composite, full-depth bituminous, and partial-design bituminous. Rutting code, fatigue cracking codes, transverse cracking codes, block cracking code, equivalent axle loads were used as input variables and international roughness index was selected as output variable. Based on estimated future pavement deterioration, future IRIs can be predicted with the proposed ANN models. The ANN models overpredicted the values of IRIs below 125 while underpredicting the values of IRIs above 125 (Figure 4.4). The authors concluded that the quadratic function ANN model performed better than the dot product ANN model.

La Torre et al. (1998) applied a multilayer perceptron (MLP) neural network model to predict the IRI of flexible pavement sections for four years into the future. The input variables used in the analysis were asphalt concrete layer thickness, the asphalt concrete backcalculated elastic modulus value, the unbound-layer thickness, the unbound-layer backcalculated elastic modulus value, the annual number of days with a temperature higher than 90 ^{o}F, the freeze index, the annual precipitation level, the average annual equivalent axle loads, and the age of the pavement at the first IRI observation. The corresponding IRI value was selected as the output variable that contains four neurons which represents the predicted IRI values for the following first, second, third, and fourth years. The long-term predictions were also addressed in the paper. Results indicated that even though the overall short and long-term performances on the training set looked promising, the model needed to be further investigated on the validation set.

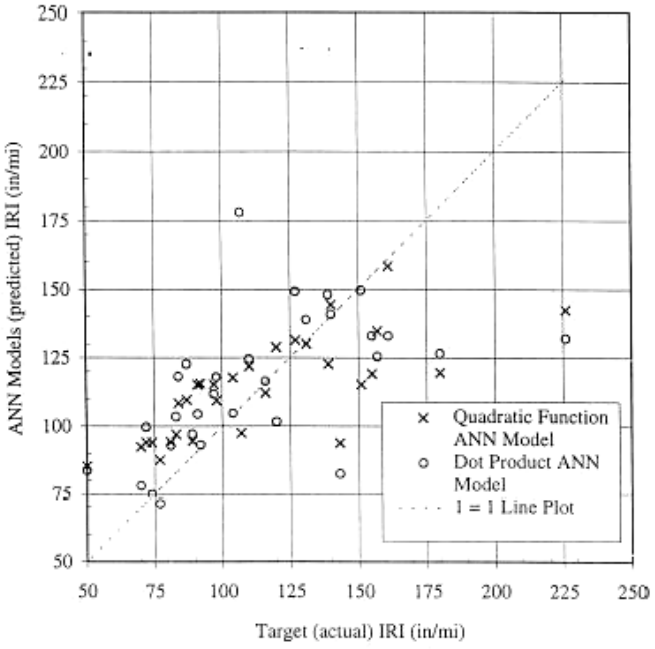

Figure 4.4. International roughness index (IRI) (in/mi) prediction values using ANN models (Roberts and Attoh-Okine 1996)

The progression of rut depths in road pavements was predicted by neural networks (Sundin 1998). The input variables were selected as the type of the pavement for the upper layer, the previous value of the rut depth, the previous change in rut depth, climate condition,

maintenance information such as the type of the last pavement action, the number of years since last maintenance action, and traffic value. It was concluded that the application of ANNs improved the quality of the predictions when ANNs were compared with those of multiple regression models.

Lu et al. (1999) and Lou et al. (2001) developed artificial neural network models to forecast the pavement crack condition by using the database composed of the Florida DOT (FDOT) pavement conditions. Seven input parameters were used in proposed models. CI(t-2), CI(t-1), CI(t), which were the crack indices (CI) in year t-2, t-1 and t, respectively, flexible type of pavement indicator (1 if flexible, 0 otherwise), rigid type of pavement indicator (if 1 is rigid, 0 otherwise), pavement cycle, and pavement age were used as inputs of the proposed model. The following year`s crack index [CI(t+1)] was predicted as the output of the neural network model. The results of the ANN model were also compared with the results of the Auto-Regression (AR) model. When the root mean square error (RMSE), average error and R^2 values were compared, it was concluded that the neural network model is an effective tool for pavement maintenance planning.

Yang et al. (2003) summarized the results of a research study carried out to implement an overall pavement condition prediction methodology using artificial neural networks. Three individual ANN models trained and tested using the Florida DOT (FDOT) pavement condition database were developed to predict the crack rating, the ride rating, and the rut rating. Results of the combination of the individual models suggested that the developed ANN models had the capability to satisfactorily forecast the overall pavement condition index up to a future period of five years. Table 4.3 summarizes the goodness of fit for each model in terms of R^2.

Dynamic artificial neural networks based on backpropagation algorithm to develop a time-dependent roughness prediction model for newly constructed Kansas jointed plain concrete pavements (JPCP) was used by Najjar and Felker (2003). The data were obtained from the Kansas pavement condition database. The international roughness index (IRI) value used in

this study represented only the right wheel path IRI. The futuristic [i.e., year (n+1)] roughness IRI value [i.e., IRI $^{(n+1)}$] was determined from a number of previously determined input parameters that were PCC slab thickness, drainable base, non-drainable base, concrete unit weight, cement factor, non-treated subgrade, lime treated subgrade, subgrade modification, percentage of natural subgrade soil material passing No. 4 sieve, percentage of natural subgrade soil material passing No. 200 sieve, plasticity index of natural subgrade soil material, cumulative yearly equivalent single axle load, average number of freeze-thaw cycles per year, cumulative total number of days below 32 ^{o}F/year, cumulative total number of days above 32 ^{o}F/year, cumulative number of wet days/year, initial right wheel path IRI values, age of pavement, and IRI value at age (n) year, i.e., $(IRI)^n$. According to the results, R^2 value decreased as extrapolation time increased. Therefore, the authors suggested that it was imperative that such a model had to be annually updated on newly acquired data.

Table 4.3. R^2 comparisons of ANN model and AR (Auto-Regressive) model (Yang et al. 2003)

Years and Forecast Models		**Goodness of Fit (R^2)**	
		Flexible Pavements	**Rigid Pavements**
1 year	ANN	0.88	0.79
	AR	0.58	0.39
2 year	ANN	0.76	0.55
	AR	0.29	0.2
3 year	ANN	0.59	0.52
	AR	-0.22	-0.15
4 year	ANN	0.48	0.4
	AR	-0.49	-0.28
5 year	ANN	0.38	0.2
	AR	-0.74	-0.14

Discussion: Pavement Distress Forecasting

Pavement condition prediction models play a crucial role in Pavement Management Systems (PMS) since these models simulates the deterioration process of pavement condition and forecast the pavement condition over time. The prediction of the forecasting models determines the actions of PMS. Therefore, the databases which ANN models were trained should be very comprehensive and be updated frequently when new data is available. ANN

model predictions were mostly compared with the multiple regression models developed for the comparison purposes. As can be seen from the summarized papers, general conclusion is that ANN models are better predictors than the traditional multiple regression models. Another advantage of the ANN models is that there is no need to specify the form of the non-linearity in advance.

CATEGORY 4: STRUCTURAL EVALUATION OF PAVEMENT SYSTEMS

Several studies utilizing ANN for predicting the elastic moduli, layer thicknesses, coefficient of subgrade reaction, shear wave velocities of the layers, and pavement surface deflections that are crucial structural parameters in the analysis and design of the pavements are summarized in this section.

In order to interpret the ground penetrating radar (GPR) thickness profile output without any destructive coring, Attoh-Okine (1993) used a feed-forward neural network model with a four layer backpropagation algorithm. GPR is a nondestructive technique that has the potential to survey pavement thickness and structure while operating at highway speed. In this study, three output nodes were used to identify the three different types of surface-base interface: composite pavements, partial-designed pavements, and full-designed pavements. Based on the analysis, the author concluded that the combination of radar output and ANN had the potential to automate nondestructive evaluation of structural conditions of pavements.

Meier and Rix (1994) developed an approach to backcalculate of pavement layer moduli from falling weight deflectometer (FWD) deflection basins by using artificial neural networks. Two backpropagation neural network models were trained to backcalculate pavement moduli for three-layered flexible pavement profiles by using synthetic deflection basins with a wide variety of layer moduli and thicknesses. The first model was trained with success using synthetic basins with no random noise added and the second model was trained using deflection basins with random noise to simulate measurement errors. Even though the

network trained and tested with noisy data exhibited much more scatter in the results, that network did a reasonably good job of predicting moduli. The authors developed a neural network model which operated 1,500 to 2,200 times faster than the conventional algorithmic programs used at that time. This study was a static analysis of pavement response. The authors also trained a different model (Meier and Rix 1995) to backcalculate pavement layer moduli from synthetic deflection basins calculated by using a dynamic analysis of pavement response based on Green functions. Similarly, this ANN model gave successful predictions in real time.

Williams and Gucunski (1995) developed backpropagation and general regression neural network models to predict the elastic moduli and layer thicknesses of pavements from the Spectral-Analysis-of-Surface-Waves (SASW) test results. The SASW test is a seismic technique for the in-situ evaluation of pavements and soil systems. Three, four, and five layer backpropagation models with jump connections were trained in the study. All neural network models produced reasonably similar results to the actual outputs. The authors concluded that backpropagation neural networks can provide a useful technique for the analysis of dispersion curves obtained from SASW tests.

In another study, Heiler et al. (1995) tackled the problem of automatic detection of asphalt thickness and depth to reinforcement in composite pavements using neural networks. The authors stated that GPR interpretation had been done manually in the past by trained engineers and technicians with the aid of standard signal processing techniques. This method of collection produced vast quantities of data, and the interpretation required a great amount of time. Recently, parallel processing in the form of artificial neural networks had been applied to the interpretation of GPR condition assessment data from highways. This paper introduced general strategy for using ANNs for the interpretation of GPR data. Results of applying this strategy to bridge deck condition assessment data were also given.

Artificial neural networks were trained to perform an inversion procedure for SASW testing of asphalt concrete (AC) pavements (Gucunski and Krstic 1996). The training of the

networks was completed by the dispersion curves for individual receiver spacings. Two different models were developed. The first model approach was on the basis of the average dispersion curve and the second model was based on the individual receiver spacing dispersion curve approach. The results of the comparison of those two models showed that both models have capability of predicting the shear wave velocities and thicknesses of all the layers with high accuracy, except the thickness of the subbase, d_3. In order to reduce this problem, the authors suggested to use the individual receiver spacing model, $V_{S2} / V_{S1} < 1$ (V_{S1}: shear wave velocity of the AC surface layer; V_{S2}: shear wave velocity of the bituminous stabilized base course layer), and the average dispersion curve model for higher ratios.

The use of the artificial neural networks for assessing the deflection and stress load transfer efficiencies of concrete pavement joints and for backcalculating joint parameters was investigated by Ioannides et al. (1996). The database was generated using numerical integration of Westergaard-type integrals to train the ANNs for joint evaluation. In this study, the ANN model was a multilayer, feed-forward network consisting of 2 hidden layers in addition to the input and output layers. The input layer consisted of the values of the ε / l and LTE_δ ratios, and the output layer consisted of the LTE_δ and the logarithm of the dimensionless joint stiffness, f. The predictive values of LTE_δ by ANN and statistical regression tool results were compared and it was observed that the ANN predictions were better than those obtained from the statistical regression algorithms. The authors also indicated that the dimensional analysis reduced the number of variables used in the ANN model permitting real-time determination during testing.

Meier et al. (1997) augmented the WESDEF (Van Cauwelaert et al. 1989) backcalculation program (minimizes the difference between a calculated basin and the measured basin by adjusting the modulus of the various layers through a series of iterations) by four artificial neural networks trained to compute pavement surface deflections as a function of pavement layer moduli for a wide range of three-layered flexible pavements. The authors noted that

WESDEF can backcalculate pavement layer moduli 42 times faster with success than it did before with the addition of the neural networks.

An ANN-based backcalculation procedure was developed for asphalt concrete over Portland cement concrete (PCC) overlays (3-layers) as composite pavement systems and implemented into a computer program called DIPLOBACK (Khazanovich and Roesler 1997). The pavement layer thicknesses and deflection profiles were given to the model as input variables to predict the elastic modulus of the AC (E_{AC}) and PCC (E_{PCC}) layers, and coefficient of subgrade reaction (k_S). Theoretical deflection basins were generated by DIPLOMAT (Khazanovich and Ioannides 1995) program (which solves AC overlays over PCC as elastic layers over a dense liquid subgrade) to create an ANN-based procedure to backcalculate E_{AC}, E_{PCC}, and k_S. The results of backcalculation were compared with the actual elastic parameters of the theoretical deflection basins and good agreement was observed. In addition, the results of the backcalculation using field test data were compared with the results obtained by using WESDEF. Based on the comparison, similar trends were observed for elastic parameters of all three pavement layers.

Kim and Kim (1998) presented a study related to the prediction of layer moduli from falling weight deflectometer (FWD) tests and surface wave measurements. Based on the observations and investigations in this study, a new modulus prediction algorithm was developed and presented. Hankel transforms were used in this study as a forward model. On the other hand, neural networks were used for the inverse process. This method was applied to the evaluation of two pavement sites in North Carolina and it was concluded that the analysis procedure developed in this study was more sensitive to upper layer conditions and resulted in less variable sub-surface layer moduli.

The capability of ANN models to compute lateral and longitudinal tensile stresses as well as deflections at the bottom of jointed concrete airfield pavements as a function of type, level, and location of the applied gear load, slab thickness, slab modulus, subgrade support, pavement temperature gradient, and the load transfer efficiencies of the joints was illustrated

by Ceylan et al. (1998, 1999a, 2000) and Ceylan (2002). The training sets were developed for prescribed gear and temperature loads using the ILLI-SLAB (Tabatabaie 1977) finite element program. The findings of these studies proved that ANN models could be successfully trained to capture the complex multi-dimensional mapping of a large-scale finite element pavement analysis problem in their connection weights and node biases.

Ceylan et al. (1999b) and Ceylan (2004) trained artificial neural networks to predict stresses and deflections in jointed concrete airfield pavements serving the Boeing B-777 aircraft. The results of the ILLI-SLAB finite element program were used to train the ANN models producing stress and deflections with average errors less than 0.5 % of those obtained directly from the finite element analyses. The prediction capability of the ANN models appeared to be accurate when predicting the maximum stresses and deflections, slab thicknesses, subgrade supports, and the joint load transfer efficiencies matched exactly on the piecewise continuous functional relations obtained from the training of the models. Figure 4.5 shows the prediction ability of the 7-60-60-12 network at 10,000 learning cycles for the simultaneous aircraft and temperature gradient loading cases. The authors concluded that trained neural network models will eventually enable pavement engineers to easily incorporate current sophisticated state-of-the-art technology into routine practical analysis and design.

In order to estimate the elastic modulus of the asphalt concrete layer and the thickness in flexible pavements, Saltan et al. (2002) developed an ANN model. Seven different deflection values obtained from the FWD tests were used as input variables in the ANN model. The authors utilized the asphalt concrete elastic modulus and thickness of asphalt mixture as output variables in the backpropagation type ANN model. Base on the analysis results, Saltan et al. (2002) concluded that the ANNs can be used for backcalculation of the thickness of layers with great improvement and accuracy.

Ceylan and Guclu (2004a) demonstrated the use of ANNs as pavement analysis and design tools by analyzing concrete airfield pavements under the following three loading cases: (1)

Airbus A380-800 new generation aircraft (NGA) gear loading only, (2) climatic loading only, and most importantly, (3) simultaneous aircraft gear and climatic loading. For the three different loading cases, the ANN model predicted maximum bending stresses and deflections with an overall average absolute error of less than 2.1 %. The authors concluded that ANNs are capable of successfully predicting the critical responses of a large scale nonlinear finite element model and such ANN models provide invaluable help to pavement engineers for studying the effects of heavy loading new generation aircraft.

In another study, Ceylan et al. (2004b) also investigated the use of the ANN-based structural models for rapid analysis of flexible pavements with unbound aggregate layers. The ANN models successfully predicted the layer moduli and critical pavement responses computed by the ILLI-PAVE finite element solutions and were much superior to the liner-elastic-layered forward and backcalculation analyses due to the non-linear material characterization employed. Figure 4.6 depicts the prediction ability of the 6-60-60-2 network that was designed to predict the elastic modulus of the AC layer and the resilient modulus of the subgrade layer using only four pavement surface deflections, and two layer thicknesses: asphalt concrete and granular base layer thicknesses. The authors concluded that such ANN structural analysis tools can provide pavement engineers and designers with sophisticated finite element solutions, without the need for a high degree of expertise in the input and output of the problem, to rapidly analyze a large number of pavement deflection basins needed for routine pavement evaluation.

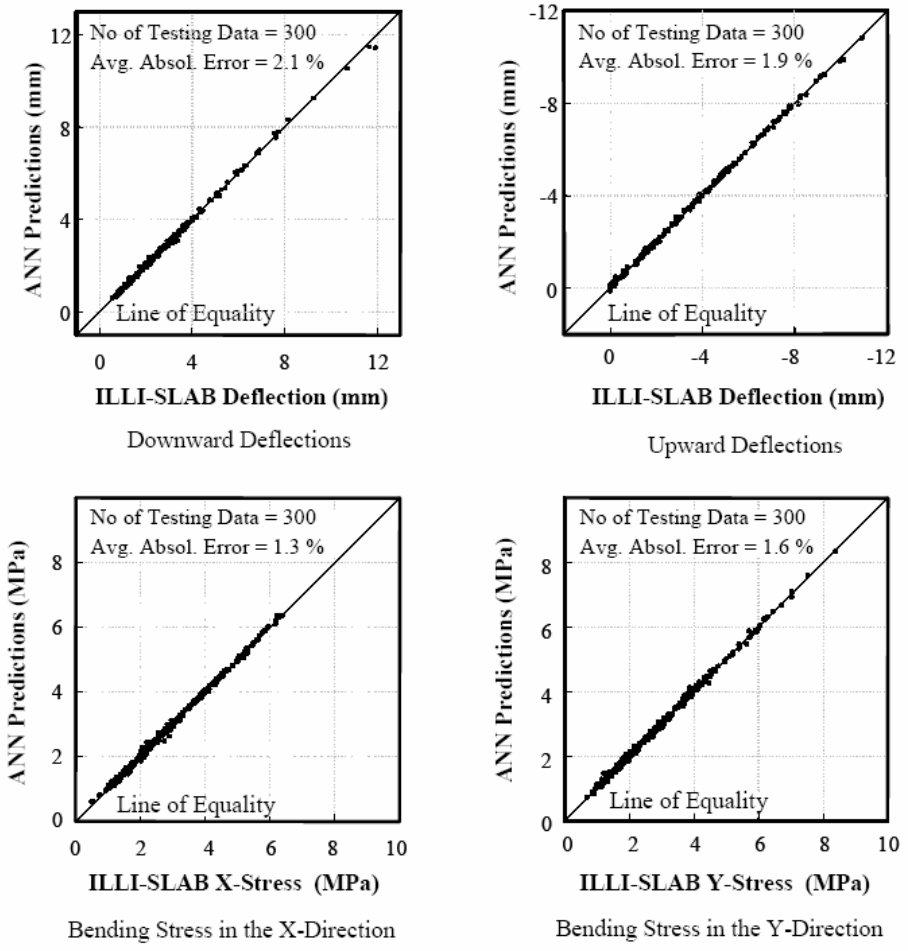

Figure 4.5. Accuracy of the 7-60-60-12 network for predicting the critical pavement responses under the simultaneous aircraft and temperature loading (Ceylan et al. 1999)

Ceylan et al. (2005a) also showed that ANN models could be developed to perform rapid and accurate predictions of flexible pavement layer moduli and critical pavement responses (stresses, strains, and deflections) from FWD deflection basins for a number of pavement input parameters considered in analysis and design. The virgin and the noise-introduced (robust) ANN models successfully predicted the pavement layer moduli and critical pavement responses obtained from the ILLI-PAVE finite element solutions and were much more superior to the linear-elastic-layered backcalculation analyses. Noise introduced ANN models have been found to be more robust compared to the models trained with the virgin training data. Such ANN models provide more realistic predictions of pavement layer

moduli and critical pavement responses because of their ability to tolerate the inaccuracies in the pavement deflection basins and the layer thicknesses due to poor construction practices.

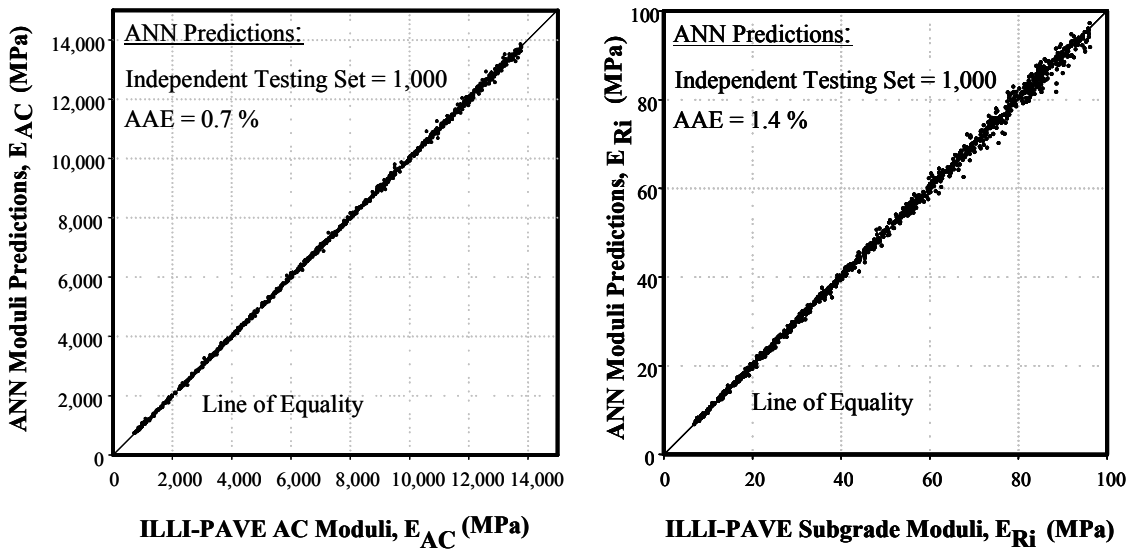

Figure 4.6. Prediction performance of the 6-60-60-2 BCM-1 network for 10,000 learning cycles (Ceylan et al. 2004)

Seven ANN-based backcalculation and forward calculation models using some 26,000 nonlinear ILLI-PAVE finite element (FE) solutions for the full depth and conventional flexible pavements were developed (Ceylan et al. 2005b). In the study, six conventional flexible pavement sections were selected to further evaluate the performances of the ANN backcalculation models. ANN models predicted the layer moduli and critical pavement responses computed by the ILLI-PAVE FE solutions and were much superior to the linear-elastic-layered forward and backcalculation analyses.

ANN-based backcalculation and forward calculation pavement structural models were developed in another study (Ceylan et al. 2005c) for full-depth flexible pavements using the ILLI-PAVE finite element solutions with non-linear, stress-dependent subgrade soil properties. The comparison of the ANN model predictions and ILLI-PAVE based algorithm results are shown in Figure 4.7. The authors concluded that that ANNs are capable of mapping complex relationships, such as those studied in complex finite element analyses,

between the input parameters and the output variables for non-linear, stress-dependent systems. ANN models can rapidly (50,000 analyses in less than a second) output the required solutions in analyzing a large number of pavement deflection basins needed for routine pavement evaluation. The rapid prediction ability of the ANN backcalculation models makes them perfect evaluation tools for analyzing the FWD deflection data, and thus assessing the condition of the pavement sections, in real time for both project specific and network level FWD testing.

In another work (Rakesh et al. 2006), ANN models were developed for computing surface deflections using elastic moduli and thicknesses of pavement layers as inputs. The ANN models have been used in BACKGA (developed by the Indian Institute of Technology) for forward calculation of surface deflections to combine the computational efficiency of ANNs with the robustness of the genetic algorithms. The authors stated that the performance of the resulting model, BACKGA-ANN, has been evaluated and found to be satisfactory.

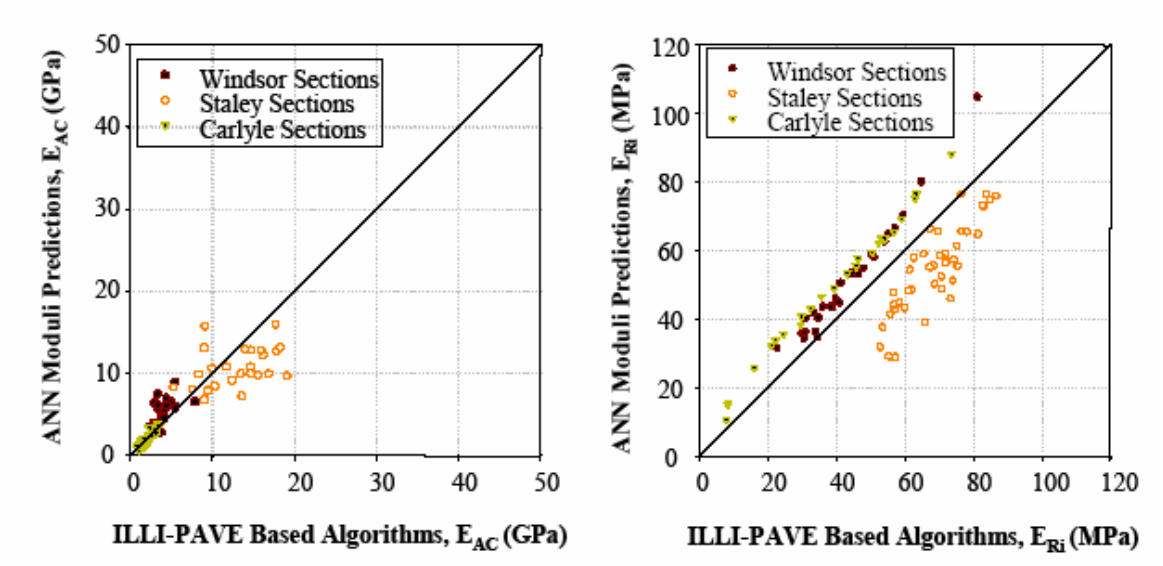

Figure 4.7. Comparison of the ILLI-PAVE based algorithms and ANN predictions (Ceylan et al. 2005)

Finally, Goktepe et al. (2006) analyzed the role of learning algorithm and ANN architecture in ANN-based backcalculation of flexible pavements. In this study, 284 different ANN models were developed using synthetic training and testing databases obtained by layered

elastic theory. Results indicated that both the learning algorithm and network architecture play important roles in the performance of the ANN-based backcalculation process to reach realistic results.

Discussion: Structural Evaluation of Pavement Systems

Artificial neural networks are applied in effective ways in the area of structural evaluation of pavement systems. The successfully developed models can be incorporated into the routine project specific and network level testing easily. Most of the ANN models summarized in this section were trained with the synthetic data as well as field test data such as FWD, GPR, and SASW. The reliability of ANN-based models can be increased when more actual field / lab data is used for the training process instead of synthetic databases. Another issue is the validation of the proposed ANN models. Getting a field or lab data, result, or interpretation for a specific problem is not always possible. For some problems, generally accepted correlations, algorithms, software programs are used in the practice. Therefore, most ANN-based models developed for the structural evaluation of pavement systems are validated by comparing with other techniques instead of actual field or lab results.

CATEGORY 5: IMAGE ANALYSIS / CLASSIFICATION

Quantification of pavement crack data is one of the most important criteria in determining optimum pavement maintenance strategies. Over the years, a significant amount of effort has been spent on developing methods to objectively evaluate the condition of pavements. A different pavement crack detection approach was investigated in this section. Basically, digital pavement images were utilized to classify the cracks by using the artificial neural networks. Some of the papers using this technique have been summarized in this section.

Kaseko et al. (1991, 1992, 1993a) proposed a purely image-processing-oriented methodology for crack identification and classification. The pavement images used in these studies were collected by the ROADRECON instrumentation vehicle acquiring the images for the US Strategic Highway Research Program (SHRP). Images extracted from the entire database were digitized to 512 x 464 pixel digital images with an 8-bit gray scale. In order to segment

and classify the images, the backpropagation algorithm was used in the neural network analysis. Images were classified into four different categories according to the nature of cracks which are “transverse”, “longitudinal”, “alligator”, and “block cracking”. The authors concluded that ANN-classifiers had a significant advantage in real-time applications with high computation rates required in pattern-recognition problems.

In a similar study, Kaseko et al. (1993b) used mean, standard deviation of gray scale level histogram of the image and a co-occurrence parameter as input variables. The threshold value was assumed as the output of the ANN model. The ANN approach and regression approach were compared in the study and as a result the ANN approach performed considerably better than the regression approach. The authors stated that the effect of co-occurrence parameter or noise reduction was significant in the analysis.

In another study, the neural network classifiers and traditional classifiers were compared by Kaseko et al. (1994). Three different models were investigated: Bayesian classifier, k-nearest-neighbor classifier, and MLP neural networks. The overall objective of this study was to develop an ANN-based methodology for processing video images for automated detection, classification, and quantification of cracking on pavement surfaces. Each selected sub-image was classified into one of the five classes that were “no cracking”, “transverse”, “longitudinal”, “diagonal”, and “combination cracking”. In conclusion, the authors demonstrated that ANN classifiers had a significant advantage in real-time applications with high computation rates.

Nallamothu and Wang (1996) studied the classification of pavement distresses using the radial basis function neural networks. Pavement distresses were classified as “transverse cracks”, “longitudinal cracks”, “raveling”, and “no crack”. Each feature vector consisted of an image that represented a distress of compressed size 24 x 9 pixels. According to the results, 85 percent success rate was obtained in the test set used in this study.

Cheng et al. (2001) presented an approach to pavement cracking detection based on neural networks and CVPRIP (computer vision, pattern recognition, and image processing) techniques. This approach is based on the assumption that the crack pixels in pavement images are darker than their surroundings and crack pixels can be separated from the background using the threshold approach. Mean and standard deviation values were used as features and these statistical values were employed to train the neural network model selecting the thresholds and then the images would become binary images (crack pixels and background) after thresholding. Finally, Hough transformation was used to detect and classify all cracks in parallel. Figure 4.8 shows the original image (a), images after applying the desire threshold values (b), and images after applying the outputs of the neural network (c). It can be seen that Figure 4.8(b) and Figure 4.8(c) are very similar. The authors concluded that the cracks were correctly and effectively detected by the proposed method which would be useful for pavement management.

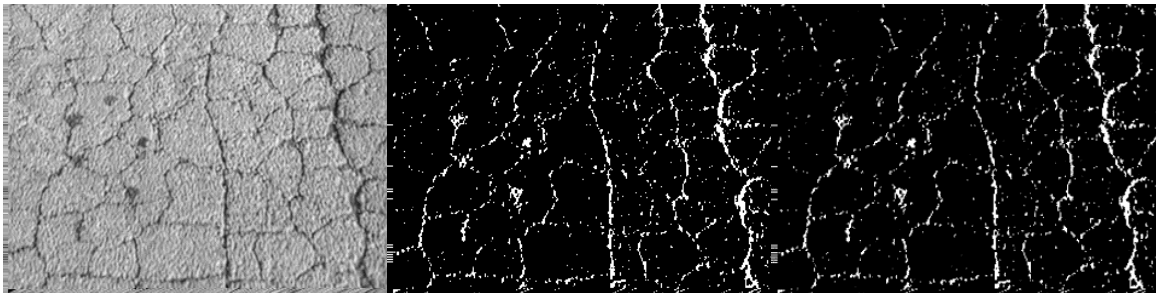

(a) (b) (c)

Figure 4.8. (a) The original image with alligator crack. (b) The result using the desired threshold. (c) The result using the neural network computed threshold (Cheng et al.2001)

In another study, Lee and Lee (2004) developed an integrated ANN-based crack imaging system to classify crack types of digital pavement images. Three different types of neural networks were used in the analyses: image-based neural network (INN), histogram-based neural network (HNN), and proximity-based neural network (PNN). Various crack types based on the subimages (crack tiles) rather than crack pixels in digital pavement images were classified by using these three neural networks. From the FHWA guidelines, 300 artificial images were generated. Actual pavement pictures taken from pavements as well as the

computer-generated data were used in order to validate the system. The outputs of the proposed model were “alligator crack”, “block crack”, “longitudinal crack”, “transverse crack”, and “no crack”. Based on the analysis, the authors concluded that the proximity-based neural networks produced the results with very high success rate. As shown in Table 4.4, all neural networks achieved a high accuracy of 95% or higher for the training sets and relatively low accuracy of 70% or higher for the testing sets.

Table 4.4. Three types of neural networks and their performances (Lee and Lee 2004)

Neural network	Training Data		Testing Data			
	Artificial Data (300)		Artificial Data(150)		Actual Images(124)	
	# of data	Accuracy	# of data	Accuracy	# of data	Accuracy
Image-based NN	291	97.0%	114	76.0%	87	70.2%
Histogram-based NN	297	99.0%	137	91.3%	93	75.0%
Proximity-based NN	287	95.7%	140	93.3%	778	95.2%

Discussion: Image Analysis / Classification

Real-time applications in pavement engineering are very important in terms of pavement management in order to speed up the process. Reliable crack detection approaches were developed by using artificial neural networks. The processing of the digital pavement surface images by artificial neural networks prevent is an advance technique which decrease the analysis time significantly. In addition, the visual quantifications of the pavement conditions rated by the pavement engineers are not always very objective and might change from someone to another. The time spent on the evaluation of the pavement condition is also another important issue. With these ANN-based image analysis methods, pavement condition evaluation can be standardized with real-time applications.

CATEGORY 6: PAVEMENT MATERIAL MODELING

The accurate and effective modeling of pavement materials is critical to the prediction of the pavement performance. Soil properties and behavior is an area that has attracted many researchers to modeling pavement materials using ANNs. Also, constitutive models describing the relationships between stresses and strains of materials are crucial elements in the design and analysis of engineering systems. This section summarizes the studies that

discuss the use of artificial neural networks as an alternative method for pavement material modeling.

The behavior of concrete in the state of plane stress under monotonic biaxial loading and compressive uniaxial cycle loading was modeled with a backpropagation neural network (Ghaboussi et al. 1991). The training data set of the proposed ANN model was obtained from the experimental results containing the relevant information about the material behavior. Therefore, the trained neural network would contain sufficient information about the material behavior to qualify as a material model. The results of proportional stress paths were utilized in the neural network model and the trained network was expected to simulate the test results for other proportional and non-proportional stress paths. The authors stated that the degree of accuracy in this generalization depended on how comprehensive the training set was. Two examples of material modeling, ANN model representing the biaxial behavior of plain concrete and the ANN model on uniaxial cyclic tests on plain concrete, were presented in the paper. Stresses and strains were used as inputs and output for both models and stress paths were predicted by ANN models. Then, the results obtained form the neural network models were compared with the experiment results, analytical model results, and mathematical material model results. The authors concluded that the ANN predictions were quite reasonable.

Eldin and Senouci (1994) examined some engineering properties of rubberized concrete and developed a neural network model to predict the rubberized concrete`s compressive and tensile strengths. The input variables that may affect the strength of rubberized concrete were selected as the rubber type (shape), size, percentage, and concrete age (curing time). In addition, the output parameters were identified as the compressive and tensile strengths of rubberized concrete specimens as a fraction of that of plain concrete. On the basis of experimental tests and neural network analyses, one of the most important conclusions was that the reduction of up to 85% of compressive strength and up to 50% of splitting-tensile strength resulted when coarse aggregate was replaced by rubber.

Tutumluer and Meier (1996) attempted at training an artificial neural network constitutive model for computing the resilient modulus of aggregates as a function of the stress state and various physical properties. The authors attempted to model the resilient modulus of aggregates because pavements were subjected to repeated wheel loads, it had been customary to use resilient modulus (M_R) to characterize the elastic stiffness of the pavement materials rather than Young's modulus. The neural networks used in this research were conventional multilayer, feed-forward neural networks trained by error backpropagation algorithm. The coefficient of uniformity (C_u), the average aggregate size (D_{50}), the dry unit weight (γ_d), the fines content (F_{200}, percent passing No. 200 sieve), the deviator stress (σ_d), and the confining pressure (σ_3) were chosen as input variables to predict the resilient modulus of the soil which was the output parameter of the proposed ANN model. Figure 4.9(a) compared the computed and target outputs for the entire independent test set. On the basis of the results, it appeared that the neural network was successfully trained to compute resilient modulus. On the other hand, as shown in Figure 4.9(b) the neural network model produced poor agreement with the experimental results in the check made with the material not included in the original data set to predict the resilient moduli. Therefore, Tutumluer and Meier (1996) concluded that the appearance of success was only skin deep.

Penumadu and Jean-Lou (1997) presented an approach of modeling the soil behavior within a unified environment based on the artificial neural networks introduced for representing the behavior of sand and clay type soil. Current stress ($\sigma`_{1i}$, $u_i$) and strain ($\varepsilon_{1i}$) states, confining pressure ($\sigma`_{3C}$), initial relative density (D_r), previous stress history (OCR), and coefficient of uniformity (C_u) variables were used as inputs and $\sigma`_{1i+1}$ and u_{i+1} were used as outputs for the ANN-based sand model. Initial shear stress (τ_i), initial strain (ε_i), current strain (ε), and strain increments ($\Delta\varepsilon_i$) were used as inputs and $\Delta\tau_i$ and τ_{i+1} variables were used as output parameters of two ANN-based clay models. Based on the analysis, the authors concluded that a well trained neural network model for a specified soil type and stress path can be combined along with the finite element method for solving complex boundary value problems.

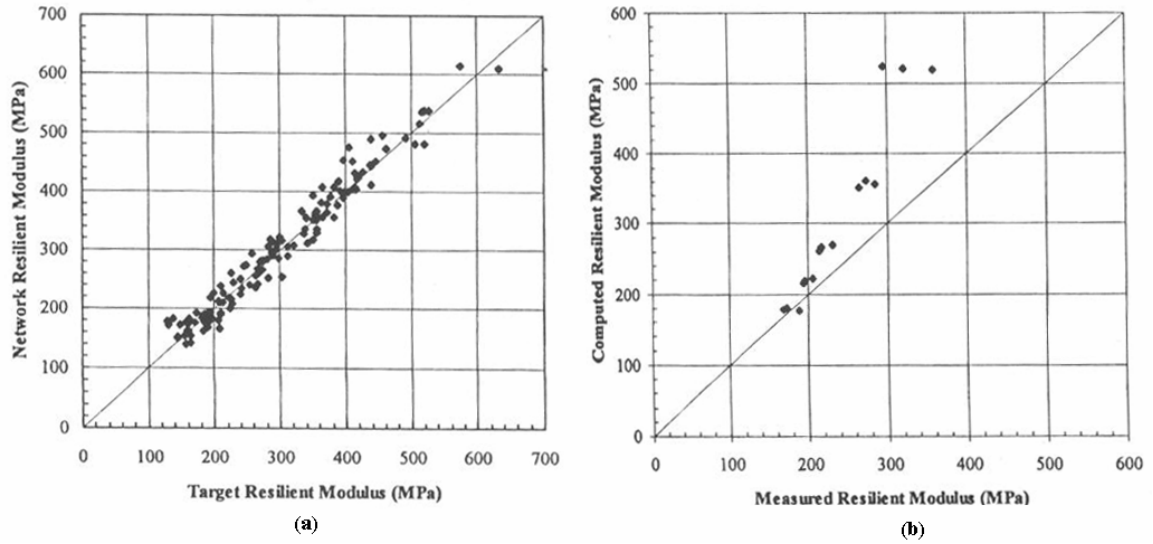

Figure 4.9. (a) Accuracy of trained 6-5-5-1 network (b) Neural network accuracy on an unfamiliar material (Tutumluer and Meier 1996)

Nested adaptive neural networks were introduced and a new type of neural network was developed by Ghaboussi and Sidarta (1998). The authors applied this neural network in modeling of the constitutive behavior of drained and undrained behavior of sand in triaxial tests. The authors utilized the strains as input variables and the stresses as outputs in the proposed ANN model. The authors concluded that these types of neural networks were capable of learning the drained and undrained behavior of sand for a range of initial void ratios and confining pressures. Sidarta and Ghaboussi (1998) also developed another method that was applied to a series of triaxial compression tests with end friction on sand.

The anisotropic aggregate behavior from repeated load triaxial tests utilizing the neural network modeling was investigated by Tutumluer and Seyhan (1998). Two triaxial stresses (confining pressure and applied deviator stress), measured vertical deformation, and two aggregate properties (compacted dry density and crushed particle percentage) were used as input variables in the trained feed-forward backpropagation type neural network. The output variables were the horizontal and shear moduli for which the actual (target) values were derived and computed from test results. The ANN models predicted the horizontal and shear moduli with mean errors less than 3% when compared to those computed using experimental

stresses and strains. The authors concluded that in the absence of lateral deformation data, such successful applications of ANNs were encouraged for determining anisotropic aggregate response and improving anisotropic modeling / characterization of granular materials. Tutumluer and Seyhan also stated that this kind of advancement was currently needed for example on designing flexible pavements with substantially thick granular base layers. The ANN model predictions for the horizontal and shear moduli were compared with the target values in Figure 4.10(a) and Figure 4.10(b), respectively.

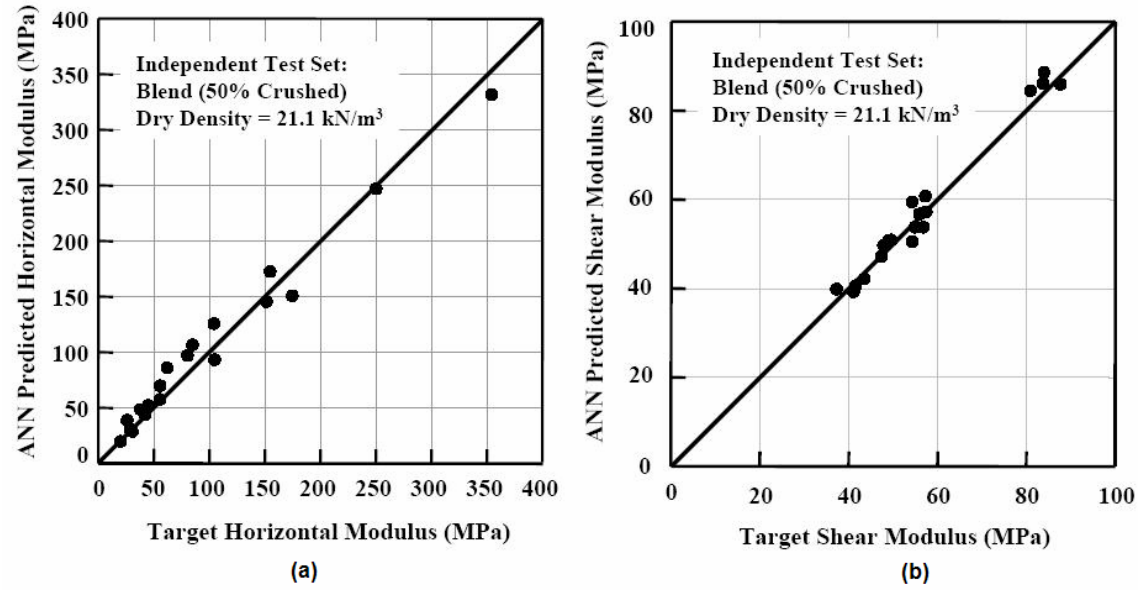

Figure 4.10. Accuracy of the (a) 5-4-1 Horizontal modulus network (b) 5-4-1 Shear modulus network (Tutumluer and Seyhan 1998)

The recurrent neural network (RNN) that is a dynamic neural system appearing effective in the input-output modeling of complex non-linear behavior of cohesionless soils was utilized by Zaman and Zhu (1998). The database was obtained from a series of triaxial compression shear tests performed on dune sand including unloading and reloading stages. Eight sets of data from triaxial compression shear tests at different effective confining stresses were employed in ANN modeling, four of which were used as training data, and the other four sets were used as testing data. The deviator stress (σ_{di}), increment of deviator stress ($\Delta\sigma_{di}$), major principle stress (σ_{1i}), increment of major principle stress ($\Delta\sigma_{1i}$), previous axial strain (ε_{1i}),

volumetric strain (ε_{vi}) and relative density (D_r) were used as input variables in the ANN model and current axial strain (ε_{1i+1}), and volumetric strain (ε_{vi+1}) were used as the outputs of the proposed model. Neural network model predictions were compared to a three invariant–dependent CAP model (a stress-strain constitutive model). The authors concluded that stress-strain behavior including unloading and reloading stages predicted by the ANN model agreed well with the measured values. The results also illustrated that ANN model was efficient in simulating non-linear behavior of cohesionless soil.

Basheer (2000) investigated the simulation of hysteresis stress-strain ($\sigma - \varepsilon$) response of geomaterials under repeated reversal loading with the time-delay artificial neural networks (TDANNs), highly non-linear mapping tools. Basheer designed a nonlinear recursive simulator containing the developed TDANNs in order to enable forecasting of complete $\sigma - \varepsilon$ curves from the knowledge of only the initial $\sigma - \varepsilon$ condition of the tested material. The author extracted the training data from a set of experimentally-obtained $\sigma - \varepsilon$ curves for the geomaterial. Stress and strain values shown in Figure 4.11(a) were used as input and output variables in the ANN model. Based on the results of the analyses, the author concluded that TDANNs were found to be viable tools for modeling the hysteresis behavior in loading reversal environmental and could be used to simulate such behavior with high accuracy for an unlimited number of cycles within and beyond the training data domain.

In a similar study, Basheer (2002) discussed the several techniques that may be used as frameworks for developing neural network based models for approximating hysteresis data. As shown in Figure 4.11(b) the input layer consisted of eight neurons, namely, (1) compaction conditions (ω and γ), (2) three-element stage label vector (virgin loading, unloading, and reloading), (3) current states of strain and stress, and the output layer consisted of one neuron: the futuristic strain for which the stress was to be predicted. The author concluded that the designed networks demonstrated high ability in simulating the real behavior of soil in all stages of loading in the neighborhood of the hysteresis and away from it.

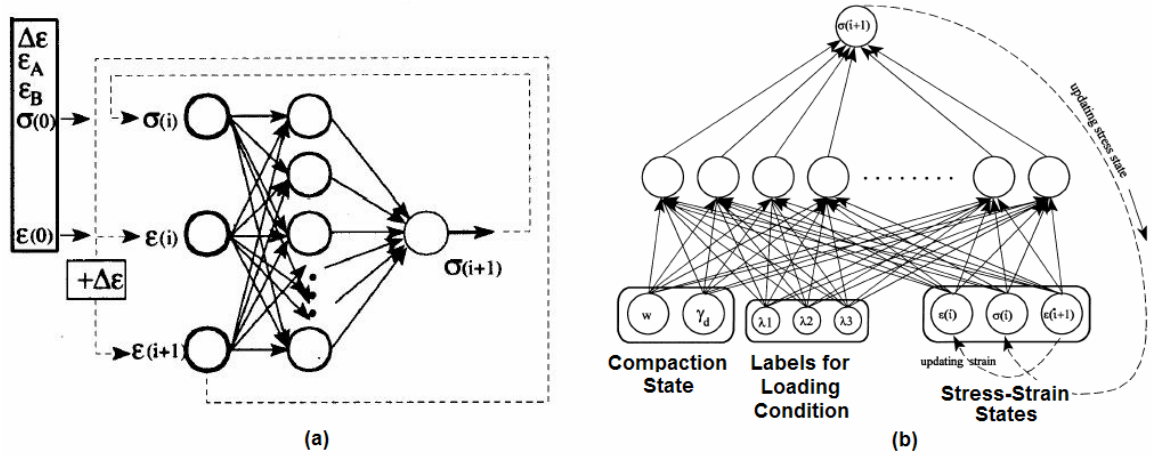

Figure 4.11. (a) Neural network architecture of the ANN-based simulator (b) Schematic of constitutive ANN-based model for the cyclic behavior of soil (Basheer 2000)

Ceylan et al. (2005d) developed ANN-based advanced aggregate rutting models and compared their performance using laboratory test data. The primary goal was to properly characterize the loading stress path dependent permanent deformation behavior from advanced repeated load triaxial tests that can simulate in the laboratory the varying stress states under actual moving wheel load conditions. Due to the complex loading regimes followed in the laboratory tests and the full-scale NAPTF (National Airport Pavement Test Facility) testing, the ANN rutting models that altogether considered as inputs the static and dynamic components of the applied stresses and the loading stress path slope produced the greatest accuracy. The authors concluded that such advanced neural network models can better describe the aggregate rutting behavior under actual field loading conditions.

Discussion: Pavement Material Modeling

Several researchers attempted to model the complex non-linear behavior of pavement materials using artificial neural networks. Pavement structure materials, especially soils are highly non-linear materials, and each type of soil shows a different behavior under different loading and environmental conditions. In the studies under this topic, ANN models were generally trained with experiment results. There are always some boundary conditions and assumptions on these experiments. Certain conditions that these experiments were conducted should be taken into account in the ANN analysis. Therefore, the limitations of the developed

ANN models (material type, loading and environmental conditions) should be clarified very clearly. It is much easier to validate the developed ANN-based models with new experiment results since the outputs of the ANN models summarized in this section are generally directly material properties.

DISCUSSION

This paper reviews a significant number of research publications which specifically deals with applications of ANNs in pavement engineering, transportation infrastructure systems between 1987 and 2007. These studies have been briefly summarized in this paper in six different categorizations: (1) predictions of pavement performance and pavement condition, (2) pavement management and maintenance strategies, (3) pavement distress forecasting, (4) structural evaluation of pavement systems, (5) image analysis and classification, and (6) pavement material modeling.

Among these categories, a main focus might be given on the structural evaluation of pavement systems since evaluating the structural condition of existing, in-service pavements is a part of the routine maintenance and rehabilitation activities undertaken by most state Department of Transportations. Several studies utilizing ANN methodology for predicting the elastic moduli, layer thickness, coefficient of subgrade reaction, shear wave velocities of pavement layers, and pavement surface deflections that are crucial structural parameters in the analysis and design of the pavements are summarized under this section. As the studies under “Structural evaluation of pavement systems” section are analyzed, it is seen that most of the proposed ANN-based models are developed for flexible (asphalt) pavement sections. In addition, developed ANN-based models use too many input parameters sometimes which is not very practical in the real life applications. Therefore, additional special interest should be given to the concrete pavements with as few practical parameters as possible in order to overcome these shortcomings. Bayrak (2007) studied the jointed Portland cement concrete pavement systems in his Ph.D. dissertation to analyze the concrete pavement parameters using the backpropagation type ANN-based models in order to fill the gap in this area. This

dissertation documented the research efforts related to the development of ANN-based concrete pavement backcalculation and forward calculation techniques which are not studied earlier. Based on the results of this research, elastic modulus of PCC slab, coefficient of subgrade reaction of pavement foundation system, radius of relative stiffness of the pavement system, maximum tensile stress at the bottom of the PCC layer, and total effective linear temperature difference between top and bottom of the PCC layer can be successfully predicted with very low average absolute error values from FWD deflection basins. One of the most important advantages of the developed ANN models in Bayrak's dissertation (2007) is the practicality and ease of use of the proposed models. The required input parameters needed for this study are falling weight deflectometer deflection basins and pavement layer thicknesses. In the developed approach, there is also no need a seed moduli or iteration process of the solution in order to predict the JPCP system parameters.

It is also well known that environmental conditions have a huge influence on the in-service pavement conditions and on the remaining life of pavements. For example, slab curling and warping in concrete pavements due to temperature and moisture differentials throughout the thickness of a slab affect the nondestructive testing results which are conducted to measure the pavement surface deflections. These erroneous measurements may divert the pavement engineers to inaccurate predictions of pavement and foundation properties and critical pavement responses. That's why curling and warping effects should be taken into account in the evaluation process of concrete pavements. Therefore, the equivalent effect of total amount of curling and warping in terms of temperature difference between the top and bottom of the concrete slabs in JPCP systems was also analyzed in Bayrak's dissertation (2007). Such an approach that takes into accounts both the traffic and environmental loading is invaluable since there is not an existing method which analyzes these effects together in JPCP systems. However, the validation of the proposed ANN-based models is a challenging problem since there is not an available method that can measure every single component of the total curling and warping in JPCP systems. The predictions of the proposed models should be used carefully and typical ranges should be taken into account in the analyses. Also, more realistic ANN-based models can be developed by using actual field data in the

training set of the ANN-based models instead of computer simulations. Bayrak (2007) concluded that trained neural network models will eventually enable pavement engineers to easily incorporate current sophisticated state-of-the-art technology into routine practical analysis and design.

SUMMARY AND CONCLUSIONS

Artificial neural network models are useful complements to more-traditional numerical and statistical methods such as regression. Once fully trained or developed, ANNs provide engineers with sophisticated, real time analysis and prediction tools with no complex analysis input requirements, such as those of finite element numerical solution techniques, and no large computer resources needed. They do not provide a priori function such as one generated by regression analysis, yet, they are not meant to be black boxes for practitioners either. ANNs commonly outperform their traditional modeling counterparts in solving complex engineering problems.

Artificial neural network modeling has shown great promise as a useful and nontraditional computing tool for analyzing too complex, non-linear problems inherent to pavement engineering. ANNs have the potential to investigate, properly model and, as a result, better understand some of the complex pavement engineering mechanisms that have not been well understood and formulated yet. This is especially possible with the vastly powerful and non-linear interconnections provided in the network architecture that enables an ANN to even model very sophisticated finite element method numerical solutions as the state-of-the-art pavement structural analysis results. As an example, the recent Mechanistic-Empirical Pavement Design Guide utilizes an ANN model to analyze rigid concrete pavements and solve for concrete pavement critical responses under environmental and traffic loading conditions.

Several successful ANN applications were reviewed in this paper for solving various pavement engineering problems in the areas of prediction of pavement performance and

condition, pavement management and maintenance strategies, pavement distress forecasting, pavement structural evaluations, image analysis and classification, and pavement material modeling. Most of the studies reviewed utilized the backpropagation type neural network models. Backpropagation ANNs are indeed very powerful and versatile networks that can be taught a mapping from one data space to another using a representative set of pattern/examples to be learned. ANN models were also noted to be able to rapidly present the required solutions by analyzing the pavement data in real time. This aspect becomes especially important in data collection and processing in real time for pavement condition and performance studies.

Use of artificial neural networks in infrastructure systems in pavement engineering has significantly increased in the past ten years. Moreover, there is still considerable work to be done in the area of infrastructural analysis in which ANNs could be used. A further issue that needs to be given some attention in the future development of ANNs is to include treatment of uncertainties associated with pavement engineering parameters. Also, more ANN-based model validations are needed with the actual laboratory and field test results and more ANN-based model interpretations should be done by field expert where the available data is very scarce. Lastly, more and larger comprehensive datasets are needed to build the models, especially for the problems where the data used to develop the ANN model is very limited. Some ANN models should be re-trained when additional data becomes available. Additionally, more comprehensive studies should be performed to see the differences between the results of different approaches on the same problem.

The use of ANNs in pavement engineering should be further pursued to make it more widespread and common among both researchers and practitioners in the field of pavement engineering. The practical use of artificial neural networks in transportation engineering is still not very common due to the lack of understanding and current skepticism even though ANNs have already proved to outperform traditional modeling techniques in solving various complex engineering problems. Transportation Research Circular (1999) stated that most of the reported ANN-based studies have not been implemented in practice since practicing

engineers are still doubtful of their use. In order to overcome these obstacles, Transportation Research Circular recommends that practicing engineers should be provided with sources of necessary background information and involved in specifically-oriented ANN workshops and tutorials.

Over the past ten years, pavement analysis and design methodologies have evolved from empirical to mechanistic-empirical and ANNs offer significant benefits in this context. Mechanistic-empirical design procedures will be based on structural analyses of pavements throughout their design life and ANNs can be used to predict the input parameters required in the mechanistic-empirical design. In addition, ANNs can also be modeled to provide the connection between the critical pavement responses and pavement performance during the design life.

Overall, despite the limitations of ANNs, they have a number of significant benefits that make them a powerful and practical tool for solving many problems in the field of pavement engineering.

ACKNOWLEDGEMENTS

The authors gratefully acknowledge the Iowa Department of Transportation (IA-DOT) for sponsoring this study. The contents of this paper reflect the views of the authors who are responsible for the facts and accuracy of the data presented within. The contents do not necessarily reflect the official views and policies of the IA-DOT. This paper does not constitute a standard, specification, or regulation.

ABBREVIATIONS / NOTATIONS

The following are the abbreviations and symbols used in this paper:

Abbrevations:

AADT = average annual daily traffic;

AASHO = American Association of State Highway Officials;
AC = asphalt concrete;
ANN = artificial neural network;
AR = auto-regression;
BPNN = back-propagation neural network;
CESAL = cumulative ESAL (equivalent single axle load, 18-kip);
CRCP = continuously reinforced concrete pavement;
CVPRIP = computer vision, pattern recognition, and image processing;
DOT = department of transportation;
ESAL = equivalent single axle load (18-kip);
FE = finite element;
FHWA = Federal Highway Administration;
FWD = falling weight deflectometer;
GANNT = genetic adaptive neural network training;
GPS = general pavement studies;
GRNN = generalized regression neural network;
HNN = histogram-based neural network;
INN = image-based neural network;
IRI = international roughness index;
JPCP = jointed plain concrete pavement;
LTE = joint load transfer efficiency;
LTPP = long term pavement performance;
M&C = material and construction;
M&R = maintenance and repair;
MC-HARP = Monte Carlo Hierarchical Adaptive Random Partitioning;
MLP = multilayer perceptron;
MLR = multiple linear regression;
NAPTF = National Airport Pavement Test Facility;
NGA = new generation aircraft;
OCR = overconsolidation ratio;

PCC = Portland cement concrete;
PCI = pavement condition index;
PCR = pavement condition rating;
PMS = pavement management system;
PNN = probabilistic neural network;
PSI = present serviceability index;
R&S = routing and sealing;
RBF = radial basis function;
RCI = riding condition index;
RMSE = root mean square error;
RNN = recurrent neural network;
SASW = spectral analysis of surface waves;
SHRP = strategic highway research program;
SN = structural number;
SPS = specific pavement studies;
TDANN = time-delay artificial neural networks;
UAB = unbound aggregate base; and
VCI = visual condition index.

Notations:

C_u = coefficient of uniformity;
E_{AC} = young's modulus of elasticity of asphalt concrete layer;
E_{PCC} = young's modulus of elasticity of Portland cement concrete layer;
ε_1 = axial strain;
ε_v = volumetric strain;
F_{200} = percent passing no. 200 sieve;
D_0 = deflection at center of loading plate (mils);
D_8 = deflection at 8 in. from the center of the FWD loading plate (mils);
D_{12} = deflection at 12 in. from the center of the FWD loading plate (mils);
D_{18} = deflection at 18 in. from the center of the FWD loading plate (mils);

D_{24} = deflection at 24 in. from the center of the FWD loading plate (mils);

D_{36} = deflection at 36 in. from the center of the FWD loading plate (mils);

D_{48} = deflection at 48 in. from the center of the FWD loading plate (mils);

D_{60} = deflection at 60 in. from the center of the FWD loading plate (mils);

D_r = relative density;

D_{50} = average aggregate size;

k = modulus of subgrade reaction;

M_R = resilient modulus;

γ_d = dry unit weight;

S = slope;

σ_1 = major principle stress;

σ_3 = confining pressure;

σ_d = deviator stress;

$\Delta\sigma_d$ = increment of deviator stress;

$\Delta\sigma_1$ = increment of major principle stress;

R^2 = coefficient of multiple determination;

τ = shear stress;

$\Delta\tau$ = increment of shear stress;

u = pore pressure;

V = shear wave velocity; and

w = crack width.

REFERENCES

Abdelrahim, A.M., and George, K. P. 2000. Artificial neural network for enhancing pavement maintenance strategy selection. Transportation Research Record, 1699, Transportation Research Board, Washington, D.C., pp. 16-22.

Adeli, H. and Hung, S.L. 1995. Machine learning: Neural networks. Genetic Algorithms, and Fuzzy Systems, Wiley, New York.

Adeli, H. and Park, H.S. 1998. Neurocomputing in design automation. CRC Press, Boca Raton, FL.

Adeli, H. 2001. Neural networks in civil engineering: 1989-2000. Computer-Aided Civil and Infrastructure Engineering, 16: 126-142.

Alsugair, A.M., and Al-Quadrah, A.A. 1998. Artificial neural network approach for pavement maintenance. Journal of Computing in Civil Engineering, ASCE, 12(4): 249-255.

Attoh-Okine, N.O. 1993. Using neural network to identify pavement structure based on radar output. Pacific Rim TransTech Conf. ASCE, NY, pp. 450-456.

Attoh-Okine, N.O. 1994. Predicting roughness progression in flexible pavements using artificial neural networks. Third International Conference on Managing Pavements, Conference Proceedings, Vol. 1, pp. 55-62.

Attoh-Okine, N.O. 1996. Predicting cracking index in flexible pavements: Artificial neural network approach. Reflecting Cracking in Pavements, Proceedings of the Third International RILEM Conference, London, England, pp. 153-160.

Attoh-Okine, N. O. 1999. Analysis of learning rate and momentum term in backpropagation neural network algorithm trained to predict pavement performance. Advances in Engineering Software, 30: 291-302.

Attoh-Okine, N.O. 2001. Grouping pavement condition variables for performance modeling using self-organizing maps. Computer-Aided Civil and infrastructure Engineering, 16: 112-125.

Banan, M.R., and Hjelmstad, K.D. 1996. Neural networks and AASHO road tests. Journal of Transportation Engineering, 122 (5): 358-366.

Basher, I.A. 2000. Selection of methodology for neural network modeling of constitutive hystereses behavior of soils. Computer-Aided Civil and Infrastructure Engineering, 15: 440-458.

Basher, I. A. 2002. Stress-strain behavior of geomaterials in loading reversal simulated by

time-delay neural networks. Journal of Materials in Civil Engineering, ASCE, 14(3): 270-273.

Bosurgi, G. and Trifiro, F. 2005. A model based on artificial neural networks and genetic algorithms for pavement maintenance management. International Journal of Pavement Engineering, 6(3): 201-209.

Ceylan, H., Tutumluer, E., and Barenberg, E. J. 1998. Artificial neural networks as design tools in concrete airfield pavement design. Proceedings of the 25th ASCE International Air Transportation Conference, Austin, Texas, USA, pp. 447-465.

Ceylan, H., Tutumluer, E., and Barenberg, E.J. 1999a. Analysis of concrete airfield slabs serving the Boeing 777 aircraft using artificial neural networks. Journal of the Transportation Research Board, 1684: 110-117.

Ceylan, H., Tutumluer, E., and Barenberg, E.J. 1999b. Artificial neural network analysis of concrete airfield pavements serving the Boeing B-777 aircraft. Transportation Research Record, 1684, Transportation Research Board, Washington, D.C., pp. 110-117.

Ceylan, H., Tutumluer, E., and Barenberg, E.J. 2000. Effects of simultaneous temperature and gear loading on the response of concrete airfield pavements serving the Boeing 777 aircraft. Proceedings of the ASCE 26th International Air Transportation Conference, San Francisco, California, USA, pp. 25-44.

Ceylan, H. 2002. Analysis and design of concrete pavement systems using artificial neural networks. Ph.D. Dissertation, University of Illinois at Urbana-Champaign, Department of Civil Engineering, Urbana, IL, USA, 256 pp.

Ceylan, H. 2004. Use of artificial neural networks for the analysis & design of concrete pavement systems. 5th International CROW-workshop on Fundamental Modeling of the design and performance of concrete pavements, Istanbul, Turkey, March 30-April 2.

Ceylan, H. and Guclu, A. 2004a. Use of artificial neural networks for the analysis and

design of concrete pavement systems serving the A380-800 aircraft. Intelligent Engineering Systems Through Artificial Neural Networks, ANNIE-2004, 14, pp. 665-670.

Ceylan, H., Guclu, A., Tutumluer, E., Thompson, M.R., and Gomez-Ramirez F. 2004b. Neural network-based structural models for rapid analysis of flexible pavements with unbound aggregate layers. In Proceedings of the 6th International Symposium on Pavements Unbound (UNBAR6), Nottingham, England, July 6-8, pp. 139-147.

Ceylan, H., Bayrak, M.B. and Guclu, A. 2005a. Use of neural networks to develop robust backcalculation algorithms for nondestructive evaluation of flexible pavement systems. Intelligent Engineering Systems Through Artificial Neural Networks, ANNIE-2005, 15, 731-740.

Ceylan, H., Bayrak, M.B., Guclu, A., Tutumluer, E. 2005b. Forward and Backcalculation of Nonlinear Pavement Systems Using Neural Networks. In Proceedings of the 11th International Conference of the Association for Computer Methods and Advances in Geomechanics (IACMAG), Turin, Italy, June 19-24, 571-578.

Ceylan, H., Guclu, A., Tutumluer, E., and Thompson, M.R. 2005c. Use of Artificial Neural Networks for Analyzing Full Depth Asphalt Pavements. International Journal of Pavement Engineering, 6 (3): 171-182.

Ceylan, H., Guclu, A., Tutumluer, E., and Pekcan, O. 2005d. Advanced Models for Predicting Aggregate Rutting Behavior. In Proceedings of the 7th International Conference on the Bearing Capacity of Roads, Railways and Airfields, Trondheim, Norway, June 27-29, 2005.

Cheng, H. D., Jingli Wang, J., Hu, Y. G. and Glazier, C. 2001. A novel approach to pavement cracking detection based on neural network. Transportation Research Records, 1764, pp. 119-127.

Choi, J., Adams, T.M., and Bahia, H.U. 2004. Pavement roughness modeling using back-propagation neural networks. Computer-Aided Civil and infrastructure Engineering,

19: 295-303.

Construction Engineering Laboratory and Facilities Group. 1982. ILLIPAVE-A Finite Element Program for the Analysis of Pavements. Department of Civil Engineering, University of Illinois at Urbana.

Dougherity, M. 1995. A review of neural networks applied to transport. Transportation Research, Part C, 3(4): 247-260.

Duncan, J.M., Monismith, C.L., and Wilson, E.L. 1968. Finite element analysis of pavements. Highway Research Record 228, Highway Research Board, Washington, D.C., pp.18-33.

Eldin, N.N. and Senouci, A.B. 1994. Measurement and prediction of the strength of rubberized concrete. Cement & Concrete Composites, 16: 287-298.

Eldin, N.N. and Senouci, A.B. 1995a. Condition rating of rigid pavements by neural networks. Can. J. Civ. Eng., 22: 861-870.

Eldin, N.N. and Senouci, A.B. 1995b. Use of neural networks for condition rating of jointed concrete pavements. Advances in Engineering Software, 23:133-141.

Eldin, N.N. and Senouci, A.B. 1995c. A pavement condition rating model using backpropagation neural networks. Microcomputers in Civil Engineering, 10 (6): 433-441.

Fausett, L. 1994. Fundamentals of Neural Networks. Prentice-Hall, Inc., New York.

Flintsch, G., Zaniewski, J. and Delton, J. 1996. Artificial neural network for selecting pavement rehabilitation projects. Transportation Research Record, 1524, Transportation Research Board, Washington, D.C., pp. 177-193.

Fwa, T.F. and Chan, W.T. 1991. Priority rating of highway maintenance needs by neural networks. Journal of Transportation Engineering, ASCE, 119(3): 419-432.

George, K.P., El-Rahim, A. and Shekharan, A.R. 1998. Updates of pavement performance modeling. Third International Conference on Road and Airfield Pavement

Technology, Proceedings, Beijing, China, Vol.1, pp. 402-410.

Ghaboussi, J., Garrett Jr., J.H., and Wu, X. 1991. Knowledge-Based modeling of material behavior with neural networks. Journal of Engineering Mechanics, 117(1): 132-153.

Ghaboussi J. and Sidarta, D.E. 1998. New nested adaptive neural networks (NANN) for constitutive modeling. Computer and Geotechnics, 22(1): 29-52.

Goh, A.T.C. 1997. A hybrid neural network based pavement management system. Road & Transport Research, 6(4): 62-71.

Goktepe, B.A., Agar, E., and Lav, H.A. 2006. Role of learning algorithm in neural network-based backcalculation of flexible pavements. Journal of Computing in Civil Engineering, 20(5): 370-373.

Golden, R.M. 1996. Mathematical methods for neural network analysis and design. MIT Press, Cambridge, MA.

Gucunski, N., and Krstic, V. 1996. Backcalculation of pavement profiles from Spectral-Analysis-of-Surface-Waves test by neural networks using individual receiver spacing approach. Transportation Research Record, 1526, Transportation Research Board, Washington, D.C., pp. 6-13.

Hajek, J.J., Haas, R.C.G. and Phang, W.A. 1987. ROSE: A knowledge-based expert system for routing and sealing. Proceedings of the Second North American Pavement Management Conference, Toronto, Canada, 2.301-2.341.

Haykin, S. 1994. Neural Networks: A Comprehensive Foundation. Macmillan Publishing, New York.

Haykin, S. 1999. Neural Networks: A Comprehensive Foundation. Prentice-Hall Inc., New York.

Hegazy, T., Fazio, P., and Moselhi, O. 1994. Developing practical neural network applications using backpropagation. Microcomputers in Civil Engineering, 9(2): 145-159.

Heiler, M., McNeil, S., and Garrett, J.J. 1995. Ground-penetrating radar for highway and bridge deck condition assessment and inventory. SPIE - The International Society for Optical Engineering, Nondestructive Evaluation of Aging Bridges and Highways, 2456, Oakland, CA, pp. 195-206.

Huang, Y. and Moore, R.K. 1997. Roughness level probability prediction using artificial neural networks. Transportation Research Record, 1952, Transportation Research Board, Washington, D.C., pp. 89-97.

Ioannides, A.M., Alexender, D.R., Hammons, M.I., and Davis, C.M. 1996. Application of artificial neural networks to concrete pavement joint evaluation. Transportation Research Record, 1540, Transportation Research Board, Washington, D.C., pp. 56-64.

Issa, R. and Zaman, M. 1999. Estimating resilient modulus of aggregate base by backpropagation neural network model. Proc. 4th Int. Conf. on Constitutive Laws for Engineering Materials, RPI, Troy, New York, pp. 493-496.

Kaseko, M.S., and Ritchie, S.G. 1991. Pavement image processing using neural networks. Proceedings of the Second International Conference on Applications of Advanced Technologies in Transportation Engineering, ASCE, NY, pp. 238-242.

Kaseko, M.S., and Ritchie, S.G. 1992. A neural network-based methodology for automated distress classification of pavement images. Proceedings of the International Conference on Artificial Intelligence Applications in Transportation Engineering, pp. 195-214.

Kaseko, M.S., Ritchie, S.G. and Lo, Z.P. 1993a. A neural network-based methodology for pavement crack detection and classification. Transportation Research, Part C:Emerging Tech.,1C(4), pp. 275-291.

Kaseko, M.S., Ritchie, S.G. and Lo, Z.P. 1993b. Evaluation of two automated thresholding techniques for pavement images. Proc. of the Infrastructure Planning and Management, ASCE, pp. 277-284.

Kaseko, M.S., Lo, Z.P., and Ritchie, S.G. 1994. Comparison of traditional and neural

classifiers for pavement-crack detection. Journal of Transportation Engineering, ASCE, 120(4): 552-569.

Khazanovich, L., and Ioannides, A.M. 1995. DIPLOMAT: Analysis program for bituminous and concrete pavements. Transportation Research Record, 1482, Transportation Research Board, Washington, D.C., pp. 52-60.

Khazanovich, L. and Roesler, J. 1997. DIPLOBACK: A neural networks-based backcalculation program for composite pavements. Transportation Research Record, 1570, Transportation Research Board, Washington, D.C., pp. 143-150.

Kim, Y. and Kim, Y.R. 1998. Prediction of layer moduli from FWD and surface wave measurements using artificial neural network. Transportation Research Record, 1639, Transportation Research Board, Washington, D.C., pp. 53-61.

La Torre, F., Domenichini, L. and Darter, M.I. 1998. Roughness prediction model based on the artificial neural network approach. Fourth International Conference on Managing Pavements, pp. 599-612.

Lee, B.J., and Lee, H.D. 2004. Position-Invariant neural network for digital pavement crack analysis. Computer-Aided Civil and infrastructure Engineering, 19: 105-118.

Lin, J.D., Yau, J.T., and Hsiao, L.H. 2003. Correlation analysis between international roughness index (IRI) and pavement distress by neural network. 82th Annual Meeting, Transportation Research Board, Washington D.C., USA.

Lou, Z., Gunaratne, M., Lu, J.J., and Dietrich, B. 2001. Application of neural network model to forecast short-term pavement crack condition: Florida case study. Journal of Infrastructure Systems, ASCE, 7(4): 166-171.

Lu, J. J., Lou, Z., and Gunaratne, M. 1999. Road surface crack condition forecasting using neural network models. Florida Department of Transportation Report, Florida, USA.

Mehrotra, K., Mohan, C.K., and Ranka, S. 1997. Elements of artificial neural networks, MIT Press, Cambridge, MA.

Mei. X., Gunaratne, M., Lu, J.J., and Dietrich, B. 2004. Neural network for rapid depth

evaluation of shallow cracks in asphalt pavements. Computer-Aided Civil and Infrastructure Engineering, 19: 223-230.

Meier, R.W. and Rix, G.J. 1994. Backcalculation of flexible pavement moduli using artificial neural network. Transportation Research Record, 1448, Transportation Research Board, Washington, D.C., pp. 75-82.

Meier, R.W. and Rix, G.J. 1995. Backcalculation of flexible pavement moduli from dynamic deflection basins using artificial neural network. Transportation Research Record, 1473, Transportation Research Board, Washington, D.C., pp. 72-81.

Meier, R.W., Alexander, D.R., and Freeman, R.B. 1997. Using artificial neural networks as a forward approach to backcalculation. Transportation Research Record, 1570, Transportation Research Board, Washington, D.C., pp. 126-133.

Najjar, Y. and Felker V. 2003. Modeling the time dependent roughness performance of Kansas PCC pavements. Smart Engineering System Design: Neural Networks, Fuzzy Logic, Evolutionary Programming, Complex Systems and Artificial Life - Proceedings of the Artificial Neural Networks in Engineering Conference, Vol.13, pp 883-888.

Nallamothu, S. and Wang, K.C.P. 1996. Experimenting with recognition accelerator for pavement distress identification. Transportation Research Record, 1536, Transportation Research Board, Washington, D.C., pp. 130-135.

National Cooperative Highway Research Program. 2004. Development of the 2002 Guide for the Design of New and Rehabilitated Pavement Structures: Phase II, Project 1-37A, NCHRP.

Owusu-Ababio, S. 1995. Modeling skid resistance for flexible pavements: A comparison between regression and neural network models. Transportation Research Record, 1501, Transportation Research Board, Washington, D.C., pp. 60-71.

Owusu-Ababio, S. 1998. Effect of neural network topology on flexible pavement cracking prediction.Computer-Aided Civil and infrastructure Engineering, 13: 349-355.

Owusu-Ababio, S. 1998. Application of neural networks to modeling thick asphalt pavement performance. Artificial Intelligence and Mathematical Methods in Pavement and Geomechanical Systems, pp.23-30.

Patterson, D. 1996. Artificial Neural Networks. Prentice-Hall, Inc., Singapore.

Penumadu, D. and Jean-Lou, C. 1997. Geomaterial modeling using artificial neural networks. Artificial Neural Networks for Civil Engineers: Fundamentals and Applications, pp. 160-184.

Rakesh, N., Jain, A. K., Reddy, M. A., and Reddy, K. S. 2006. Artificial neural networks - Genetic algorithm based model for backcalculation of pavement layer moduli. International Journal of Pavement Engineering, 7(3): 221-230.

Robert, C.A. and Attoh-Okine, N.O. 1998. A comparative analyses of two artificial neural networks using pavement performance prediction. Computer-Aided Civil and Infrastructure Engineering, 13: 339-348.

Rumelhart, D.E., Hinton, G.E., and Williams, R.J. 1986. Learning integral representation by error propagation, in Rumelhart, D.E. et al., eds., Parallel Distributed Processing, MIT Press, Cambridge, MA, pp. 318-362.

Saltan, M., Tigdemir, M., and Karasahin, M. 2002. Artificial neural network application for flexible pavement thickness modeling. Turkish J. Eng. Env. Sci. 26: 243-248.

Schwartz, C.W. 1993. Infrastructure condition forecasting using neural networks. Proc. of the Infrastructure Planning and Management, ASCE, pp. 282-284.

Shekharan, A.R. 2000. Pavement performance prediction by artificial neural network. Computational Intelligence Applications in Pavement and Geomechanical Systems, pp 89-98.

Sidarta, D.E. and Ghaboussi J. 1998. Constitutive modeling of geomaterials from non-uniform material tests. Computer and Geotechnics, 22(1): 53-71.

Sundin, S. 1998. Predicting rut depth in pavements using artificial neural networks. Nimes `98 Conference on Complex Systems, Intelligent Systems, & Interfaces, La Lettre de

1`IA Nimes 98, pp. 263-266.

Sundin, S. and Braban-Ledoux, C. 2001. Artificial intelligence-based decision support technologies in pavement management. Computer-Aided Civil and Infrastructure Engineering, 16:143-157.

Tabatabaie, A.M. 1977. Structural analysis of concrete pavement joints. PhD thesis, Univ. of Illinois at Urbana-Champaign, Urbana, IL, USA.

Taha, M.A. and Hanna, Awad, S. 1995. Evolutionary neural network model for the selection of pavement maintenance strategy. Transportation Research Record, 1497, Transportation Research Board, Washington, D.C., pp. 70-76.

Transportation Research Circular. 1999. Use of Artificial Neural Networks in Geomechanical and Pavement Systems. Transportation Research Board / National Research Council, Number E-CO12.

Tutumluer, E. and Meier, R. W. 1996. An Attempt at Resilient Modulus Modeling Using Artificial Neural Networks. Transportation Research Record No. 1540, TRB, National Research Council, Washington, D. C., 1-6.

Tutumluer, E., and Seyhan, U. 1998. Neural network modeling of anisotropic aggregate behavior from repeated load triaxial tests. Transportation Research Record. 1615, Transportation Research Board, Washington, D.C., pp. 86–93.

Van Cauwelaert, F.J., Alexander, D.R., White, T.D., and Barker, W.R. 1989. Multilayer elastic program for backcalculating layer moduli in pavement evaluation. ASTM STP 1026, West Conshohocken, Pa.

Van der Gryp, A., Bredenhann, S.J., Henderson, M.G. and Rohde, G.T. 1998. Determining the visual condition index of flexible pavements using artificial neural networks. Fourth International Conference on Managing Pavements, Durban, South Africa, 2, pp. 115-129.

Wang, K.C.P. 1995. Feasibility of applying embedded neural net chip to improve pavement surface image processing. Journal of Computing in Civil Engineering, ASCE, 1:589-

595.

Williams, T.P., and Gucunski, N. 1995. Neural networks for backcalculation of moduli from SASW test. Journal of Computing in Civil Engineering, ASCE, 9(1): 1-8.

Yang, J., Lu, J.J., Gunaratne, M., and Xiang, Q. 2003. Forecasting overall pavement condition using neural networks: - Application on Florida highway network. Transportation Research Record, 1853, Transportation Research Board, Washington, D.C., pp. 3-12.

Zaman, M. and Zhu, J.H. 1998. A neural network model for a cohesionless soil. Proc. Int. Workshop on Artificial Intelligence and Math. Methods in Pavement and Geomechanical Sys., Florida Atlantic Univ., Miami, pp. 39-54.

Zhu, J.H., Zaman, M., and Trafalis, T.B. 1996. Prediction of shear stress-strain behavior of soil with recurrent neural network. Proc. Artificial Neural Networks in Engineering (ANNIEÆ96), Vol. 6, Smart Engineering Systems: Neural Networks, Fuzzy Logic and Evolutionary Programming, St. Louis, Missouri, pp. 809-814.

CHAPTER 5. USE OF NEURAL NETWORKS TO DEVELOP ROBUST BACKCALCULATION AND FORWARD CALCULATION MODELS FOR CONCRETE PAVEMENT SYSTEMS

A paper to be submitted to *The Journal of Transportation Engineering (ASCE)*

Mustafa Birkan Bayrak and Halil Ceylan

ABSTRACT:

This paper presents a study to develop artificial neural network (ANN)-based backcalculation and forward calculation models for predicting the concrete pavement parameters, i.e., the elastic modulus of Portland cement concrete (PCC) slab (E_{PCC}), the coefficient of subgrade reaction (k_S) of the pavement foundation, the radius of relative stiffness (RRS) of the pavement system, and the maximum tensile stresses at the bottom of the Portland cement concrete layer (σ_{MAX}) from falling weight deflectometer (FWD) deflection basin data and the thickness of the concrete pavement structure. The ISLAB2000 finite element (FE) program, extensively tested and validated for over 20 years, has been used as an advanced structural model for solving the responses of the concrete pavement systems and generating a large knowledge database. The trained ANN-based models were capable of predicting the concrete pavement parameters and critical pavement responses with very low average absolute error (AAE) values. In order to develop more robust networks that can tolerate the noisy or inaccurate pavement deflection patterns collected from the FWD field tests, several network architectures were trained with varying levels of noise in them. Applied noise levels in deflection basins ranged from ± 2% to ± 10% to train the robust ANN models that can account for the variations in deflection measurements due to poor testing practices. ANN-based model predictions were also compared with the other methods. A sensitivity study was conducted to determine the most suitable ANN architecture for this specific problem. In addition, another sensitivity study was conducted to verify the significance of the layer thicknesses and the effect of bonding between the PCC and the base layer in the backcalculation procedure. Finally, the results of this study demonstrated that the

developed ANN-based models can successfully predict the concrete pavement parameters and critical pavement responses with high accuracy.

Key Words: Artificial Neural Networks, Falling Weight Deflectometer, Finite Element Analysis, Concrete Pavements, Pavement Layer Backcalculation and Forward Calculation.

INTRODUCTION

Falling weight deflectometer (FWD) and heavy weight deflectometer (HWD) testing have become the main nondestructive testing (NDT) techniques to structurally evaluate the in-service pavements over the last twenty years. Falling weight deflectometer testing is often preferred over destructive testing methods because FWD testing is faster than destructive tests and do not entail the removal of pavement materials. In addition, the testing apparatus is easily transportable. Pavement properties are "backcalculated" from the observed dynamic response of the pavement surface to an impulse load (the falling weight). To evaluate the structural condition of in-service pavements and to characterize the layer properties as inputs into available numerical or analytical programs, backcalculation of pavement layer properties is a very useful tool. Most backcalculation procedures estimate pavement properties by matching measured and calculated pavement surface deflection basins.

There are many advantages to using FWD tests, in lieu of, or supplement traditional destructive tests for pavement structural evaluation. Most important, is the capability to quickly gather data at several locations while keeping a runway, taxiway, or apron operational during these 2-minute to 3-minute tests, provided the testing is performed in close coordination with the Air Traffic Control. Without FWD/HWD testing, structural data must be obtained from numerous cores, borings, and excavation pits on existing highway/airport pavements. This can be very disruptive to highway/airport operations. FWD tests are economical to perform and data can be collected at up to 250 locations per day. The FWD/HWD equipment measures pavement surface deflections from an applied dynamic load that simulates a moving wheel (FAA 2004).

Backcalculated pavement layer parameters play a crucial role in pavement management systems in project specific and network level pavement testing and evaluation for Department of Transportations (DOTs) to make decisions on overall maintenance and budget plans. The primary focus of this study is to rapidly analyze large number of pavement deflection basins needed for routine pavement evaluation for both project specific and network level FWD testing. The backcalculated pavement parameters for the jointed plain Portland cement concrete pavement (JPCP) systems in this study are elastic modulus of the PCC slab, and coefficient of subgrade reaction of the pavement foundation. In addition to these concrete pavement parameters, radius of relative stiffness and maximum tensile stress at the bottom of the PCC layer were also forward calculated by developed ANN-based models since there is a strong relationship between critical pavement responses and the pavement performance.

Over the years, researchers have developed several different methodologies for backcalculation of concrete pavement layer moduli from FWD measurements, including the AREA method for concrete pavements (Ioannides et al. 1989; Ioannides 1990; Barenberg and Petros 2006), ILLI-BACK (Ioannides 1994), graphical solution using ILLI-SLAB (Foxworthy and Darter 1989), use of regression analysis to solve AREA method for concrete pavements (Hall 1992; Hall et al. 1996), use of best fit algorithm to find radius of relative stiffness (Hall et al. 1996; Smith et al. 1996), and many others. FWD deflection basins and PCC slab thickness are the only information needed for predicting the concrete pavement parameters with developed ANN-based models. There is no need for the provision of seed moduli in the developed approach. The use of the ANN models also results in a drastic reduction in computation time compared to other methodologies.

FINITE ELEMENT PROGRAMS FOR CONCRETE PAVEMENTS

Today, a variety of finite element (FE) programs are available for the analysis and design of pavement systems. The two main categories of FE programs are those: (1) programs

specifically designed for the analysis of pavement systems, and (2) general-purpose programs. Finite element programs such as ABAQUS, ANSYS, and DYNA3D are powerful general-purpose programs with three-dimensional non-linear dynamic analysis capabilities. In several research studies, these programs have successfully been used for pavement analysis. A number of FE models built using these programs have been reported in the literature (Mallela and George 1994; Darter et al. 1995; Kennedy 1998). On the other hand, considerable computational resources and time needed for analyzing a structural system are among the limitations of the general-purpose FE programs.

There are also FE-based programs developed specifically for analysis of concrete pavement systems such as ISLAB2000 (Tabatabaie and Barenberg 1978; Khazanovich 1994; Khazanovich et al. 2000), DIPLOMAT (Khazanovich and Ioannides 1995), KENSLABS (Huang 1985), WESLIQID (Chou 1981), J-SLAB (Tayabji and Colley 1983), FEACONS-IV (Tia et al. 1988), KOLA (Kok 1990), and EverFE (Davids et al. 1998). Most of these programs can analyze multi-wheel loading of one- or two-layered medium thick plates resting on a Winkler foundation or elastic solid (ISLAB2000, KENSLABS, WESLIQID). EverFE can analyze multi-layered pavement systems using a 3D-continuum brick element for the Portland cement concrete (PCC) and base layers. ISLAB2000 contains many advanced features that distinguish it from other pavement programs that are based on the plate theory.

In addition to the FE programs, Westergaard (1926) solutions (plate theory) for PCC pavements are also used to analyze the concrete pavements. ANN trainings are also used to interpret results from databases of deflection profiles to estimate pavement properties (Ceylan 2004; Ceylan et al. 2004; Ceylan et al. 2005). Although there are different FE programs and other approaches to analyze the concrete pavements, all methods do not produce exactly the same results. In order to better understand the results produced by different programs, a sensitivity analysis was performed as part of this study.

Comparison of Finite Element Models and Closed-Form Solutions

A sensitivity study was performed to analyze the differences in the slab-center deflections (D_0, the maximum FWD deflection) obtained from ISLAB2000, DIPLOMAT, KENSLABS and Westergaard solutions. ISLAB2000 is a FE modeling program designed specifically for analyzing concrete pavements. In large part, it is an extension and improvement of the ILLI-SLAB (Foxworthy and Darter 1989) and ILSL2 (Khazanovich 1994) programs. ISLAB2000 is a significant improvement over it's predecessors for the analysis of concrete pavement systems, enabling users to analyze a wide range of problems.

ISLAB2000 allows the user to define an "unlimited" number of nodes, pavement layers, and wheel loads. It also includes an improved void analysis model. DIPLOMAT was developed by Khazanovich and Ioannides (1995), which is an extension of elastic layer and plate theories. Several programs have been developed based on Burmister elastic layer solutions, but only DIPLOMAT can model pavement layers as plates, springs and/or elastic layers together. On the other hand, one disadvantage of DIPLOMAT and other elastic layer programs (ELPs) is that joints cannot be modeled because layers are assumed infinite in the horizontal direction. The KENSLABS computer program is based on the FE method, in which slabs are divided into rectangular FE with a large number of nodes. KENSLABS can be applied to a maximum of 6 slabs, 7 joints, and 420 nodes. Both wheel loads and subgrade reactions are applied to the slab as vertical concentrated forces at the nodes.

In this study, plate theory was used in the analyses and the pavement foundation is assumed as dense-liquid foundation (as Winkler-spring method). Different configurations of E_{PCC}, h_{PCC}, and k_S were defined and the D_0 deflections obtained from ISLAB2000, DIPLOMAT, and KENSLABS FE programs and Westergaard solutions were compared with each other (see Figure 5.1). The deflection profiles obtained from ISLAB2000, DIPLOMAT, and KENSLABS FE models for two pavement configurations were also presented in Figure 5.2.

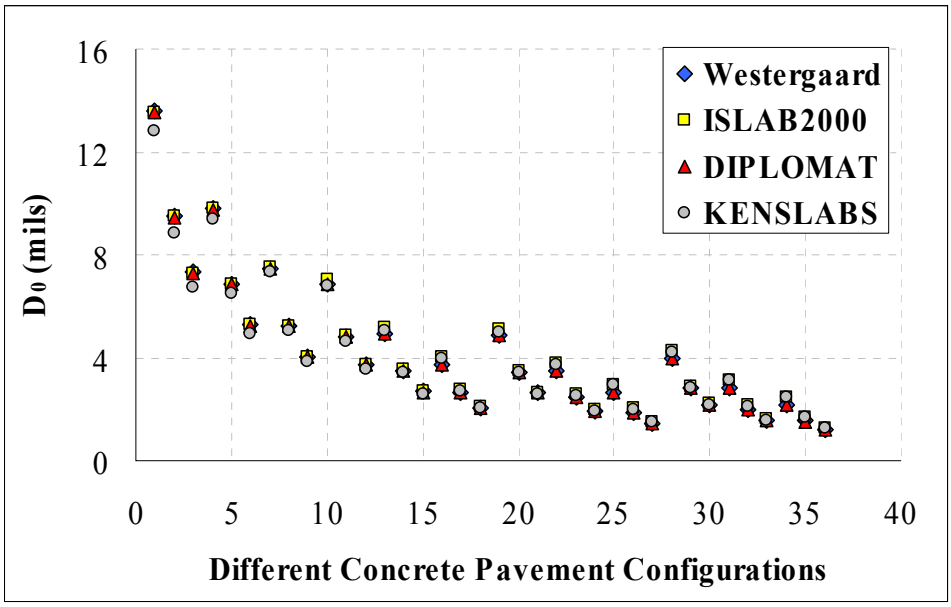

Figure 5.1. Comparison of ISLAB2000, DIPLOMAT, and KENSLABS finite element model solutions with Westergaard theoretical solutions

As can be seen from Figures 5.1 and 5.2, a good match was obtained for results from different models. Finally, a solution database using the ISLAB2000 FE model was created since the ISLAB2000 is convenient due to the ease of modeling and flexibility in the analysis compared to other methods. ISLAB2000 can also analyze partially bonded layers, the effects of non-linear temperature distribution throughout the constructed layers, the mismatched joints and cracks and the effect of voids under the slab. On the other hand, there might be various reasons of the observed differences in the deflection profiles obtained from different methods. These reasons can be listed as follows.

- ISLAB2000 and KENSLABS use finite slabs in the analysis (slab sizes, joints, and load transfer efficiencies must be identified in the programs) but DIPLOMAT and Westergaard solutions do not take into account the slab size, joints and load transfer efficiencies.
- ISLAB2000 and KENSLABS use a rectangular or square loading area. On the other hand, DIPLOMAT and Westergaard solutions consider circular loading area.

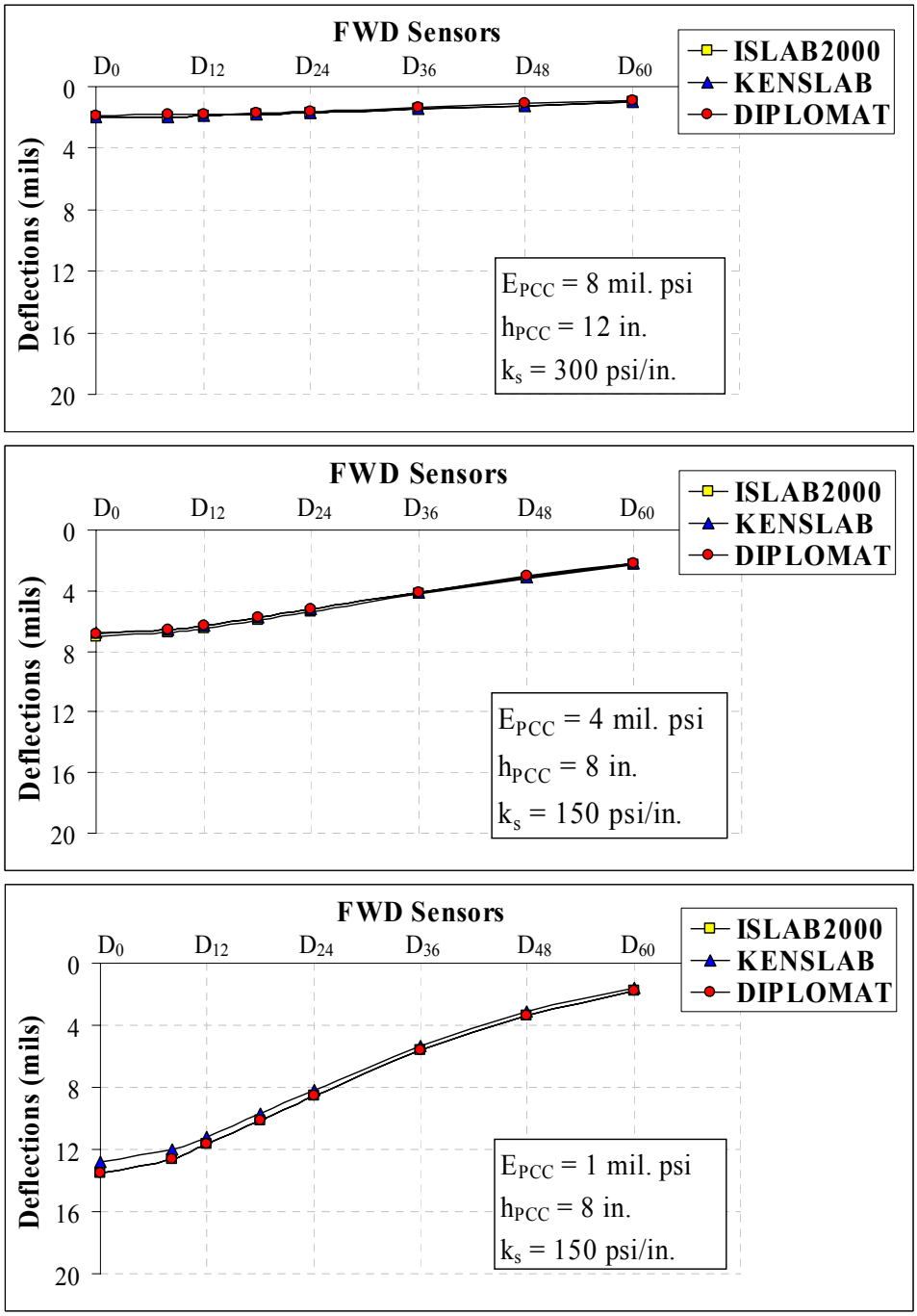

Figure 5.2. Comparison of ISLAB2000, DIPLOMAT, and KENSLAB finite element model solutions for different pavement configurations

GENERATING ISLAB2000 FINITE ELEMENT SOLUTION DATABASE

ISLAB2000 (Khazanovich et al. 2000) runs were generated by modeling slab-on-grade concrete pavement systems in order to train the ANN-based models. A single slab layer resting on a Winkler foundation was analyzed in all cases. Concrete pavements analyzed in this study were represented by a six-slab assembly, each slab having dimensions of 20 ft by 20 ft (see Figure 5.3). A standard ISLAB2000 FE mesh (10,004 elements with 10,209 nodes) was constructed for the slab to maintain the same level of accuracy in the results from all analyses. A general view of the ISLAB2000 FE solution used in the study is shown in Figure 5.4.

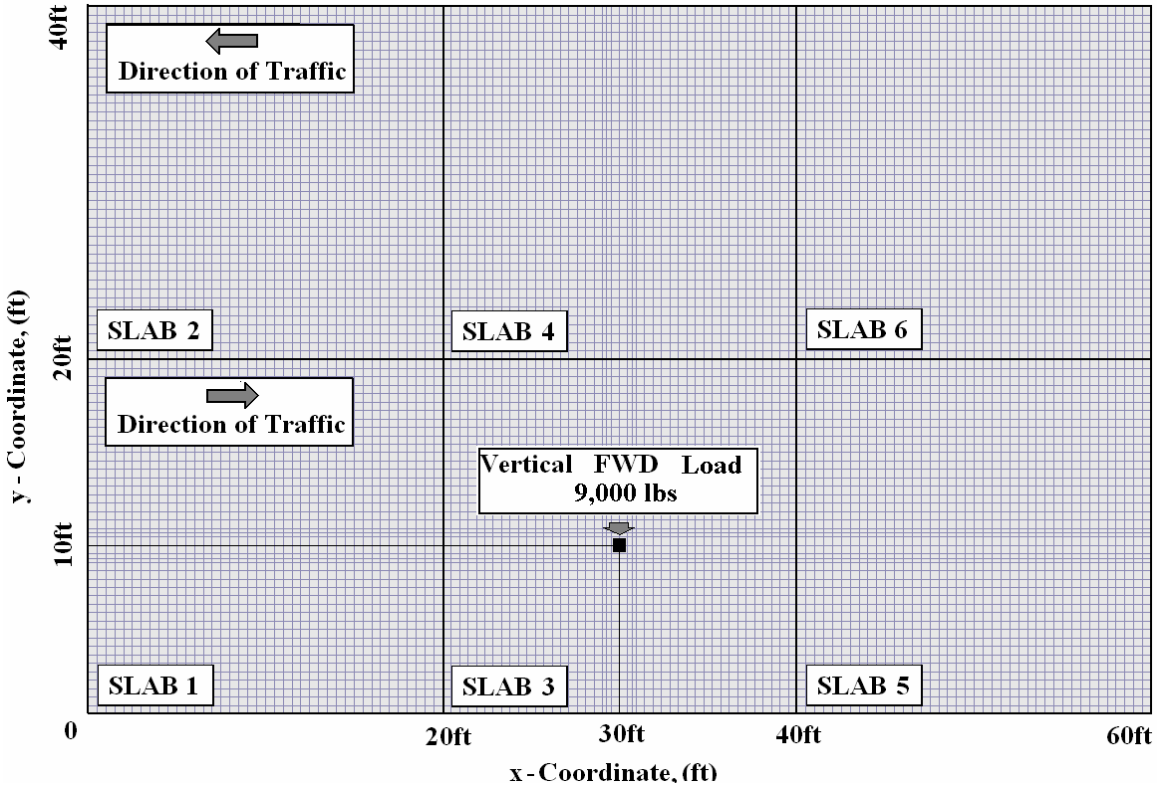

Figure 5.3. ISLAB2000 finite element model meshing for the six-slab JPCP assembly

The ISLAB2000 solutions database was generated by varying the elastic modulus of PCC slab, coefficient of subgrade reaction, and thickness of the PCC layer (h_{PCC}) over a range of values representative of realistic variations in the field. The ranges used in the ISLAB2000 analyses are shown in Table 5.1. Poisson's ratio, slab width, slab length, PCC slab unit weight, and coefficient of thermal expansion were set equal to 0.15, 20 ft, 20 ft, 0.087 lb/in^3,

$5.5x10^{-6}$ 1/°F, respectively. The total number of ISLAB2000 runs conducted in this study was 51,539. For each training, the ISLAB2000 solution database was first portioned to create a training set and an independent testing set of 2,000 patterns to check the prediction performance of the trained ANN-based models.

Table 5.1. Ranges of the input parameters used in the ISLAB2000 database generation

Pavement slab inputs	**Min. Value**	**Max. Value**
E_{PCC}, ksi	1,000	15,000
h_{PCC}, in.	6	25
Pavement foundation inputs	**Min. Value**	**Max. Value**
k_S, psi/in.	50	1,000

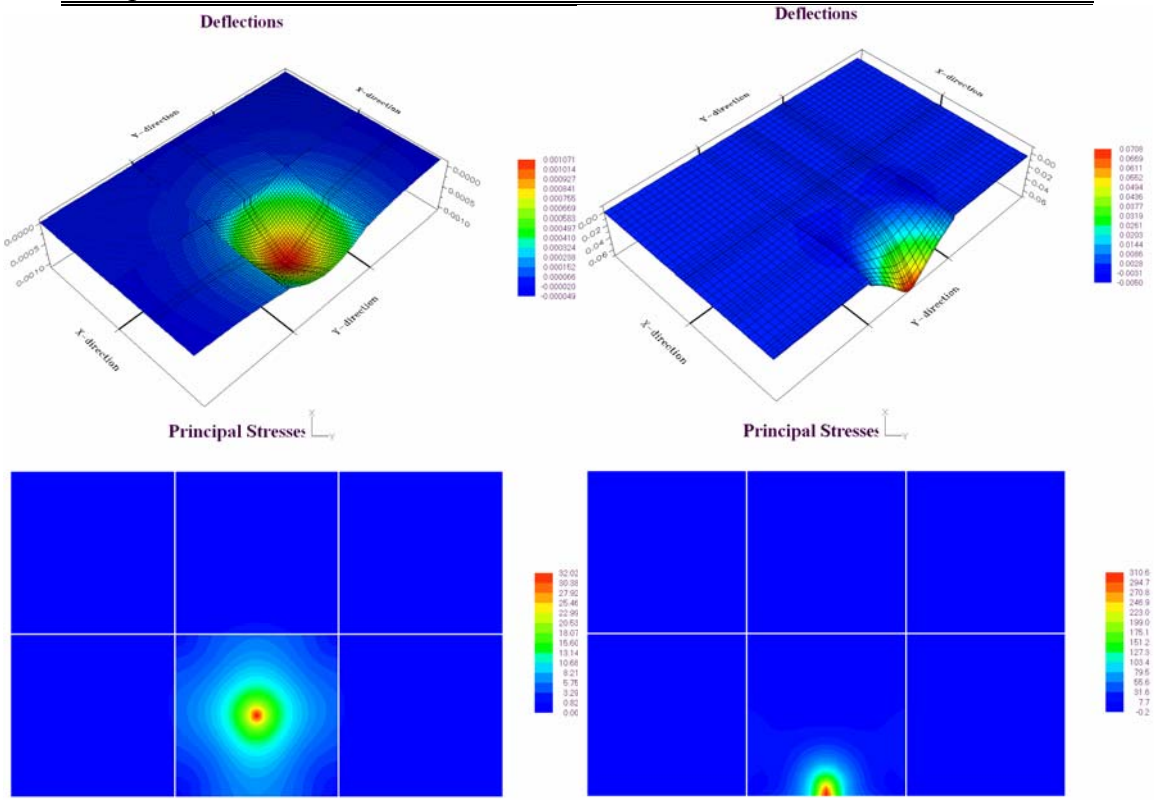

Figure 5.4. A general view of the deflections and stresses at the bottom of the PCC slab under 9-kip loading in six-slab assembly

The ranges of the pavement surface deflections calculated by ISLAB2000 are given in Table 5.2. All pavement surface deflection values were normalized between the maximum value of the D_0 (36.26 mils) and the minimum value of D_{60} (0 mils). According to LeCun (1993), each

input variable should be preprocessed so that its mean value, averaged over the entire training set, is close to zero. Thus, inputs were normalized between +2 and -2. In a similar way, outputs were normalized between 0.1 and 0.9 because of the effective ranges of the sigmoid activation function considered in the backpropagation type ANN trainings.

Table 5.2. Pavement surface deflections range (inputs of the ANN-based models)

	D_0 (mils)	D_8 (mils)	D_{12} (mils)	D_{18} (mils)	D_{24} (mils)	D_{36} (mils)	D_{48} (mils)	D_{60} (mils)
Min. Value	0.29	0.29	0.28	0.27	0.27	0.25	0.22	0.00
Max. Value	36.26	33.95	31.69	27.82	23.78	16.26	10.25	6.84

The dense liquid (DL) model, proposed by Winkler (1864), was used to characterize the subgrade behavior in this study. Accurate modeling of subgrade support for pavement systems is not a simple task since many soil types exhibit non-linear, stress dependent elasto-plastic behavior especially under the moving heavy wheel loads. Nevertheless, experience in concrete pavements analysis and design has shown that subgrade layer may be modeled as linear elastic because of the lower levels of vertical stresses acting on concrete pavement foundations. A plate on a dense liquid foundation is the most widely adopted mechanistic idealization for analysis of concrete pavements (NCHRP, 2003). Dense liquid foundation is implemented in several FE models, such as ISLAB2000, DIPLOMAT, KENSLABS, WESLIQID, J-SLAB, and FEACONS III (Tia et al., 1987). Consideration of the critical load transfer phenomena, occurring at the PCC slab joints, and the concomitant development of major distress types, such as faulting, pumping and corner breaking are the significant advantages of this approach. The DL foundation is the simplest foundation model and requires only one parameter, the coefficient of subgrade reaction, k_S, which is the proportionality constant between the applied pressure and the load plate deflection. Subgrade deformations are local in character, that is, they develop only beneath the load plate. Furthermore, their behavior is considered linear-elastic and deformations are recoverable upon removal of load (Tia et al. 1987).

SENSITIVITY STUDY FOR ACHIEVING OPTIMUM ANN ARCHITECTURE

The selection of ANN architecture is not a straightforward decision-making process. Most of the time is spent to determine the appropriate architecture for a particular problem. Therefore, a sensitivity study was conducted to determine the most suitable architecture for the backcalculation of the concrete pavement parameters. For this purpose, different architectures were tried in order to obtain the minimum Average Absolute Error (AAE) value which is an indication of the success of the developed ANN-based models. The number of hidden layers, the number of neurons in each hidden layer, learning rate, and momentum factor were varied and the AAE values were compared. The results of the sensitivity study in determining the optimum architecture are presented in Figure 5.5. Based on the results of this sensitivity study and previous studies (Ceylan et al. 2005; Bayrak et al. 2006; Bayrak and Ceylan 2006), networks with two hidden layers with 60 neurons in each hidden layer were exclusively chosen for all models trained in this study. In addition, the learning rate and momentum factor values which are the internal ANN architecture parameters were chosen as 0.2 and 0.6, respectively.

Similar to the traditional regression methods, the output variables in ANN architecture are the dependent variables, which are defined according to the problem under study. Also, variables that appear in the input layer are independent variables. In order to show the individual effect of each deflection (ANN model inputs) on the concrete pavement parameters (ANN model outputs), multivariate correlation analyses were conducted and R^2 values obtained from these statistical analyses are presented in Figure 5.6. As seen from the results, the correlation between the pavement surface deflections and E_{PCC}, RRS, and σ_{max} is much higher for the deflections close to the loading point (D_0, D_{12}) than the outer deflections (D_{48}, D_{60}). On the other hand, the opposite is true for the k_S which is highly correlated with the outer deflections (D_{48}, D_{60}). In addition, as the number of sensors increases, the mean value of elastic modulus of PCC slab increases and the mean value of coefficient of subgrade reaction decreases (Rufino et al. 2002). D_0 and D_{12} deflections are relatively more sensitive to changes in the elastic modulus of PCC slab, compared to D_{48} and D_{60} deflections.

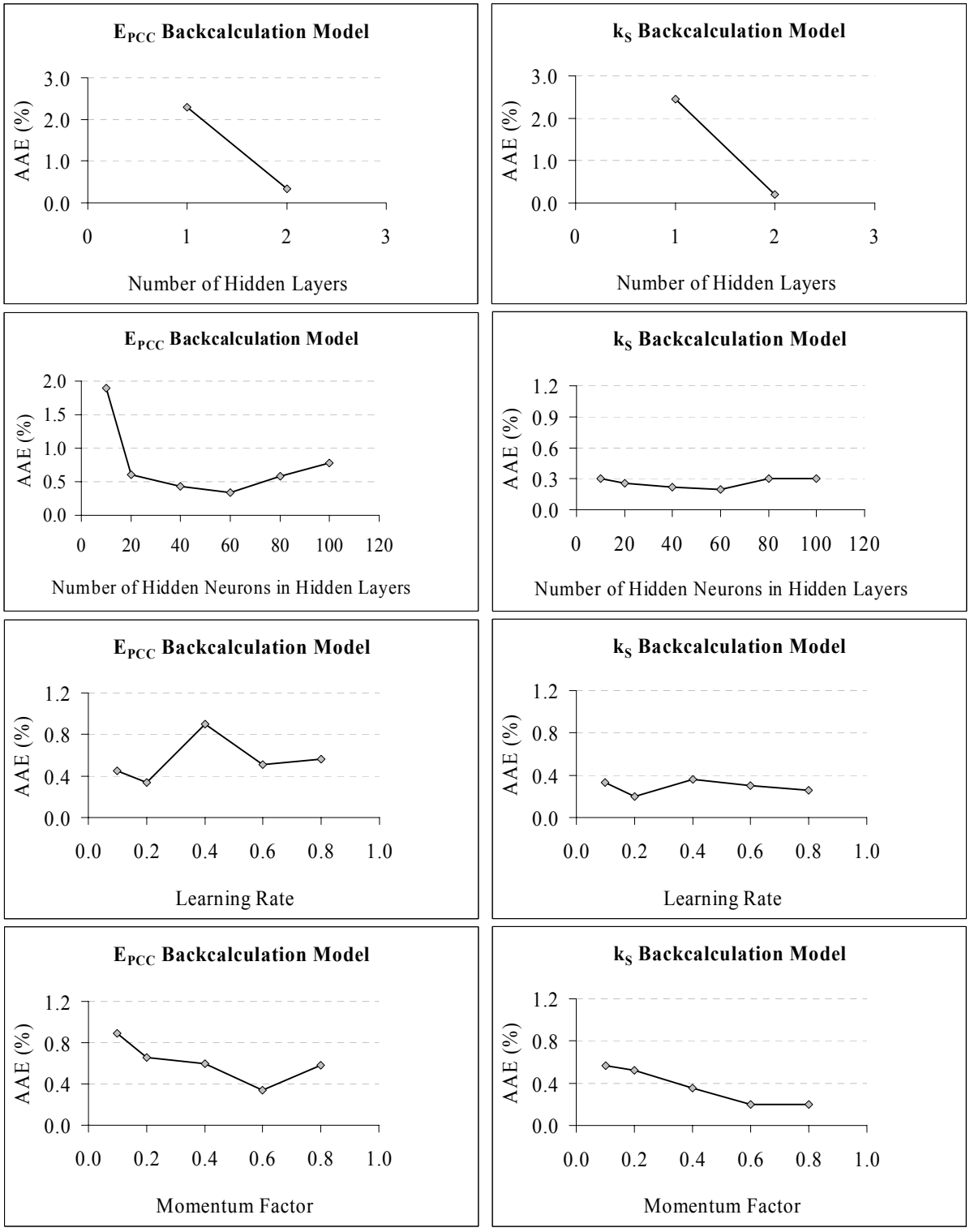

Figure 5.5. Sensitivity study results for ANN architecture parameters

On the other hand, D_{48} and D_{60} deflections are much more sensitive to the changes in the subgrade support (k_S). In order to be able to compare the backcalculated and forward calculated concrete pavement parameters, four-, six-, seven-, and eight-deflection ANN-based models were developed in this study. The results are presented in the following sections.

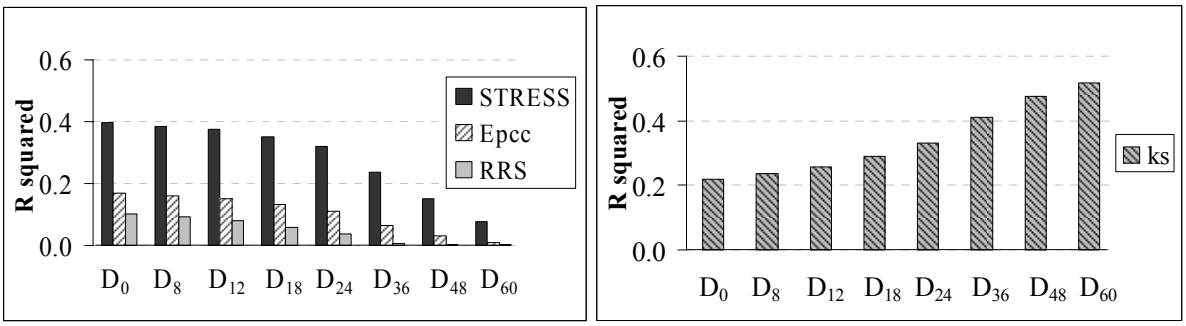

Figure 5.6. Correlations between deflections and concrete pavement parameters

ANN-BASED PAVEMENT LAYER BACKCALCULATION AND FORWARD CALCULATION MODELS

Artificial neural network methodology was chosen as the backcalculation and forward calculation method in this study. There are several different types of ANN such as backpropagation neural networks (BPNN), radial basis function networks (RBFNN), probabilistic neural networks (PNN), and generalized regression neural networks (GRNN), to name a few. Computing abilities of ANNs have been proven in the fields of prediction and estimation, pattern recognition, and optimization (Adeli and Hung 1995; Golden 1996; Mehrotra 1997; Adeli and Park 1998; Haykin 1999). The best-known example of a neural network training algorithm is backpropagation (Rumelhart et al. 1986; Fausett 1994; Patterson 1996; Haykin 1999) which is based on a gradient-descent optimization technique. The backpropagation neural networks are described in many sources (Hegazy 1994; Adeli and Hung 1995; Mehrotra 1997; Topping and Bahreininejad 1997; Haykin 1999). A comprehensive description of ANNs is beyond the scope of this paper. The adoption and use of ANN modeling techniques in the recently released Mechanistic-Empirical Pavement Design Guide (NCHRP project 1-37A: Development of the 2002 Guide for the Design of

New and Rehabilitated Pavement Structures: Phase II) has especially placed the emphasis on the successful use of neural networks in geomechanical and pavement systems.

Backpropagation type artificial neural network models were trained in this study with the results from the ISLAB2000 finite element program and were used as backcalculation tools for predicting the elastic modulus of the PCC slab, and coefficient of subgrade reaction, and as forward calculation tools for predicting the radius of relative stiffness, and maximum tensile stresses at the bottom of the PCC layer. A network with two hidden layers was exclusively chosen for all models trained in this study. Satisfactory results were obtained in the sensitivity study with this type of networks due to their ability to better facilitate the nonlinear functional mapping. The detailed information of the developed models is shown in Table 5.3. The comparison of the ISLAB2000 solutions and developed ANN-based model predictions for E_{PCC}, k_S, RRS, and σ_{MAX} were shown in Figure 5.7 to Figure 5.10, respectively.

In the current study, basically four different ANN-based models have been developed which are BCM-E_{PCC}, BCM-k_S (for backcalculation), FCM-RRS, and FCM-σ_{MAX} (for forward calculation) models. Falling weight deflectometer deflections [D_0(0 in.), D_8(8 inches), D_{12}(12 inches), D_{18}(18 inches), D_{24}(24 inches), D_{36}(36 inches), D_{48}(48 inches), and D_{60}(60 inches)] and PCC slab thickness (h_{PCC}) were used as input variables in the developed ANN-based models. ANN models with different architectures (4-, 6-, 7-, and 8-deflection models) have been developed for backcalculation and forward calculation of concrete pavement parameters and critical pavement responses (see Table 5.3).

Table 5.3. Architectures and AAE values of the ANN-based models

ANN Models	Input Parameters	ANN Architecture	AAE (%)
BCM-E_{PCC}-(4)	D_0, D_{12}, D_{24}, D_{36} + h_{PCC}	5-60-60-1	0.34
BCM-E_{PCC}-(6)	D_0, D_{12}, D_{24}, D_{36}, D_{48}, D_{60} + h_{PCC}	7-60-60-1	0.32
BCM-E_{PCC}-(7)	D_0, D_8, D_{12}, D_{18}, D_{24}, D_{36}, D_{60} + h_{PCC}	8-60-60-1	0.29
BCM-E_{PCC}-(8)	D_0, D_8, D_{12}, D_{18}, D_{24}, D_{36}, D_{48}, D_{60} + h_{PCC}	9-60-60-1	0.30
BCM-k_S-(4)	D_0, D_{12}, D_{24}, D_{36}	4-60-60-1	0.28
BCM-k_S-(6)	D_0, D_{12}, D_{24}, D_{36}, D_{48}, D_{60}	6-60-60-1	0.22
BCM-k_S-(7)	D_0, D_8, D_{12}, D_{18}, D_{24}, D_{36}, D_{60}	7-60-60-1	0.19
BCM-k_S-(8)	D_0, D_8, D_{12}, D_{18}, D_{24}, D_{36}, D_{48}, D_{60}	8-60-60-1	0.22
FCM-RRS-(4)	D_0, D_{12}, D_{24}, D_{36} + h_{PCC}	5-60-60-1	0.14
FCM-RRS-(6)	D_0, D_{12}, D_{24}, D_{36}, D_{48}, D_{60} + h_{PCC}	7-60-60-1	0.14
FCM-RRS-(7)	D_0, D_8, D_{12}, D_{18}, D_{24}, D_{36}, D_{60} + h_{PCC}	8-60-60-1	0.23
FCM-RRS-(8)	D_0, D_8, D_{12}, D_{18}, D_{24}, D_{36}, D_{48}, D_{60} + h_{PCC}	9-60-60-1	0.14
FCM-σ_{MAX}-(4)	D_0, D_{12}, D_{24}, D_{36} + h_{PCC}	5-60-60-1	0.82
FCM-σ_{MAX}-(6)	D_0, D_{12}, D_{24}, D_{36}, D_{48}, D_{60} + h_{PCC}	7-60-60-1	0.75
FCM-σ_{MAX}-(7)	D_0, D_8, D_{12}, D_{18}, D_{24}, D_{36}, D_{60} + h_{PCC}	8-60-60-1	0.72
FCM-σ_{MAX}-(8)	D_0, D_8, D_{12}, D_{18}, D_{24}, D_{36}, D_{48}, D_{60} + h_{PCC}	9-60-60-1	0.70

Noise-Introduced Backcalculation Models

In addition to the training and testing sets prepared for the zero-noise BCM-E_{PCC} and BCM-k_S models, more ANN training sets were generated by introducing 4% ($\pm$2%), 10% ($\pm$5%) and 20% ($\pm$10%) noise to the FWD deflection basin data. The purpose of introducing noisy patterns in the training sets was to develop more robust networks that can tolerate the noisy or inaccurate deflection patterns collected from the FWD deflection basins. Noise introduction was as follows: ISLAB2000 solution databases were first partitioned to create training set patterns and an independent testing set of 2,000 patterns to check the performance of the trained ANN-based models. Uniformly distributed random numbers ranging from 0 to 4% ($\pm$2%) and 10% ($\pm$5%) for low-noise levels and ranging from 0 to 20% ($\pm$10%) for high-noise patterns were generated each time to create noisy training patterns. After adding randomly selected noise values only to the pavement surface deflections of D_0, D_8, D_{12}, D_{18}, D_{24}, D_{48}, and D_{60}, new training data sets were developed for each noisy training set. By repeating the noise introduction procedure, four more training data sets were formed for each backcalculation model. Including the original training set with no noise in it, a total

of 195,130 for E_{PCC} and 247,695 for k_S patterns were used to train the noise-introduced ANN-based backcalculation models. The architectures of the noise-introduced ANN-based backcalculation models were given in Table 5.4. As can be seen from the results, AAE values increase when high levels of noise are introduced to the deflection data as expected.

Table 5.4. Architectures and AAE values of the noise-introduced ANN-based models

ANN Models	**Input Parameters**	**ANN Architecture**	**AAE (%)**
BCM-E_{PCC}-(4) ($\pm$2%)	D_0, D_{12}, D_{24}, D_{36} + h_{PCC}	5-60-60-1	2.57
BCM-E_{PCC}-(4) ($\pm$5%)	D_0, D_{12}, D_{24}, D_{36} + h_{PCC}	5-60-60-1	5.96
BCM-E_{PCC}-(4) ($\pm$10%)	D_0, D_{12}, D_{24}, D_{36} + h_{PCC}	5-60-60-1	11.61
BCM-E_{PCC}-(6) ($\pm$2%)	D_0, D_{12}, D_{24}, D_{36}, D_{48}, D_{60} + h_{PCC}	7-60-60-1	1.11
BCM-E_{PCC}-(6) ($\pm$5%)	D_0, D_{12}, D_{24}, D_{36}, D_{48}, D_{60} + h_{PCC}	7-60-60-1	2.59
BCM-E_{PCC}-(6) ($\pm$10%)	D_0, D_{12}, D_{24}, D_{36}, D_{48}, D_{60} + h_{PCC}	7-60-60-1	5.22
BCM-E_{PCC}-(7) ($\pm$2%)	D_0, D_8, D_{12}, D_{18}, D_{24}, D_{36}, D_{60} + h_{PCC}	8-60-60-1	1.04
BCM-E_{PCC}-(7) ($\pm$5%)	D_0, D_8, D_{12}, D_{18}, D_{24}, D_{36}, D_{60} + h_{PCC}	8-60-60-1	2.37
BCM-E_{PCC}-(7) ($\pm$10%)	D_0, D_8, D_{12}, D_{18}, D_{24}, D_{36}, D_{60} + h_{PCC}	8-60-60-1	4.54
BCM-E_{PCC}-(8) ($\pm$2%)	D_0, D_8, D_{12}, D_{18}, D_{24}, D_{36}, D_{48}, D_{60} + h_{PCC}	9-60-60-1	1.42
BCM-E_{PCC}-(8) ($\pm$5%)	D_0, D_8, D_{12}, D_{18}, D_{24}, D_{36}, D_{48}, D_{60} + h_{PCC}	9-60-60-1	1.75
BCM-E_{PCC}-(8) ($\pm$10%)	D_0, D_8, D_{12}, D_{18}, D_{24}, D_{36}, D_{48}, D_{60} + h_{PCC}	9-60-60-1	3.33
BCM-k_S-(4) ($\pm$2%)	D_0, D_{12}, D_{24}, D_{36}	4-60-60-1	1.65
BCM-k_S-(4) ($\pm$5%)	D_0, D_{12}, D_{24}, D_{36}	4-60-60-1	4.23
BCM-k_S-(4) ($\pm$10%)	D_0, D_{12}, D_{24}, D_{36}	4-60-60-1	7.51
BCM-k_S-(6) ($\pm$2%)	D_0, D_{12}, D_{24}, D_{36}, D_{48}, D_{60}	6-60-60-1	1.46
BCM-k_S-(6) ($\pm$5%)	D_0, D_{12}, D_{24}, D_{36}, D_{48}, D_{60}	6-60-60-1	2.69
BCM-k_S-(6) ($\pm$10%)	D_0, D_{12}, D_{24}, D_{36}, D_{48}, D_{60}	6-60-60-1	3.60
BCM-k_S-(7) ($\pm$2%)	D_0, D_8, D_{12}, D_{18}, D_{24}, D_{36}, D_{60}	7-60-60-1	1.21
BCM-k_S-(7) ($\pm$5%)	D_0, D_8, D_{12}, D_{18}, D_{24}, D_{36}, D_{60}	7-60-60-1	1.74
BCM-k_S-(7) ($\pm$10%)	D_0, D_8, D_{12}, D_{18}, D_{24}, D_{36}, D_{60}	7-60-60-1	2.71
BCM-k_S-(8) ($\pm$2%)	D_0, D_8, D_{12}, D_{18}, D_{24}, D_{36}, D_{48}, D_{60}	8-60-60-1	1.17
BCM-k_S-(8) ($\pm$5%)	D_0, D_8, D_{12}, D_{18}, D_{24}, D_{36}, D_{48}, D_{60}	8-60-60-1	1.58
BCM-k_S-(8) ($\pm$10%)	D_0, D_8, D_{12}, D_{18}, D_{24}, D_{36}, D_{48}, D_{60}	8-60-60-1	2.23

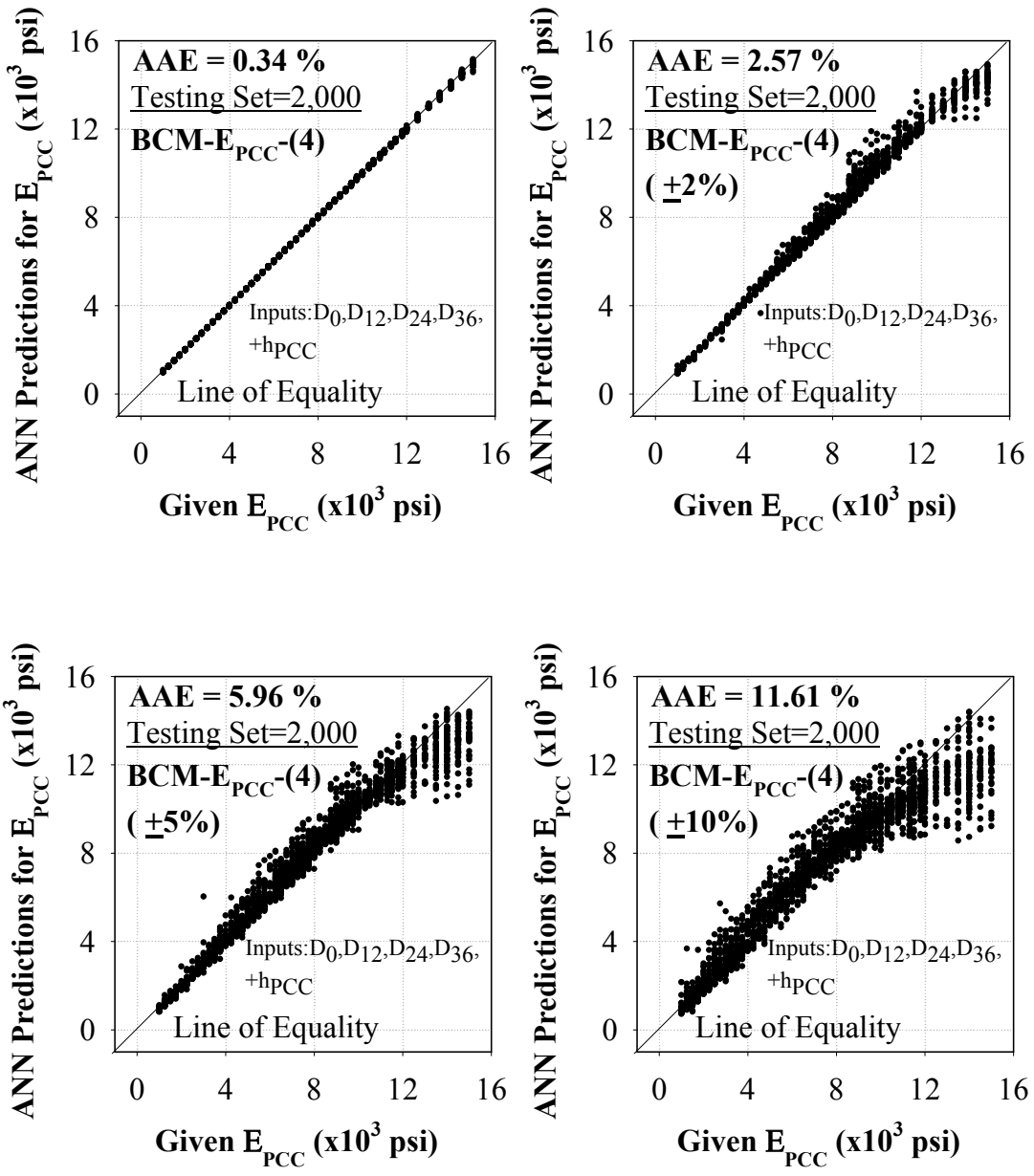

Figure 5.7. Prediction performance of ANN-based models for backcalculating the elastic modulus of PCC slab, E_{PCC}

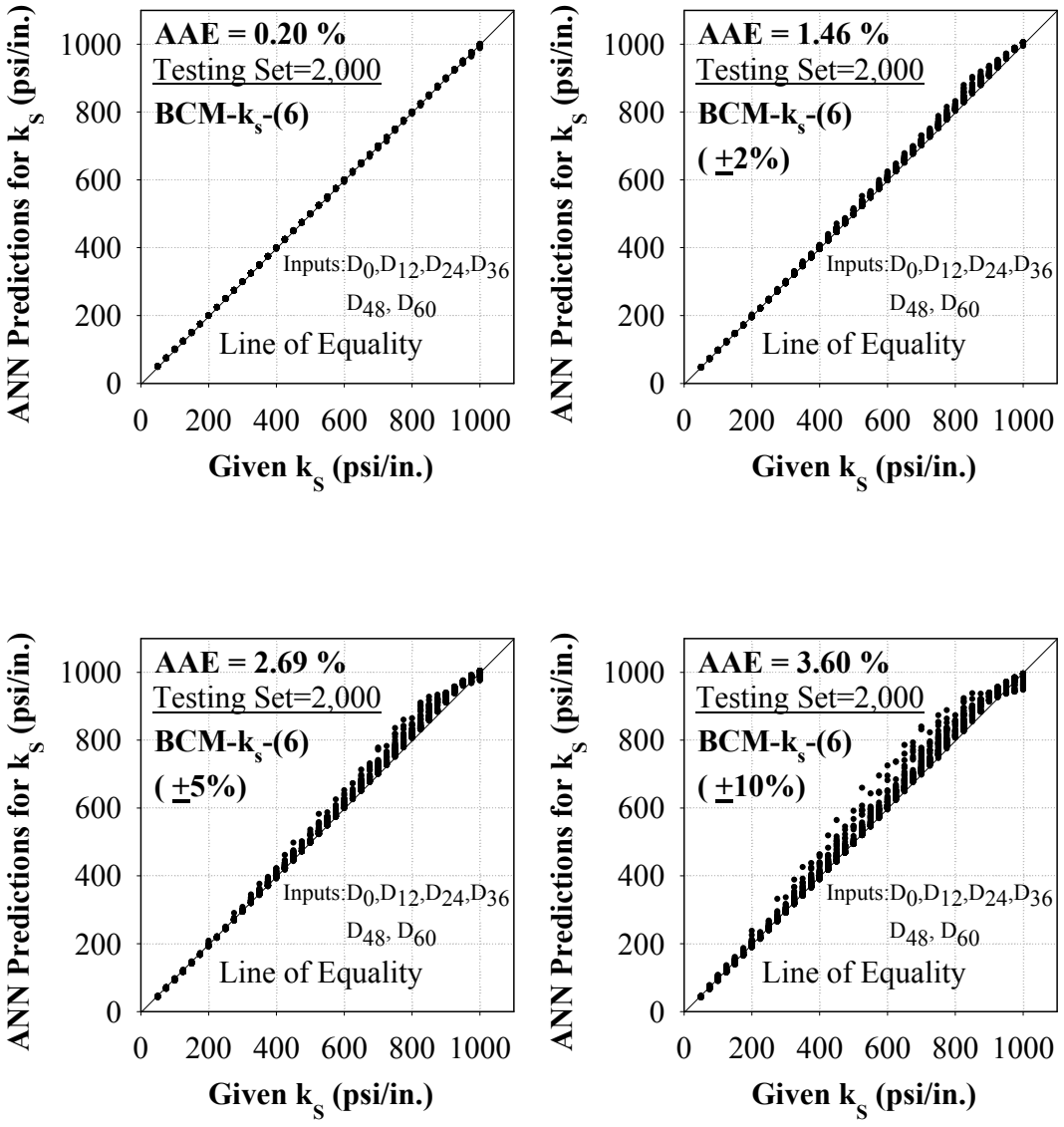

Figure 5.8. Prediction performance of ANN-based models for backcalculating the coefficient of subgrade reaction, k_s

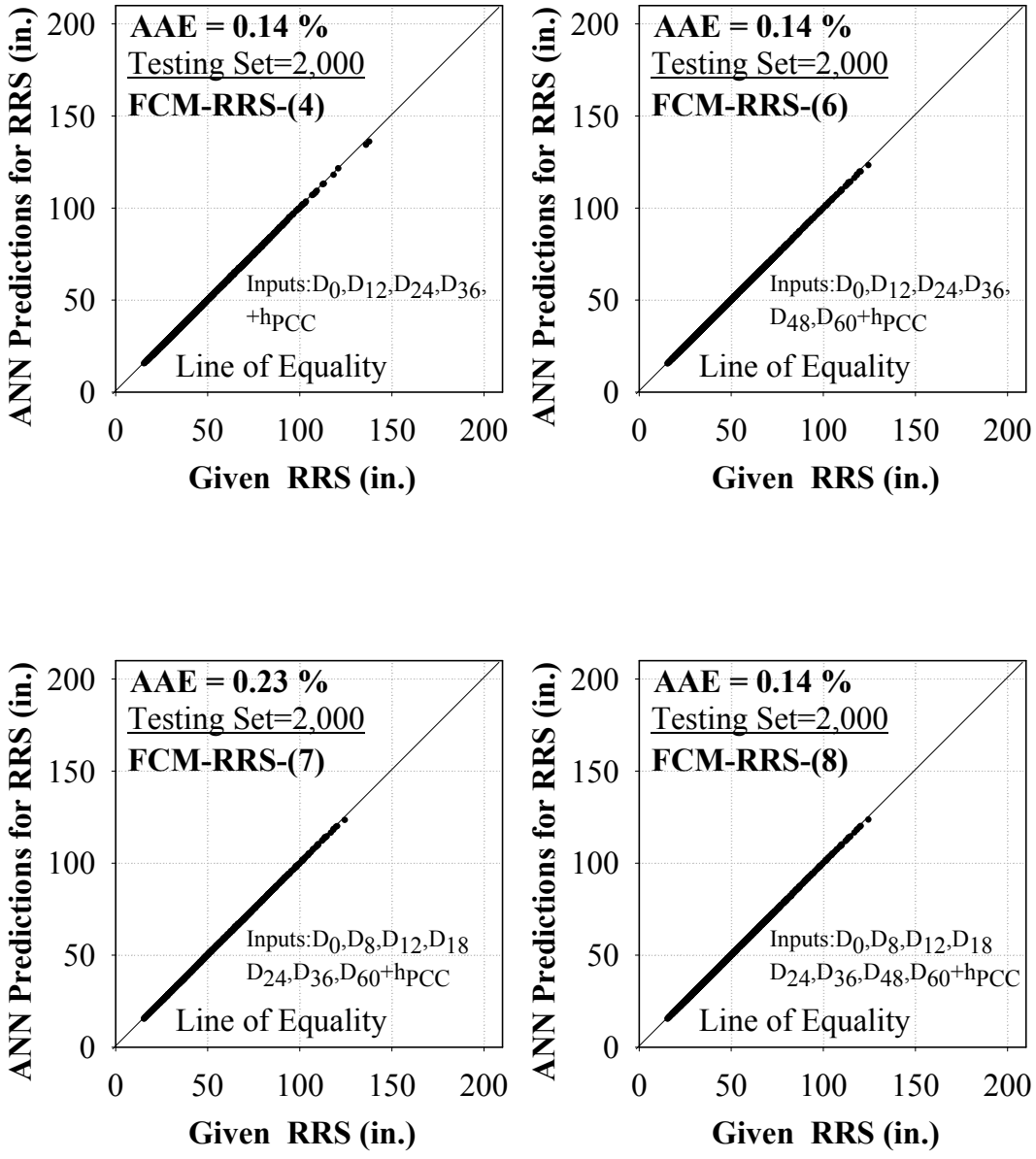

Figure 5.9. Prediction performance of ANN-based models for forward calculating the radius of relative stiffness, RRS

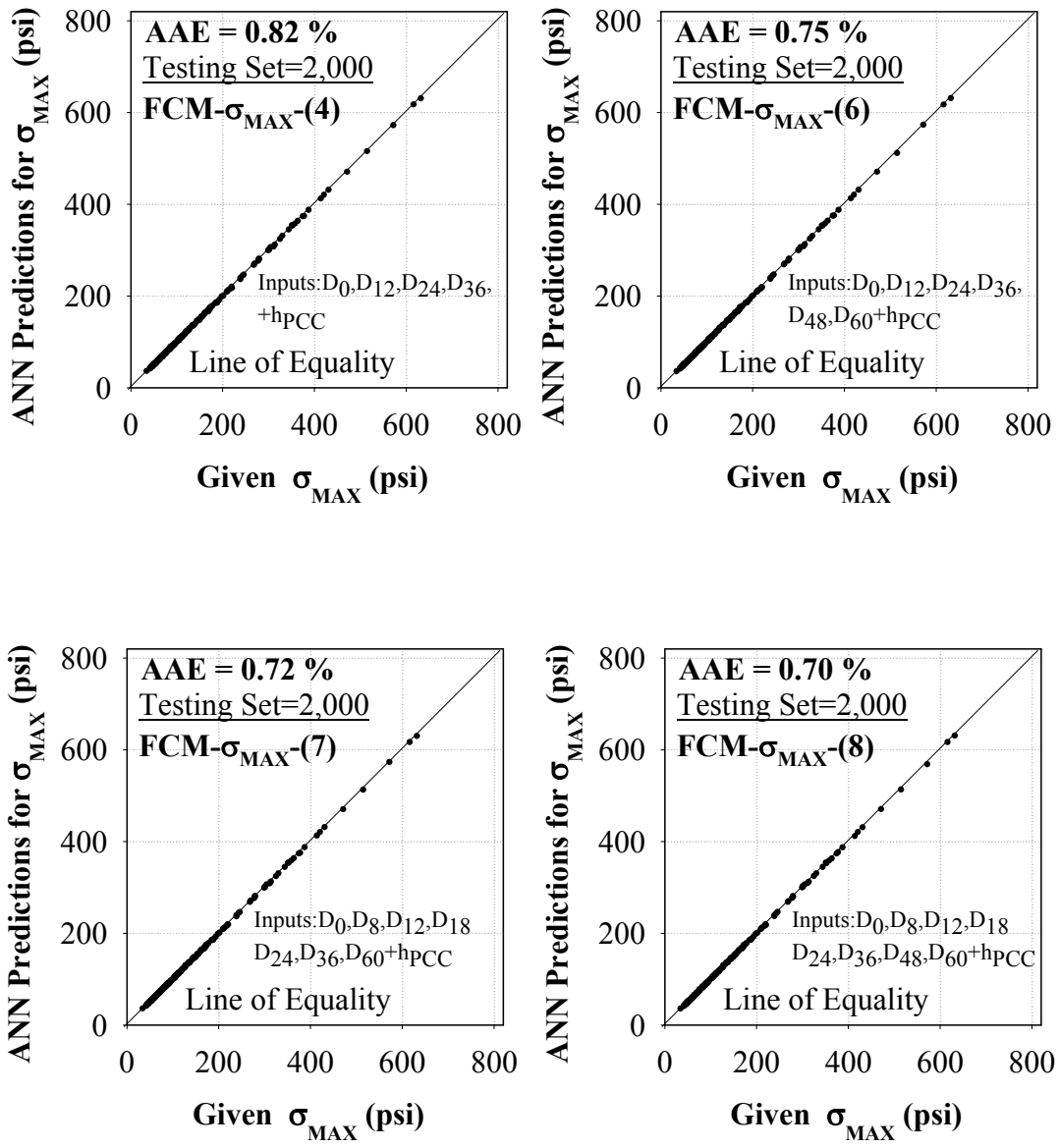

Figure 5.10. Prediction performance of ANN-based models for forward calculating the maximum tensile stress at the bottom of the PCC layer, σ_{MAX}

THE SIGNIFICANCE OF LAYER BONDING AND THICKNESS IN THE PAVEMENT LAYER BACKCALCULATION

Two of the important issues in the backcalculation of the concrete pavement parameters are the degree of bonding between layers and thickness of the PCC and base layers. To simplify

the ANN-based backcalculation methodology developed in this study, only one thickness value (effective PCC thickness) was considered in the analysis. The effective thickness of the pavement structure is directly related to the bonding conditions between the PCC layer and the base layer. Since it is difficult to construct a long pavement section with a uniform thickness value, it is assumed, during the backcalculation of the pavement parameters, that pavement thickness is uniform for a given section and it's the value taken from the project files. To determine the effective thickness of a two-layer pavement section for bonded, unbonded, and partially bonded cases, the equations given below are considered (Ioannides et al., 1992)**.**

Effective thickness for fully bonded PCC layers was computed using the following equations:

$$h_{e-b} = \left\{ h_1^3 + \frac{E_2}{E_1} h_2^3 + 12\left[\left(x_{na} - \frac{h_1}{2} \right)^2 h_1 + \frac{E_2}{E_1} \left(h_1 - x_{na} + \frac{h_2}{2} \right)^2 h_2 \right] \right\}^{1/3} \tag{5.1}$$

$$x_{na} = \frac{E_1 h_1 \dfrac{h_1}{2} + E_2 h_2 \left(h_1 + \dfrac{h_2}{2} \right)}{E_1 h_1 + E_2 h_2} \tag{5.2}$$

Effective thickness for unbonded PCC layers was computed using the following equations:

$$h_{e-u} = \left(h_1^3 + \frac{E_2}{E_1} h_2^3 \right)^{1/3} \tag{5.3}$$

Effective thickness for partially bonded PCC layers was computed using the following equations:

$$h_{e-p} = (1-x) h_{e-u} + (x) h_{e-b} \tag{5.4}$$

$$x = \frac{h_{e-p} - h_{e-u}}{h_{e-b} - h_{e-u}} \tag{5.5}$$

where as;

$h_{e\text{-}b}$ = Effective thickness of the fully bonded PCC layers

$h_{e\text{-}u}$ = Effective thickness of the unbonded PCC layers

$h_{e\text{-}p}$ = Effective thickness of the partially bonded PCC layers

E_1 or E_2 = Elastic modulus for layer 1 or 2

h_1 or h_2 = Thickness for layer 1 or 2

x_{na} = Neutral axis distance from top of layer

x = Degree of bonding which ranges between 0 and 1

The effect of the layer thickness in the E_{PCC} predictions

The predicted layer moduli are very sensitive to the pavement layer thickness. Even a small change in the assumed PCC layer thickness causes considerable differences in the backcalculated elastic moduli of the PCC layer. To demonstrate the effect of the PCC thickness on the backcalculated E_{PCC} values, field FWD data was used (see Figure 5.11).

The effect of pavement layer bonding in the E_{PCC} predictions

In order to investigate the sensitivity of the layer bonding between the pavement layers, again actual FWD data was used. The variation of the backcalculated E_{PCC} values with different degree of layer bonding for the concrete pavement section is presented in Figure 5.12. As seen in Figure 5.12, a change in the degree of layer bonding between the pavement layers affects the backcalculated E_{PCC} values significantly. Finally, results from this sensitivity analysis show the significance of the layer thickness and degree of bonding in the E_{PCC} backcalculation procedure. Since the exact thickness of the PCC layer and the degree of bonding between the PCC and base layers are not exactly known, more scatter is expected in the predictions. In addition, the time of the FWD testing is also crucial in the E_{PCC} backcalculation due to curling and warping problems in concrete pavements. The results of previous studies indicate that the variations in temperature between two separate FWD tests affect primarily the elastic modulus of the slab (Ioannides et al. 1989). Due to the slab curling, temperature difference across the depth of the concrete pavement in the test sections is another major reason of the scatter in E_{PCC} predictions (Bayrak et al. 2006). Therefore, the main reasons of the scatter in the predictions are basicly the curling and warping issues, the bonding degree between the PCC and base layers, and uncertainities in the thickness of the PCC layer. Also, the time of the year (spring, fall etc.) that FWD test is conducted also affects the backcalculated k_S due to the freeze and thaw effects in the pavement foundation.

To improve the E_{PCC} backcalculation, nondestructive evaluation techniques (NDT) such as Ground Penetrating Radar (GPR) readings or cores (destructive technique) can be taken along the test sections to determine the exact thickness of the layers at the FWD test points. Also, the time of the FWD tests due to curling and warping issues and the shape of the PCC slab should exactly be taken into account in the interpretations of the analyses of the concrete pavements for both E_{PCC} and k_S predictions.

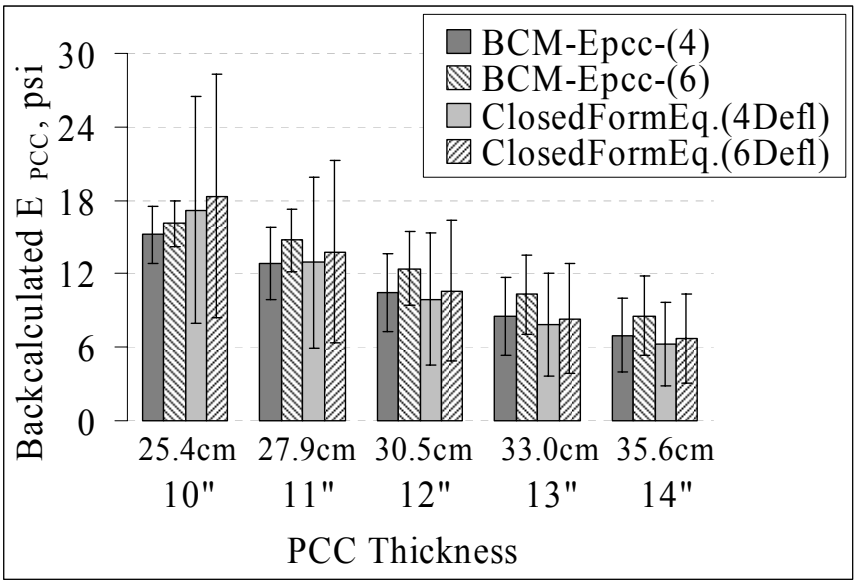

Figure 5.11. Effect of layer thickness on E_{PCC} backcalculation

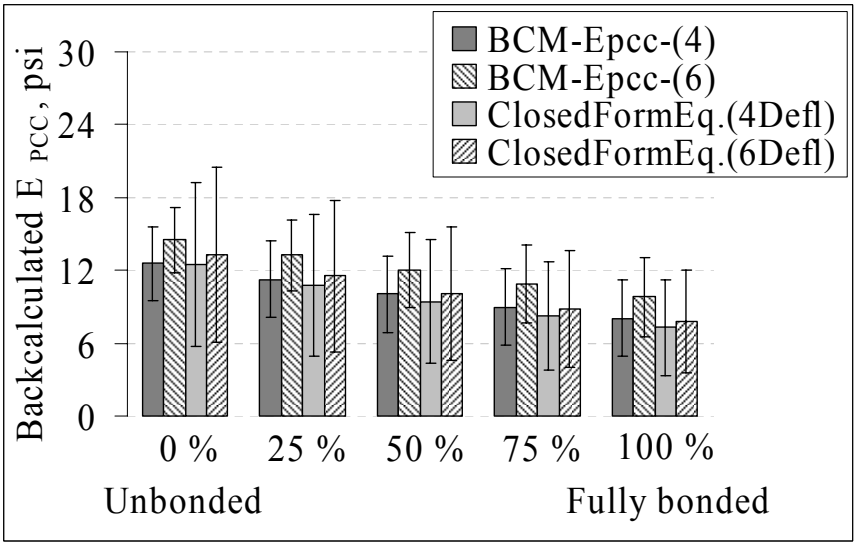

Figure 5.12. Effect of degree of layer bonding on E_{PCC} backcalculation

The closed-form equations used in this sensitivity analysis were obtained from a statistical study with the ISLAB2000 solution database used in this paper. There is a unique relationship between AREA and radius of relative stiffness (Ioannides 1989). AREA is a parameter that has been used to analyzed concrete pavement parameters and can be calculated for a given number and configuration of deflection sensors. Radius of relative stiffness (RRS) can be calculated from the AREA-RRS equations. AREA value was calculated from 4 deflections (D_0, D_{12}, D_{24}, and D_{36}) and 6 deflections (D_0, D_{12}, D_{24}, D_{36}, D_{48}, and D_{60}) as shown in Equations 5.6 and 5.7 below. Load (P), radius of load plate (a), and Poisson's ratio (μ) were set to 9,000-lbs, 5.9 inches, and 0.15, respectively. The equations used in the numerical backcalculation of the concrete pavement parameters are summarized below:

$$AREA_4(in.) = 6 * \left[1 + 2\left(\frac{D_{12}}{D_0}\right) + 2\left(\frac{D_{24}}{D_0}\right) + \left(\frac{D_{36}}{D_0}\right) \right] \tag{5.6}$$

$$AREA_6(in.) = 6 * \left[1 + 2\left(\frac{D_{12}}{D_0}\right) + 2\left(\frac{D_{24}}{D_0}\right) + 2\left(\frac{D_{36}}{D_0}\right) + 2\left(\frac{D_{48}}{D_0}\right) + \left(\frac{D_{60}}{D_0}\right) \right] \tag{5.7}$$

$$RRS_4(in.) = (-128.9885)+(5.4082*AREA_4)+(1.0224*(AREA_4-30.8637)^2)+ (0.1919*(AREA_4-30.8637)^3)+(0.0146*(AREA_4-30.8637)^4) \tag{5.8}$$

$$RRS_6(in.) = (-49.1500)+(1.9800*AREA_6)+(0.1147*(AREA_6-44.3008)^2)+ (0.0075*(AREA_6-44.3008)^3)+(0.0002*(AREA_6-44.3008)^4) \tag{5.9}$$

$$k_S = \left(\frac{P}{8D_0 RRS_i^{\,2}}\right)\left\{1 + \left(\frac{1}{2\pi}\right)\left[ln\left(\frac{a}{2RRS_i}\right) - 0.673\right]\left(\frac{a}{RRS_i}\right)^2\right\} \tag{5.10}$$

$$E_{PCC} = \left(\frac{12RRS_i^{\,4}k_S(1-\mu^2)}{h_{PCC}^{\,3}}\right) \tag{5.11}$$

COMPARISON OF THE ANN-BASED MODEL PREDICTIONS WITH RESULTS FROM OTHER METHODS

ANN-based models predictions were compared with the closed-form solutions, pavement layer backcalculation software results (EverCalc 5.0 and BAKFAA) and finite element program solutions (ISLAB2000 and EverFE 2.24) using the National Airport Pavement Test Facility (NAPTF) FWD data. The FWD tests were conducted on the NAPTF's LRS, MRS, and HRS sections. Each NAPTF test section is identified using a three-character code, where the first character indicates the subgrade strength (L for low, M for medium, and H for high), the second character indicates the test pavement type (F for flexible and R for rigid-concrete), and third character signifies whether the base material is conventional (C) or stabilized (S). The three concrete pavement sections are designated as follows: (a) LRS – concrete pavement with stabilized base over low-strength subgrade, (b) MRS – concrete pavement with stabilized base over medium-strength subgrade, and (c) HRS – concrete pavement with stabilized base over high-strength subgrade. A representative FWD deflection profile from each test section was selected (see Figure 5.13) to compare the backcalculated and forward calculated concrete pavement parameters from different methodologies. All FWD deflection basins were normalized to 9-kip in order to compare the results.

The comparison of the E_{PCC}, k_S, and RRS predictions obtained from four different methodologies are presented in Figure 5.13. As the results of the comparison shows, the predictions obtained from different methods are close to each other although there are small differences due to the nature of the using different methods. ANN-based predictions seem generally more conservative based on solutions using other approaches. ANN-based model predictions for σ_{MAX} were also compared with the closed-form solutions, ISLAB2000 and EverFE 2.24 FE program solutions for different pavement configurations (see Figure 5.14). A very good match was also obtained with the other program solutions for σ_{MAX} predictions. Please note that the slab-edge loading results were used for the σ_{MAX} analyses since the maximum (critical) tensile stress at the bottom of the PCC layer occurs in the slab edge. It is a very big advantage to be able to predict the pavement properties and critical pavement responses from FWD deflection basins in real time during the field testing without need to

any sophisticated input requirements. There is also no need to a seed moduli or any iteration which most pavement layer backcalculation programs require. In addition, as the speed of the ANN-based models (only 1 second) to backcalculate and forward calculate the concrete pavement parameters and critical pavement responses is also taken into account, it can be easily concluded that ANN approach overcomes this complex problem in an accurate, fast, easy and acceptable manner.

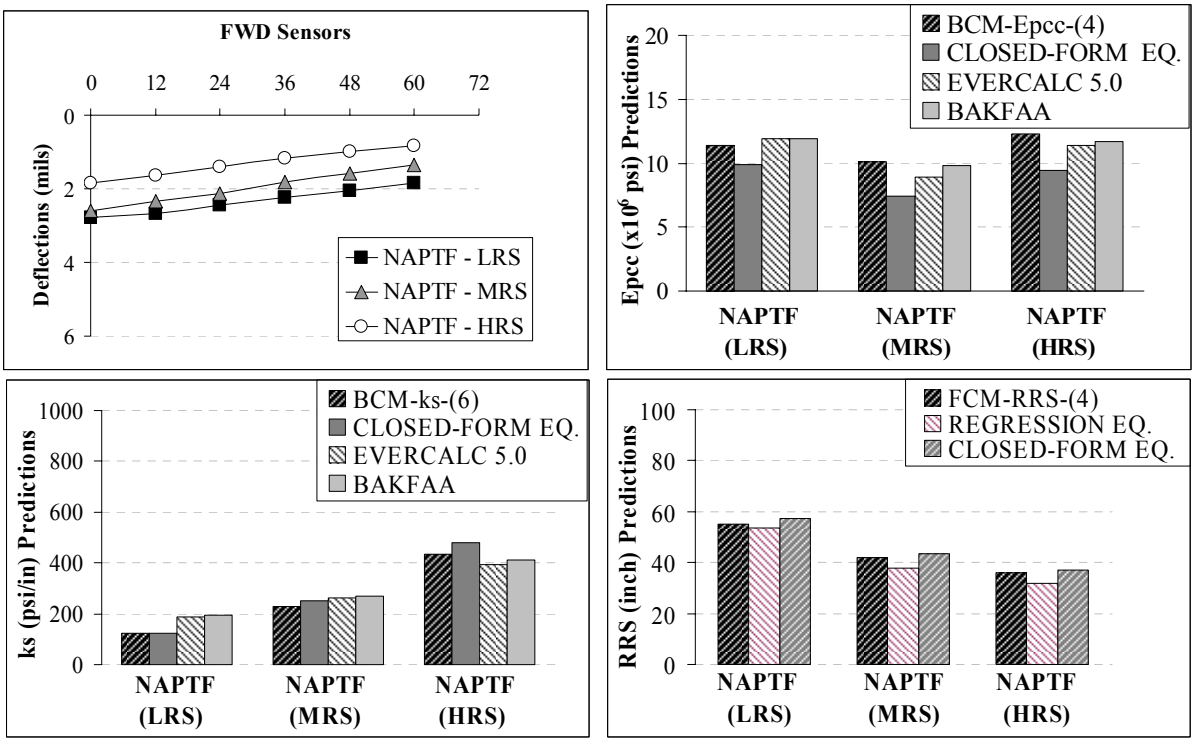

Figure 5.13. Comparison of the E_{PCC}, k_S, and RRS predictions.

APPLICATION TO ACTUAL FIELD FWD DATA

The proposed ANN-based models were also utilized to backcalculate and forward calculate the concrete pavement parameters and pavement responses using the actual FWD field tests conducted by Iowa Department of Transportation in Iowa-Allamakee (US-18) and Iowa-Wright (I-35) counties. The elastic modulus of the PCC slab, the coefficient of subgrade reaction, radius of relative stiffness, and maximum tensile stress at the bottom of the PCC layer predictions obtained from the proposed ANN-based models were shown in Figure 5.10 for these two FWD data sets. The standard deviation values obtained from these analyses are

very low and the predictions seem very consistent. All FWD test data was normalized to 9-kip in order to compare the results. PCC slab thicknesses were taken from the corresponding milepost documents. Very uniform predictions were obtained for k_S, RRS, and σ_{MAX} values in both FWD data sets. Instead of slab-edge deflection data, slab center FWD test results were used for the prediction of maximum tensile stresses at the bottom of the PCC layer by developing ANN models that uses slab center deflection data since only the slab center FWD test results were available in this particular example. Please also note that FWD deflection basins seemed to be very erroneous ($D_{24} > D_0$ etc.) were filtered from the analyzed database.

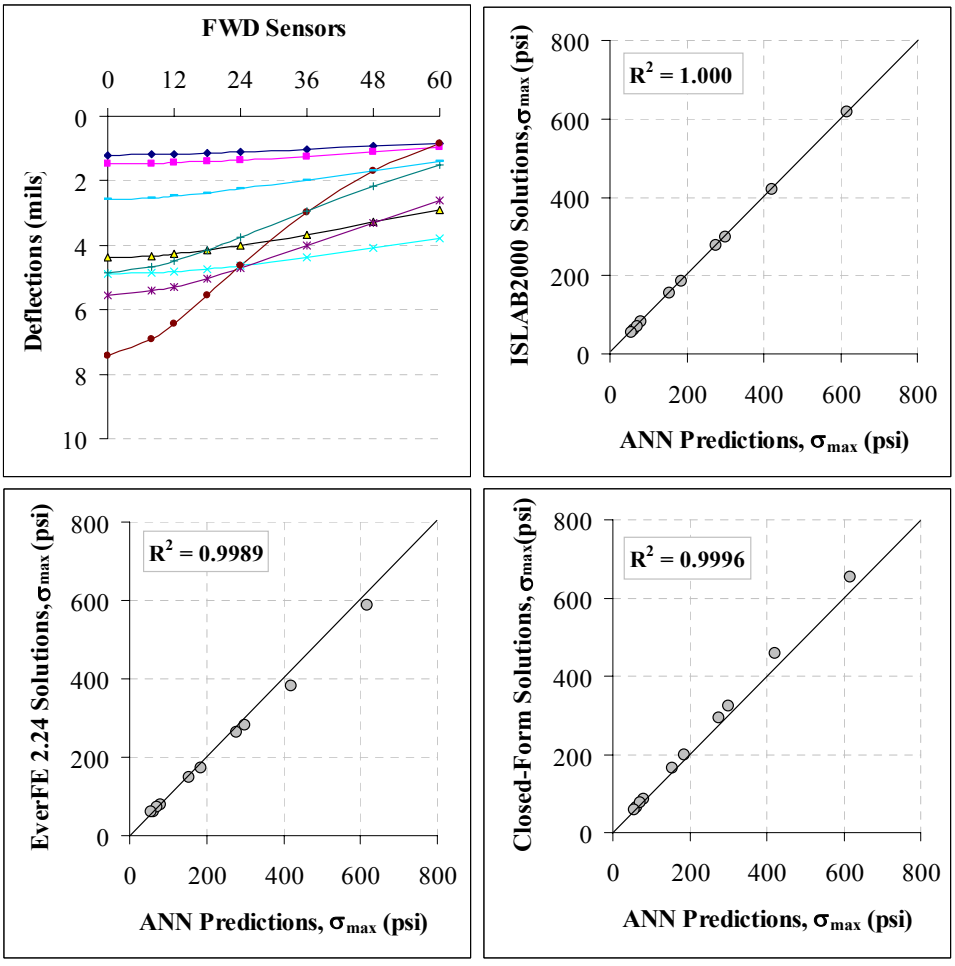

Figure 5.14. Comparison of the σ_{MAX} predictions.

Noise-introduced model predictions for E_{PCC} and k_S were also presented in Figure 5.16 to Figure 5.19 for both FWD data sets. Even though all the predictions are very close to each

other, generally noise-introduced model predictions were slightly higher for E_{PCC} and slightly lower for k_S compared to the zero-noise model predictions.

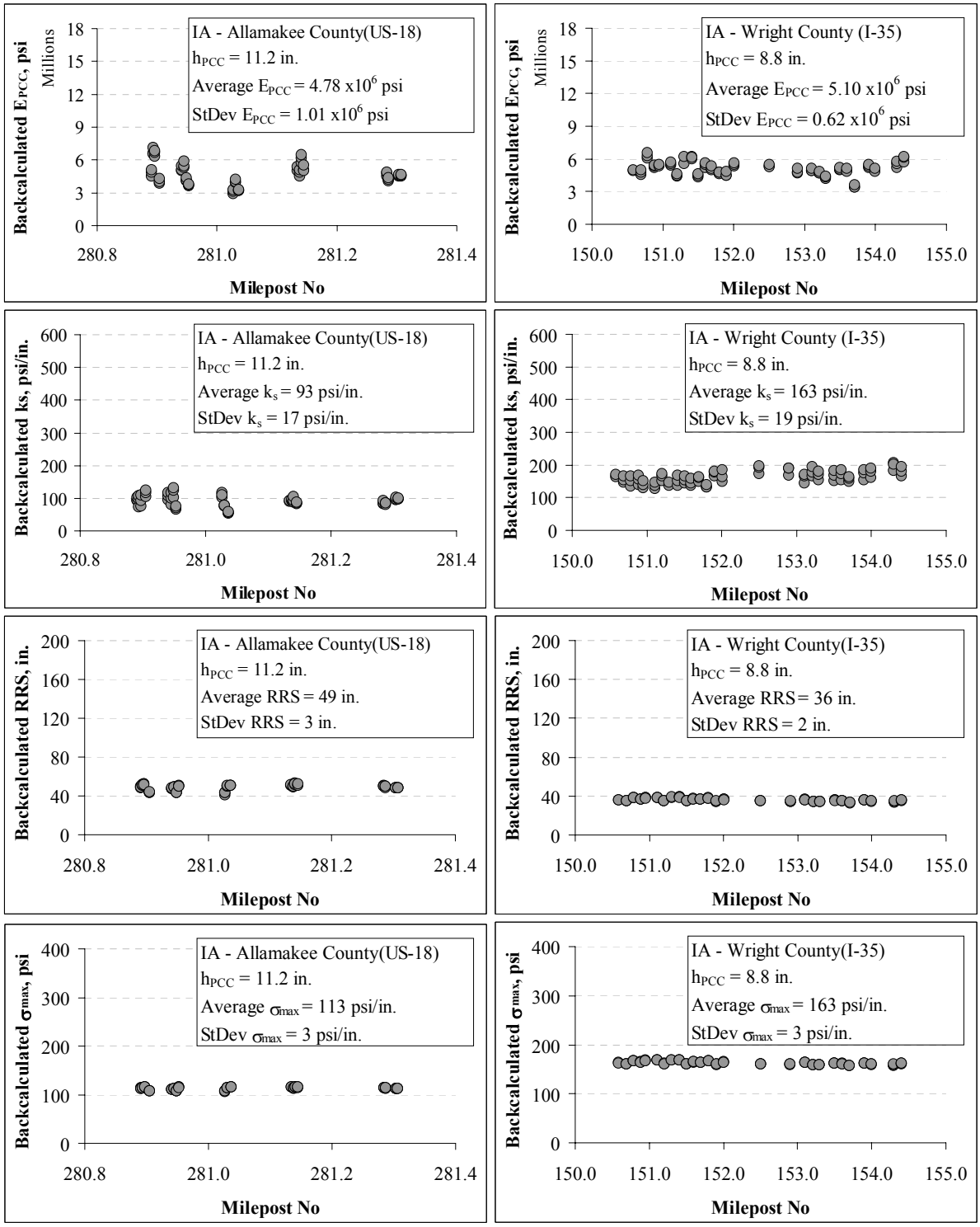

Figure 5.15. ANN-based model predictions from actual FWD deflection basin data for concrete pavement properties and responses

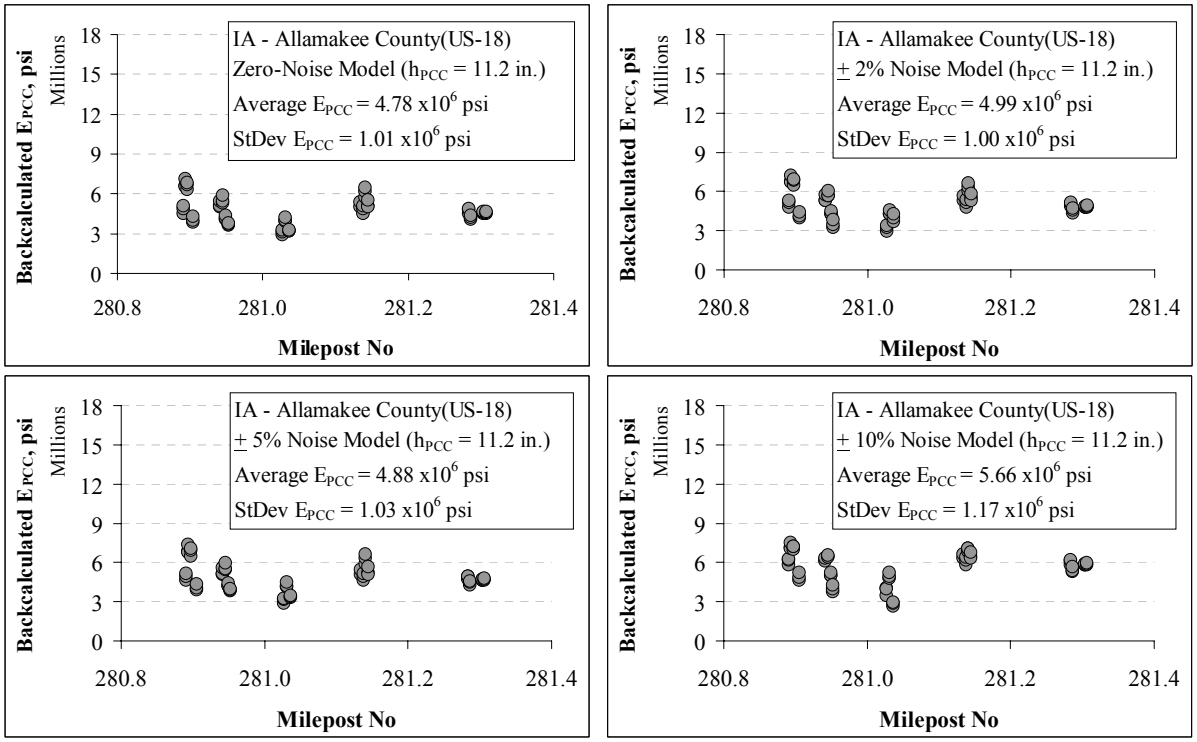

Figure 5.16. Zero-noise and noise-introduced model predictions for E_{PCC} (Allamakee County)

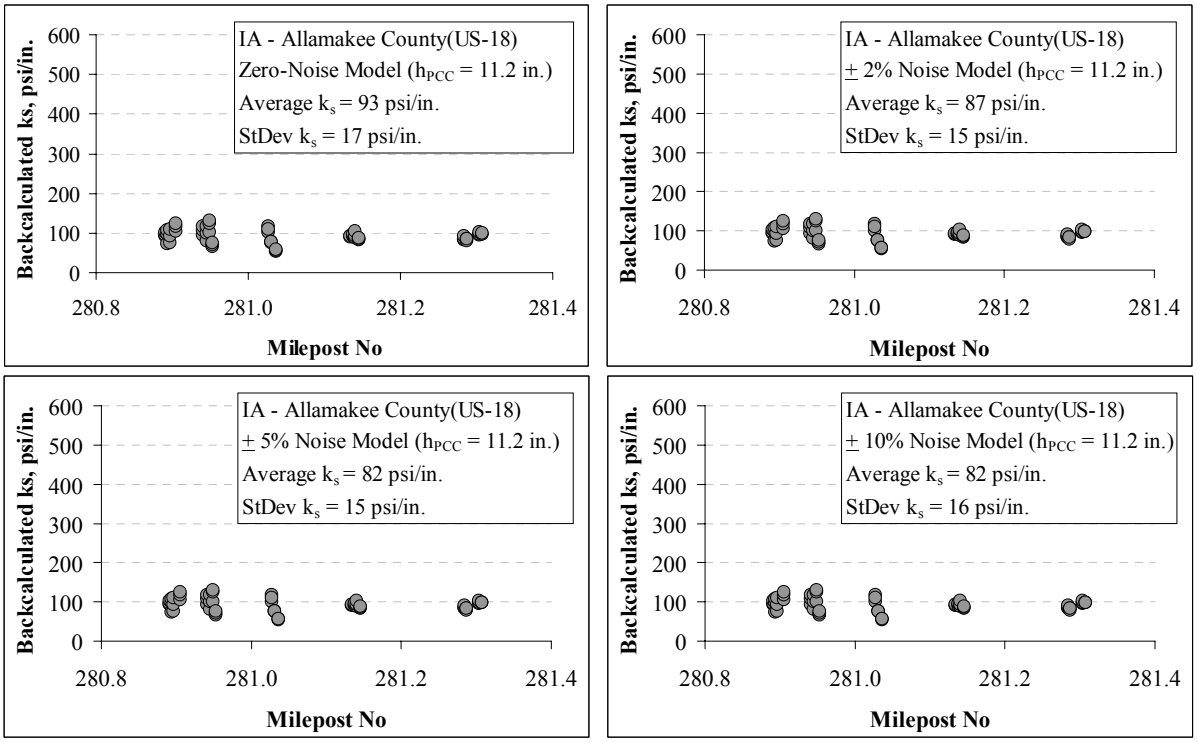

Figure 5.17. Zero-noise and noise-introduced model predictions for k_S (Allamakee County)

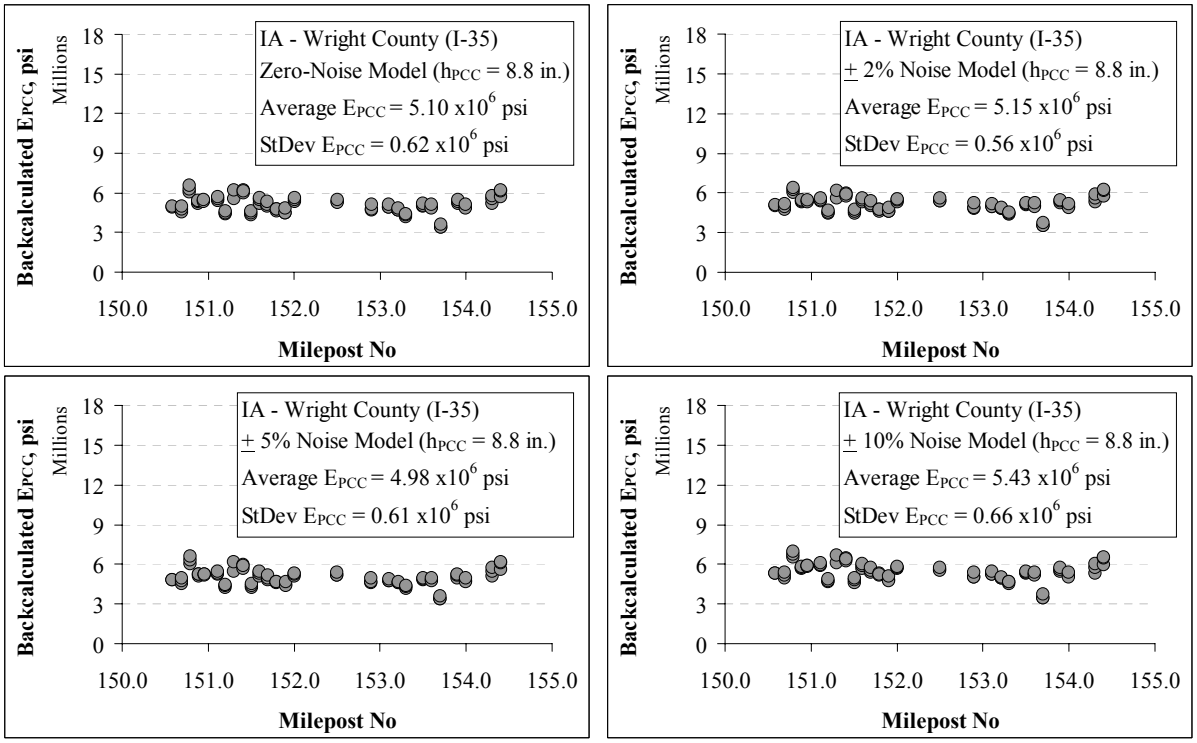

Figure 5.18. Zero-noise and noise-introduced model predictions for E_{PCC} (Wright County)

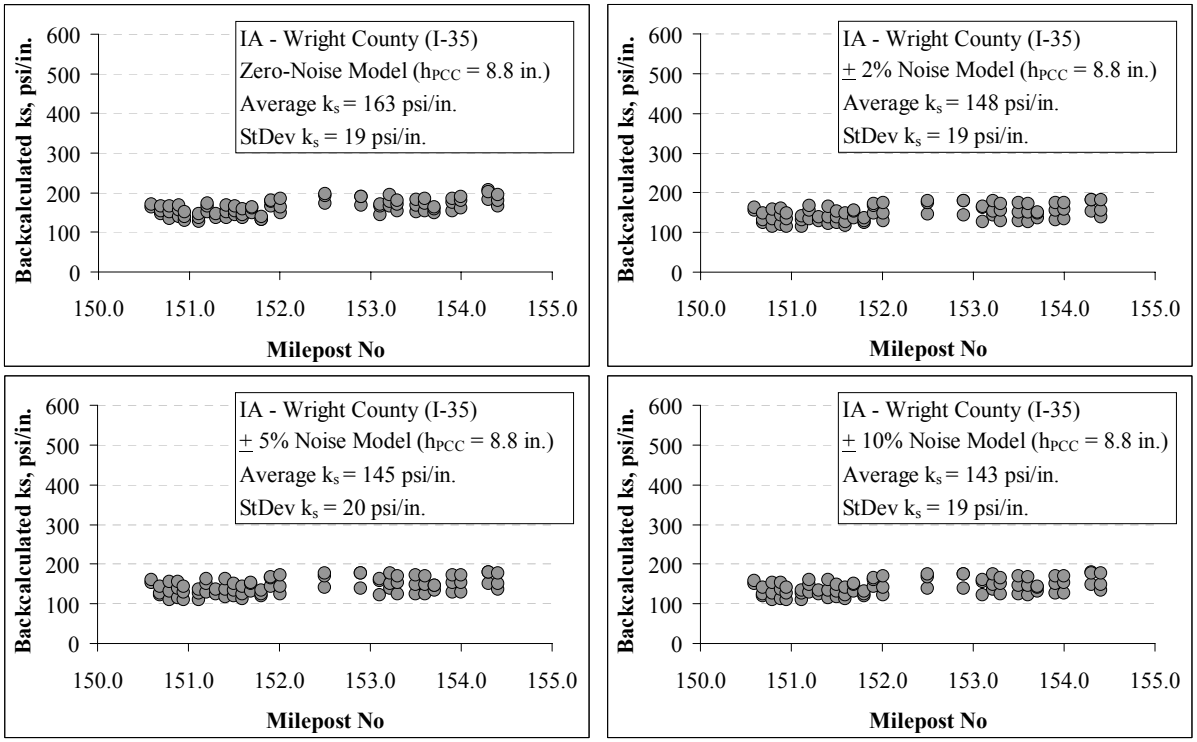

Figure 5.19. Zero-noise and noise-introduced model predictions for k_S (Wright County)

DISCUSSION OF RESULTS

A total of 40 ANN-based backcalculation and forward calculation models were developed in this study which can predict the elastic modulus of the PCC slab (E_{PCC}), coefficient of subgrade reaction (k_S), radius of relative stiffness (RRS), and maximum tensile stresses at the bottom of the PCC layer (σ_{MAX}) of concrete pavement systems from the FWD deflection basin data and PCC slab thickness.

The developed ANN-based models gave very low average absolute error values for all zero-noise models (< % 0.82) for synthetic database. On the other hand, the case is not like that when the actual FWD data is utilized in the developed models. There might be always some variability in the slab thicknesses in the field due to the poor construction which will directly affect the backcalculated pavement parameters. In addition, there might be some noise in the collected data, might be errors in data collection process due to FWD machine sensor calibration, and might be some operator mistakes. Therefore, actual FWD deflections which are the basic inputs of the backcalculation models are not always as perfect as synthetic data. Thus, noise-introduced ANN models were developed as well for the backcalculation models. As a matter of fact, meaningless FWD deflection data should be filtered and extracted from the data analysis.

A sensitivity study was conducted to determine the most appreciate architecture for the backcalculation of the concrete pavement parameters. Based on the results of this study, ANN networks with two hidden layers with 60 neurons in each hidden layer were exclusively chosen for all models trained in this study.

The predictions of the developed ANN-based models were compared with the closed-form solutions, pavement layer backcalculation softwares (EverCalc 5.0, and BAKFAA) and FE program solutions (ISLAB2000 and EverFE 2.24). Actual FWD deflection basins were selected from three different test sites from National Airport Pavement Test Facility data for the comparison study. The predictions of different methods for this specific data were presented. Even though there are some differences in the predictions obtained from different methodologies; the results seem very similar to each other but the real time prediction

capability (< 1 sec.) and the ease of the usage of the ANN-based models (no seed moduli, no itearation, etc.) make them very powerful tools over the other methods.

Also, two different sets of field FWD deflection basin data were utilized to backcalculate the elastic modulus of the PCC slab, coefficient of subgrade reaction, and to forward calculate the radius of relative stiffness, and tensile stresses at the bottom of the PCC layer in two pavement test sections. E_{PCC}, k_S, RRS, and σ_{MAX} predictions for IA-Allamakee and IA-Wright counties concrete pavement test sections were presented. Consistent results were obtained from the developed ANN-based models by using the field FWD deflection basins. It should be noted that k_S values might show considerable seasonal changes throughout the year, and the time of the FWD testing used for backcalculation should be taken into account in the design level. All FWD testings used in this case study were conducted in May, 2006.

The backcalculated coefficient of subgrade reaction is independent of the assumed PCC slab thickness values but even a small change in the assumed PCC slab thickness causes critical differences in the backcalculated elastic moduli of the PCC slab (Ioannides 1989). Therefore, the thickness of the PCC slab was not used as an input parameter in the developed BCM-k_S backcalculation models. On the other hand, the thickness of the PCC slab playing a crucial role in the E_{PCC} backcalculation is one of the most important parameters in the BCM-E_{PCC} prediction models. Generally, slab thickness exhibits considerable variability in the field and this has a large impact on the backcalculated PCC slab properties. Consequently, a given error in the estimate of the thickness of the PCC slab will have significant effects on the backcalculated slab modulus. A sensitivity study was conducted in the study to show the significance of the layer thickness and layer bonding on the backcalculated layer moduli.

In addition, the time of the day for the FWD testing is also crucial in the E_{PCC} backcalculation due to curling and warping problems in concrete pavements. The results of the previous studies indicate that the variations in temperature between two separate FWD tests on the same pavement section affect primarily the elastic modulus of the slab (Ioannides et al. 1989). Basically, more scatter is expected in E_{PCC} predictions due to the curling and

warping issues, possible variations in PCC slab thickness, and the uncertainties in bonding degree between the PCC and base layers.

The backcalculated and forward calculated concrete pavement properties and critical pavement responses are significantly affected from the number of the FWD sensors. As the number of sensors increases, the mean value of elastic modulus of PCC slab increases and the mean value of coefficient of subgrade reaction decreases (Rufino et al. 2002). D_0 and D_{12} deflections are relatively more sensitive to changes in the elastic modulus of PCC slab, compared to D_{48} and D_{60} deflections. On the other hand, D_{48} and D_{60} deflections are much more sensitive to the changes in the subgrade support (k_S). Therefore, BCM-E_{PCC}-(4) model (Inputs: D_0, D_{12}, D_{24}, D_{36}, and h_{PCC}) is proposed for the elastic modulus of PCC slab predictions, and BCM-k_S-(6) model (Inputs: D_0, D_{12}, D_{24}, D_{36}, D_{48}, and D_{60}) is proposed for the coefficient of subgrade reaction predictions. FCM-RRS-(4) model (Inputs: D_0, D_{12}, D_{24}, D_{36}, and h_{PCC}) and FCM-σ_{MAX}-(4) model (Inputs: D_0, D_{12}, D_{24}, D_{36}, and h_{PCC}) are also proposed for the radius of relative stiffness, and maximum tensile stresses at the bottom of the PCC layer predictions, respectively.

CONCLUSIONS

ANN-based backcalculation and forward calculation models developed in this study successfully predicted the elastic modulus of Portland cement concrete layer (E_{PCC}), the coefficient of subgrade reaction (k_S), the radius of relative stiffness (RRS), and the maximum tensile stresses at the bottom of the PCC layer (σ_{MAX}) from FWD deflection data in a rapid and accurate manner. Several network architectures were trained with varying levels of noise in them in order to develop more robust networks that can tolerate the noisy or inaccurate pavement deflection patterns collected from the FWD field tests. In addition, a sensitivity study was conducted for the ANN model architecture. The prediction capabilities of the ANN-based models developed in this study were compared with the pavement layer backcalculation software results (EverCalc 5.0 and BAKFAA), finite element program solutions (ISLAB2000 and EverFE 2.24) and closed-form equations. A good agreement was

satisfied on this comparison study. The significance of the layer thickness and layer bonding was also presented in a sensitivity study. The use of the ANN-based models also resulted in a drastic reduction in computation time. Finally, it can be concluded that the developed ANN-based models can be utilized to backcalculate the E_{PCC}, and k_S, and to forward calculate the RRS and σ_{MAX} with very low average absolute error values (<0.82 % for the synthetic deflection basins).

ACKNOWLEDGEMENTS

The authors gratefully acknowledge the Iowa Department of Transportation (IA-DOT) for sponsoring this study. The contents of this paper reflect the views of the authors who are responsible for the facts and accuracy of the data presented within. The contents do not necessarily reflect the official views and policies of the IA-DOT. This paper does not constitute a standard, specification, or regulation.

REFERENCES

Adeli, H. and Hung, S.L. 1995. Machine Learning: Neural Networks, Genetic Algorithms, and Fuzzy Systems, Wiley, New York.

Adeli, H. and Park, H.S. 1998. Neurocomputing in Design Automation, CRC Press, Boca Raton, FL.

BAKFAA. 2003. Computer Program for Backcalculation of Airport Pavement Properties, (Federal Aviation Administration, http://www.airtech.tc.faa.gov/naptf/download/).

Barenberg, E. J., and K. A. Petros. 1991. Evaluation of Concrete Pavements Using NDT Results. Project IHR-512, University of Illinois at Urbana-Champaign and Illinois Department of Transportation, Report No. UILU-ENG-91-2006.

Bayrak, M. B., and Ceylan, H. 2006. Backcalculation of Rigid Pavement Parameters by Artificial Neural Networks. Infra-Structure Systems Engineering, Bio-informatics and Computational Biology and Evolutionary Computation, Vol. 16, Proceedings of the Artificial Neural Networks In Engineering (ANNIE) Conference, St. Louis, Missouri.

Bayrak, B., Gopalakrishnan, K., and Ceylan, H. 2006. Neural Network-Based Backcalculation Models for Non-Destructive Evaluation of Rigid Airfield Pavement Systems, Accepted for Presentation and Publication at the 6th International DUT-Workshop on Fundamental Modelling of Design and Performance of Concrete Pavements, Old-Turnhout, Belgium, September 14-17.

Ceylan, H. 2004. Use of Artificial Neural Networks for the Analysis and Design of Concrete Pavement Systems. 5th International CROW-Workshop on Fundamental Modeling of the Design and Performance of Concrete Pavements, Istanbul, Turkey.

Ceylan, H., Guclu, A., Tutumluer, E., Thompson, M.R., and Gomez-Ramirez F. 2004. Neural Network-Based Structural Models for Rapid Analysis of Flexible Pavements with Unbound Aggregate Layers. Proceedings, Sixth International Conference on Pavements Unbound, Nottingham, England.

Ceylan, H., Bayrak, M.B. and Guclu, A. 2005. Use of Neural Networks to Develop Robust Backcalculation Algorithms for Nondestructive Evaluation of Flexible Pavement Systems. Intelligent Engineering Systems through Artificial Neural Networks, ANNIE, 15, pp.731-740.

Chou, Y.T. 1981. Structural Analysis Computer Programs for Rigid Multicomponent Pavement Structures with Discontinuities - WESLIQID and WESLAYER. Technical Report GL-81-6, U.S. Army Engineer Waterways Experiment Station.

Darter, M.I., K.T. Hall, and C. Kuo. 1995. Support Under Portland Cement Concrete Pavements. NCHRP Report 372. Washington, DC: National Cooperative Highway Research Program.

Davids, W. G., Turkiyyah, G. M., and Mahoney, J. P. 1998. EverFE: rigid pavement three – dimensional finite element analysis tool. Transportation Research Record. Vol. 1629,Transportation Research Board, Washington, D.C., pp. 41-49.

EverCalc© 5.0. 1999. Pavement Backcalculation Program, Washington State Department of Transportation.

FAA Report. 2004. Use of Nondestructive Testing in the Evaluation of Airport Pavements, FAA Advisory Circular No. 150/5370-11A, Office of Airport Safety and Standards, Federal Aviation Administration.

Fausett, L. 1994. Fundamentals of Neural Networks. New York: Prentice Hall.

Foxworthy, P. T., and M. I. Darter. 1989. ILLI-SLAB and FWD Deflection Basins for Characterization of Rigid Pavements. Nondestructive Testing of Pavements and Backcalculation of Moduli. American Society for Testing and Materials, pp. 368-386.

Golden, R.M. 1996. Mathematical Methods for Neural Network Analysis and Design, MIT Press, Cambridge, MA.

Hall, K. T. 1992. Backcalculation Solutions for Concrete Pavements, Technical Memo Prepared for SHRP Contract P-020, Long-Term Pavement Performance Data Analysis.

Hall, K. T., M. I. Darter, T. Hoerner, and L. Khazanovich. 1996. LTPP Data Analysis – Phase I: Validation of Guidelines for K Value Selection and Concrete Pavement Performance Prediction. Interim Report prepared for FHWA, ERES Consultants, Champaign, IL.

Haykin, S. 1999. Neural Networks: A Comprehensive Foundation. Prentice-Hall Inc. NJ, USA.

Hegazy, T., Fazio, P., and Moselhi, O. 1994. Developing Practical Neural Network Applications Using Backpropagation. Microcomputers in Civil Engineering, Vol.9, No.2, pp.145-159.

Huang, Y.H. 1985. A Computer Package for Structural Analysis of Concrete Pavements. Proceedings, 3rd International Conference on Concrete Pavement Design and Rehabilitation, Purdue University, pp.295-307.

Ioannides, A. M. 1990. Dimensional Analysis in NDT Rigid Pavement Evaluation. Journal of Transportation Engineering, Vol.116, No. 1, pp.23-36.

Ioannides, A.M. 1994. Concrete Pavement Backcalculation Using ILLI-BACK 3.0, Nondestructive Testing of Pavements and Backcalculation of Moduli. American Society for Testing and Materials, Vol. 2, pp.103-124.

Ioannides, A.M., E.J. Barenberg, and J.A. Lary. 1989. Interpretation of Falling Weight Deflectometer Results Using Principals of Dimensional Analysis. Proceedings, 4th International Conference on Concrete Pavement Design and Rehabilitation, Purdue University, pp.231-247.

Ioannides, A.M., Khazanovich, L., and Becque, J.L. 1992. Structural Evaluation of Base Layers in Concrete Pavement Systems. In Transportation Research Record: Journal of the Transportation Research Board, No. 1370, Washington, D.C., pp. 20-28.

Kennedy J.C. 1998. Material Nonlinear and Time-Dependent Effects on Pavement Design for Heavyweight, Multi-Wheel Vehicles. Proceedings of the First International symposium on 3D Finite Element For Pavement Analysis and Design.

Khazanovich, L. 1994. Structural Analysis of Multi-Layered Concrete Pavement Systems, Ph.D. dissertation, University of Illinois, Illinois, USA.

Khazanovich, L., and Ioannides, A.M. 1995. DIPLOMAT: Analysis Program for Bituminous and Concrete Pavements. In Transportation Research Records: Journal of the Transportation Research Board, No. 1482, pp. 52-60.

Khazanovich, L., Yu, H.T., Rao, S., Galasova, K., Shats, E., and Jones, R. 2000. ISLAB2000 - Finite Element Analysis Program for Rigid and Composite Pavements, User's Guide, ERES Consultants, A Division of Applied Research Associates, Champaign, Illinois.

Kok, A.W.M. 1990. A PC Program for the Analysis of Rectangular Pavements Structures. Proceedings, 2nd International Workshop on the Design and Rehabilitation of Concrete Pavements, Sigüenza, Spain, pp. 113-120.

LeCun, Y. 1993. Efficient learning and second-order methods, a tutorial at NIPS 93, Denver.

Mallela, J. and K.P. George. 1994. Three-Dimensional Dynamic Response Model for Rigid Pavements. In Transportation Research Record: Journal of the Transportation Research Board, No. 1448, TRB, Washington, D.C.

Mehrotra, K., Mohan, C.K., and Ranka, S. 1997. Elements of Artificial Neural Networks, MIT Press, Cambridge, MA.

NCHRP Report. 2003. Guide for Mechanistic-Empirical Design of New and Rehabilitated Pavement Structures, Appendix QQ: Structural Response Models for Rigid Pavements.

Patterson, D. 1996. Artificial Neural Networks. Singapore: Prentice Hall.

Rufino, D., Roesler, J., and Barenberg, E.J. 2002. Evaluation of Different Methods and Models for Backcalculating Pavement Properties Based on Denver International Airport Data. 2002 Federal Aviation Administration Technology Transfer Conference, Atlantic City, NJ.

Rumelhart, D.E., Hinton, G.E., and Williams, R.J. 1986. Learning integral representation by error propagation. Parallel Distributed Processing, MIT Press, Cambridge, MA, pp.318-362.

Smith, K. D., M. J. Wade, D. G. Peshkin, L. Khazanovich, H. T. Yu, and M. I. Darter. 1996. Performance of Concrete Pavements, Volume II – Evaluation of In-Service Concrete Pavements. Report No. FHWA-RD-95-110, ERES Consultants, Champaign, IL.

Tabatabaie, A.M., and Barenberg, E.J. 1978. Finite Element Analysis of Jointed or Cracked Concrete Pavements. In Transportation Research Record: No. 671, TRB, pp. 11-18.

Tayabji, S.D., and Colley, B.E. 1983. Improved Pavement Joints. In Transportation Research Records: Journal of the Transportation Research Board, No. 930.

Tia, M., Armaghani, J.M., Wu, C.L., Lei, S., and Toye, K.L. 1987. FEACONS III Computer Program for an Analysis of Jointed Concrete Pavements. In Transportation Research Record: Journal of the Transportation Research Board No.1136, TRB, pp. 12-22.

Tia, M., Wu, C.L., Ruth, B.E., Bloomquist, D., and Choubane, B. 1988. Field Evaluation of Rigid Pavements for the Development of a Rigid Pavement Design System – Phase III. Project 245-D54, Dept. of Civ. Engr., Univ. of Florida, Gainesville, Fla.

Topping, B. H. V. and Bahreininejad, A. 1997. Neural Computing for Structural Mechanics, Saxe-Coburg Publications, Edinburgh, UK.

Westergaard, H.M. 1926. Stresses in Concrete Pavements Computed by Theoretical Analysis, Public Roads, Vol. 07, pp. 25-35.

Winkler, E. 1864. Die Lehre von der Elastizitt und Festigkeit (Theory of Elasticity and Strenght), H. Dominicus, Prague, Czechoslovakia (in German).

CHAPTER 6. BACKCALCULATION OF TOTAL EFFECTIVE LINEAR TEMPERATURE DIFFERENCE (TELTD) IN JOINTED PLAIN CONCRETE PAVEMENT SYSTEMS

A paper to be submitted to *The Journal of Transportation Engineering (ASCE)*

Mustafa Birkan Bayrak and Halil Ceylan

ABSTRACT

Falling Weight Deflectometer (FWD) tests are often conducted on concrete pavements to assess the in-situ structural capacity of pavement systems. The pavement surface deflections are affected from the curling resulting from the differential expansion and contraction between the top and bottom of the concrete slabs. Generally, most of the backcalculation programs do not take into account the curling effects in the backcalculation of structural capacity of pavement systems and the first step for this goal should be to predict the total effective linear temperature difference (TELTD). The objective of this investigation is to develop a rapid methodology for backcalculating the TELTD in jointed plain concrete pavements (JPCP) from the FWD deflection basins and the thickness of the concrete pavement layer. With additional tests in the field, it is also possible to estimate the effective built-in temperature difference (EBITD) which is an important component of any mechanistic-empirical design procedure for jointed plain concrete pavements. The results of this study demonstrated that the developed ANN-based models can successfully predict the total effective linear temperature difference of in-service pavements in an efficient and cost-effective way without any need for embedded instrumentations in concrete pavements. Therefore, such ANN-based backcalculation models can be used for large number of concrete slabs in a relatively short period of time for estimating the TELTD that can be used for adjustments for the in-situ structural capacity of JPCP systems.

Key Words: Artificial Neural Networks, Falling Weight Deflectometer, Finite Element Analysis, Concrete Pavements, Curling, Total Effective Linear Temperature Difference, Pavement Layer Backcalculation, Nondestructive Testing and Evaluation.

INTRODUCTION

Daily and seasonal variations in weather conditions and fixed built-in effects in concrete layer cause the concrete slabs to curl up or down at joints and around the perimeter. Curling in concrete slabs is a combination of five nonlinear components which are temperature gradient, built-in temperature gradient, moisture gradient, differential drying shrinkage, and creep (Rao and Roesler 2005a). The total effective linear temperature difference (TELTD) is represented as the total amount of curling in a slab due to the combination of these five factors. Also, effective built-in temperature difference (EBITD) is represented as the difference between the TELTD and the temperature difference between top and bottom of a concrete slab (ΔT_{TG}). The relationship between these two definitions was shown in Equation 6.1.

$$TELTD = \Delta T_{TG} + EBITD \tag{6.1}$$

The concrete slabs tend to curl up when the slab surface is cooler and drier than base [see Figure 6.1(a)], and tend to curl down when the slab surface is at a higher temperature and moisture than base [see Figure 6.1(b)]. Rao and Roesler (2005b) indicated that temperature difference in a typical slab can vary from a night-time value of 14 ^{0}F to 23 ^{0}F to a day-time value of 59 ^{0}F to 77 ^{0}F depending on the climatic conditions, slab geometry, material properties of the slab and base, subgrade moisture content, etc. Rao and Roesler (2005b) also stated that EBITD can be in a range of -22 ^{0}F to 23 ^{0}F, or even greater.

Generally, concrete slabs are not completely flat under the normal environmental conditions due to the curling effects and concrete slab responses are affected from these curling effects throughout the day and season. Researchers have been focusing on the temperature and moisture gradient effects on concrete slab behavior for a long time (Hatt 1925; Carlson 1938; Hveem 1951; Hveem and Tremper 1957). The pavement performance is directly affected from the curling behavior of concrete slabs. Therefore, the mechanistic-empirical design procedures generally take into account the temperature gradients and EBITD values (Zollinger and Barenberg 1989; Darter et al. 2001; Hiller and Roesler 2002). In addition, backcalculated concrete slab and subgrade moduli are affected from the time of the day at

which deflection testing is done (Ioannides 1989). This effect is most likely due to temperature gradients and the resulting slab curling. Therefore, accounting for the effect of slab curling is very important for reliable interpretation of deflection data and the first step on this goal is to determine the amount of curling in concrete slabs. Then, this curling amount can be used as another input parameter in the backcalculation of concrete slab and subgrade moduli.

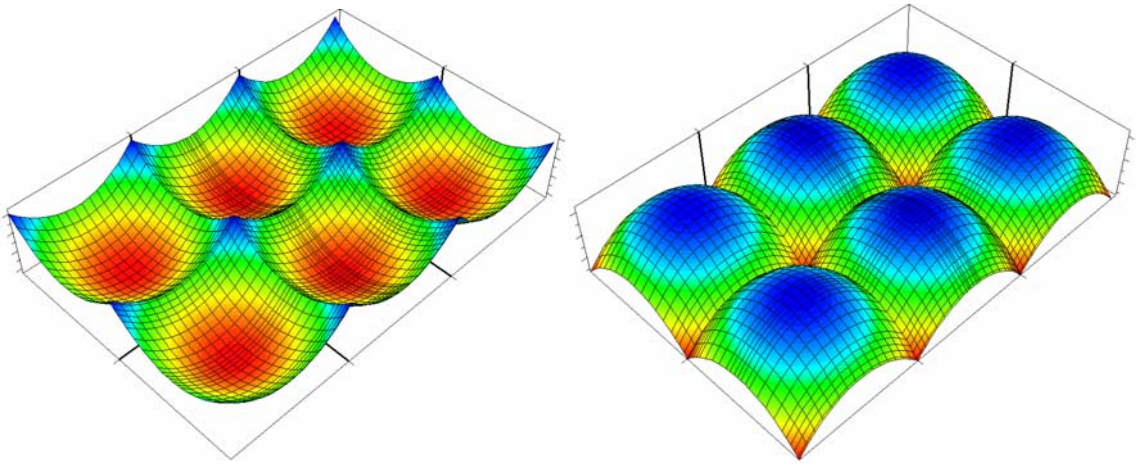

(a) (b)

Figure 6.1. (a) Typical night-time curling (b) Typical day-time curling

GENERATING ISLAB2000 FINITE ELEMENT SOLUTION DATABASE

In order to train the ANN models, ISLAB2000 (Khazanovich et al. 2000) runs were generated by modeling slab-on-grade concrete pavement systems. A single slab layer resting on a Winkler foundation was analyzed in all cases. Concrete pavements analyzed in this study were represented by a six-slab assembly, each slab having dimensions of 15 ft by 15 ft (4.5 m by 4.5 m).

To maintain the same level of accuracy in the results from all analyses, a standard ISLAB2000 finite element mesh was constructed for the slab. This mesh consisted of 10,004 elements with 10,209 nodes. The ISLAB2000 solutions database was generated by varying the elastic modulus of PCC slab (E_{PCC}), coefficient of subgrade reaction (k_S), thickness of PCC layer (h_{PCC}), total effective linear temperature difference (TELTD), and load transfer efficiency (LTE) over a range of values representative of realistic variations in the field. The

ranges used in the analyses are shown in Table 6.1. The input parameters were selected randomly between the minimum and maximum values. The Poisson's ratio (ν), the slab width (W), the slab length (L), PCC unit weight (γ), and coefficient of thermal expansion (α) were set equal to 0.15, 15 ft (4.5 m), 15 ft (4.5 m) , 0.087 lb/in^3(2,408.15 kg/m^3), 5.5x10^{-6} 1/^{o}F (9.9x10^{-6} 1/^{o}C), respectively.

Table 6.1. Ranges of the input parameters used in the ISLAB2000 database generation

Pavement System Inputs	**Minimum Value**	**Maximum Value**
E_{PCC}, (ksi)	2,000	10,000
k_S, (psi/in)	50	700
h_{PCC}, (in)	6	20
TELTD, (^{o}F)	-60	+60
LTE, (%)	1	99

A general view of the ISLAB2000 FE solution is shown in Figure 6.2(a). As the environmental effects are introduced to the pavement system in addition to the typical traffic loading, additional deflections and stresses occur in concrete slabs as can be seen from Figure 6.2(b).

PROCEDURE OF THE DEVELOPED APPROACH

Steps in the preparing the ANN training database:

Step 1. Totally 8,734 different pavement and loading configurations were prepared to be conducted in ISLAB2000 FE program. ISLAB2000 program input parameters were selected randomly between the minimum and maximum values that had been previously determined for each parameter.

Step 2. ISLAB2000 runs were applied for three different loadings for each pavement configurations.

Loading 1: 9-kip traffic loading in the center of the slab + Temperature loading,

Loading 2: 9-kip traffic loading in the corner of the slab + Temperature loading,

Loading 3: Temperature loading only.

Then, corresponding deflections were extracted from ISLAB2000 solution database.

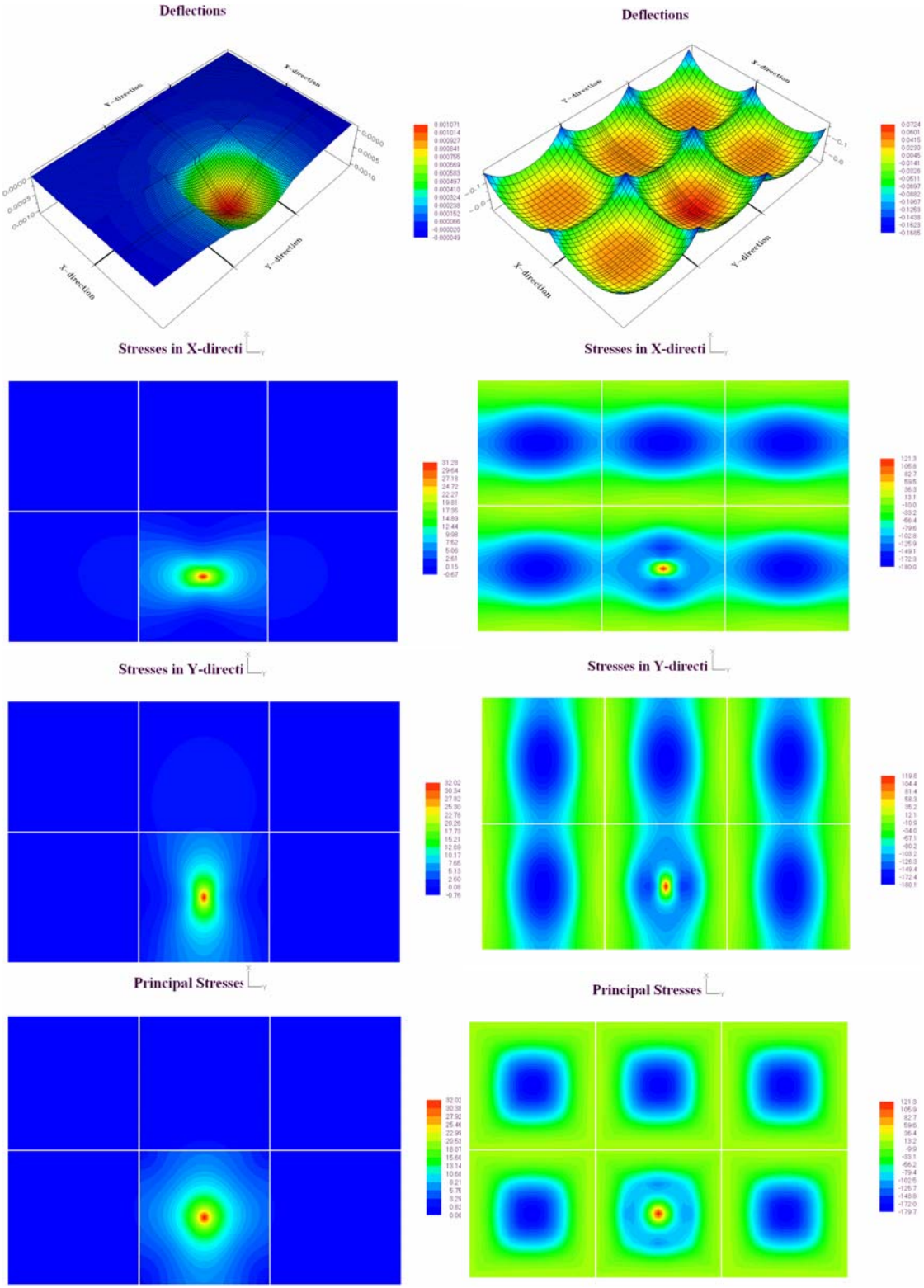

(a) (b)

Figure 6.2. A general view of the ISLAB2000 solutions for deflections and stresses: (a) Traffic load only, (b) Traffic load + Temperature

Step 3. In this step, effect of temperature on the pavement surface deflections was investigated by comparing ISLAB2000 runs. In the field, concrete slabs are generally curled up or down daily because of the fluctuations in the temperature and moisture during the day and night in addition to the built-in curling which already exists in the slab. That's why the concrete slabs are not in completely flat condition during the FWD testing. Therefore, FWD sensors are positioned in the field on a curled slab, not on a completely flat slab and the deflections measured by the FWD sensors are function of the FWD loading and the total amount of curling in the slab. When the concrete slabs curl up, some additional voids occur under the edges and corners of the slab due to the loss of contact between the pavement layer and subgrade and higher FWD deflections are obtained from the field tests conducted in the edges and corners of the concrete slabs compared to the flat-slab conditions. On the other hand, very similar deflections are obtained in the mid-slab (center) tests since there is not any loss of contact between the concrete slab and subgrade even in the curl up condition. In the curl down conditions, excessive voids occur under the mid-slab instead of edges and corners. This time loss of contact occurs under the center of the slab and it is expected to have different deflection basins from the mid-slab FWD tests for curl down condition and flat-slab conditions. The Figure 6.3 show all these four conditions for mid-slab and slab corner for curl up, curl down, and flat-slab conditions. As expected, different deflection basins are obtained in the mid-slab for positive temperature gradient and in the corner for negative temperature gradient. On the other hand, same deflection basins are obtained in the mid-slab for negative temperature gradient and in the corner for positive temperature gradient for curled and flat conditions.

Step 4. The total number of the ISLAB2000 runs conducted in this study was 8,734. Corresponding deflection basins and loading condition were extracted from the ISLAB2000 solution database for each pavement configuration (see Figure 6.4). Then, in order to find out the deflections due to the 9-kip traffic loading only in a *curled* slab (temperature-introduced slab), "Loading 1 – Loading 3" and "Loading 2 – Loading 3" (as explained in Step 2) deflection basins were calculated to create the ANN training database. These adjusted deflection basins were used as the input parameters in the ANN trainings in addition to the thickness of the PCC layer and the load transfer efficiency across the transverse joint. In the

field, all input parameters required for the proposed approach are obtained from the FWD tests except the thickness value which can be determined from the project documents, mileposts, or from other sources for each pavement section.

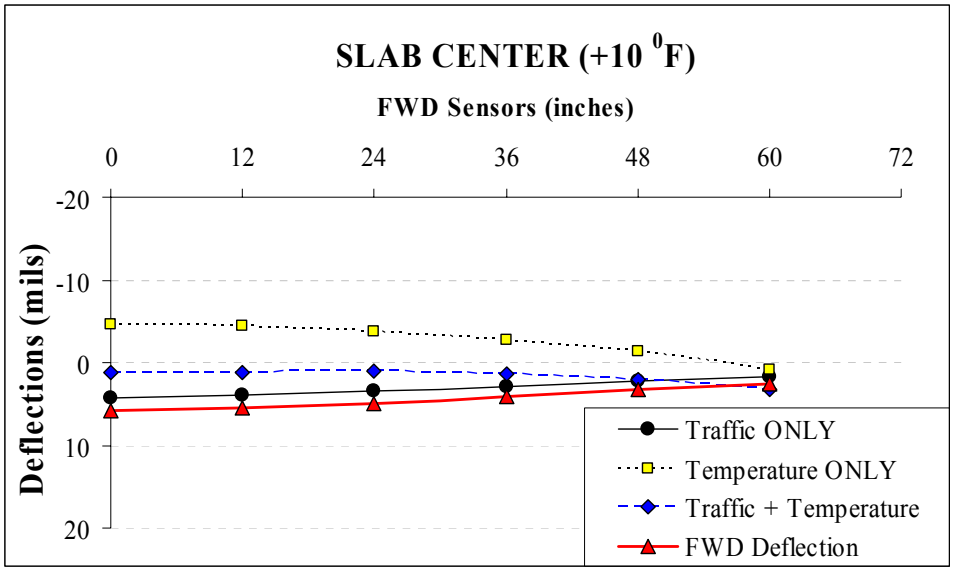

(a)

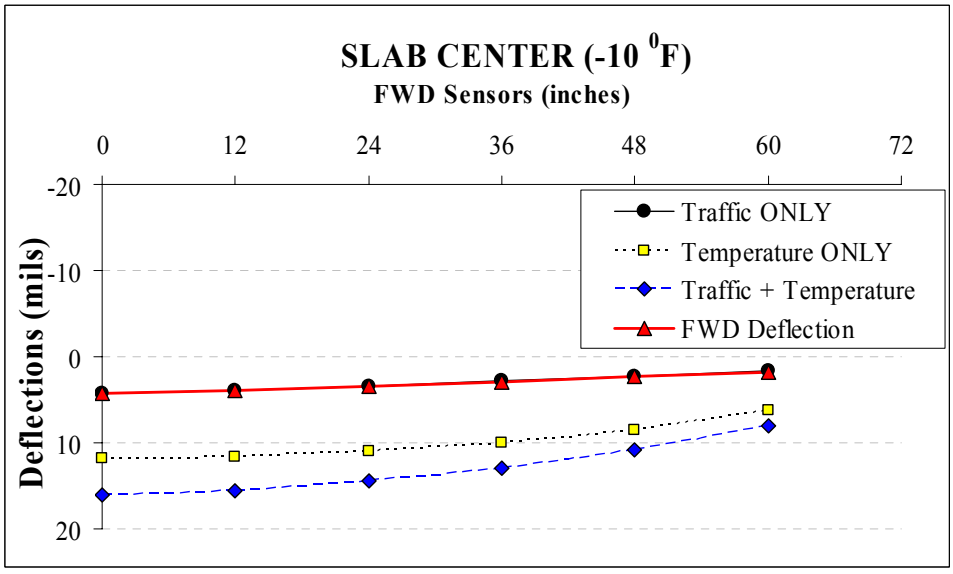

(b)

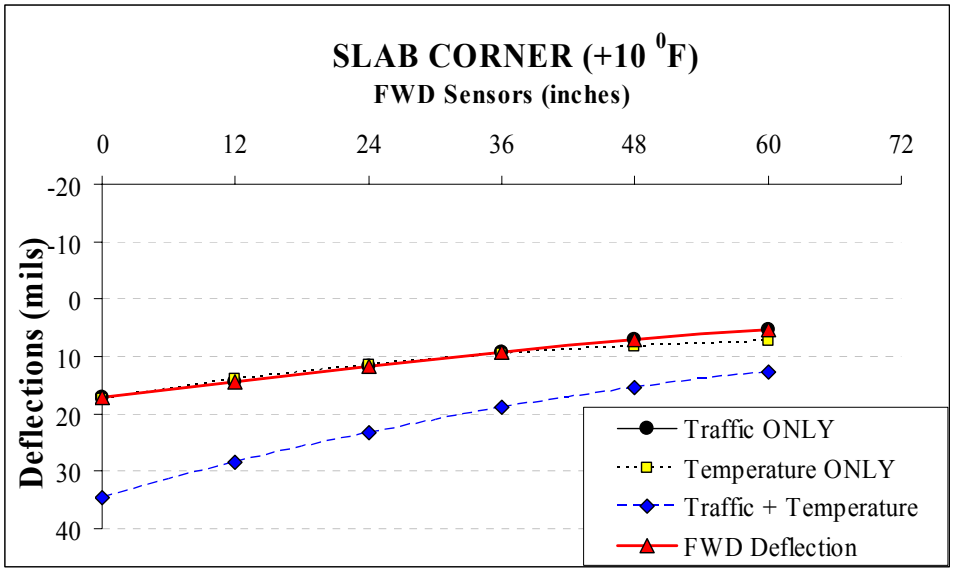

(c)

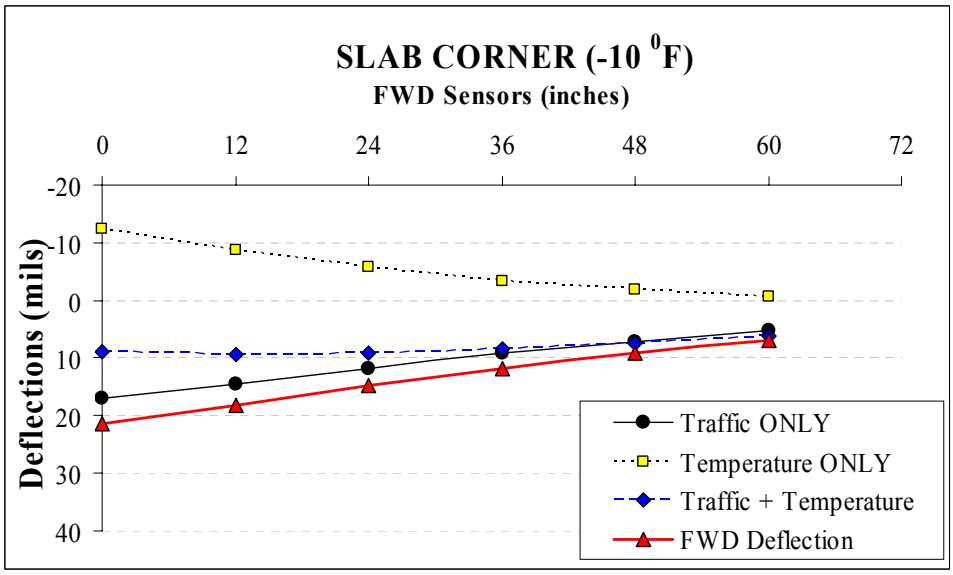

(d)

Figure 6.3. Comparison of deflection basins: (a) Slab center, $+10^0$F, (b) Slab center, -10^0F, (c) Slab corner, $+10^0$F, and (d) Slab corner, -10^0F.

Figure 6.4. The schematic view of the structural model

Steps in the development of the ANN-based TELTD backcalculation models:

Step 5. The next step in the development of ANN-based TELTD backcalculation models is the training of the ANN models. For each training, the ISLAB2000 solution database was first portioned to create a training set of 8,234 (94%) and an independent testing set of 500 (6%) patterns to check the prediction performance of the trained ANN models. Backpropagation type ANN architectures with two hidden layers were used for the training of the ANN models in this study. A general view of the ANN model can be seen in Figure 6.5.

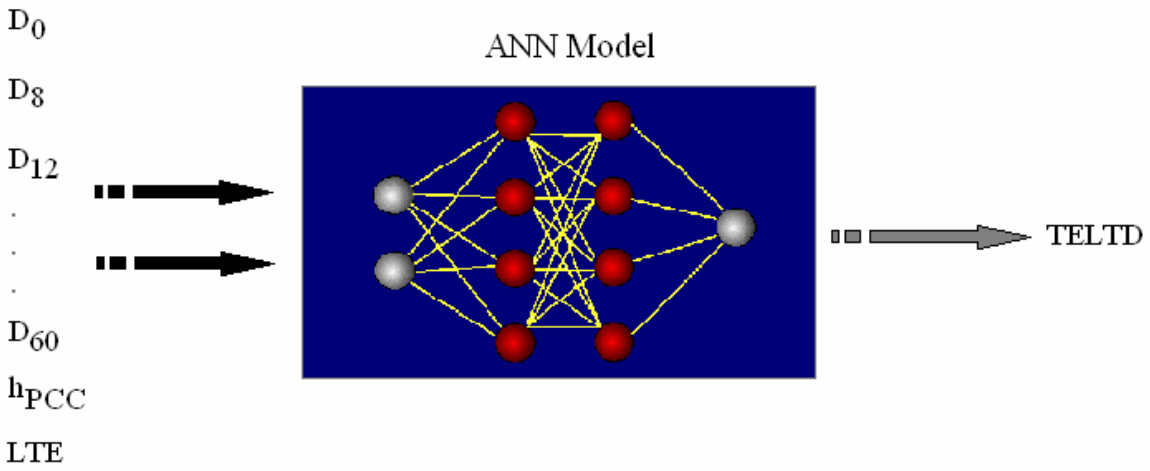

Figure 6.5. The schematic view of the ANN-based backcalculation model

Step 6. The FWD surface deflections (D_0, D_8, D_{12}, D_{18}, D_{24}, D_{36}, D_{48}, and D_{60}) are often collected at several different locations, at the drop location (0) and at radial offsets of 8-in. (203-mm), 12-in. (254-mm), 18-in. (457-mm), 24-in. (610-mm), 36-in. (914-mm), 48-in (1219-mm), and 60-in. (1524-mm), and 72-in. (1829-mm). Several ANN-based backcalculation models were developed using different FWD sensor configurations. For example, there are 4-Deflection (D_0, D_{12}, D_{24}, D_{36}), 6-Deflection (D_0, D_{12}, D_{24}, D_{36}, D_{48}, D_{60}), 7-Deflection (D_0, D_8, D_{12}, D_{18}, D_{24}, D_{36}, D_{60}), and 8-Deflection (D_0, D_8, D_{12}, D_{18}, D_{24}, D_{36}, D_{48}, D_{60}) ANN-based backcalculation models to predict TELTD. Please note that each model uses both center and corner FWD deflection basins as input parameters which means 4-Deflection model uses actually eight deflection values (four deflections from center and four deflections from corner FWD loading). The average absolute error (AAE) values were calculated to investigate the prediction capability of each model as tabulated in Table 6.2. Figure 6.6 shows the comparison of the ANN-based backcalculation model predictions and ISLAB2000 solutions. The training progress curves show also the trend of the decrease of the mean squared error (MSE) for each model (see Figure 6.7).

Table 6.2. Input/output configuration of ANN-based TELTD backcalculation models

Model Name	**Inputs**	**Output**	**AAE(^oF)**
TELTD-4DEFL	Center 4Defl.+Corner 4Defl.+h_{PCC}+LTE	TELTD	1.37
TELTD-6DEFL	Center 6Defl.+Corner 6Defl.+h_{PCC}+LTE	TELTD	1.30
TELTD-7DEFL	Center 7Defl.+Corner 7Defl.+h_{PCC}+LTE	TELTD	1.53
TELTD-8DEFL	Center 8Defl.+Corner 8Defl.+h_{PCC}+LTE	TELTD	1.33

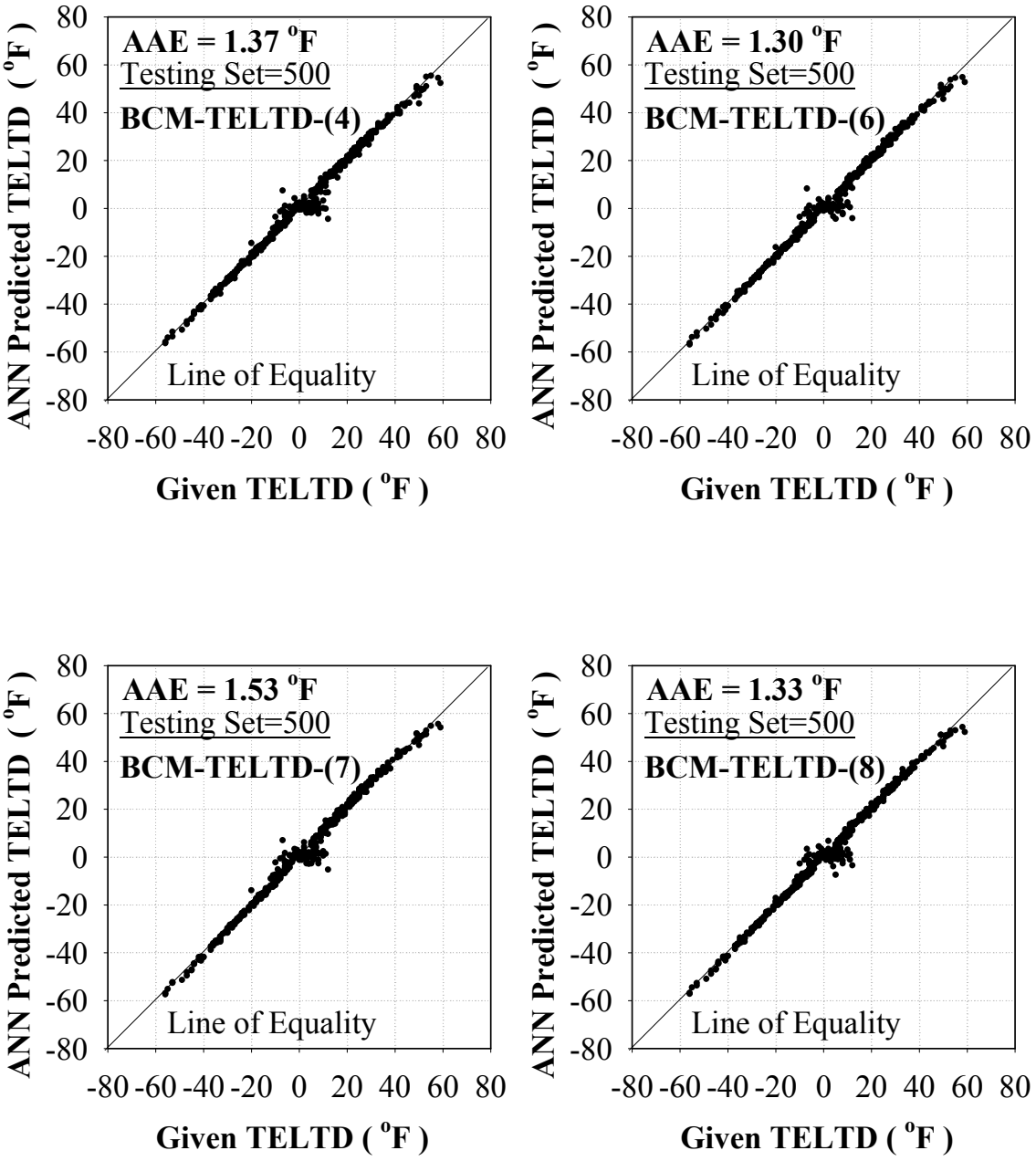

Figure 6.6. Prediction performance of the ANN-based models for backcalculating the Total Effective Linear Temperature Difference, TELTD

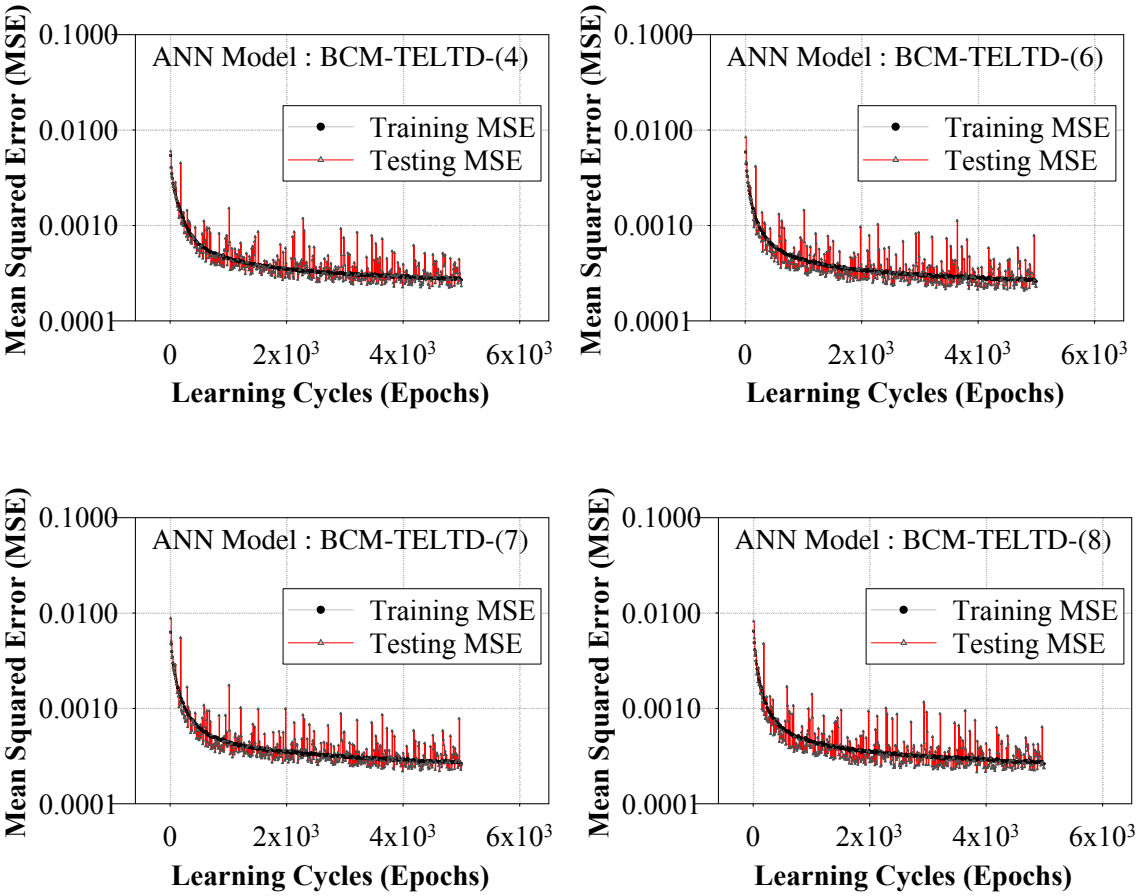

Figure 6.7. Training progress curve for the TELTD backcalculation models

Step 7. In addition to the training and testing sets prepared for backcalculation models, more ANN training sets were generated by introducing ±2%, ±5% and ±10% noise to the FWD deflection data used in backcalculation models. The purpose of introducing noisy patterns in the training sets was to develop more robust networks that can tolerate the noisy or inaccurate deflection patterns collected from the FWD deflection basins. Noise introduction to trained ANN models was as follows: ISLAB2000 solution database was first partitioned to create training sets of 8,234 training patterns and an independent testing set of 500 patterns to check the performance of the trained ANN models. Uniformly distributed random numbers ranging from -2 to +2% (± 2%), -5 to +5% (± 5%) and -10 to +10%(± 10%) were generated each time to create noisy training patterns. After adding randomly selected noise values only to the pavement surface deflections of D_0, D_8, D_{12}, D_{18}, D_{24}, D_{48},

and D_{60}, new training data sets were developed for each noisy training set. By repeating the noise introduction procedure, four more training data sets were formed for each backcalculation models. Including the original training set with no noise in it, a total of 41,170 patterns were used to train the noise-introduced ANN-based backcalculation models. The AAE values of the noise-introduced TELTD backcalculation models were tabulated in Table 6.3.

Table 6.3. Input/output configuration of noise-introduced ANN-based TELTD backcalculation models

Model Name	**Inputs**	**Output**	**AAE(^{o}F)**
TELTD-4DEFL-(±2%)	Center 4Defl.+Corner 4Defl.+h_{PCC}+LTE	TELTD	1.49
TELTD-4DEFL-(±5%)	Center 4Defl.+Corner 4Defl.+h_{PCC}+LTE	TELTD	1.91
TELTD-4DEFL-(±10%)	Center 4Defl.+Corner 4Defl.+h_{PCC}+LTE	TELTD	2.51
TELTD-6DEFL-(±2%)	Center 6Defl.+Corner 6Defl.+h_{PCC}+LTE	TELTD	1.38
TELTD-6DEFL-(±5%)	Center 6Defl.+Corner 6Defl.+h_{PCC}+LTE	TELTD	1.56
TELTD-6DEFL-(±10%)	Center 6Defl.+Corner 6Defl.+h_{PCC}+LTE	TELTD	1.85
TELTD-7DEFL-(±2%)	Center 7Defl.+Corner 7Defl.+h_{PCC}+LTE	TELTD	1.28
TELTD-7DEFL-(±5%)	Center 7Defl.+Corner 7Defl.+h_{PCC}+LTE	TELTD	1.38
TELTD-7DEFL-(±10%)	Center 7Defl.+Corner 7Defl.+h_{PCC}+LTE	TELTD	1.88
TELTD-8DEFL-(±2%)	Center 8Defl.+Corner 8Defl.+h_{PCC}+LTE	TELTD	1.41
TELTD-8DEFL-(±5%)	Center 8Defl.+Corner 8Defl.+h_{PCC}+LTE	TELTD	1.45
TELTD-8DEFL-(±10%)	Center 8Defl.+Corner 8Defl.+h_{PCC}+LTE	TELTD	1.73

Steps in the backcalculation of TELTD with field data:

Step 8. In order to be able to use this approach, FWD load must be dropped at three different locations in a concrete slab in the field (see Figure 6.8). One FWD loading is needed at the center of the slab, one is needed in the corner of the slab, and the last one is needed in the mid-transverse joint location in the slab. Load transfer efficiency (LTE) which is one of the input parameters of the developed approach can be easily calculated as the ratio of unloaded slab deflection to loaded slab deflection as shown in Figure 6.9. Then, the only information needed is the thickness of the concrete layer which can be obtained from the

project documents. In summary, TELTD in concrete slabs can be backcalculated from FWD deflection basins with the developed ANN-based models in a rapid and cost-effective way.

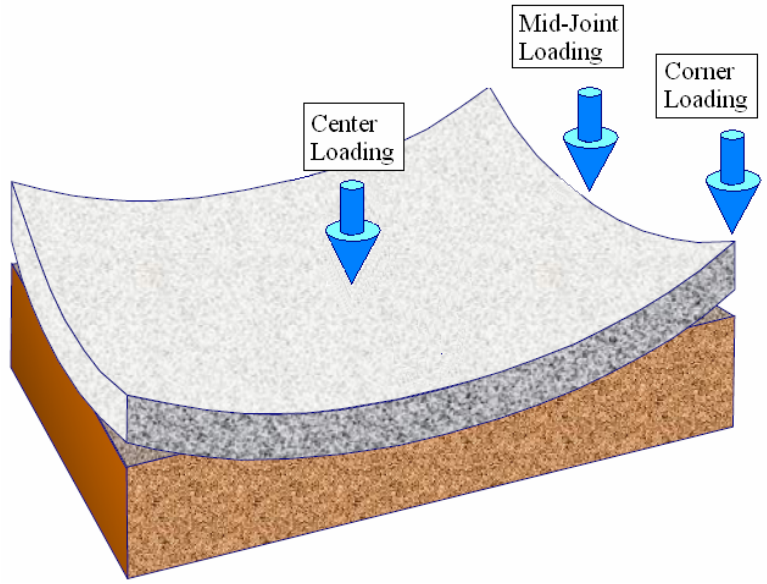

Figure 6.8. FWD loading locations for the proposed approach

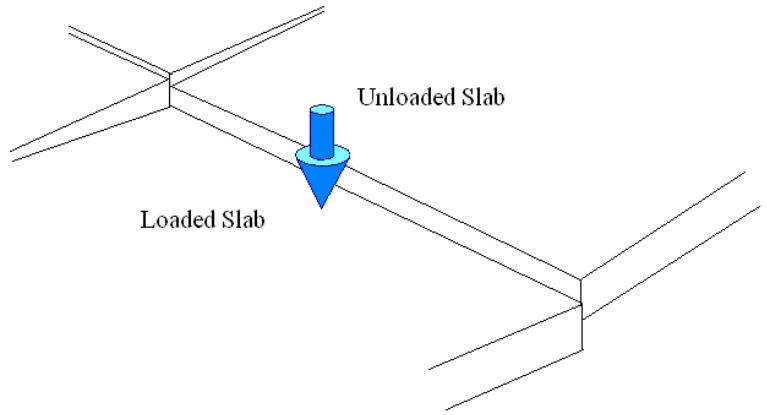

Figure 6.9. Load transfer efficiency

COMPARISON WITH THE MULTIPLE LINEAR REGRESSION ANALYSIS

The comparison of the artificial neural network approach with the multiple linear regression (MLR) analysis is summarized for the backcalculation of the total effective linear temperature difference parameter in concrete pavements. The same dataset was used for the development of the two approaches and a separate dataset was used for the calculations of AAE values and comparison of the results. The general schematic views of two approaches

and prediction capabilities are shown in Figure 6.10 and Figure 6.11, respectively. The complexity in the nature of this challenging problem does not allow a few coefficients to solve the entire problem as in regression analysis. As shown from the Figure 6.11, the artificial neural networks (AAE = 1.30%) are superior over the multiple linear regression analysis (AAE = 10.57%) for this particular problem for the backcalculation of TELTD.

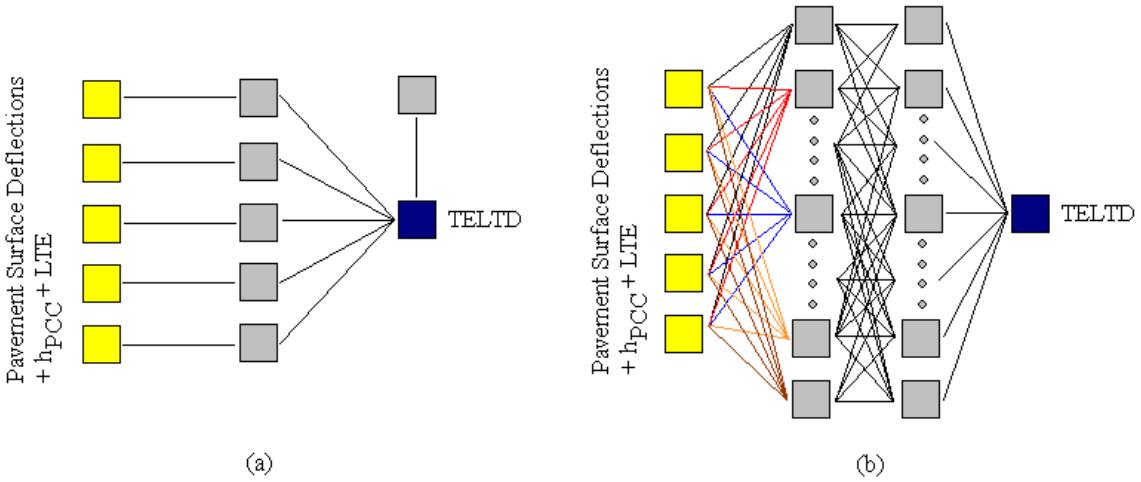

Figure 6.10. (a) Schematic view of MLR approach, (b) Schematic view of ANN approach

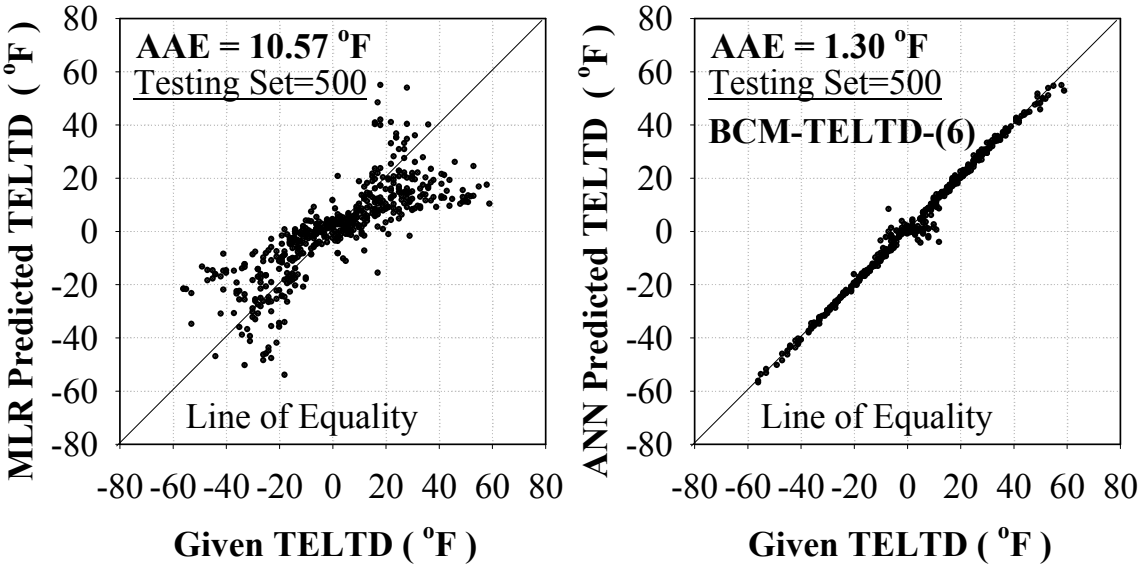

(a) (b)

Figure 6.11. (a) MLR predictions for TELTD, (b) ANN predictions for TELTD

APPLICATION OF THE DEVELOPED APPROACH TO THE ACTUAL FWD DATA

To compare the actual field TELTD values with the backcalcualetd TELTD values is a very challenging problem. In the field, temperature difference between top and bottom of a concrete slab (ΔT_{TG}) can be measured with either the installation of some instrumentation into the concrete layer during the construction process or some additional methods after the construction. Unfortunately, these tests give only ΔT_{TG} but not TELTD for that pavement section. In order to measure the EBITD, additional field tests should be conducted hour by hour on the same pavement section. Therefore, the measurement of TELTD is a really difficult and challenging process.

With the proposed method, once the TELTD is backcalculated, differentiating the ΔT_{TG} and EBITD from each other requires also some additional field tests. Therefore, there is very limited field study that can be used in the comparison process of the developed models. The developed ANN-based backcalculation models have been used to backcalculate the TELTD and EBITD by using actual field data collected by the Wisconsin Department of Transportation (WisDOT). The FWD data and ΔT_{TG} values used in the analysis were shown in Table 6.4 and Figure 6.12 (Crovetti 2002). Maximum deflections normalized to 9,000-lbs load were also shown in Figure 6.13. First of all, field study results conducted by the WisDOT were used to compare the magnitude of the backcalculated TELTD and measured ΔT_{TG} (see Figure 6.14) and then, EBITD values were calculated (see Figure 6.15) from the backcalculated TELTD and measured ΔT_{TG}. The uniformity of EBITD values of three different concrete slabs was investigated in this specific pavement sections. The field tests were conducted in both upward (night-time) and downward (day-time) curling regimes in the test sections located along US-18/151 in Iowa and Dane Counties.

Table 6.4. US-18/151 FWD deflection data and temperature measurements

Slab	Position	Load	D_0	D_{12}	D_{24}	D_{36}	ΔT_{TG}
1	Center	**9493(9000)**	3.35(3.18)	3.15(2.99)	2.68(2.54)	2.17(2.06)	-13
		13667(9000)	4.88(3.21)	4.50(2.96)	3.87(2.55)	3.20(2.11)	-13
		19349(9000)	6.92(3.22)	6.37(2.96)	5.45(2.54)	4.48(2.08)	-13
	Corner	**9176(9000)**	21.95(21.53)	20.52(20.13)			-13
		13250(9000)	28.85(19.60)	26.96(18.31)			-13
		18842(9000)	36.52(17.44)	34.08(16.28)			-13
2	Center	**9521(9000)**	3.18(3.01)	2.92(2.76)	2.47(2.33)	2.08(1.97)	-13
		13668(9000)	4.65(3.06)	4.22(2.78)	3.62(2.38)	3.02(1.99)	-13
		19409(9000)	6.53(3.03)	6.00(2.78)	5.17(2.40)	4.32(2.00)	-13
	Corner	**9262(9000)**	18.93(18.39)	16.13(15.67)			-13
		13365(9000)	24.95(16.80)	22.41(15.09)			-13
		18996(9000)	32.08(15.20)	29.7614.10)			-13
3	Center	**9498(9000)**	3.00(2.84)	2.80(2.65)	2.34(2.22)	1.92(1.82)	-13
		13677(9000)	4.37(2.88)	3.99(2.63)	3.33(2.19)	2.78(1.83)	-13
		19515(9000)	6.25(2.88)	5.72(2.64)	4.87(2.25)	3.99(1.84)	-13
	Corner	**9247(9000)**	17.24(16.78)	14.12(13.74)			-13
		13323(9000)	22.79(15.40)	19.09(12.90)			-13
		19054(9000)	29.94(14.14)	25.21(11.91)			-13
1	Center	**9479(9000)**	3.58(3.40)	3.31(3.14)	2.84(2.70)	2.37(2.25)	5
		13588(9000)	5.11(3.38)	4.74(3.14)	4.09(2.71)	3.33(2.21)	5
		19409(9000)	7.27(3.37)	6.75(3.13)	5.80(2.69)	4.78(2.22)	5
	Corner	**9317(9000)**	7.02(6.78)	6.75(6.52)			5
		13467(9000)	10.04(6.71)	9.59(6.41)			5
		19164(9000)	14.22(6.68)	13.58(6.38)			5
2	Center	**9416(9000)**	3.28(3.14)	3.03(2.90)	2.59(2.48)	2.13(2.04)	5
		13591(9000)	4.67(3.09)	4.34(2.87)	3.72(2.46)	3.05(2.02)	5
		19439(9000)	6.69(3.10)	6.16(2.85)	5.33(2.47)	4.34(2.01)	5
	Corner	**9356(9000)**	7.88(7.58)	7.47(7.19)			5
		13425(9000)	11.13(7.46)	10.55(7.07)			5
		19187(9000)	15.77(7.40)	14.78(6.93)			5
3	Center	**9489(9000)**	3.35(3.18)	3.15(2.99)	2.64(2.50)	2.15(2.04)	5
		13624(9000)	4.76(3.14)	4.39(2.90)	3.81(2.52)	3.09(2.04)	5
		19392(9000)	6.81(3.16)	6.28(2.91)	5.40(2.51)	4.46(2.07)	5
	Corner	**9380(9000)**	7.02(6.74)	6.44(6.18)			5
		13503(9000)	10.11(6.74)	9.34(6.23)			5
		19250(9000)	14.57(6.81)	13.28(6.21)			5

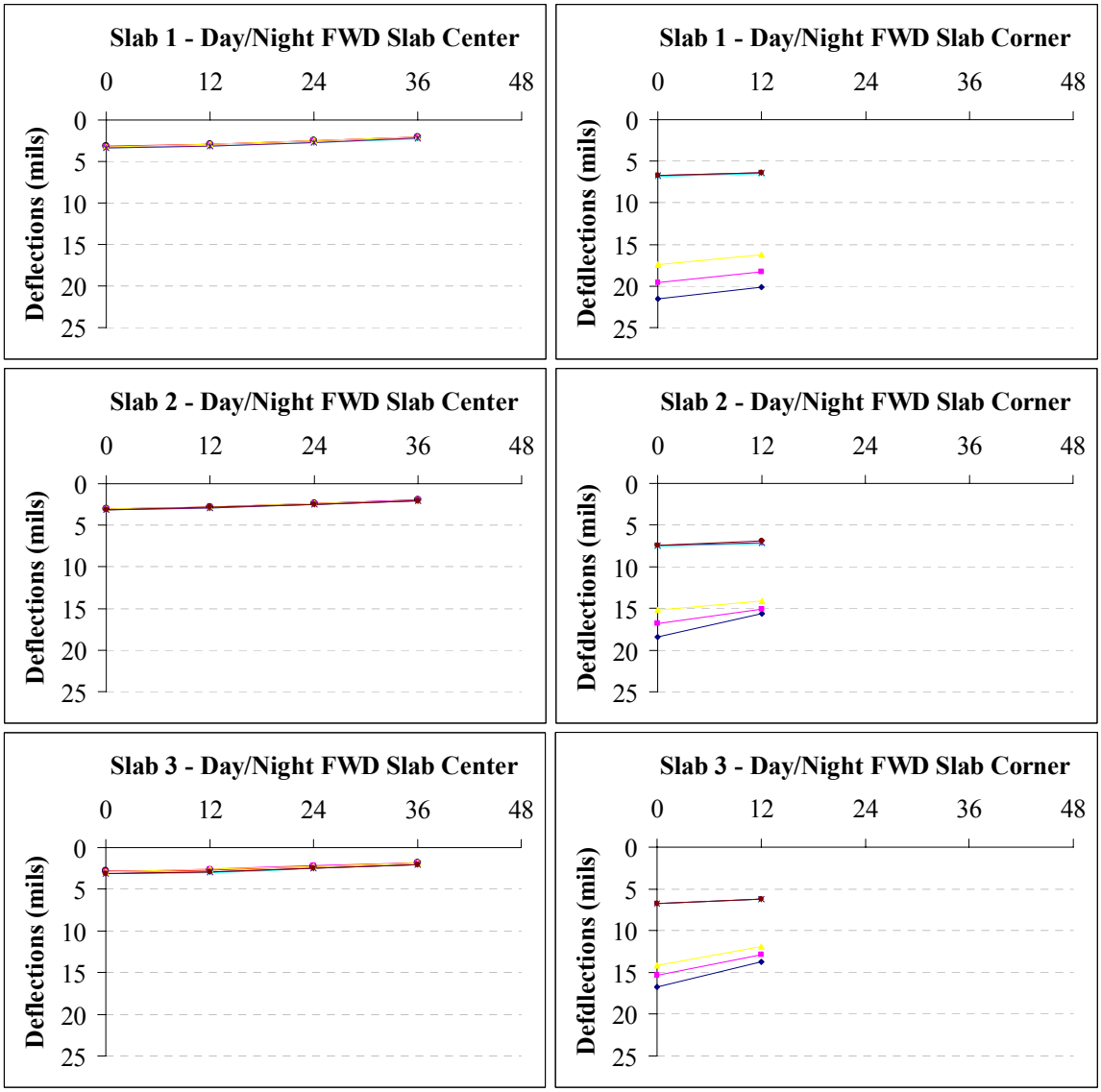

(a) (b)

Figure 6.12. (a) Normalized slab center FWD deflection basins, (b) Normalized slab corner deflection basins

The test section includes 9-in. concrete slab, 4-in. nonstabilized open-graded base layer, 4-in. dense-graded aggregate subbase layer, and select fill of variable depth (Crovetti 2002). The EBITD values obtained from two curling regimes (day-time and night-time) were compared with each other. Although there are some differences in the EBITD values obtained from day and night FWD testings, it seems that this difference is not crucial (see Figure 6.15). Also please note that it was assumed that the LTE value was 80 % between the adjacent slabs since there was not LTE information available. The backcalculated EBITD values for three

concrete slabs are approximately 0.8 ^{0}F, 3.1 ^{0}F, and 3.2 ^{0}F for slab1, slab2, and slab3, respectively. As can be seen from Figure 6.14 and 6.15, the backcalculated values give a general idea of the magnitudes of the TELTD and EBITD in this specific concrete pavement sections. The normalized FWD deflection values shows that slab1 deflections are always higher than the other slab deflections for both center and corner FWD loadings except the day-time corner FWD testing. By accepting the other FWD deflection values have no any error in them, it was expected to have higher deflection values for slab1 corner for the day-time testing as well. The reason of the negative EBITD values backcalculated from the day-time FWD tests for slab1 might be these relatively low deflection values. Another important point is that only four center (D_0, D_{12}, D_{24}, and D_{36}) and two corner (D_0 and D_{12}) FWD deflection were used in the analysis since the other deflection values were not available. More deflection values (D_0 to D_{60}) for both center and corner loadings should be used in the backcalculation of TELTD to better map the curling behavior of the concrete slabs.

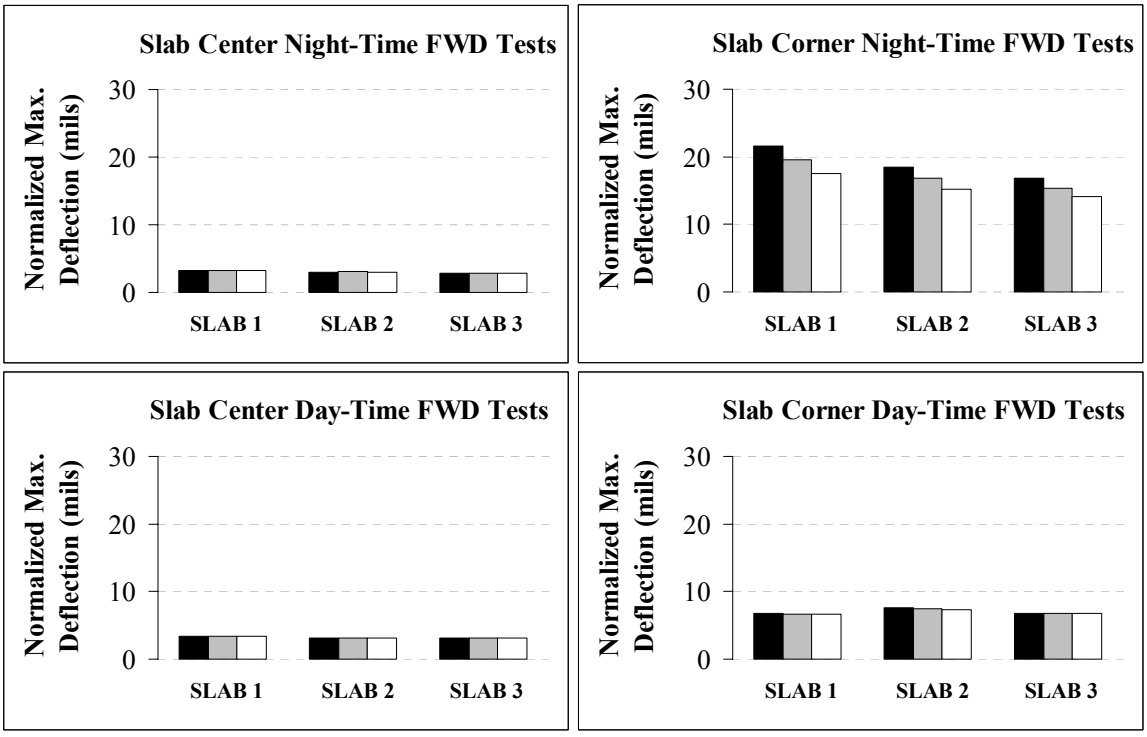

(a) (b)

Figure 6.13. (a) Normalized slab center D_0 deflections, (b) Normalized slab corner D_0 deflections

It should be also taken into account that the EBITD values shown in Figure 6.15 include the daily moisture gradient effects. On the other hand, since there was not any available moisture gradient measurements during the FWD tests, this parameter could not be taken into account in the analysis. Therefore, another reason to the small difference between the backcalculated EBITD values from day-time and night-time FWD tests might be these moisture effects.

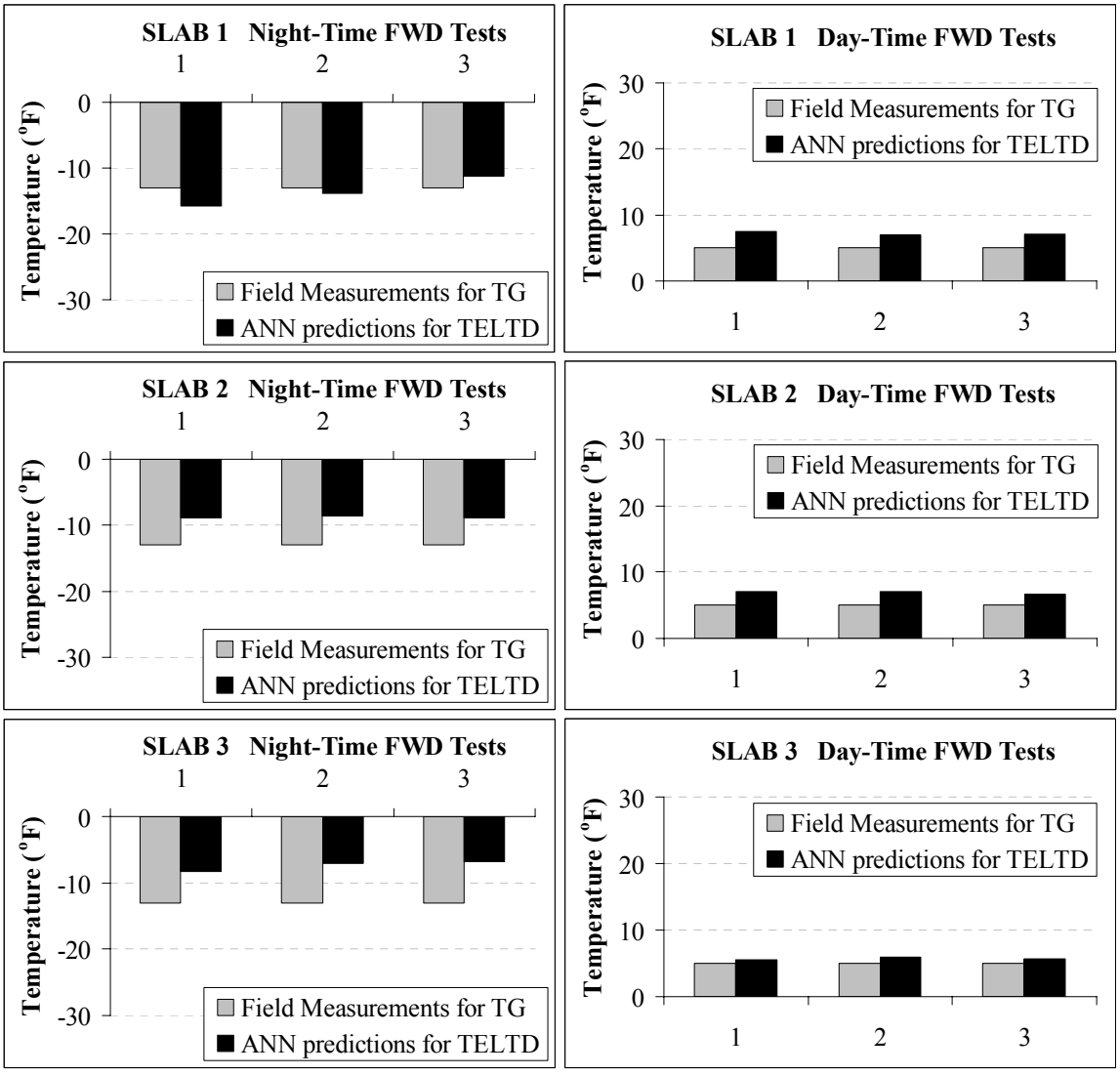

Figure 6.14. Comparison of the backcalculated TELTD and measured ΔT_{TG} values

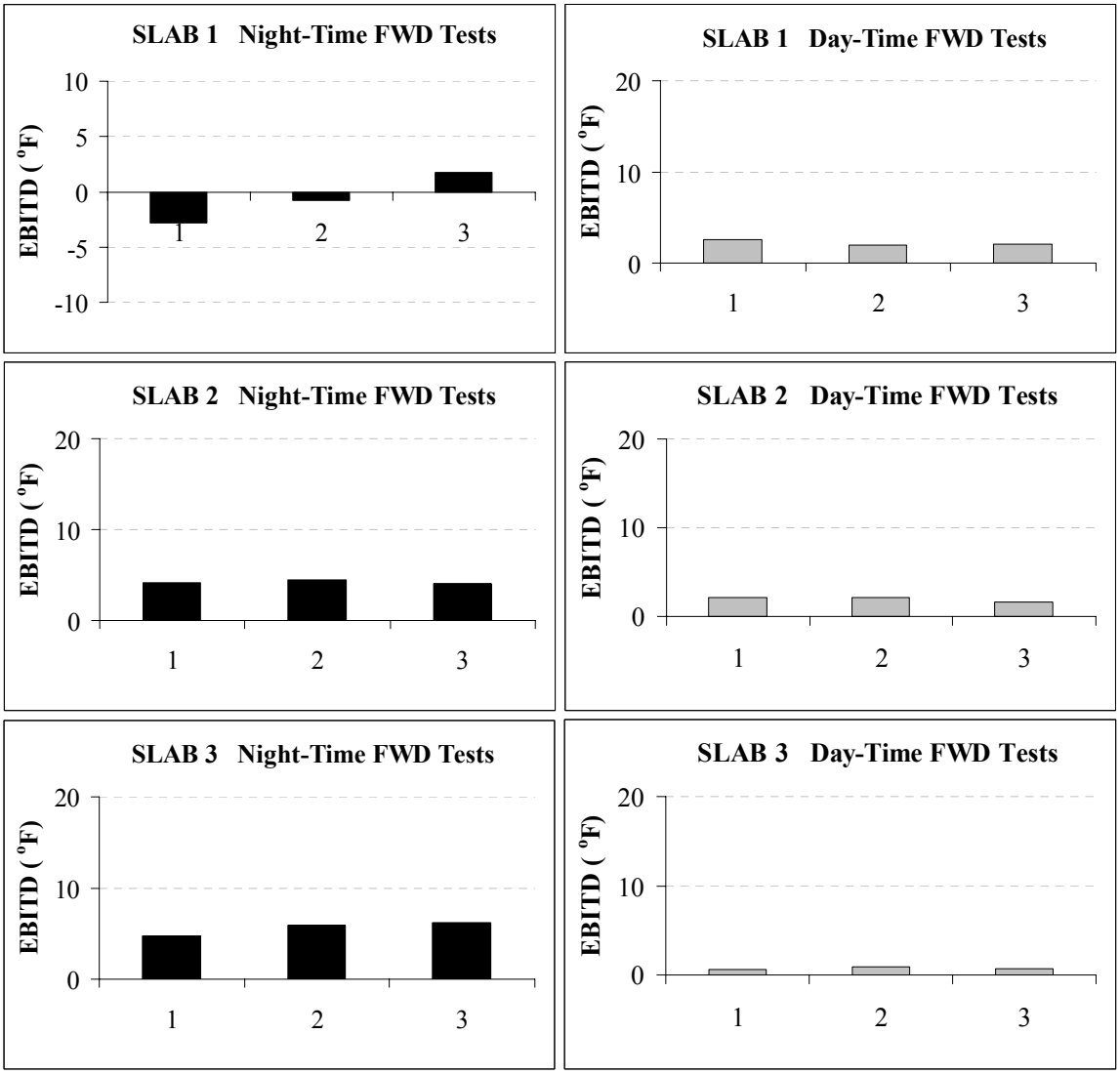

Figure 6.15. The predicted effective built-in temperature difference

DISCUSSION

In summary, total temperature effective linear temperature difference (TELTD) in concrete slabs can be successfully backcalculated from FWD deflection basins with the developed ANN-based models. It is well-known that the environmental conditions during the FWD testing have a significant influence on the deflection basins and consequently final backcalculation of the pavement moduli. Temperature differences through the concrete slab thickness results in additional slab deformations which affect the deflection basins measured during the FWD tests. Therefore, backcalculated moduli of pavement layers based on flat-

slab condition assumptions by using the FWD data may be unrealistic. Therefore, the TELTD can be used as an adjustment parameter in the backcalculation of the concrete pavement layer moduli in the future studies. The objective of this study is to develop a rapid methodology for predicting the TELTD of concrete pavements in real-time considering the influence of environmental effects.

Backcalculating EBITD of in-service pavements with the traditional methods requires instrumentation and measurement of individual unloaded slabs' movements over a 24-hour period which is a difficult, time-consuming, and expensive method. In addition, very little information can be obtained about the EBITD at the end of this difficult method. To backcalculate the EBITD by using this approach is also possible if the actual field temperature difference between top and bottom of the concrete layer (ΔT_{TG}) is measured in the field with some additional methods. Thermocouples can be installed during the construction of the concrete layer or holes can be drilled in several slabs and the temperature at the bottom of the concrete layer by using oil can be measured. Then, the field temperature difference between top and bottom of the concrete layer can easily be calculated since the surface temperature of the slab is measured with the temperature sensor on the FWD. Since the TELTD is backcalculated with the developed ANN-based models and ΔT_{TG} is measured in the field, EBITD which changes to a smaller extent through the life of the pavement can be determined by calculating the difference between TELTD and ΔT_{TG}.

As explained previously, the required input parameters to predict the TELTD with the developed approach are pavement surface deflection basins obtained from center and corner slab FWD loadings, the thickness of the slab, and the load transfer efficiency across the transverse joint. It is crucial to use both the center and corner deflection basins together in the analysis, because some additional voids might occur under the center of the slab, and corner of the slab during the day-time and night-time curling, respectively. Therefore, the some excessive deflections might be obtained in the center of the slab during daytime and in the corner of the slab during the nighttime. Figure 6.16 summarizes the prediction capabilities of the ANN-based TELTD models that use either only center or only corner

deflection basins. The AAE value was 1.33 ^{0}F in the model that uses both deflection basins. In order to map the entire slab behavior anytime, both center and corner deflection basins were used in the developed approach. Consequently, the most significant advantages of the proposed approach is that FWD tests can be conducted anytime during day and night in this approach.

The thickness of the slab is another important factor that affects the total amount of curling in concrete pavements since the weight of the concrete slab is proportional to the thickness of the slab. As the thickness of the slab increases, the total amount of downward curling in the center and upward curling in the corners of the slab decreases. In addition, load transfer efficiency also affects the amount of curling especially in the corners of the slab. Therefore, in the developed approach, the slab thickness and load transfer efficiency were used as input parameters in addition to the deflection basins.

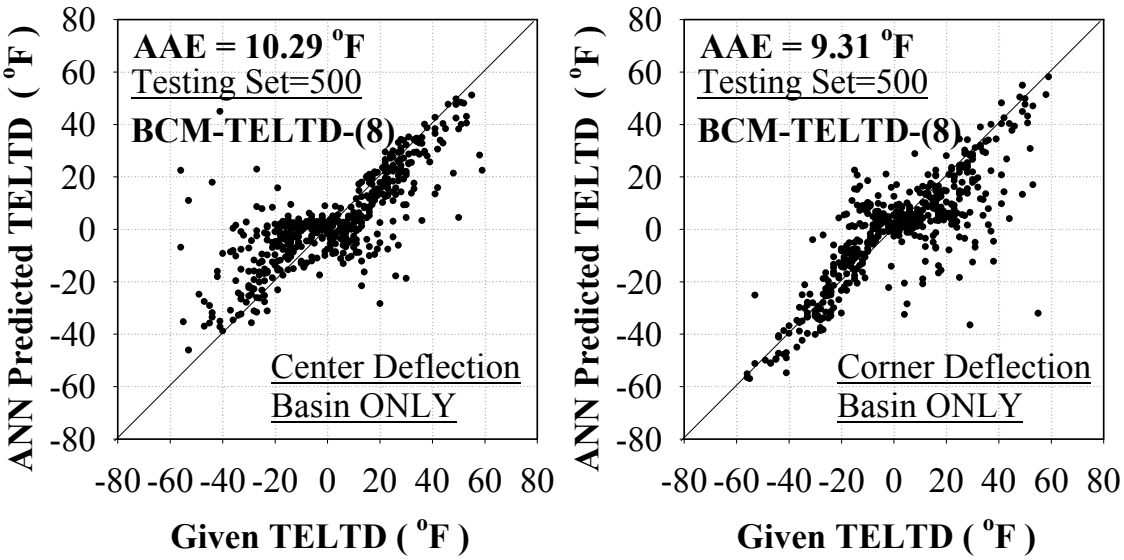

(a) (b)

Figure 6.16. (a) BCM-TELTD-(8) that uses only center FWD loading data, (b) BCM-TELTD-(8) that uses only corner FWD loading data

CONCLUSIONS

The use of ANNs as pavement analysis tool was demonstrated in this study by analyzing jointed Portland cement concrete pavements. Totally, sixteen ANN-based backcalculation models were developed for predicting total effective linear temperature difference using solutions from state-of-the-art structural analysis program, ISLAB2000. It was demonstrated that ANN-based models are capable of successfully predicting the total effective linear temperature difference using the FWD field deflection measurements. Such methodology will be an invaluable tool for pavement engineers for evaluating the total amount of curling of JPCP systems. Rapid prediction ability of the ANN models provide a tremendous advantage to the pavement engineers by allowing them to nondestructively assess the condition of the transportation infrastructure systems in real time while the FWD testing takes place in the field. Such a methodology will enable pavement engineers to easily and quickly incorporate the needed sophistication in structural analysis, such as from finite element modeling with proper characterization of pavement layers, into routine practical mechanistic-based analysis and design. Also, it would provide realistic pavement layer stiffness properties considering the slab curling behavior in the future studies. Elimination of any additional field tests with the integration of ANN-based backcalculation approach can be invaluable for the state and federal agencies for rapidly analyzing large number of pavement deflection basins needed for routine deflection testing.

ACKNOWLEDGEMENTS

The authors gratefully acknowledge the Iowa Department of Transportation (IA-DOT) for sponsoring this study. The contents of this paper reflect the views of the authors who are responsible for the facts and accuracy of the data presented within. The contents do not necessarily reflect the official views and policies of the IA-DOT. This paper does not constitute a standard, specification, or regulation.

REFERENCES

Carlson, R.W. 1938. Drying Shrinkage of Concrete as Affected by Many Factors, Proceedings, American Society for Testing and Materials, ASTM, West Conshohocken, Pa, 38(2), pp.419-440.

Crovetti, J.A. 2002. Deflection-Based Analysis Techniques for Jointed Concrete Pavement Systems. Transportation Research Record, 1809, Paper No.02-4029, pp.3-11.

Darter, M., and Khazanovich, L., Snyder, M., Rao, S., and Hallin, J. 2001. Development of Calibration of a Mechanistic Design Procedure for Jointed Plain Concrete Pavements, Proceedings, 7th International Conference on Concrete Pavements, Orlando, FL.

Hatt, W.K. 1925. The Effect of Moisture on Concrete, Trans. Am. Soc. Civ. Eng., 157, pp. 270-315.

Hiller, J.E. and Roesler, J.R. 2002. Transverse Joint Analysis for use in Mechanistic-Empirical Design of Rigid Pavements, Journal of Transportation Board, 1809, National Research Council, Washington, DC, pp.42-51.

Hveem, F.N. 1951. Slab Warping Affects Pavement Joint Performance, Proceedings, American Concrete Institute, 47, pp.797-808.

Hveem, F.N., and Tremper, B. 1957. Some Factors Influencing Shrinkage of Concrete Pavements, Proceedings, American Concrete Institute, 53, pp.781-789.

Ioannides, A.M., Barenberg E.J., and Lary, J.A. 1989. Interpretation of Falling Weight Deflectometer Results Using Principals of Dimensional Analysis. Proceedings, 4th International Conference on Concrete Pavement Design and Rehabilitation, Purdue University, pp.231-247.

Khazanovich, L., Yu, H.T., Rao, S., Galasova, K., Shats, E., and Jones, R. 2000. ISLAB2000 - Finite Element Analysis Program for Rigid and Composite Pavements, User's Guide, ERES Consultants, A Division of Applied Research Associates, Champaign, Illinois.

Rao, S. and Roesler, J.R. 2005a. Characterizing Effective Built-In Curling from Concrete Pavement Field Measurements, Journal of Transportation Engineering, American Society of Civil Engineers, 131 (4), pp.320-327.

Rao, S. and Roesler, J.R. 2005b. Nondestructive Testing of Concrete Pavements for Characterization of Effective Built-In Curling, Journal of Testing and Evaluation, 33 (5), pp. 356-363.

Zollinger, D.G. and Barenberg, E.J. 1989. Proposed Mechanistic Based Design Procedure for Jointed Concrete Pavements, Illinois Cooperative Highway Research Program Project IHR-518, University of Illinois, Urbana, IL.

CHAPTER 7. REHABILITATION DESIGN APPLICATIONS

The predictions obtained from ANN-based models can be used as an input parameter in the Mechanistic-Empirical Pavement Design Guide software in the rehabilitation of the PCC pavements section. Predicted in-service elastic modulus of the PCC layer and coefficient of subgrade reaction values can be used in the PCC overlay section in MEPDG to define the existing pavement properties. The effective built-in curling/warping value is another input parameter in the Mechanistic-Empirical Pavement Design Guide. In order to analyze the effect of the existing pavement properties on the faulting and international roughness index (IRI) over the 20 years, a sensitivity study was conducted by varying E_{PCC}, h_{PCC}, k_S, and effective built-in temperature difference values. Based on the results of such a study by using the existing pavement properties predicted by the developed ANN-based models, pavement engineers can reach an optimum solution for the rehabilitation of a specific pavement section. The values used in this sensitivity study, faulting and IRI plots were presented below.

Table 7.1. The existing and overlay PCC pavement layer properties

	Overlay PCC Layer Properties		**Existing PCC Layer Properties**			**Subgrade Stiffness**
Case #	**E_{PCC} (psi)**	**h_{PCC} (psi)**	**E_{PCC} (psi)**	**h_{PCC} (psi)**	**EBITD(^oF)**	**k_S (psi/in)**
1	4,000,000	10	4,000,000	10	-10	200
2	4,000,000	10	5,000,000	10	-10	200
3	4,000,000	10	4,000,000	10	-10	500
4	4,000,000	8	4,000,000	10	-10	200
5	4,000,000	12	4,000,000	10	-10	200
6	4,000,000	10	4,000,000	10	+10	200
IA-Bremer	4,000,000	10	3,000,000	10	-10	120
IA-Allamakee	4,000,000	10	4,500,000	10	-10	90

Table 7.2. MEPDG software results for each pavement configuration

Case #	Faulting Limit (years)	IRI limit (years)
1	8.3	16.5
2	9.5	17.6
3	10.4	18.7
4	8.2	15.6
5	13.5	22
6	22	24
IA-Bremer	5.8	14.7
IA-Allamakee	7.6	15.1

In faulting prediction plots, there are three different lines: Horizontal red line represents the faulting limit, the black line (below) represents the expected faulting, and the blue line (above) represents the expected faulting value at 90% reliability. In the same way, there are three different lines in the international roughness index plots: Horizontal red line represents the international roughness index limit, the black line (below) represents the expected international roughness index, and the blue line (above) represents the expected international roughness index value at 90% reliability.

As the results of the sensitivity study show, the time needed to reach the faulting limit ($Faulting_{limit}$ = 0.12 in.) and the international roughness index (IRI_{limit} = 172) limit increases with an increase in elastic modulus of PCC layer (E_{PCC}), thickness of PCC layer (h_{PCC}), and coefficient of subgrade reaction (k_S). In addition, positive permanent curling/warping in concrete slabs instead of negative permanent curling/warping helps the pavement stability and performance and as a result it increases the pavement remaining life significantly. The schematic views of the each pavement section and predicted faulting and international roughness index values over the 20 years are given in Figure 7.1 to Figure 7.24.

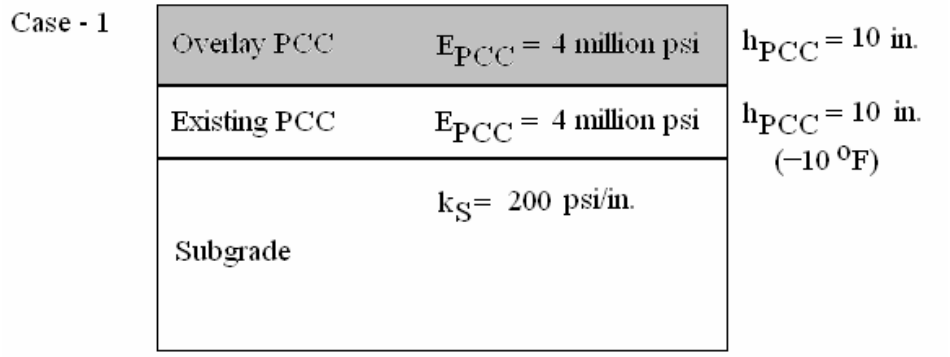

Figure 7.1. Schematic view of the Case-1 pavement structure

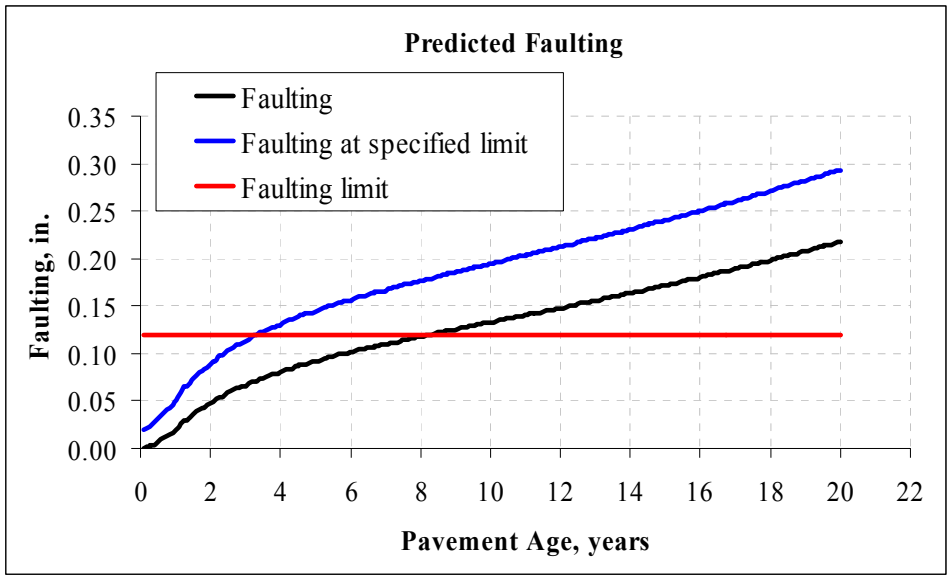

Figure 7.2. Faulting predictions for Case-1 pavement structure

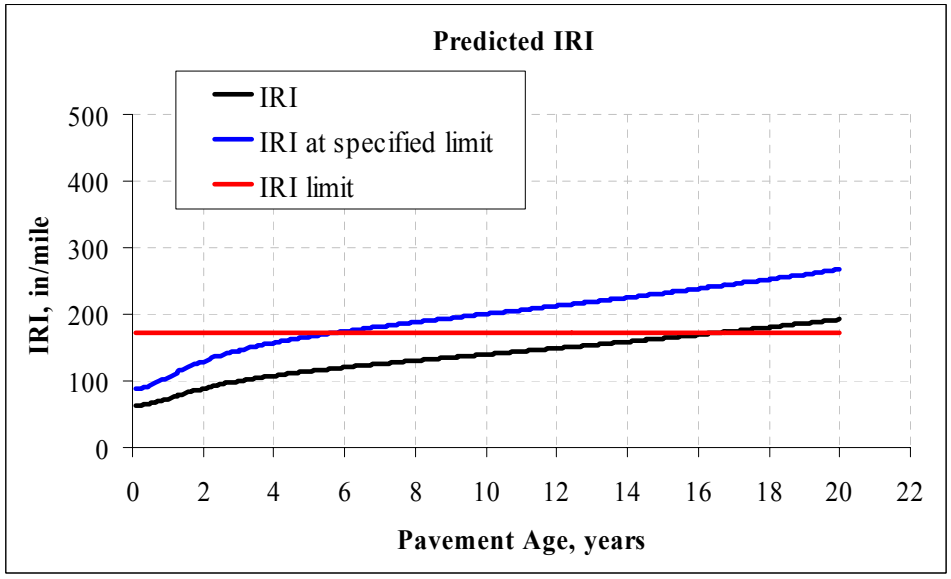

Figure 7.3. International rougness index predictions for Case-1 pavement structure

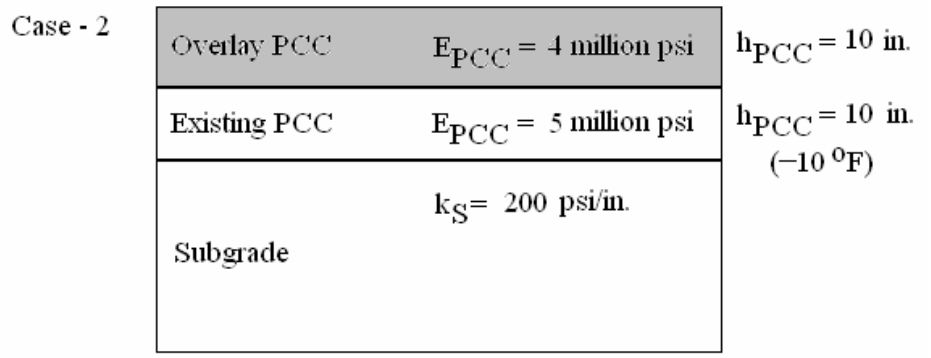

Figure 7.4. Schematic view of the Case-2 pavement structure

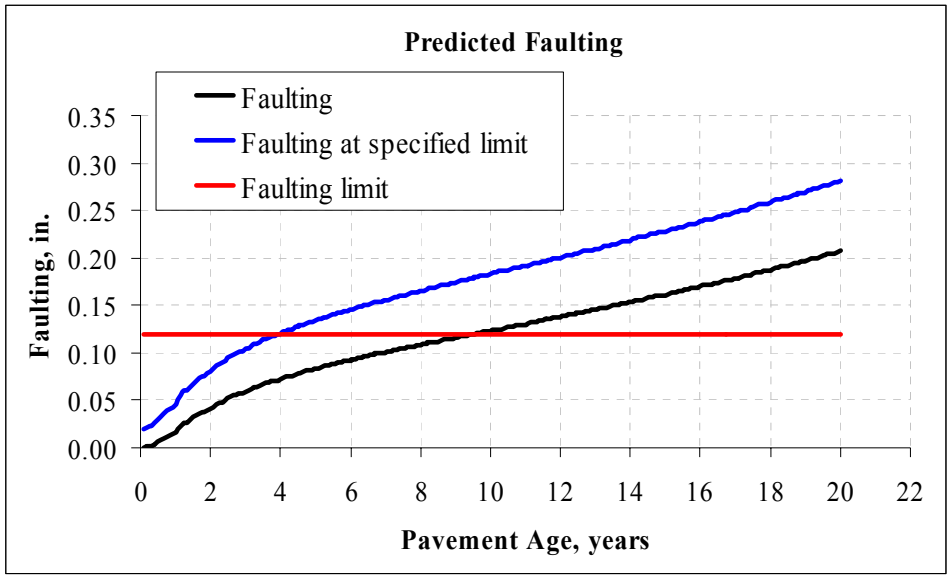

Figure 7.5. Faulting predictions for Case-2 pavement structure

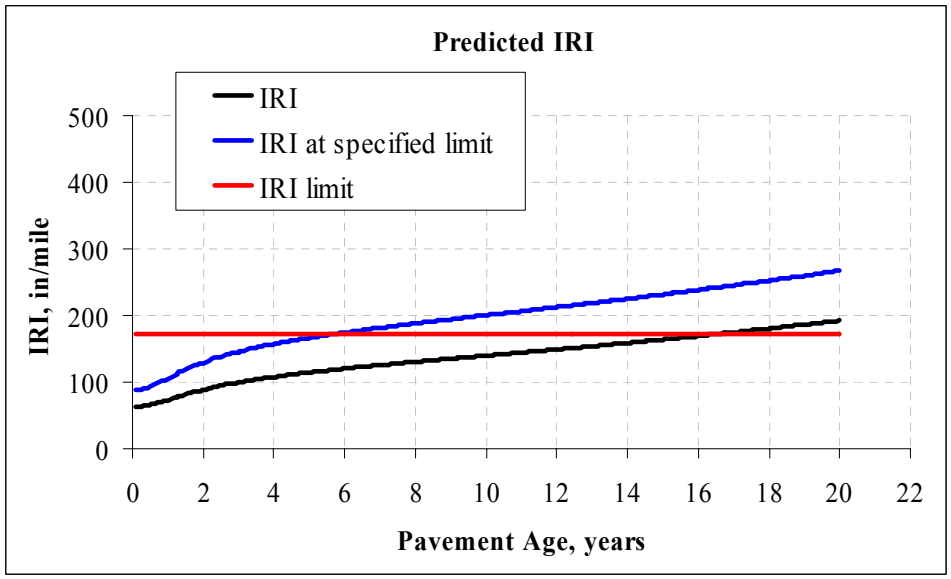

Figure 7.6. International rougness index predictions for Case-2 pavement structure

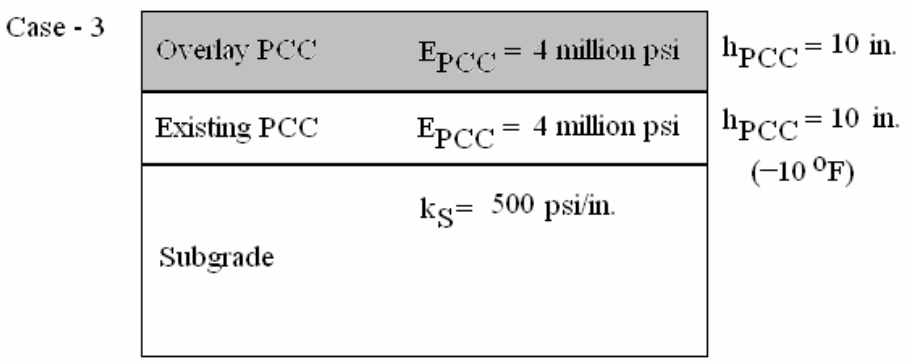

Figure 7.7. Schematic view of the Case-3 pavement structure

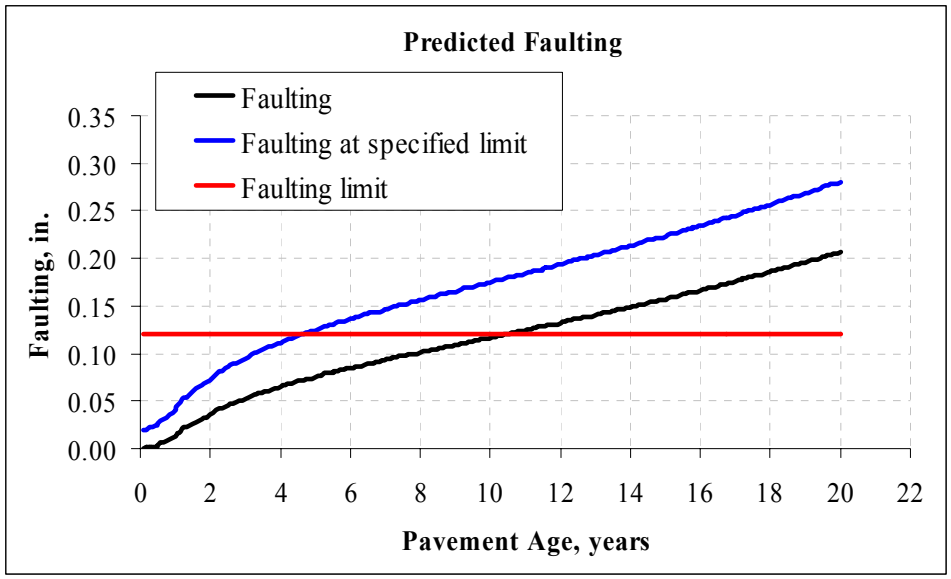

Figure 7.8. Faulting predictions for Case-3 pavement structure

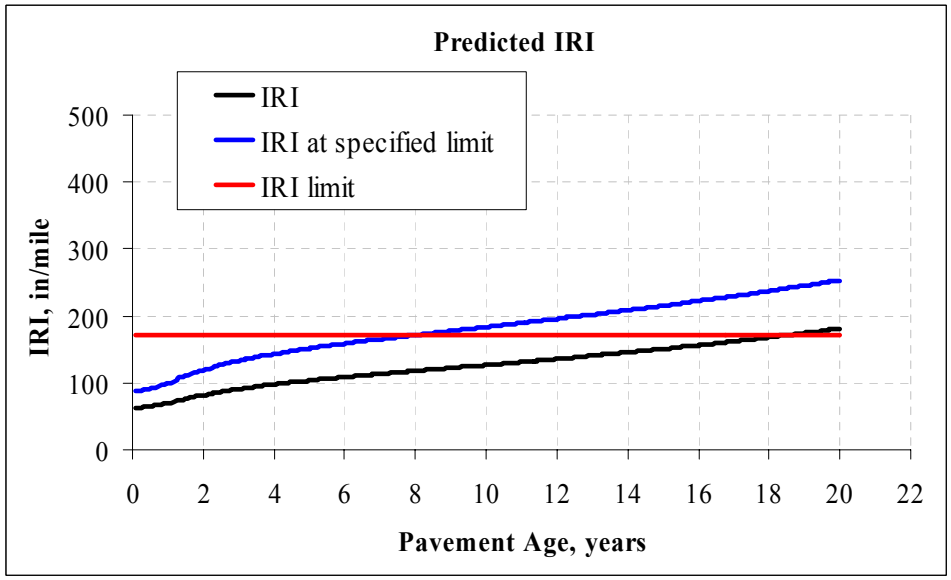

Figure 7.9. International rougness index predictions for Case-3 pavement structure

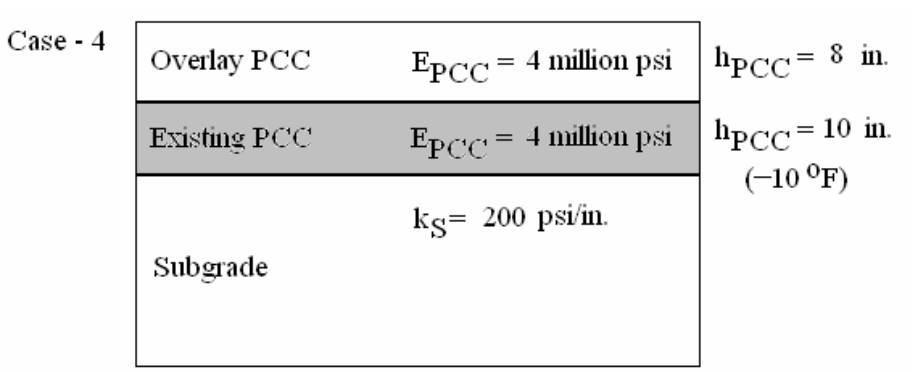

Figure 7.10. Schematic view of the Case-4 pavement structure

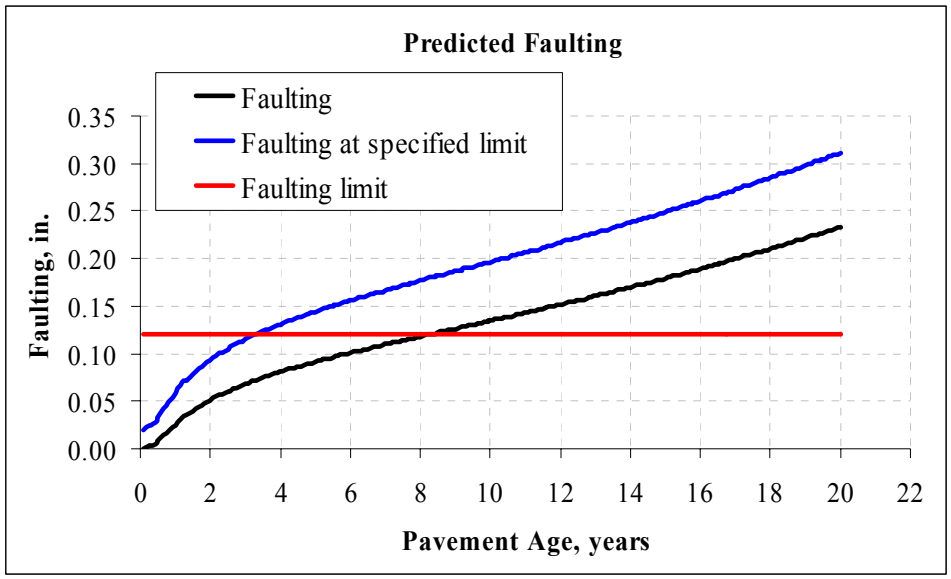

Figure 7.11. Faulting predictions for Case-4 pavement structure

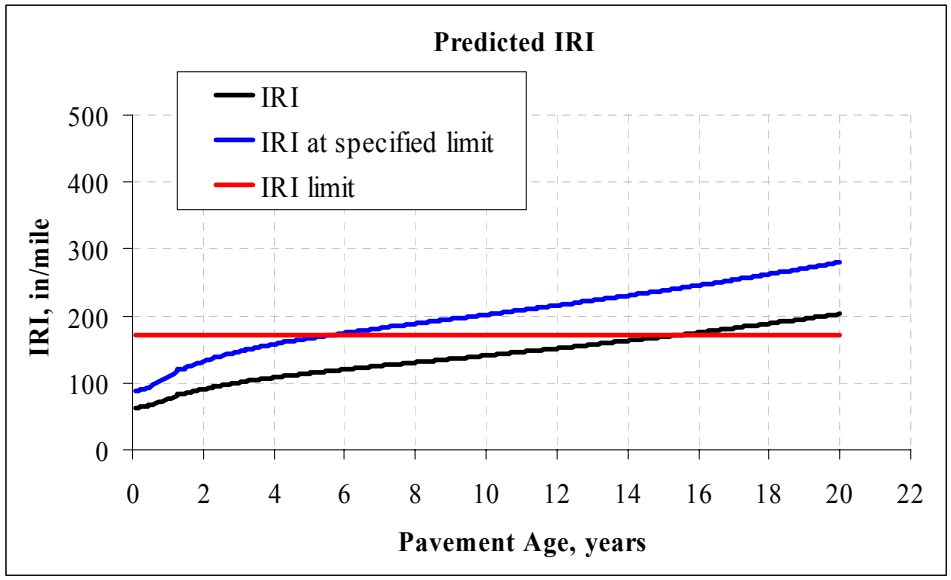

Figure 7.12. International rougness index predictions for Case-4 pavement structure

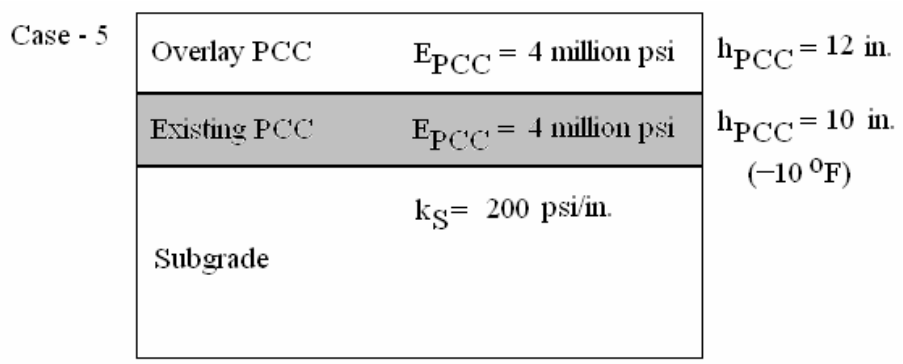

Figure 7.13. Schematic view of the Case-5 pavement structure

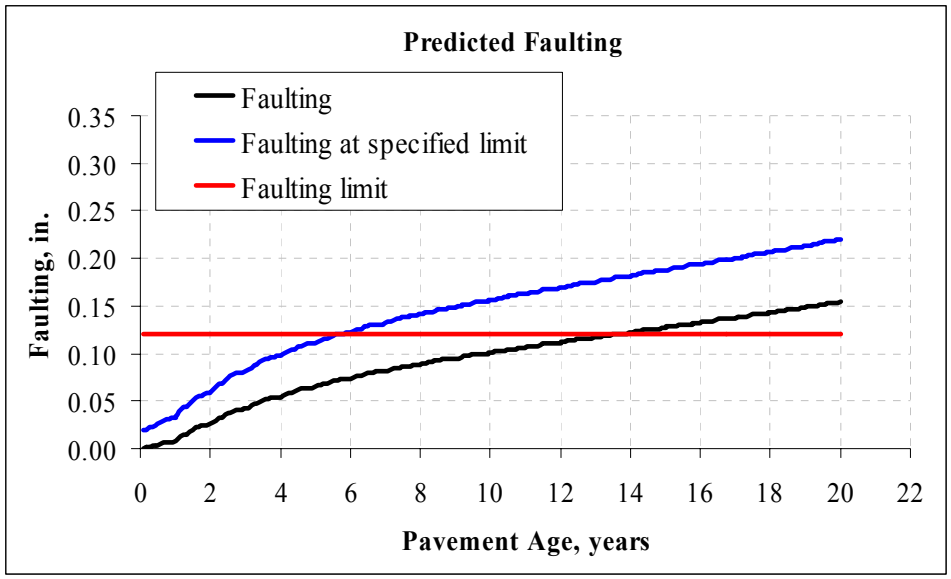

Figure 7.14. Faulting predictions for Case-5 pavement structure

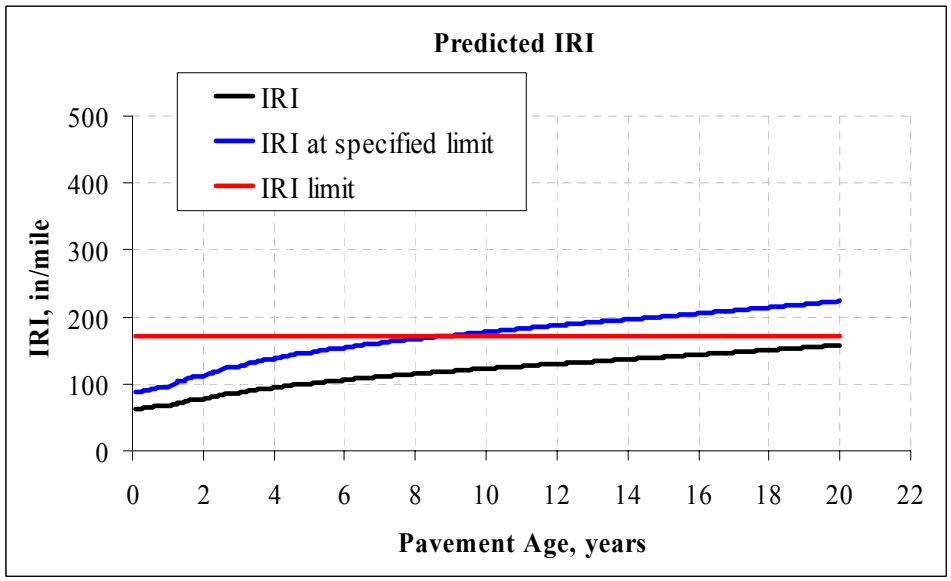

Figure 7.15. International rougness index predictions for Case-5 pavement structure

Case - 6

Overlay PCC	E_{PCC} = 4 million psi	h_{PCC} = 10 in.
Existing PCC	E_{PCC} = 4 million psi	h_{PCC} = 10 in. (+10 ^{o}F)
Subgrade	k_S = 200 psi/in.	

Figure 7.16. Schematic view of the Case-6 pavement structure

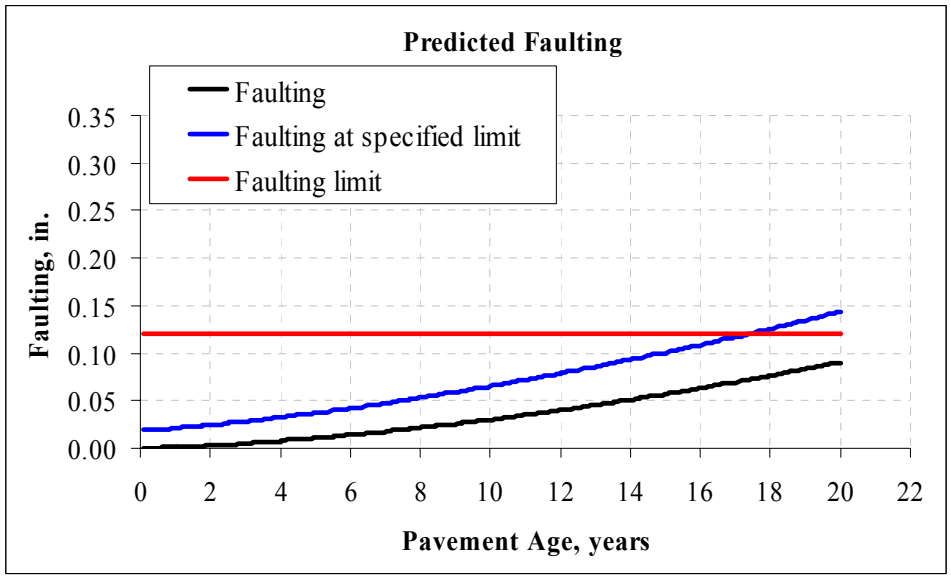

Figure 7.17. Faulting predictions for Case-6 pavement structure

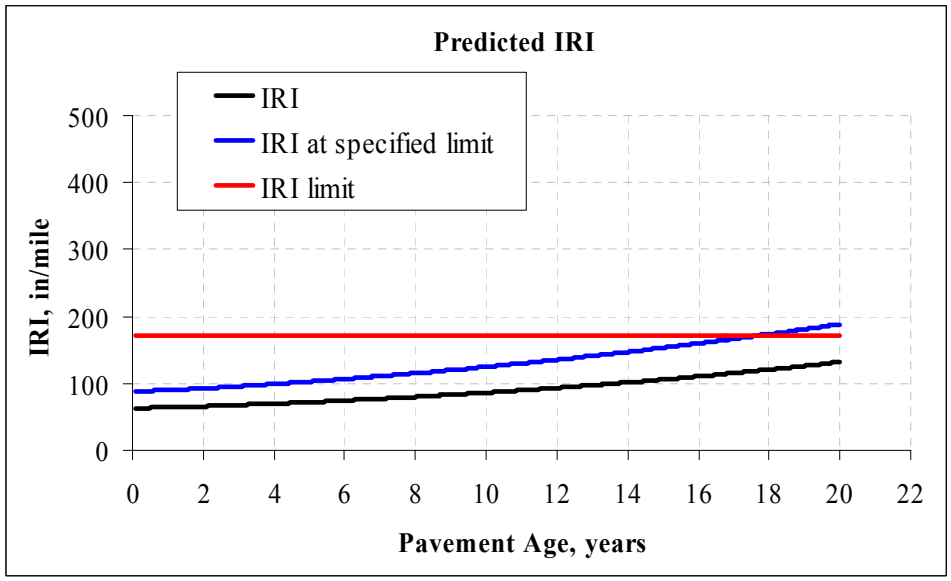

Figure 7.18. International rougness index predictions for Case-6 pavement structure

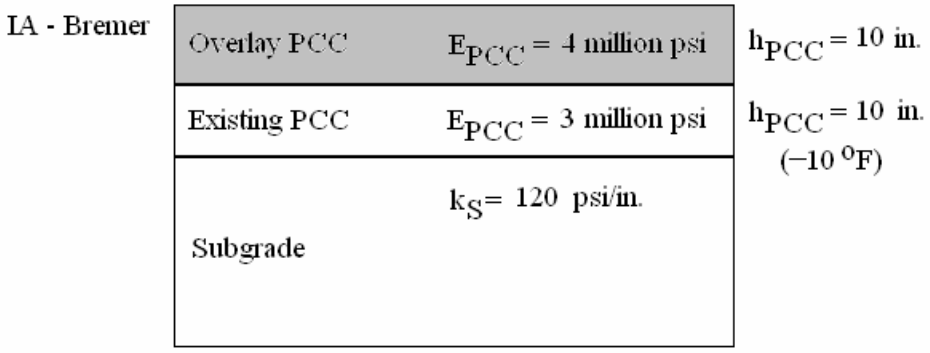

Figure 7.19. Schematic view of the IA-Bremer pavement structure

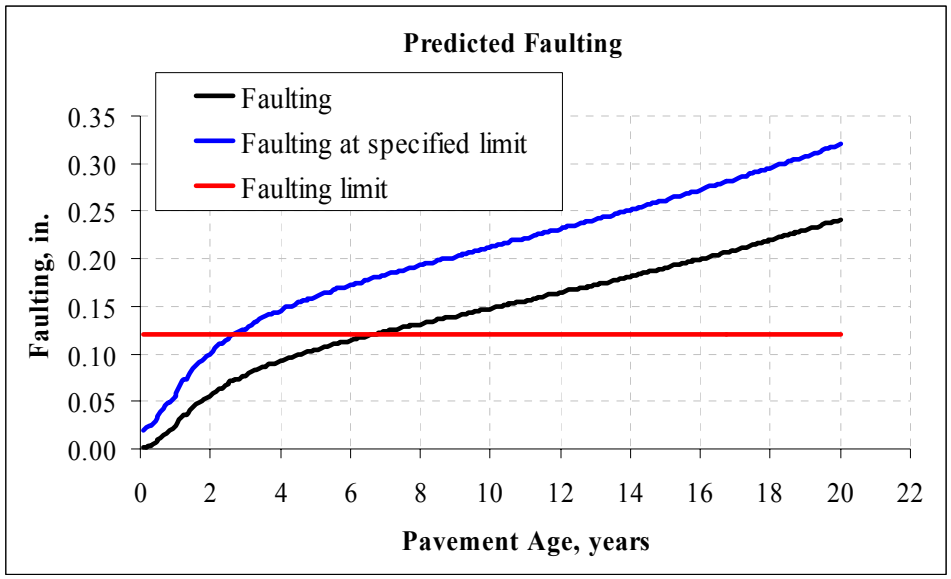

Figure 7.20. Faulting predictions for IA-Bremer pavement structure

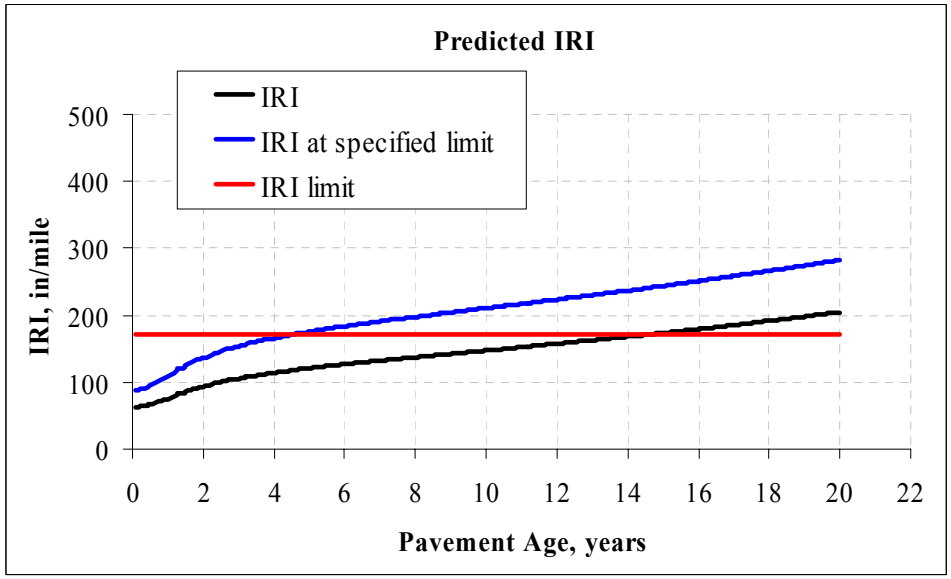

Figure 7.21. International rougness index predictions for IA-Bremer pavement structure

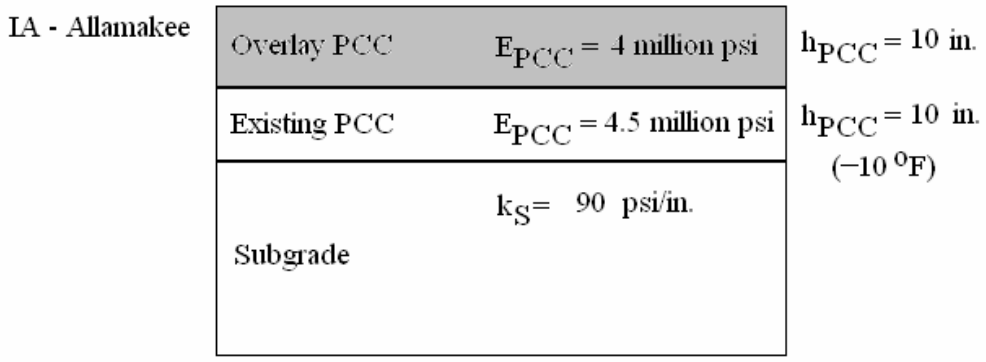

Figure 7.22. Schematic view of the IA-Allamakee pavement structure

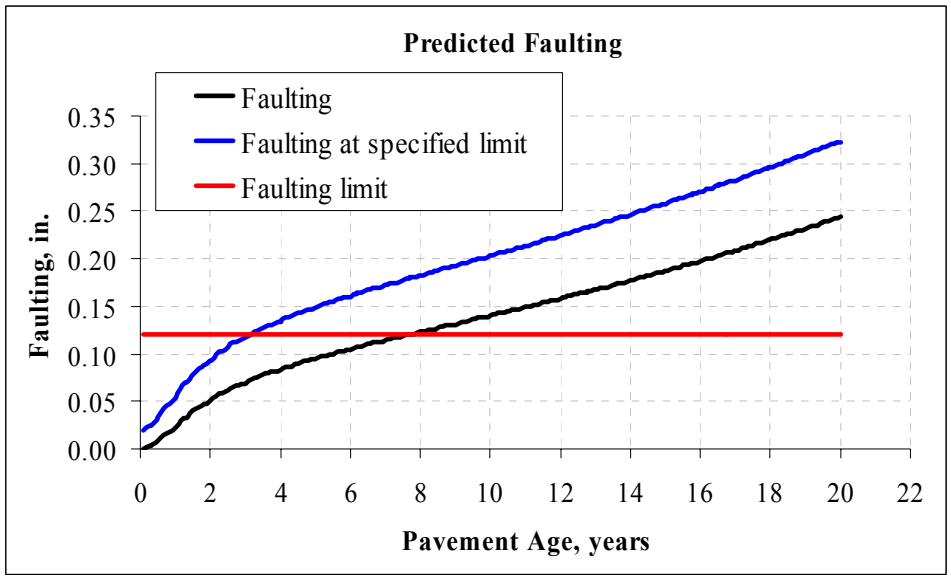

Figure 7.23. Faulting predictions for IA-Allamakee pavement structure

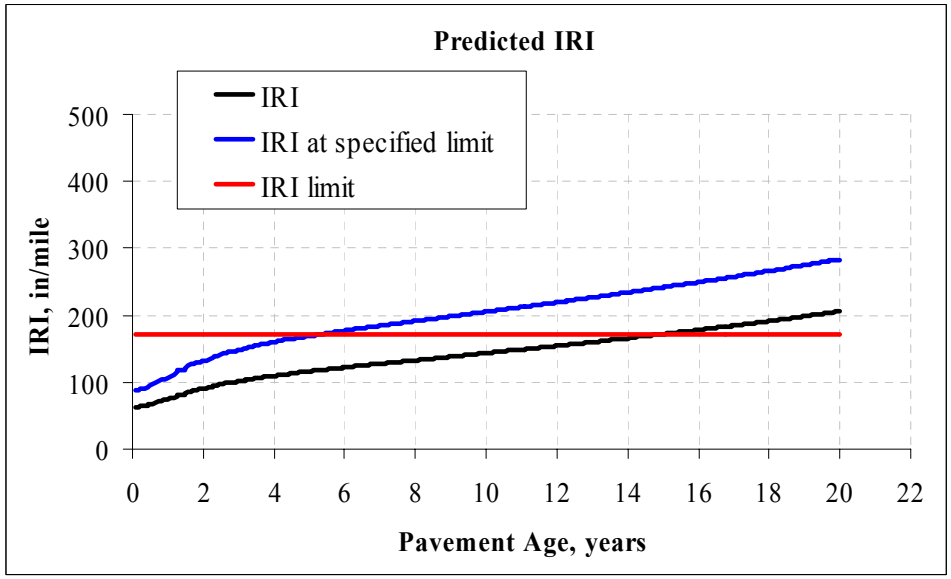

Figure 7.24. International rougness index predictions for IA-Allamakee pavement structure

CHAPTER 8. GENERAL CONCLUSIONS

SUMMARY

This study is an in-depth and comprehensive investigation of the feasibility of employing artificial neural networks (ANNs) in predicting the jointed plain concrete pavement (JPCP) system parameters in a rapid and accurate manner from falling weight deflectometer (FWD) deflection basins in real-time and consequently incorporation of the state-of-the-art finite element solutions into routine practical design. The research therefore mainly focused on the development and performance of comprehensive ANN-based models based on the ISLAB2000 finite element solutions for the analysis of JPCP systems under different traffic and temperature loadings. In order to generate the design pavement parameters and critical pavement responses as inputs, results from the ISLAB2000 finite element analyses were used for the training ANN-based models.

This research documented the research efforts related to the development of ANN-based concrete pavement backcalculation and forward calculation techniques. Based on the results of this research, elastic modulus of PCC slab (E_{PCC}), coefficient of subgrade reaction of pavement foundation system (k_S), radius of relative stiffness of the pavement system (RRS), maximum tensile stress at the bottom of the PCC layer (σ_{MAX}), and total effective linear temperature difference in the PCC layer (TELTD) can be successfully predicted with very low average absolute error values from FWD deflection basins. Rapid prediction ability of the ANN-based models (capable of analyzing 100,000 FWD deflection profiles in one second) provides a tremendous advantage to the pavement engineers by allowing them to nondestructively assess the condition of the transportation infrastructure in real time while the FWD testing takes place in the field. It is also well known that environmental conditions have a huge influence on the in-service pavement conditions and on the remaining life of pavements. Therefore, curling and warping of concrete slabs were taken into account in the developed approach.

Since slab curling and warping in concrete pavements due to temperature and moisture differentials throughout the thickness of a slab affect the nondestructive testing results, these erroneous measurements may divert the pavement engineers to inaccurate predictions of pavement and foundation properties. Therefore, ANN-based models were developed which can predict the equivalent effect of total amount of curling and warping in terms of temperature difference between the top and bottom of the concrete slab in JPCP systems. Therefore, such ANN-based backcalculation models can be used for the analysis of large number of concrete slabs in a relatively short period of time for estimating the total amount of curling and warping that can be used for adjustments for the in-situ structural capacity and remaining life estimations of JPCP systems.

Backcalculated concrete pavement parameters and forward calculated critical pavement responses play also a crucial role in pavement management systems (PMS) at the network level. Since the developed models can predict the JPCP system parameters and critical pavement responses instantly by use of the trained ANN-based models, it is much easier to make a decision on overall maintenance and budget plans in routine practical design. For example, backcalculated in-service concrete pavement parameters can be used to make a final decision on the pavement maintenance and rehabilitation or concrete fatigue life predictions (from critical pavement responses) can be made in real-time during the FWD testing in the field based on the ANN-based model predictions for critical pavement responses.

Finally, it can be concluded that ANN-based analysis models can provide pavement engineers and designers with state-of-the-art solutions, without the need for a high degree of expertise in the input and output of the problem, to rapidly analyze a large number of concrete pavement deflection basins needed for project specific and network level pavement testing and evaluation.

CONCLUSIONS

A total of twenty zero-noise and thirty-six noise-introduced ANN-based backcalculation and forward calculation models were developed in this study which can predict the elastic modulus of the PCC slab (E_{PCC}), coefficient of subgrade reaction of pavement foundation (k_S), radius of relative stiffness of pavement system (RRS), maximum tensile stress at the bottom of the PCC layer (σ_{MAX}), and total effective linear temperature difference between the top and bottom of the PCC layer (TELTD) from FWD deflection basin data and PCC slab thickness.

Several ANN-based backcalculation models were developed that use different FWD sensor configurations. For example, there are 4-Deflection (D_0, D_{12}, D_{24}, D_{36}), 6-Deflection (D_0, D_{12}, D_{24}, D_{36}, D_{48}, D_{60}), 7-Deflection (D_0, D_8, D_{12}, D_{18}, D_{24}, D_{36}, D_{60}), and 8-Deflection (D_0, D_8, D_{12}, D_{18}, D_{24}, D_{36}, D_{48}, D_{60}) ANN-based models developed in this research to predict the concrete pavement parameters and critical pavement responses.

A sensitivity study was conducted to determine the most appreciate architecture for the backcalculation of the concrete pavement parameters. Based on the results of this study, ANN networks with two hidden layers with 60 neurons in each hidden layer were exclusively chosen for all models trained in this study. In addition, learning rate and momentum factor parameters were chosen as 0.2 and 0.6, respectively.

The developed ANN-based models gave very low average absolute error values for all zero-noise models (< 1 %) for synthetic database. On the other hand, the case is not like that when the actual FWD data is utilized in the developed models. There might be always some variability in the slab thicknesses in the field due to the poor construction which will directly affect the backcalculated pavement parameters and responses. In addition, there might be some noise in the collected data, might be errors in data collection process due to FWD machine sensor calibration, and might be some operator mistakes. Therefore, actual FWD deflections which are the basic inputs of the backcalculation models are not always as perfect

as synthetic data. Thus, thirty-six noise-introduced ANN-based backcalculation models were developed in this research as well. As a matter of fact, meaningless FWD deflection data should be filtered and extracted from the data analysis.

The predictions of the developed ANN-based models were compared with the closed-form solutions, backcalculation softwares (EverCalc 5.0, and BAKFAA) and finite element program solutions (ISLAB2000 and EverFE 2.24). Even though there are some differences in the predictions obtained from different methodologies; the results seem very similar to each other but the real time prediction capability (< 1 sec.) and the ease of the usage of the ANN-based models (no seed moduli, no iteration, prediction of total curling and warping amount etc.) make them very powerful tools over the other methods.

Elimination of seed layer moduli selection step combined with the integration of ANN-based direct backcalculation approach can be invaluable for the state and federal agencies for rapidly analyzing large number of pavement deflection basins needed for routine pavement evaluation for both project specific and network level FWD testing.

The thickness of the PCC slab playing a crucial role in the E_{PCC} backcalculation is one of the most important parameters in the E_{PCC} prediction models. On the other hand, the thickness of the PCC slab was not used as an input parameter in the developed ANN-based k_S backcalculation models since it has not an effect on the backcalculated k_S predictions. Generally, slab thickness exhibits considerable variability in the field and this has a large impact on the backcalculated PCC slab properties. Consequently, the results of the analyses showed that a given error in the estimate of the thickness of the PCC slab will have significant effects on the backcalculated slab modulus.

In addition, the time of the day for the FWD testing is also crucial in the E_{PCC} backcalculation due to curling and warping problems in concrete pavements. The results of the previous studies indicate that the variations in temperature between two separate FWD tests on the same pavement section affect primarily the elastic modulus of the slab (Ioannides

et al. 1989). Basically, more scatter is expected in E_{PCC} predictions due to the curling and warping issues, possible variations in PCC slab thickness, and the uncertainties in bonding degree between the PCC and base layers.

The limitations of the developed ANN-based backcalculation and forward calculation models can be listed as below:

- The developed ANN-based models use only D_0, D_8, D_{12}, D_{18}, D_{24}, D_{36}, D_{48}, and D_{60} deflection values.

- Erroneous deflection basins should be filtered from the data set and realistic FWD deflection basins should be used in the analyses. For example, there must be a pattern between deflections such as $D_0>D_8>D_{12}>D_{18}>D_{24}>D_{36}>D_{48}>D_{60}$.

- There are certain ranges for each backcalculated or forward calculated parameter and thickness of PCC layer. If the value of the parameter is out of this range, the developed ANN-based models can not predict realistic values.

Table 8.1 Ranges of the JPCP system parameters used in this research

Pavement System Inputs	**Minimum Value**	**Maximum Value**
E_{PCC}, (ksi)	1,000	15,000
k_S, (psi/in)	50	1,000
h_{PCC}, (in)	6	25
RRS, (in)	15	140
σ_{MAX}, (psi)	30	710
TELTD, (^oF)	-60	+60
Temperature Gradient, (^0F/in)	-3.0	+3.0
LTE, (%)	1	99

- If there are two PCC layers in the concrete pavement system instead of one layer, these two layers should be transformed into one layer by calculating effective layer thickness (Ioannides et al. 1992).

RECOMMENDATIONS

The backcalculated concrete pavement properties and forward calculated critical pavement responses are significantly affected from the number of the FWD sensors. As the number of sensors increases, the mean value of elastic modulus of PCC slab increases and the mean value of coefficient of subgrade reaction decreases (Rufino et al. 2002). D_0 and D_{12} deflections are relatively more sensitive to changes in the elastic modulus of PCC slab, compared to D_{48} and D_{60} deflections. On the other hand, D_{48} and D_{60} deflections are much more sensitive to the changes in the subgrade support (k_S). Therefore, BCM-E_{PCC}-(4) model (Inputs: D_0, D_{12}, D_{24}, D_{36}, and h_{PCC}) is proposed for the elastic modulus of PCC slab predictions, and BCM-k_S-(6) model (Inputs: D_0, D_{12}, D_{24}, D_{36}, D_{48}, and D_{60}) is proposed for the coefficient of subgrade reaction predictions. FCM-RRS-(4) (Inputs: D_0, D_{12}, D_{24}, D_{36}, and h_{PCC}), FCM-σ_{MAX}-(4) (Inputs: D_0, D_{12}, D_{24}, D_{36}, and h_{PCC}) and BCM-TELTD-(6) [Inputs: Center(D_0, D_{12}, D_{24}, D_{36}, D_{48}, D_{60}), Corner(D_0, D_{12}, D_{24}, D_{36}, D_{48}, D_{60}), h_{PCC}, LTE] models are also proposed for the radius of relative stiffness, maximum tensile stresses at the bottom of the PCC layer, and total effective linear temperature difference predictions, respectively.

To improve the E_{PCC} backcalculation, nondestructive evaluation techniques (NDT) such as Ground Penetrating Radar (GPR) readings or cores (destructive technique) can be taken along the test sections to determine the exact thickness of the layers at the FWD test points. Also, the time of the FWD tests due to curling and warping issues and the shape of the PCC slab should exactly be taken into account in the interpretations of the analyses of the concrete pavements.

Actual field pavement deflection data obtained from both falling weight deflectometer and heavy weight deflectometer tests can be used in the training process of the developed ANN-based models instead of using finite element solutions. Thus, there is no need to introduce noise to the pavement surface deflections by an artificial method. In order to be able to suse

such a database, elastic moduli of the PCC layers and subgrade stiffness should be know for those pavement sections.

Temperature differences through the concrete slab thickness results in additional slab deformations which affect the deflection basins measured during the FWD tests. Therefore, new models/techniques can be developed in the future to predict the pavement moduli that use the TELTD as an input adjustment parameter. These model predictions can be compared with the actual deflection, temperature, and moisture measurements from newly constructed and instrumented concrete pavements since the environmental conditions during the FWD testing have a significant influence on the deflection basins and consequently final backcalculation of the pavement moduli and estimation of pavement remaining life.

Although advanced approaches to pavement layer backcalculation and forward calculation have been developed in this research, the accuracy of results will largely depend on the quality and integrity of FWD deflection data collected in the field. Future research efforts should focus on developing guidelines for state DOTs that clearly define the FWD testing requirements, data analysis approach, and reporting requirements. The guidelines can provide state DOTs with an improved specification for acquiring FWD testing and backcalculation services as well as provide guidance for state DOTs internal staff conducting FWD testing and analysis. Also, the guidelines can provide procedures for standardized FWD calibration.

REFERENCES

BAKFAA. 2003. Computer Program for Backcalculation of Airport Pavement Properties. Federal Aviation Administration, www.airtech.tc.faa.gov/naptf/download/

Davids, W.G., Turkiyyah, G.M., and J. Mahoney. 1998. EverFE - A New Rigid Pavement Finite Element Analysis Tool. In Transportation Research Record, National Research Council, Washington, DC, pp. 69-78.

EverCalc© 5.0. 1999. Pavement Backcalculation Program. Washington State Department of Transportation.

Ioannides, A.M., Barenberg E.J., and Lary, J.A. 1989. Interpretation of Falling Weight Deflectometer Results Using Principals of Dimensional Analysis. Proceedings, 4th International Conference on Concrete Pavement Design and Rehabilitation, Purdue University, pp.231-247.

Khazanovich, L., Yu, H.T., Rao, S., Galasova, K., Shats, E., and Jones, R. 2000. ISLAB2000 - Finite Element Analysis Program for Rigid and Composite Pavements, User's Guide, ERES Consultants, A Division of Applied Research Associates, Champaign, Illinois.

Rufino, D., Roesler, J., and Barenberg, E.J. 2002. Evaluation of Different Methods and Models for Backcalculating Pavement Properties Based on Denver International Airport Data. 2002 Federal Aviation Administration Technology Transfer Conference, Atlantic City, NJ.

ACKNOWLEDGEMENTS

The authors gratefully acknowledge the Iowa Department of Transportation (IA-DOT) for sponsoring this study. The contents of this paper reflect the views of the authors who are responsible for the facts and accuracy of the data presented within. The contents do not necessarily reflect the official views and policies of the IA-DOT. This paper does not constitute a standard, specification, or regulation.

APPENDIX A. ANN-BASED BACKCALCULATION MODELS FOR ELASTIC MODULUS OF PCC LAYER

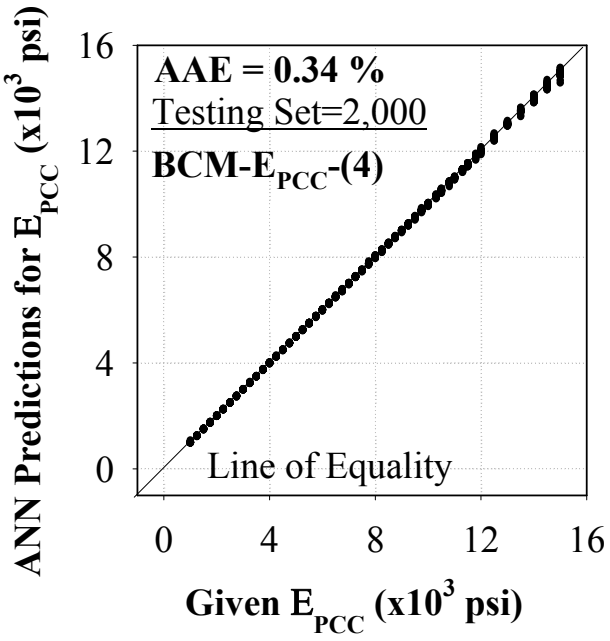

Figure A.1. Prediction performance of the BCM-E_{PCC}-(4) model for backcalculating the PCC layer modulus, E_{PCC}

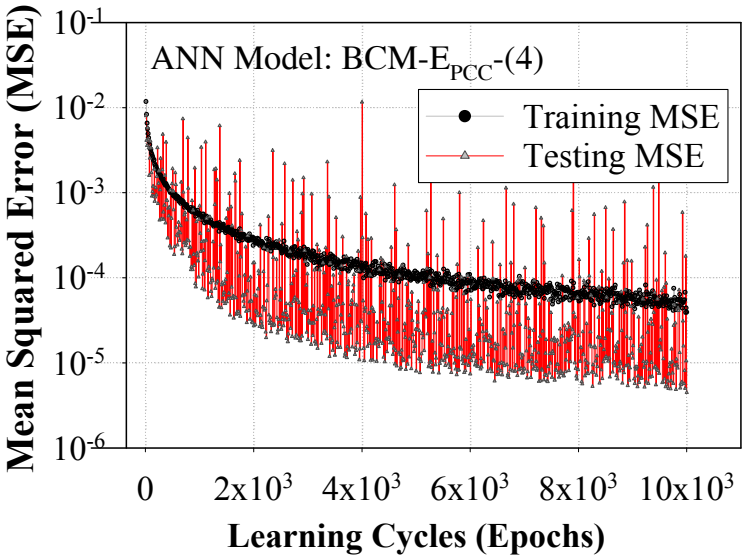

Figure A.2. Training progress curve for the BCM-E_{PCC}-(4) model

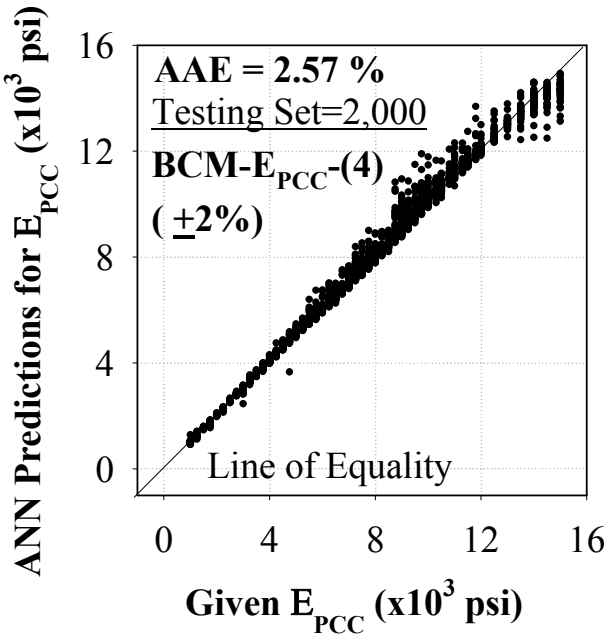

Figure A.3. Prediction performance of the BCM-E_{PCC}-(4) (±2%) model for backcalculating the PCC layer modulus, E_{PCC}

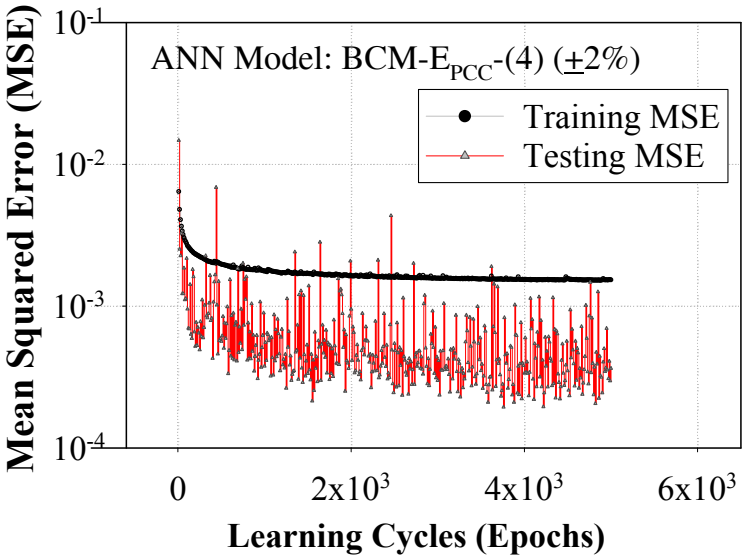

Figure A.4. Training progress curve for the BCM-E_{PCC}-(4) (±2%) model

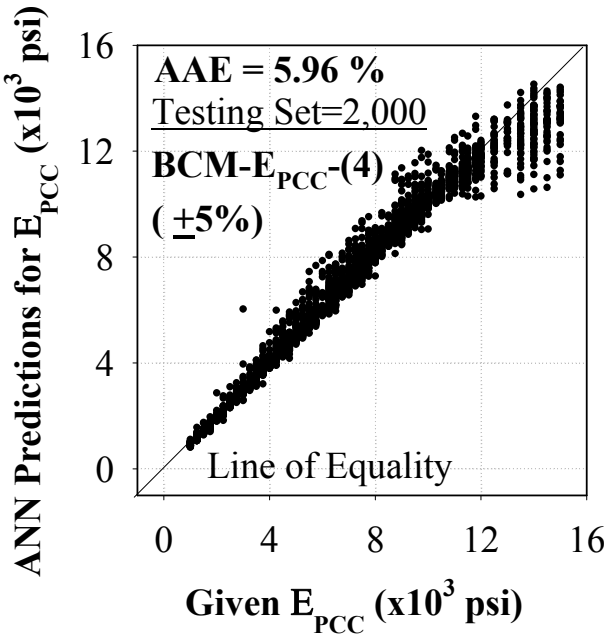

Figure A.5. Prediction performance of the BCM-E_{PCC}-(4) (±5%) model for backcalculating the PCC layer modulus, E_{PCC}

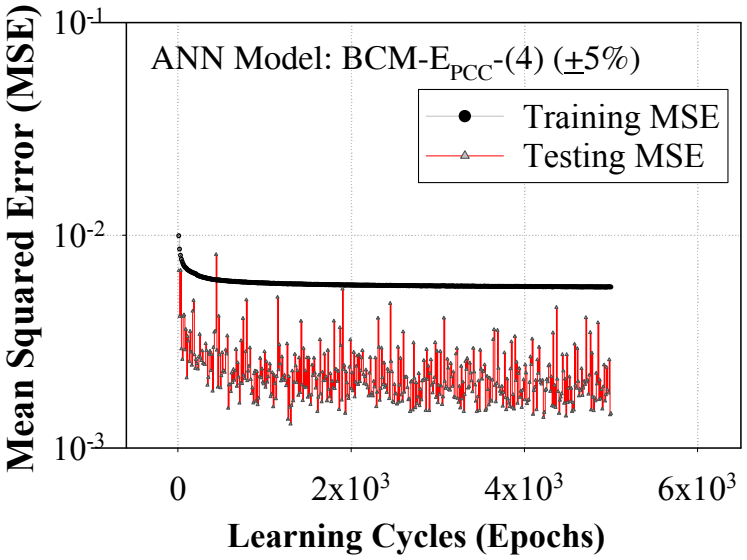

Figure A.6. Training progress curve for the BCM-E_{PCC}-(4) (±5%) model

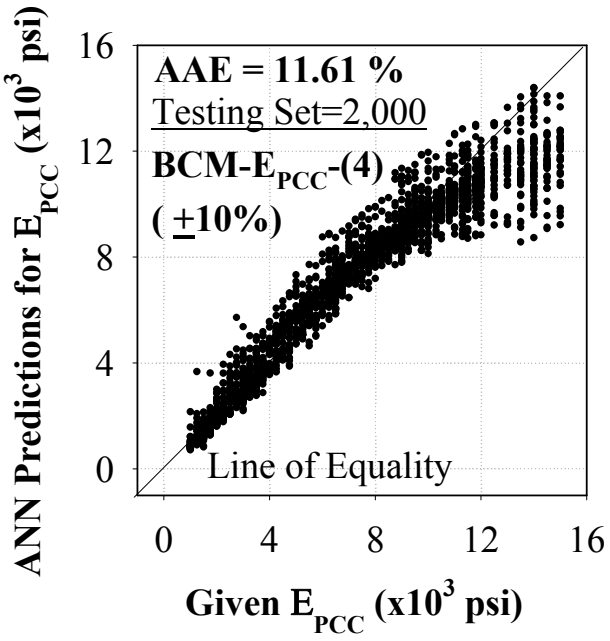

Figure A.7. Prediction performance of the BCM-E_{PCC}-(4) (±10%) model for backcalculating the PCC layer modulus, E_{PCC}

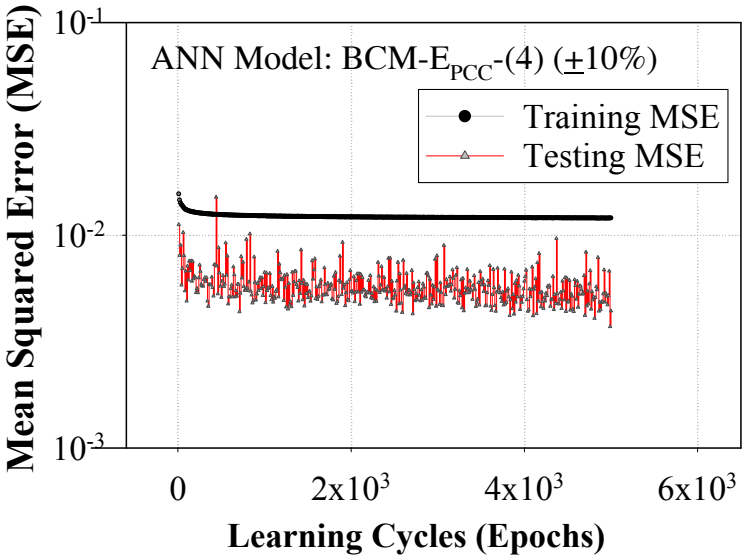

Figure A.8. Training progress curve for the BCM-E_{PCC}-(4) (±10%) model

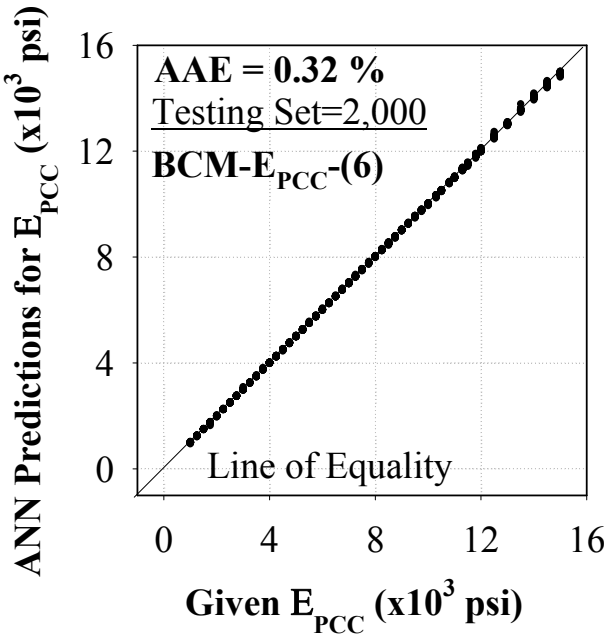

Figure A.9. Prediction performance of the BCM-E_{PCC}-(6) model for backcalculating the PCC layer modulus, E_{PCC}

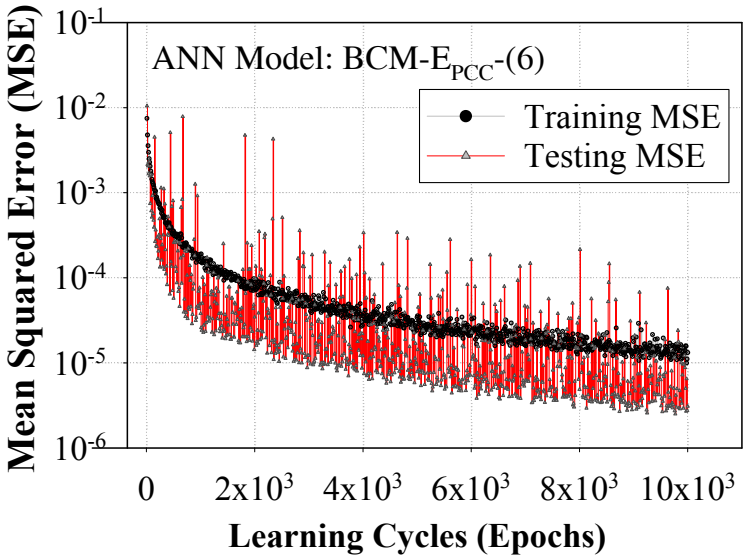

Figure A.10. Training progress curve for the BCM-E_{PCC}-(6) model

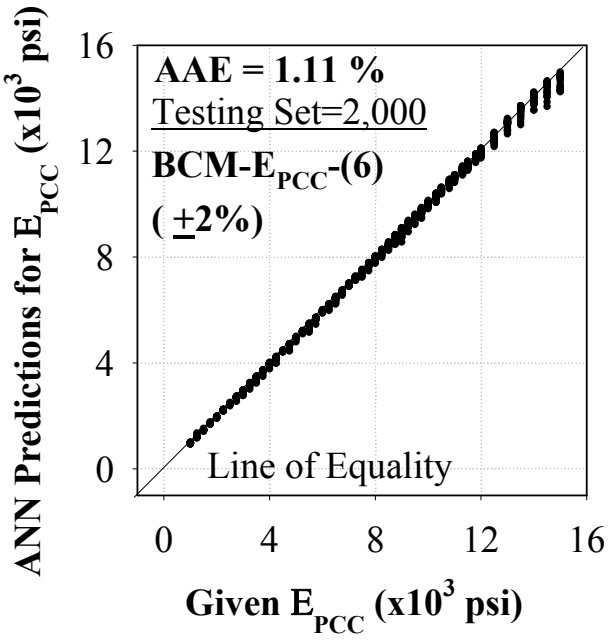

Figure A.11. Prediction performance of the BCM-E_{PCC}-(6) ($\pm$2%) model for backcalculating the PCC layer modulus, E_{PCC}

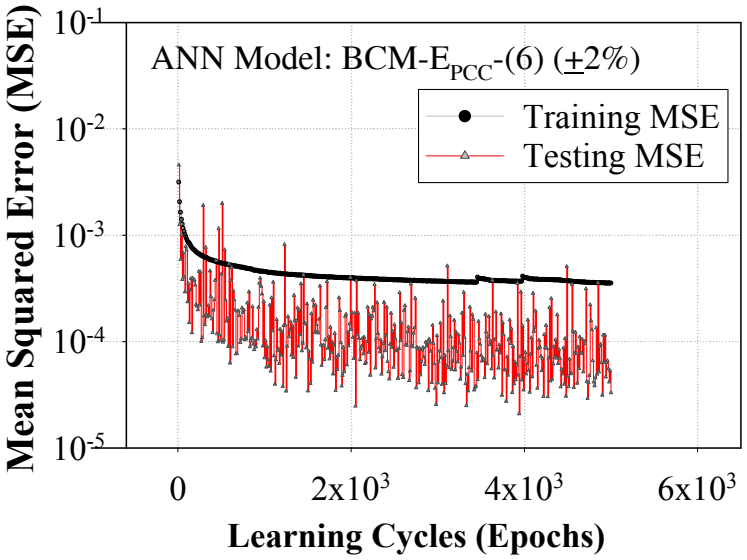

Figure A.12. Training progress curve for the BCM-E_{PCC}-(6) ($\pm$2%) model

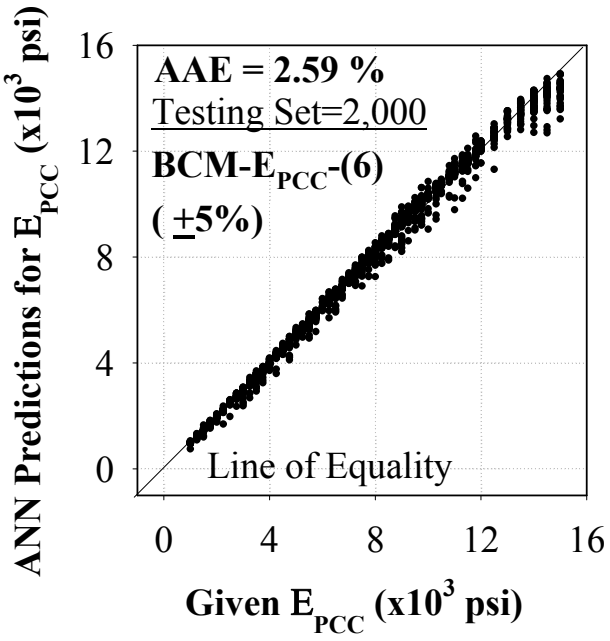

Figure A.13. Prediction performance of the BCM-E_{PCC}-(6) (±5%) model for backcalculating the PCC layer modulus, E_{PCC}

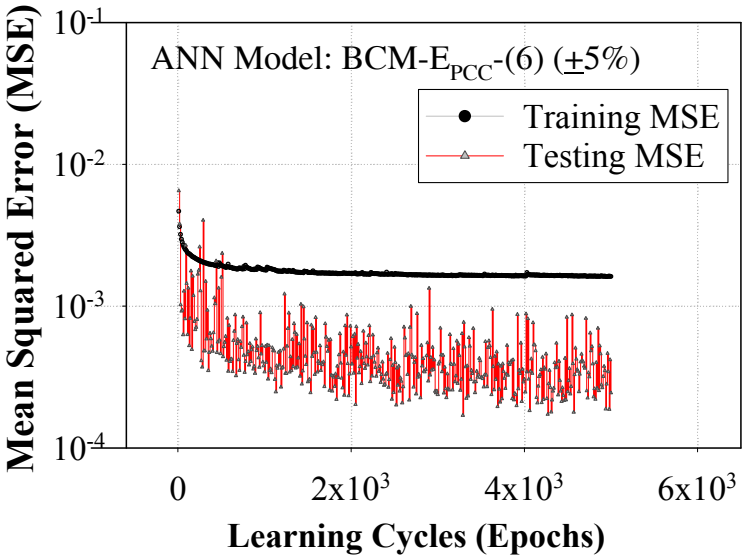

Figure A.14. Training progress curve for the BCM-E_{PCC}-(6) (±5%) model

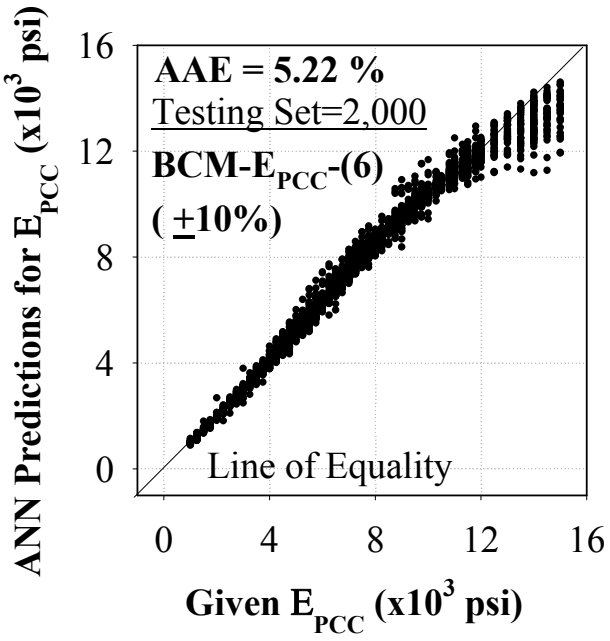

Figure A.15. Prediction performance of the BCM-E_{PCC}-(6) (±10%) model for backcalculating the PCC layer modulus, E_{PCC}

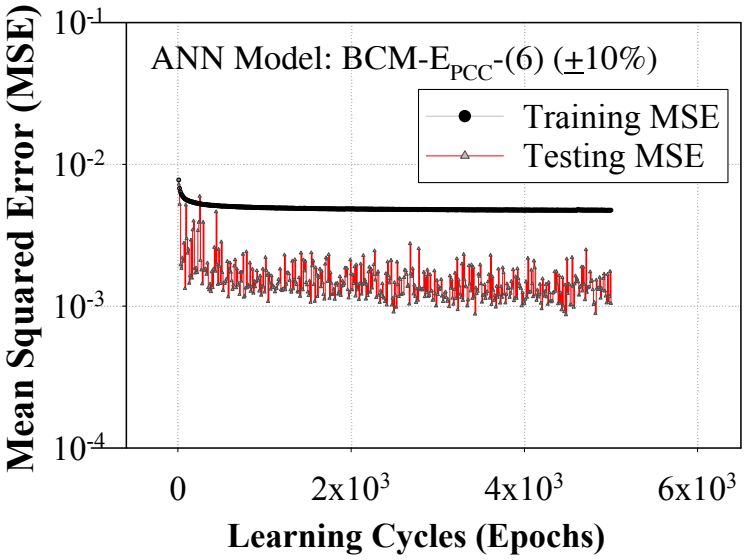

Figure A.16. Training progress curve for the BCM-E_{PCC}-(6) (±10%) model

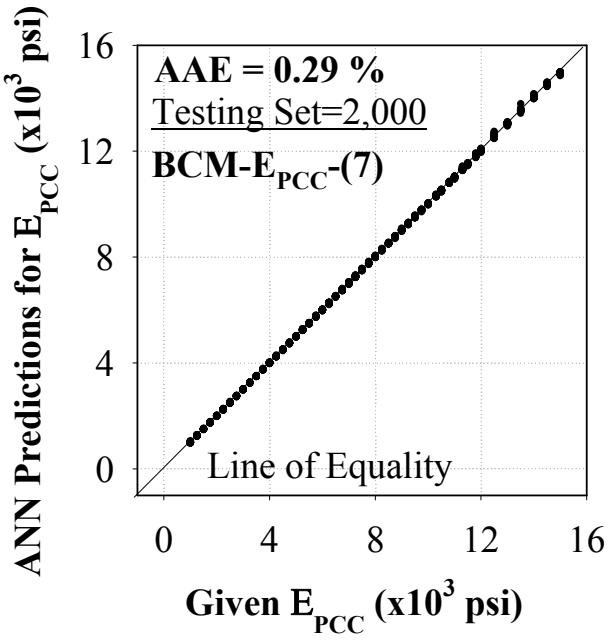

Figure A.17. Prediction performance of the BCM-E_{PCC}-(7) model for backcalculating the PCC layer modulus, E_{PCC}

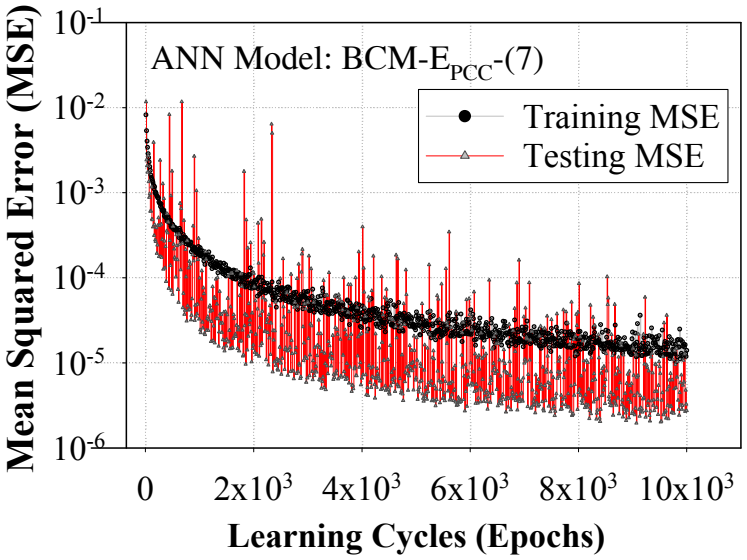

Figure A.18. Training progress curve for the BCM-E_{PCC}-(7) model

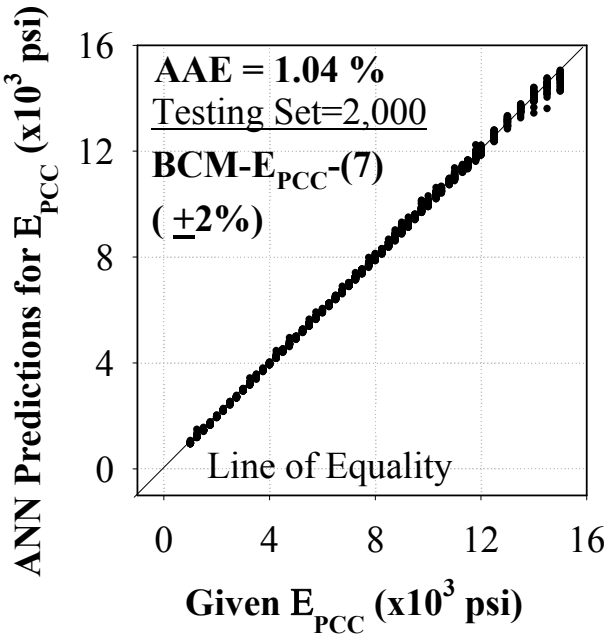

Figure A.19. Prediction performance of the BCM-E_{PCC}-(7) ($\pm$2%) model for backcalculating the PCC layer modulus, E_{PCC}

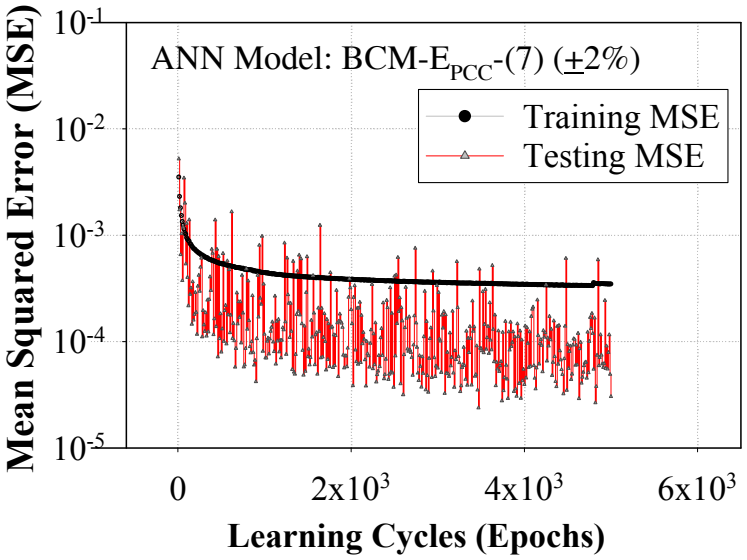

Figure A.20. Training progress curve for the BCM-E_{PCC}-(7) ($\pm$2%) model

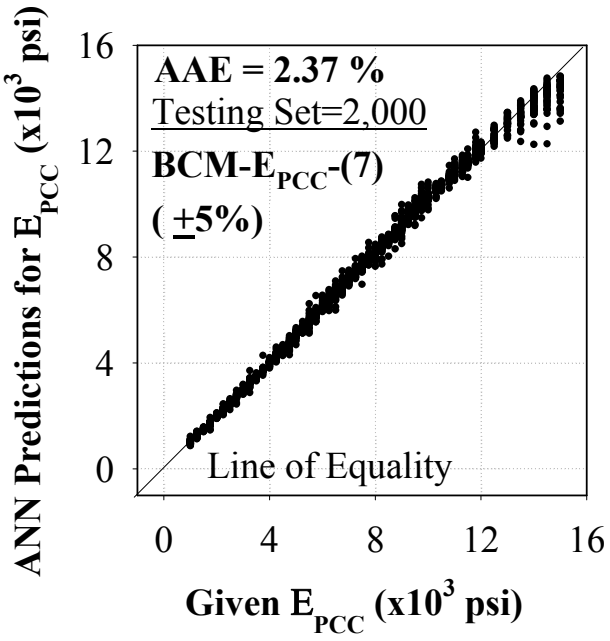

Figure A.21. Prediction performance of the BCM-E_{PCC}-(7) (±5%) model for backcalculating the PCC layer modulus, E_{PCC}

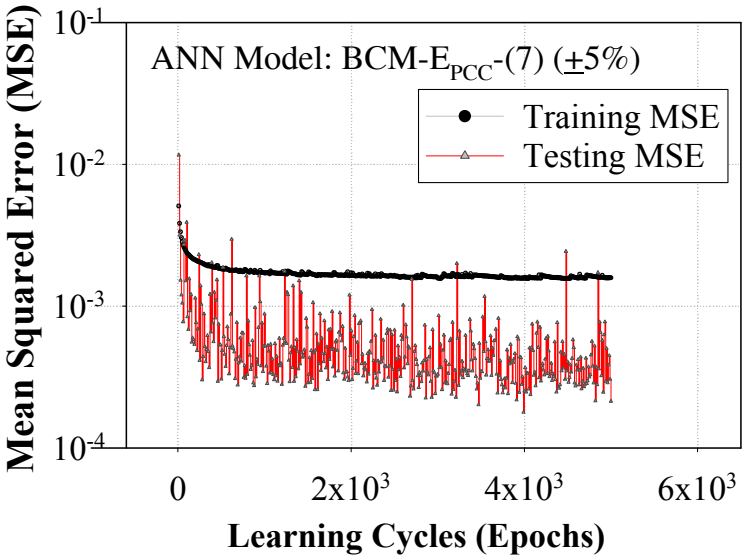

Figure A.22. Training progress curve for the BCM-E_{PCC}-(7) (±5%) model

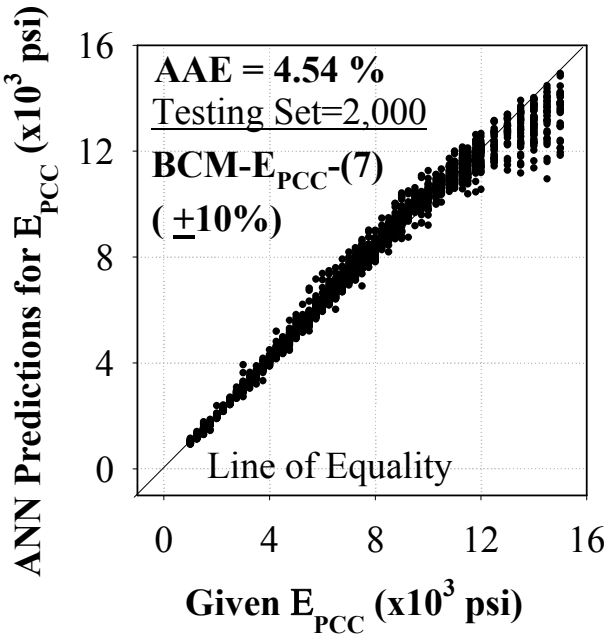

Figure A.23. Prediction performance of the BCM-E_{PCC}-(7) (±10%) model for backcalculating the PCC layer modulus, E_{PCC}

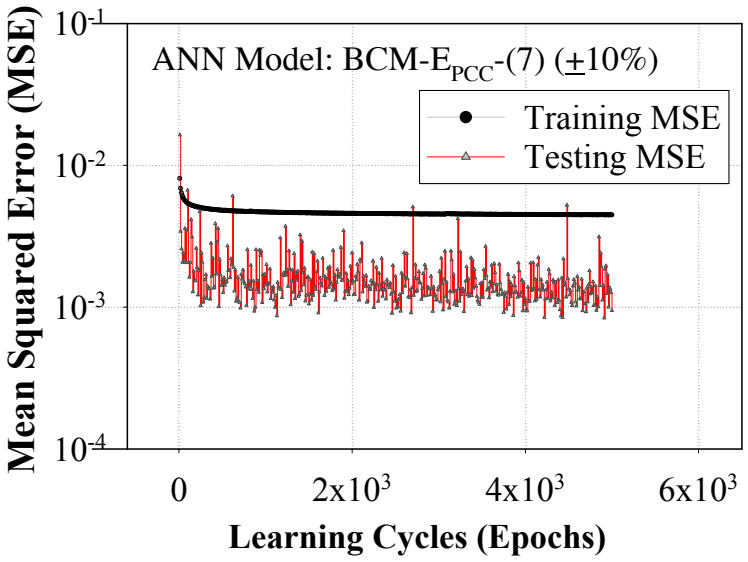

Figure A.24. Training progress curve for the BCM-E_{PCC}-(7) (±10%) model

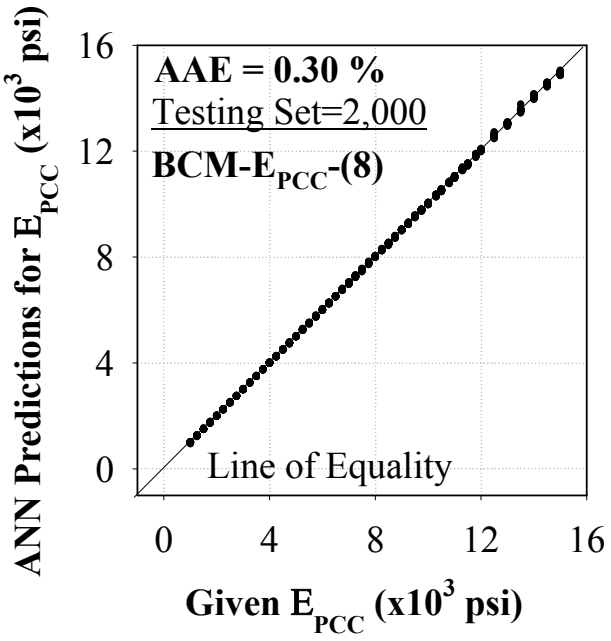

Figure A.25. Prediction performance of the BCM-E_{PCC}-(8) model for backcalculating the PCC layer modulus, E_{PCC}

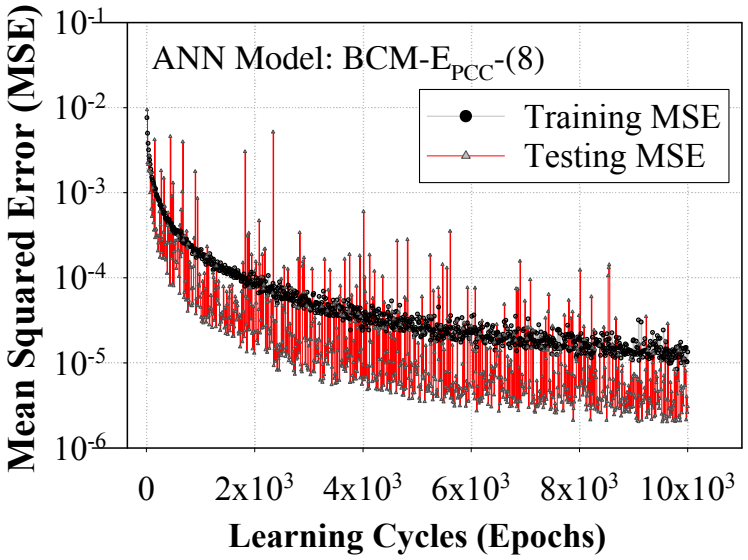

Figure A.26. Training progress curve for the BCM-E_{PCC}-(8) model

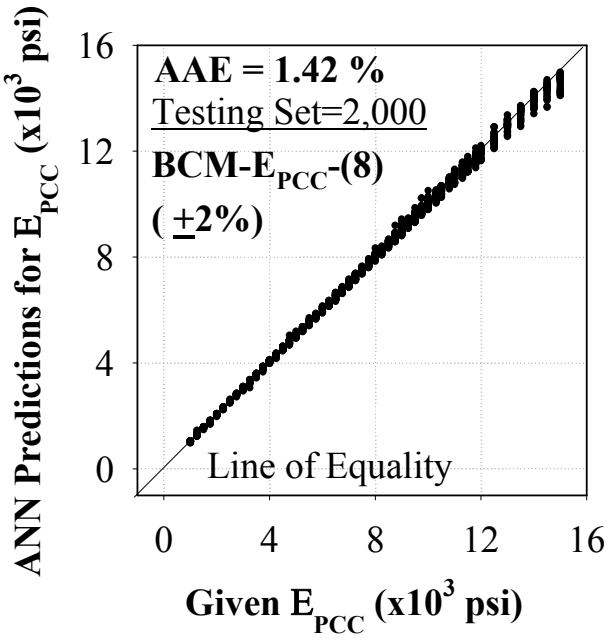

Figure A.27. Prediction performance of the BCM-E_{PCC}-(8) ($\pm$2%) model for backcalculating the PCC layer modulus, E_{PCC}

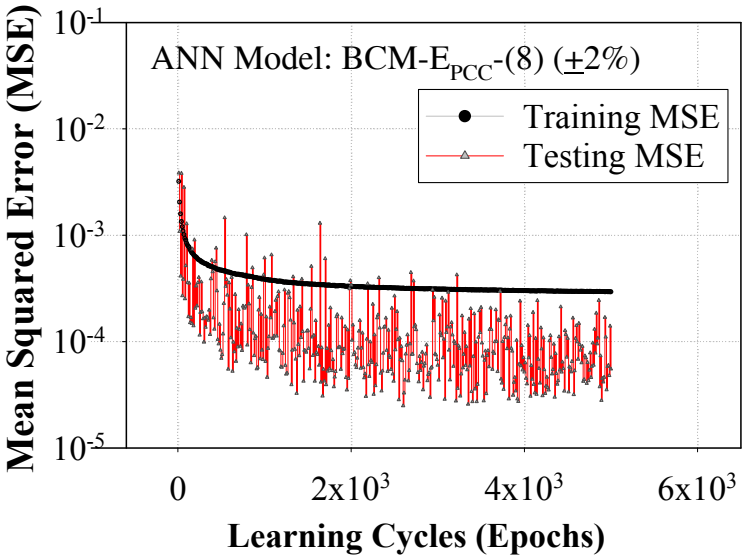

Figure A.28. Training progress curve for the BCM-E_{PCC}-(8) ($\pm$2%) model

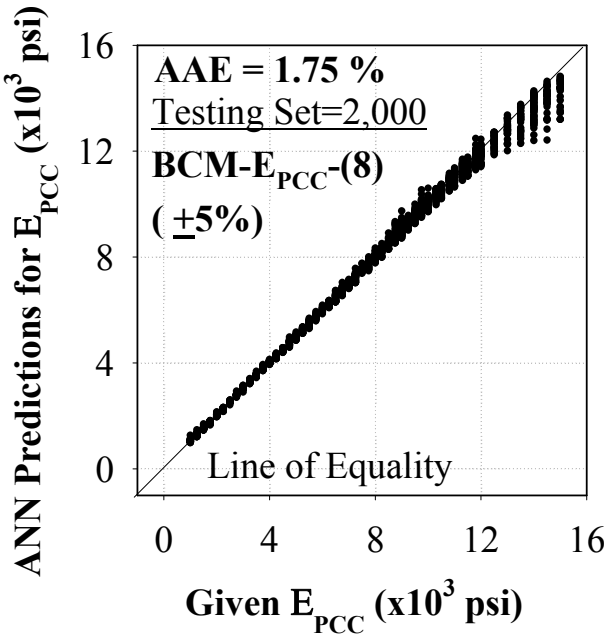

Figure A.29. Prediction performance of the BCM-E_{PCC}-(8) (±5%) model for backcalculating the PCC layer modulus, E_{PCC}

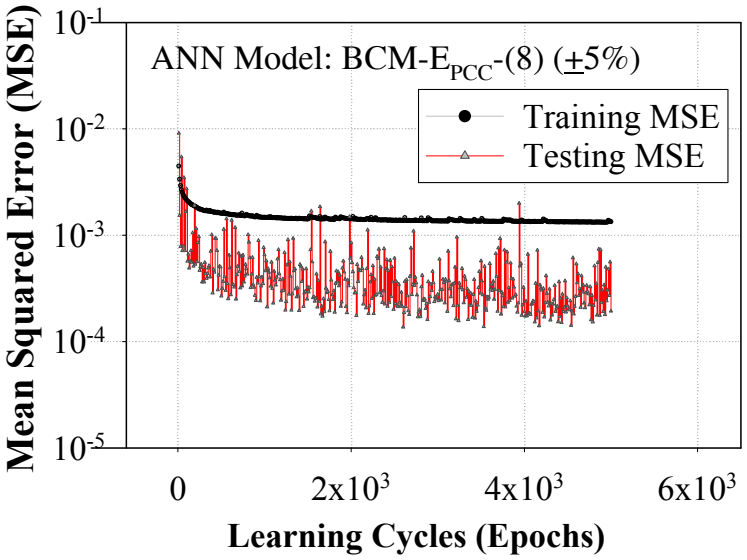

Figure A.30. Training progress curve for the BCM-E_{PCC}-(8) (±5%) model

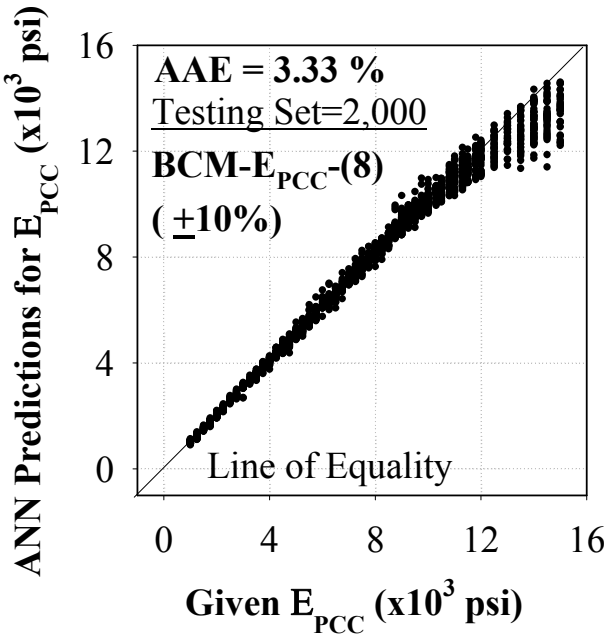

Figure A.31. Prediction performance of the BCM-E_{PCC}-(8) ($\pm$10%) model for backcalculating the PCC layer modulus, E_{PCC}

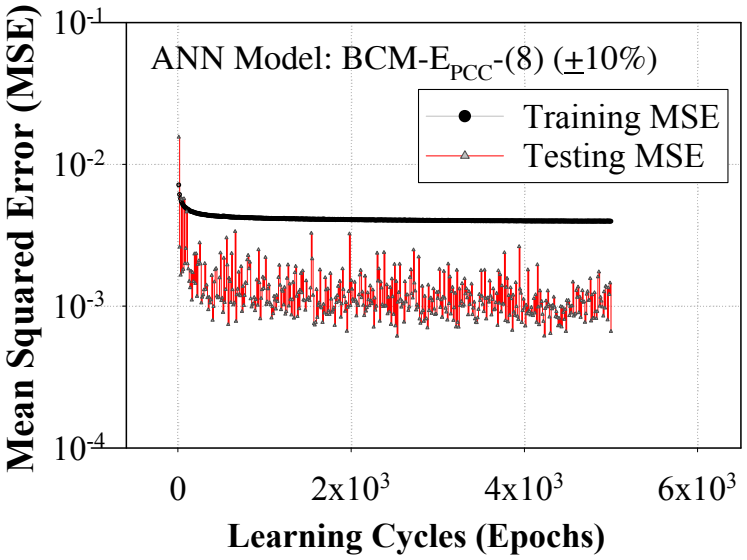

Figure A.32. Training progress curve for the BCM-E_{PCC}-(8) ($\pm$10%) model

APPENDIX B. ANN-BASED BACKCALCULATION MODELS FOR COEFFICIENT OF SUBGRADE REACTION

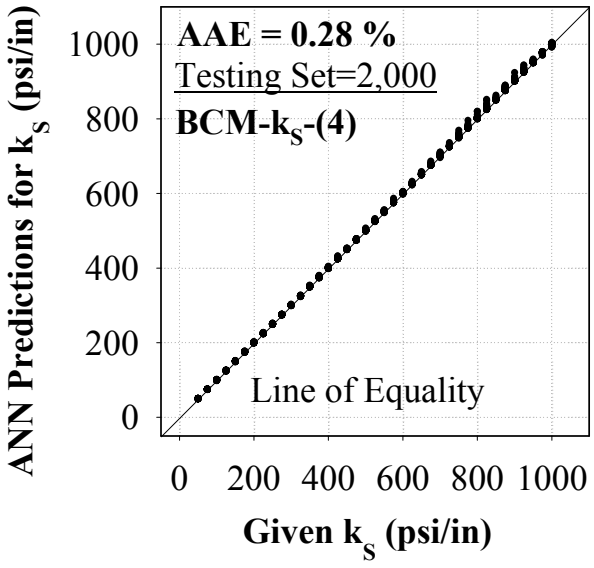

Figure B.1. Prediction performance of the BCM-k_S-(4) model for backcalculating the coefficient of subgrade reaction, k_S

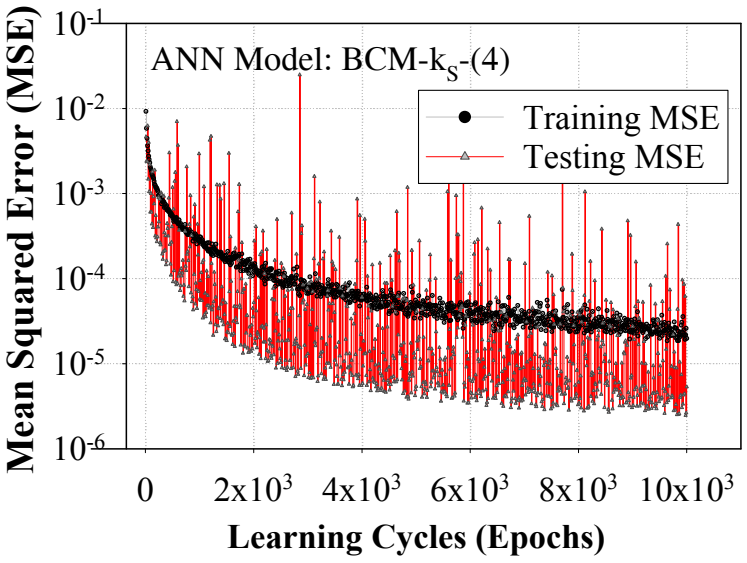

Figure B.2. Training progress curve for the BCM-k_S-(4) model

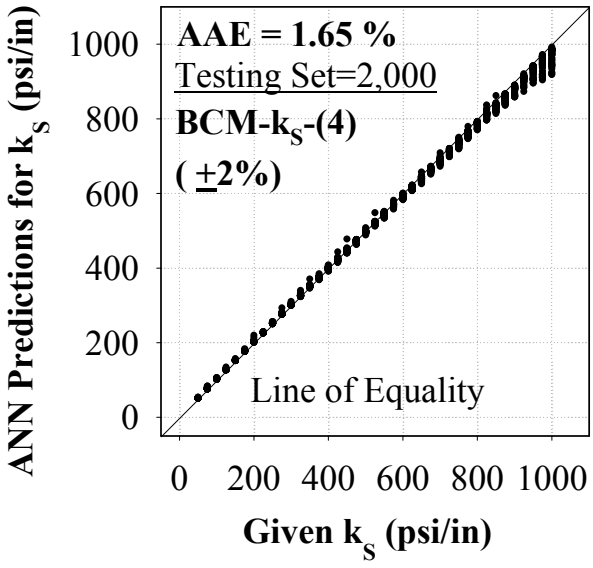

Figure B.3. Prediction performance of the BCM-k_S-(4) (±2%) model for backcalculating the coefficient of subgrade reaction, k_S

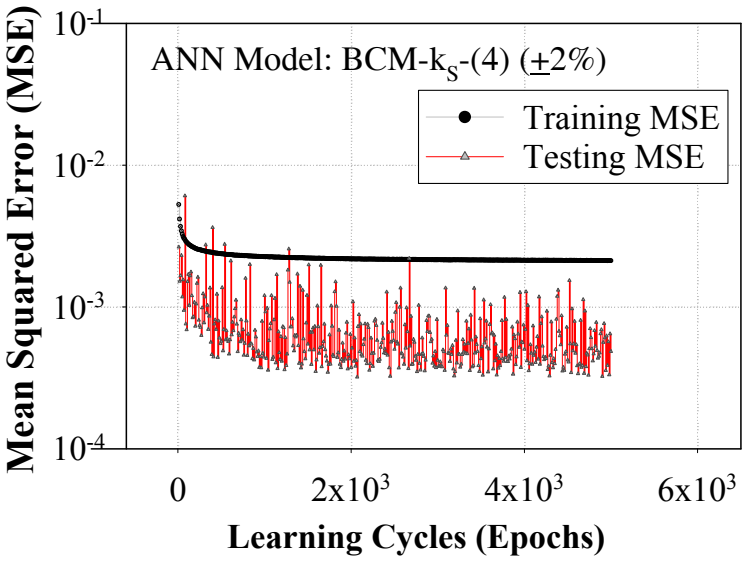

Figure B.4. Training progress curve for the BCM-k_S-(4) (±2%) model

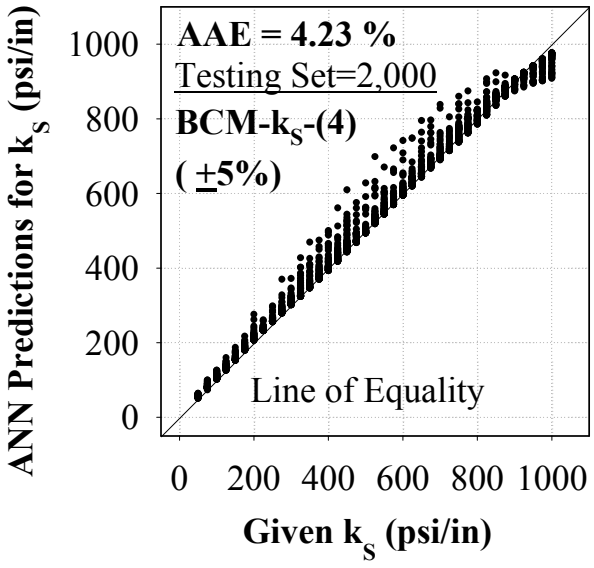

Figure B.5. Prediction performance of the BCM-k_S-(4) (±5%) model for backcalculating the coefficient of subgrade reaction, k_S

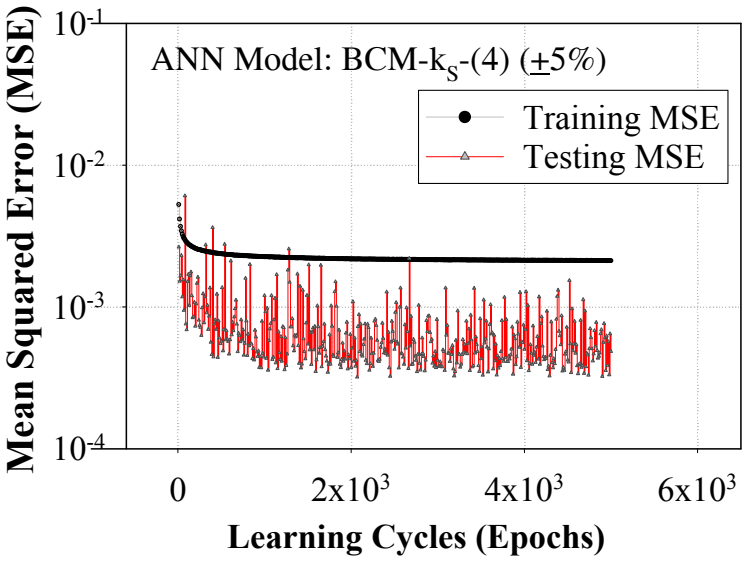

Figure B.6. Training progress curve for the BCM-k_S-(4) (±5%) model

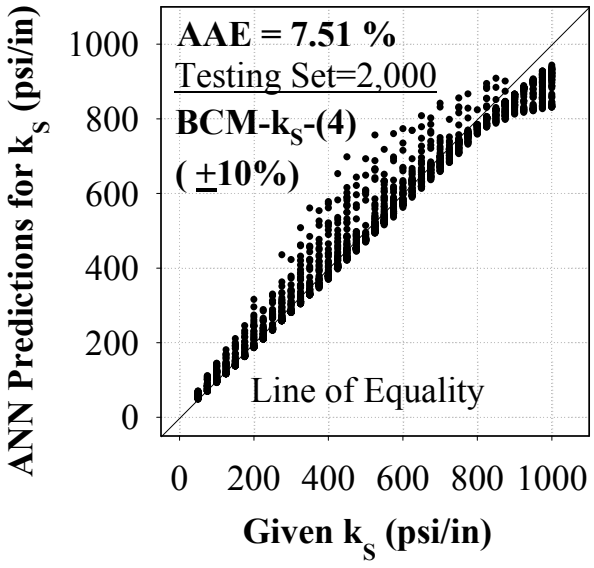

Figure B.7. Prediction performance of the BCM-k_S-(4) (±10%) model for backcalculating the coefficient of subgrade reaction, k_S

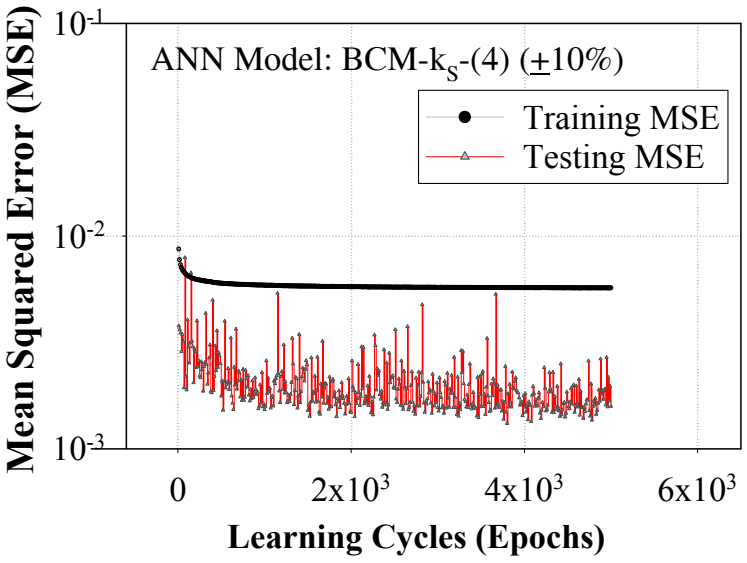

Figure B.8. Training progress curve for the BCM-k_S-(4) (±10%) model

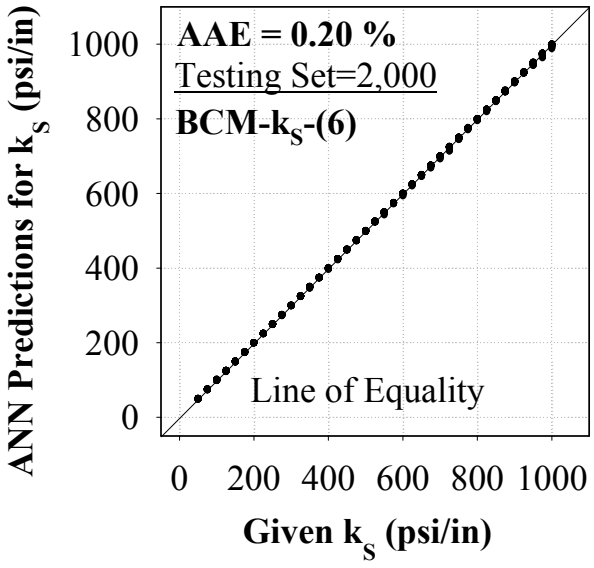

Figure B.9. Prediction performance of the BCM-k_S-(6) model for backcalculating the coefficient of subgrade reaction, k_S

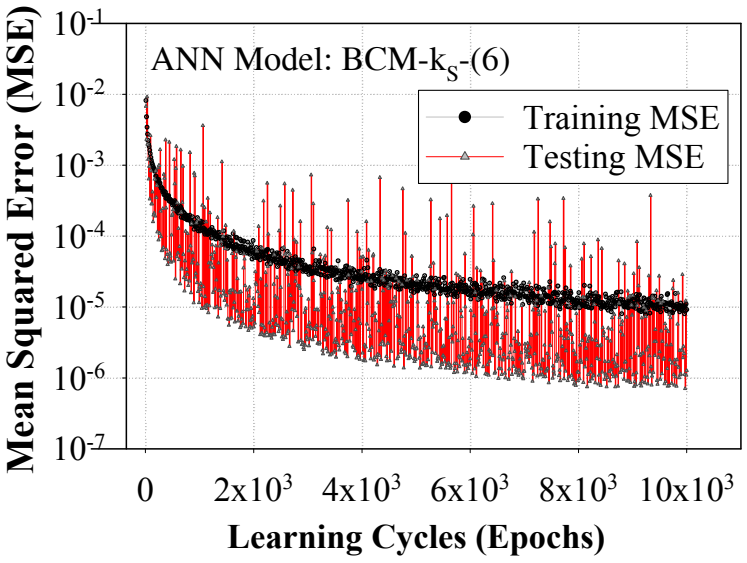

Figure B.10. Training progress curve for the BCM-k_S-(6) model

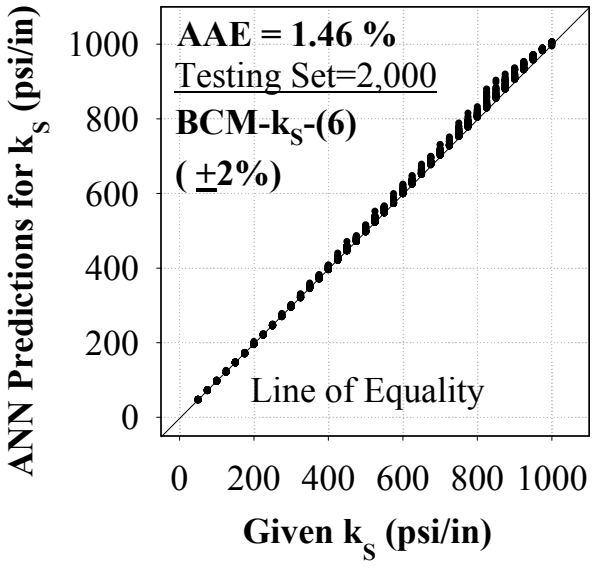

Figure B.11. Prediction performance of the BCM-k_S-(6) (±2%) model for backcalculating the coefficient of subgrade reaction, k_S

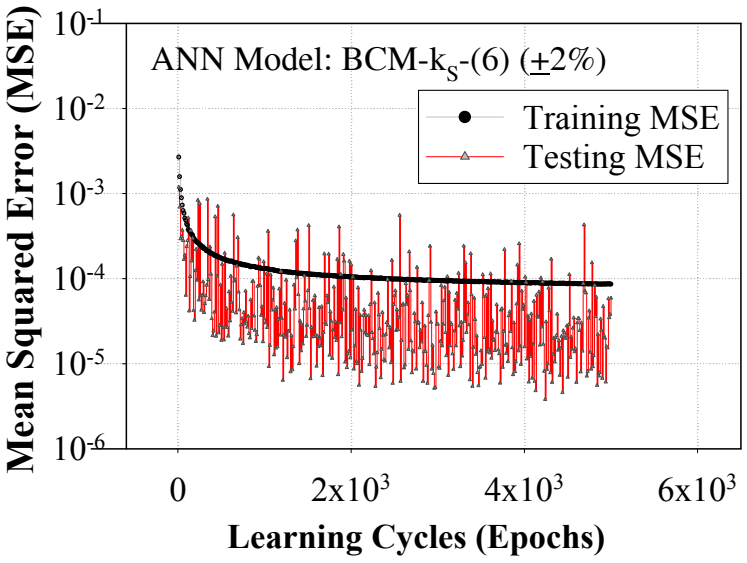

Figure B.12. Training progress curve for the BCM-k_S-(6) (±2%) model

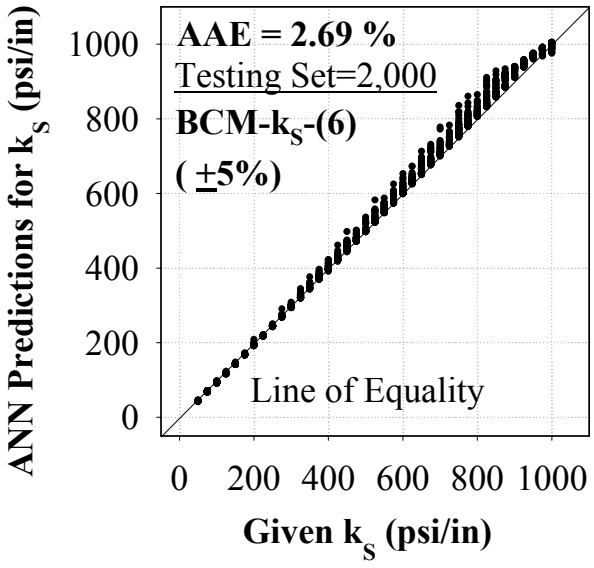

Figure B.13. Prediction performance of the BCM-k_S-(6) (±5%) model for backcalculating the coefficient of subgrade reaction, k_S

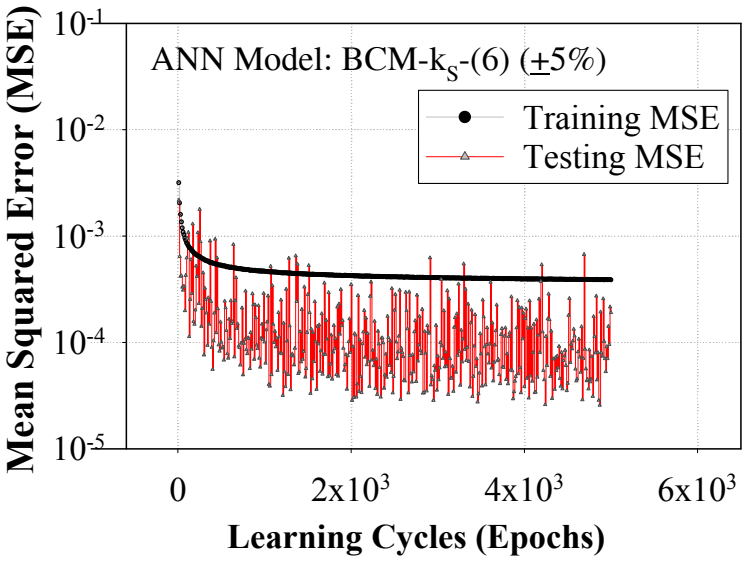

Figure B.14. Training progress curve for the BCM-k_S-(6) (±5%) model

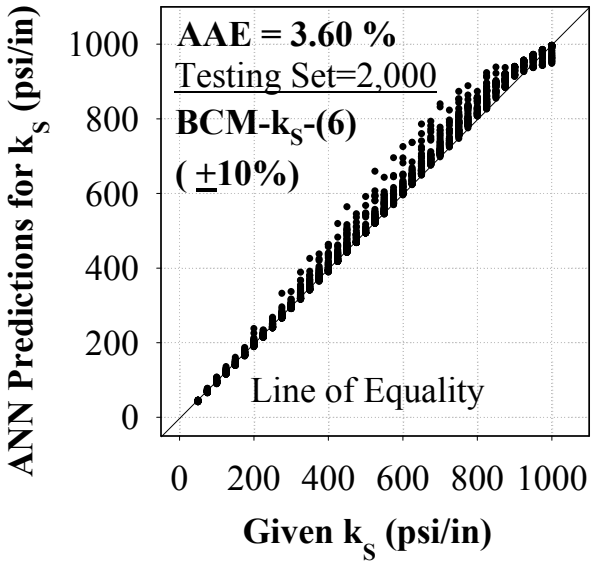

Figure B.15. Prediction performance of the BCM-k_S-(6) (±10%) model for backcalculating the coefficient of subgrade reaction, k_S

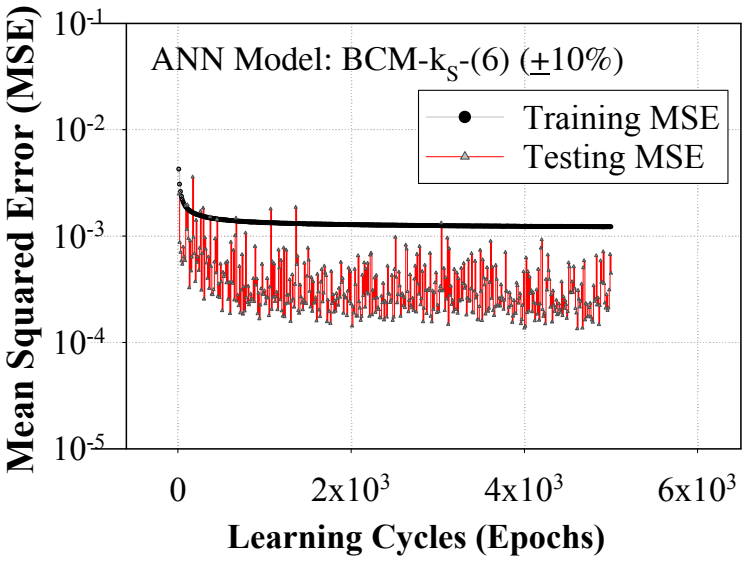

Figure B.16. Training progress curve for the BCM-k_S-(6) (±10%) model

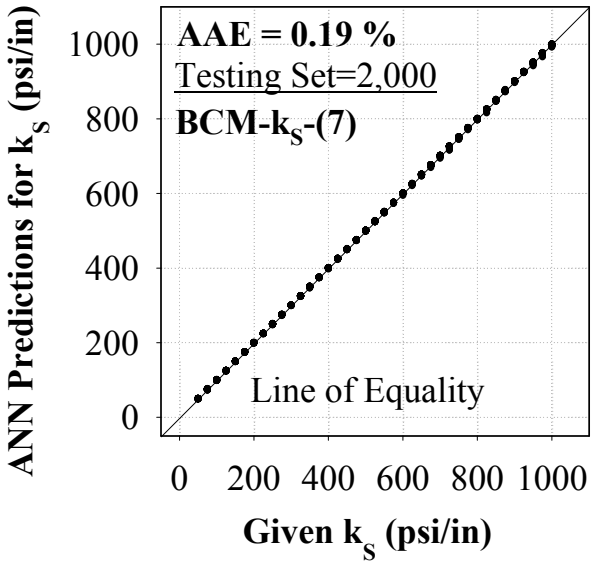

Figure B.17. Prediction performance of the BCM-k_S-(7) model for backcalculating the coefficient of subgrade reaction, k_S

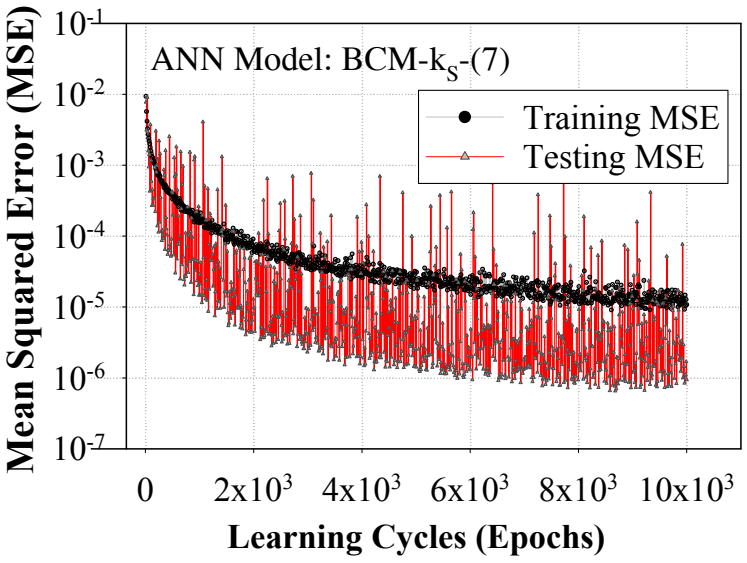

Figure B.18. Training progress curve for the BCM-k_S-(7) model

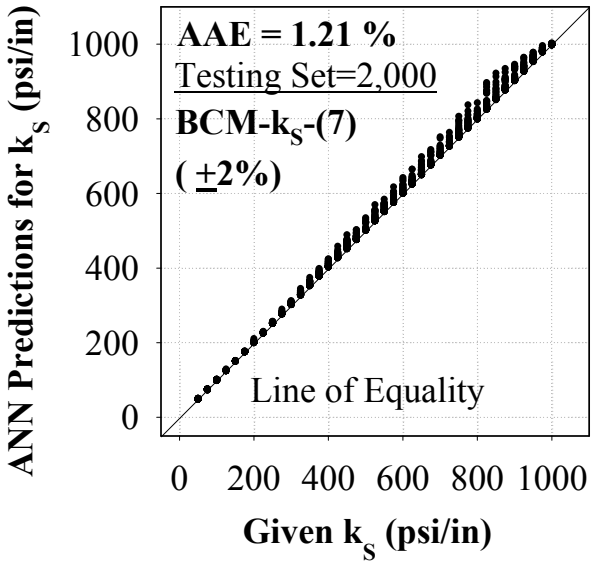

Figure B.19. Prediction performance of the BCM-k_S-(7) (±2%) model for backcalculating the coefficient of subgrade reaction, k_S

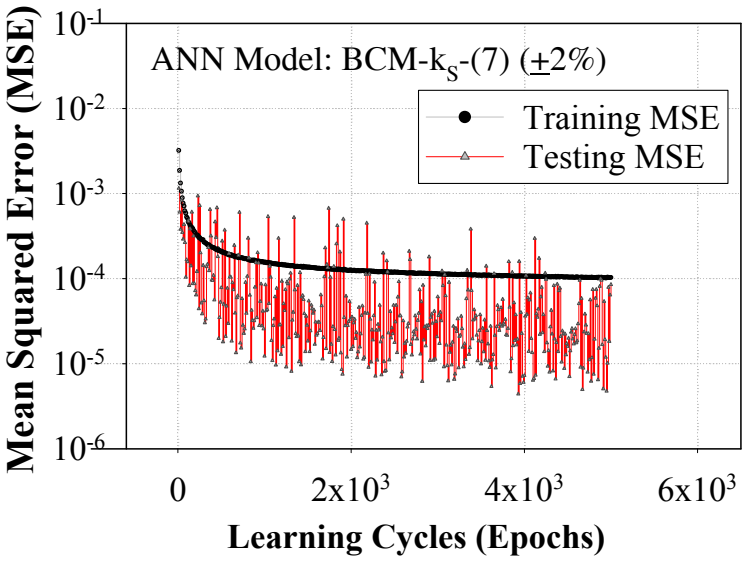

Figure B.20. Training progress curve for the BCM-k_S-(7) (±2%) model

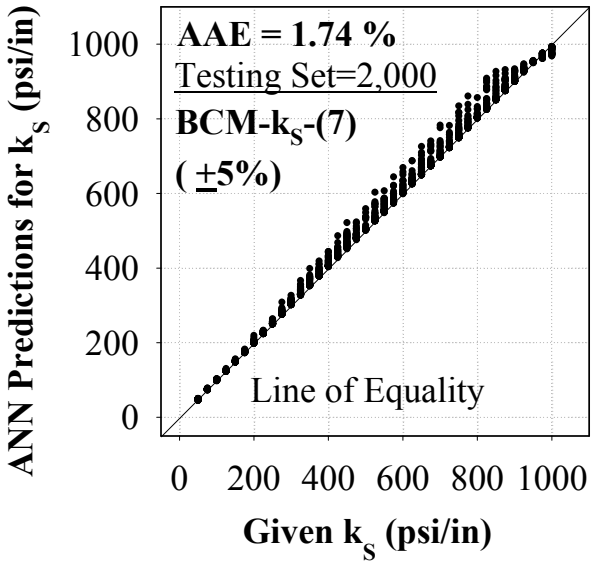

Figure B.21. Prediction performance of the BCM-k_S-(7) ($\pm$5%) model for backcalculating the coefficient of subgrade reaction, k_S

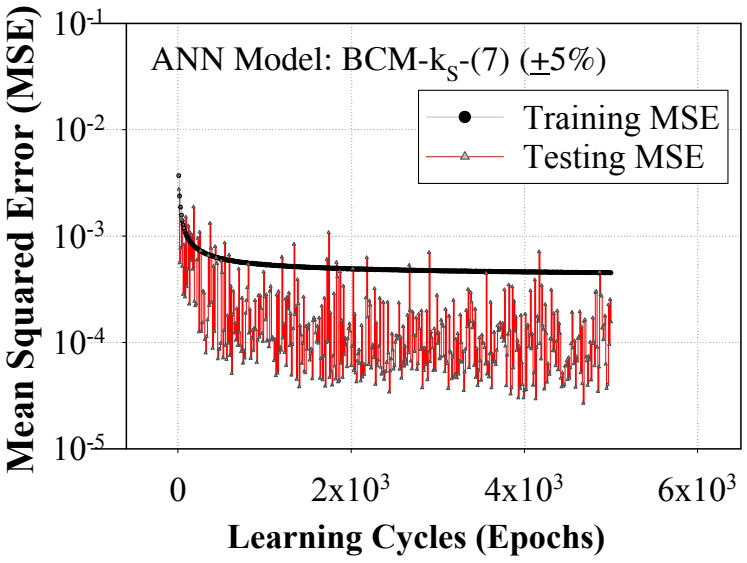

Figure B.22. Training progress curve for the BCM-k_S-(7) ($\pm$5%) model

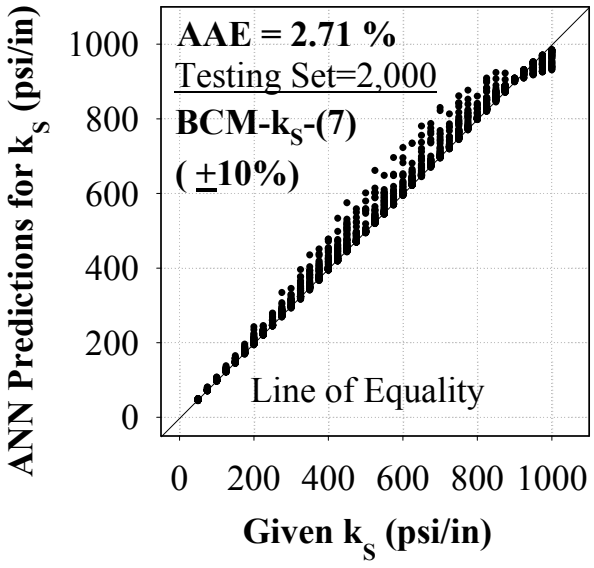

Figure B.23. Prediction performance of the BCM-k_S-(7) (±10%) model for backcalculating the coefficient of subgrade reaction, k_S

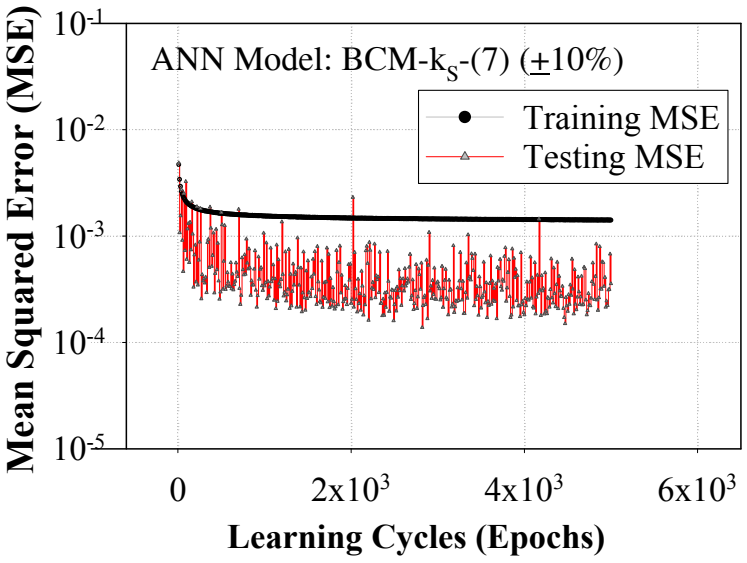

Figure B.24. Training progress curve for the BCM-k_S-(7) (±10%) model

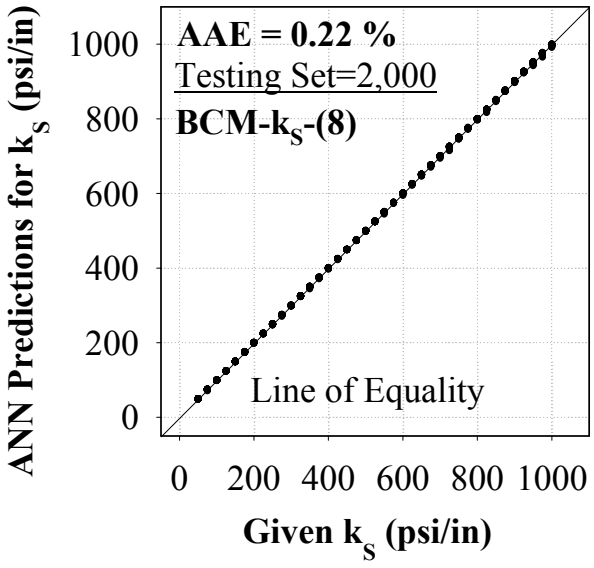

Figure B.25. Prediction performance of the BCM-k_S-(8) model for backcalculating the coefficient of subgrade reaction, k_S

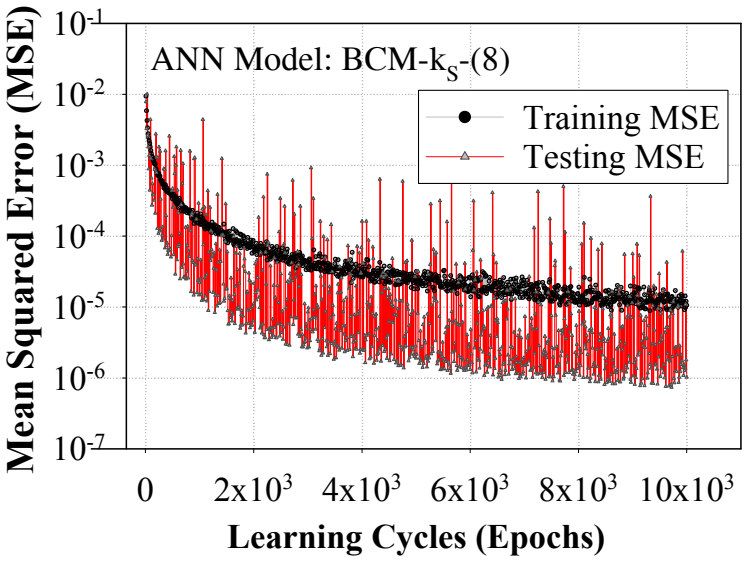

Figure B.26. Training progress curve for the BCM-k_S-(8) model

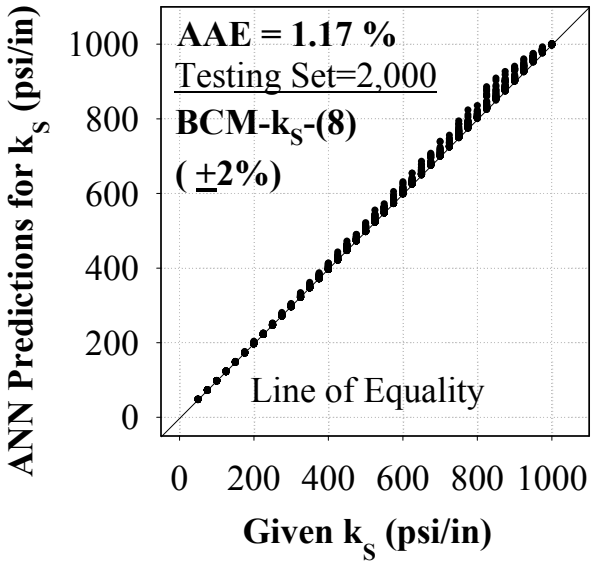

Figure B.27. Prediction performance of the BCM-k_S-(8) (±2%) model for backcalculating the coefficient of subgrade reaction, k_S

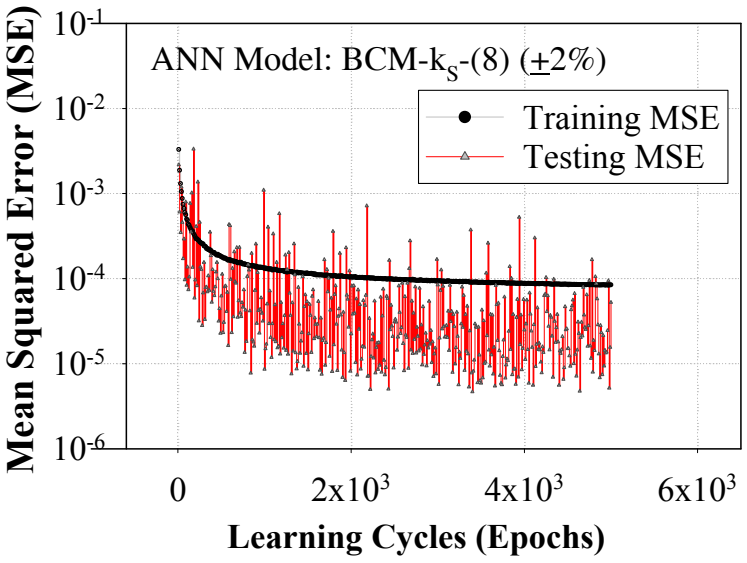

Figure B.28. Training progress curve for the BCM-k_S-(8) (±2%) model

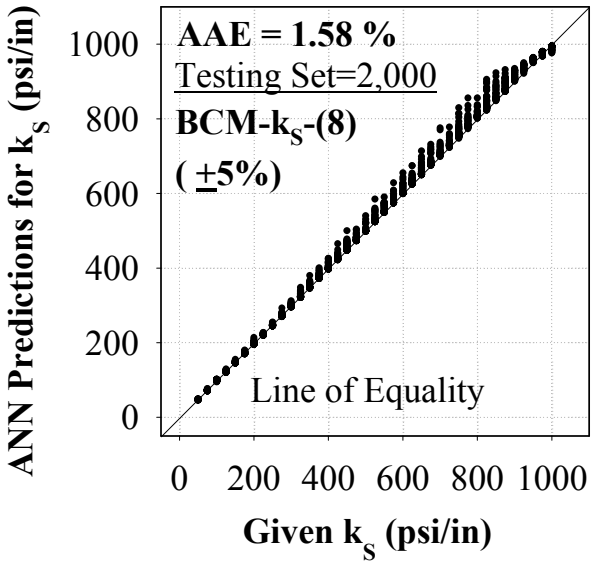

Figure B.29. Prediction performance of the BCM-k_S-(8) (±5%) model for backcalculating the coefficient of subgrade reaction, k_S

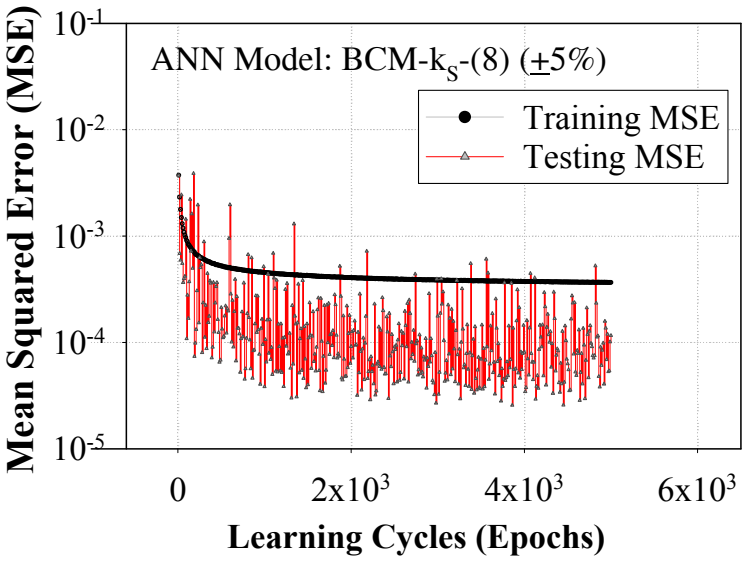

Figure B.30. Training progress curve for the BCM-k_S-(8) (±5%) model

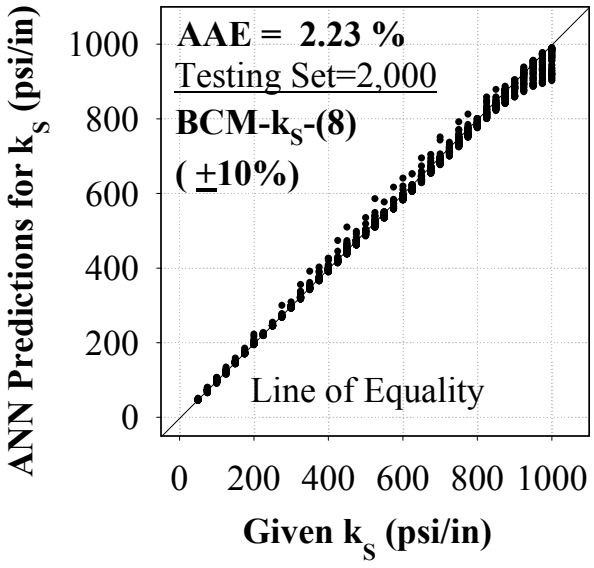

Figure B.31. Prediction performance of the BCM-k_S-(8) (±10%) model for backcalculating the coefficient of subgrade reaction, k_S

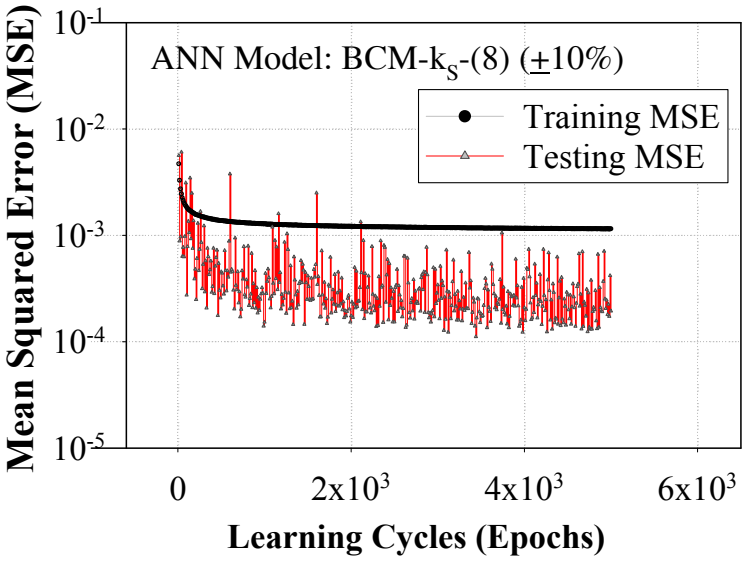

Figure B.32. Training progress curve for the BCM-k_S-(8) (±10%) model

APPENDIX C. ANN-BASED BACKCALCULATION MODELS FOR TOTAL EFFECTIVE LINEAR TEMPERATURE DIFFERENCE

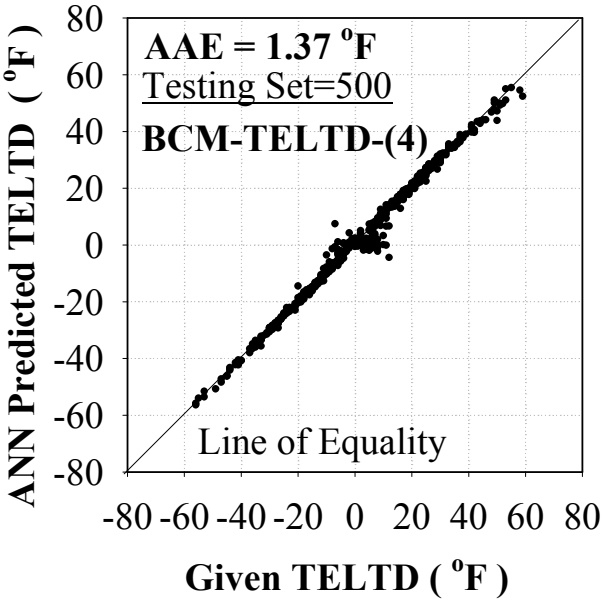

Figure C.1. Prediction performance of the BCM-TELTD-(4) model for backcalculating the total effective linear temperature difference, TELTD

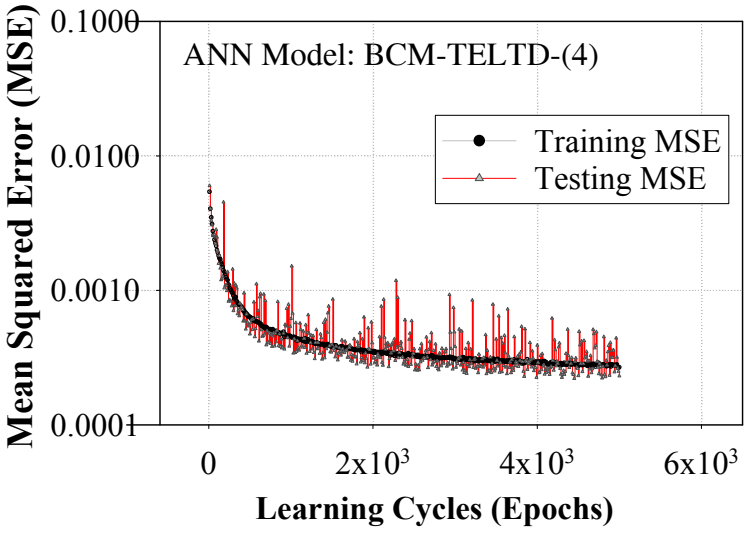

Figure C.2. Training progress curve for the BCM-TELTD-(4) model

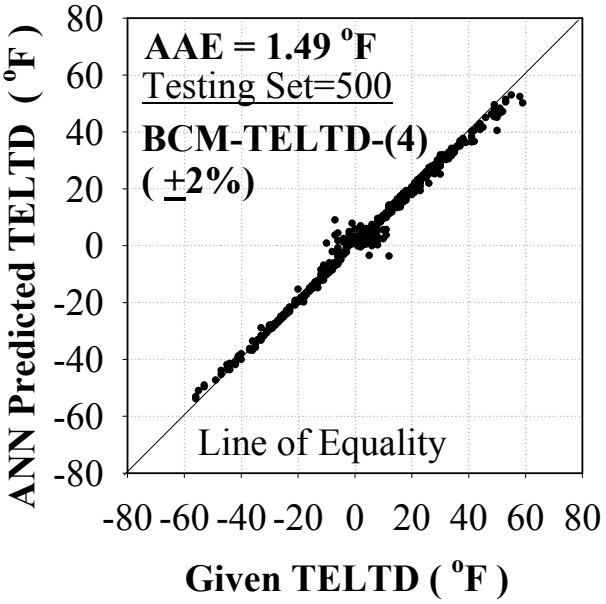

Figure C.3. Prediction performance of the BCM-TELTD-(4) (±2%) model for backcalculating the total effective linear temperature difference, TELTD

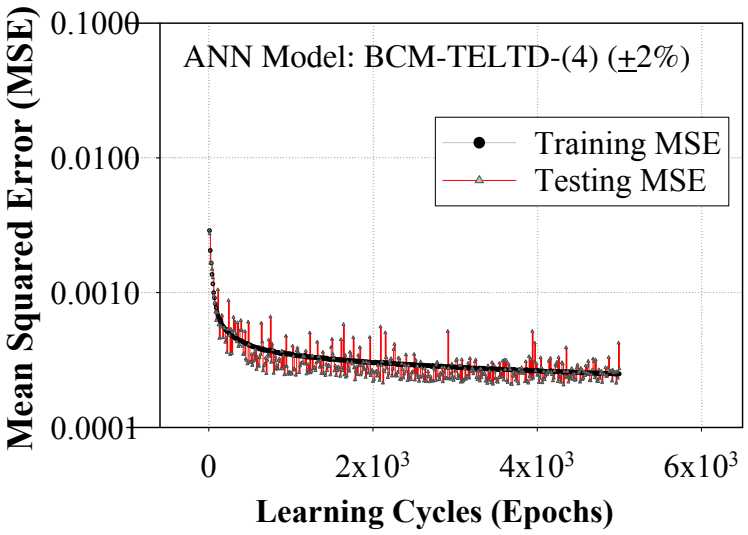

Figure C.4. Training progress curve for the BCM-TELTD-(4) (±2%) model

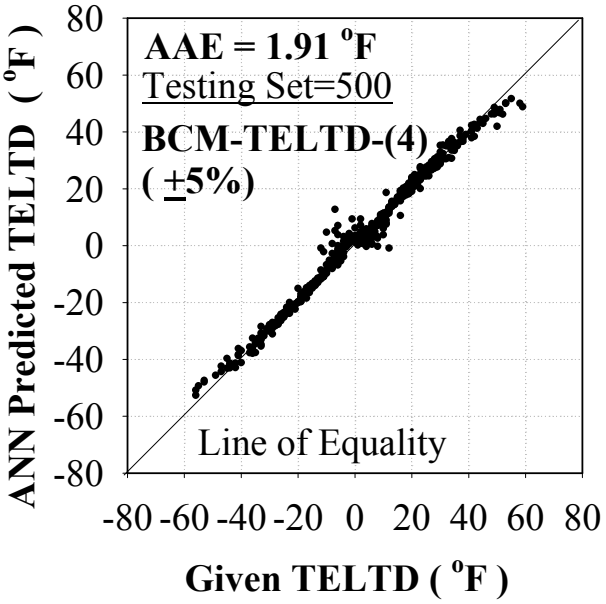

Figure C.5. Prediction performance of the BCM-TELTD-(4) (±5%) model for backcalculating the total effective linear temperature difference, TELTD

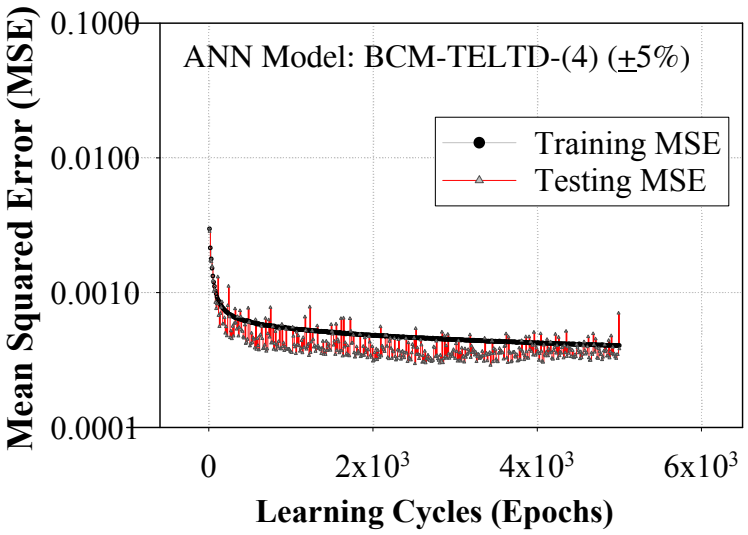

Figure C.6. Training progress curve for the BCM-TELTD-(4) (±5%) model

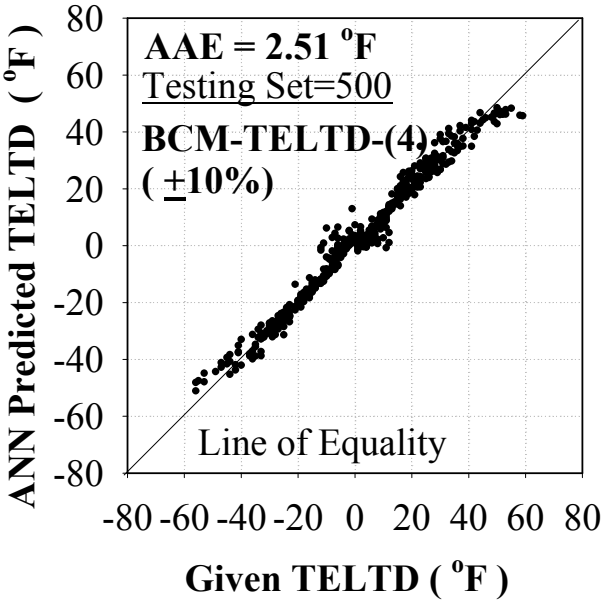

Figure C.7. Prediction performance of the BCM-TELTD-(4) (±10%) model for backcalculating the total effective linear temperature difference, TELTD

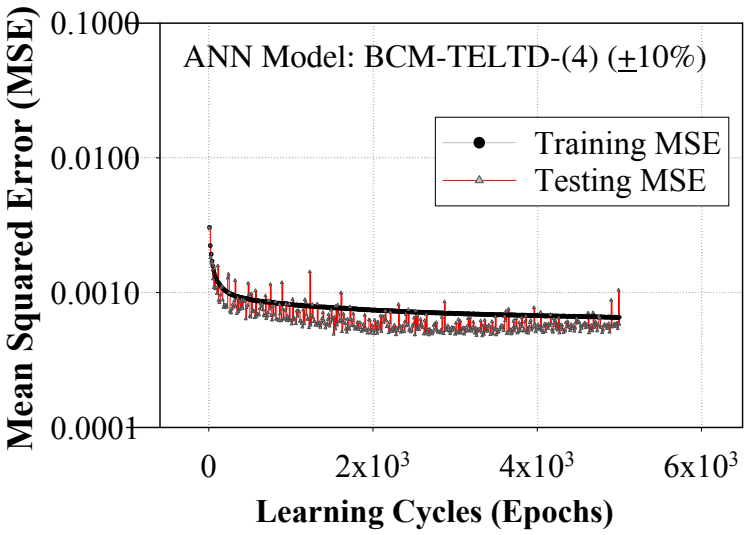

Figure C.8. Training progress curve for the BCM-TELTD-(4) (±10%) model

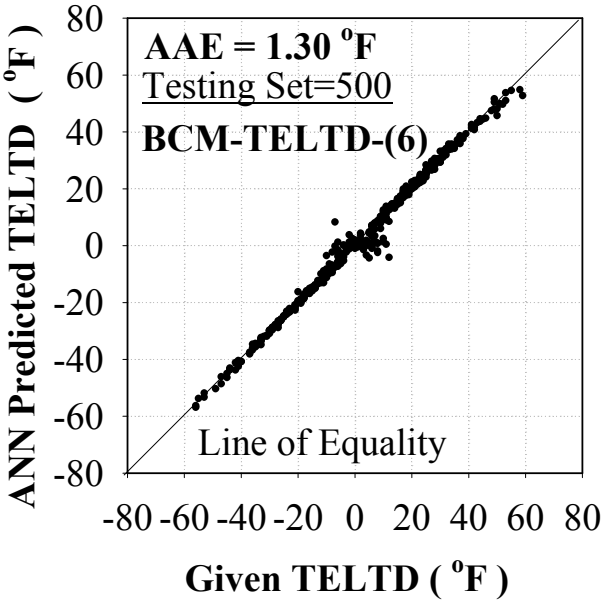

Figure C.9. Prediction performance of the BCM-TELTD-(6) model for backcalculating the total effective linear temperature difference, TELTD

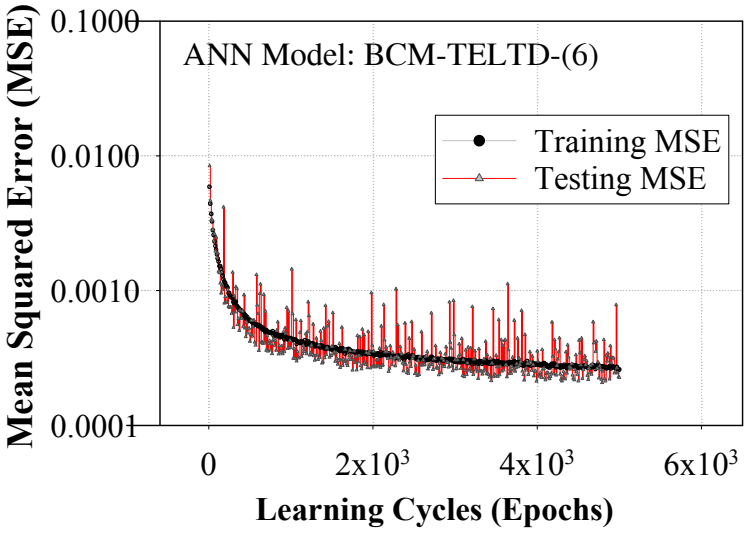

Figure C.10. Training progress curve for the BCM-TELTD-(6) model

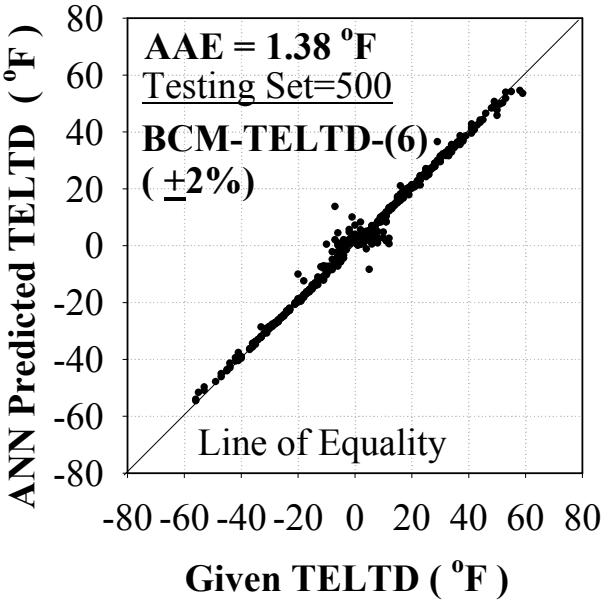

Figure C.11. Prediction performance of the BCM-TELTD-(6) (±2%) model for backcalculating the total effective linear temperature difference, TELTD

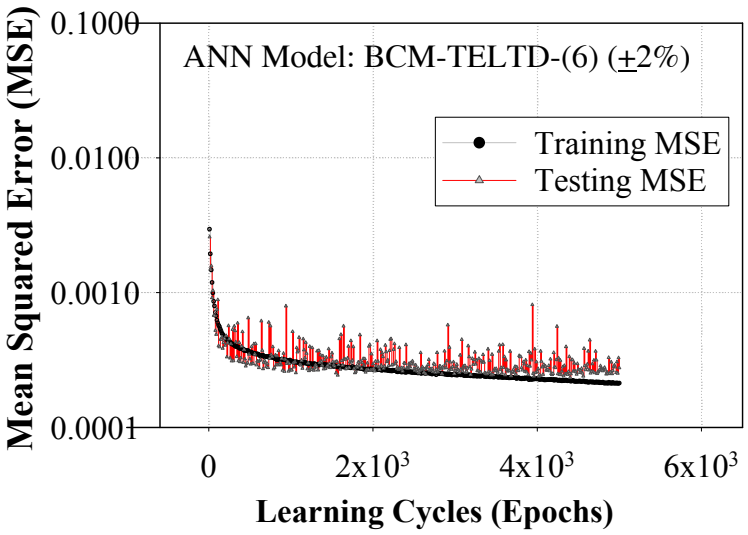

Figure C.12. Training progress curve for the BCM-TELTD-(6) (±2%) model

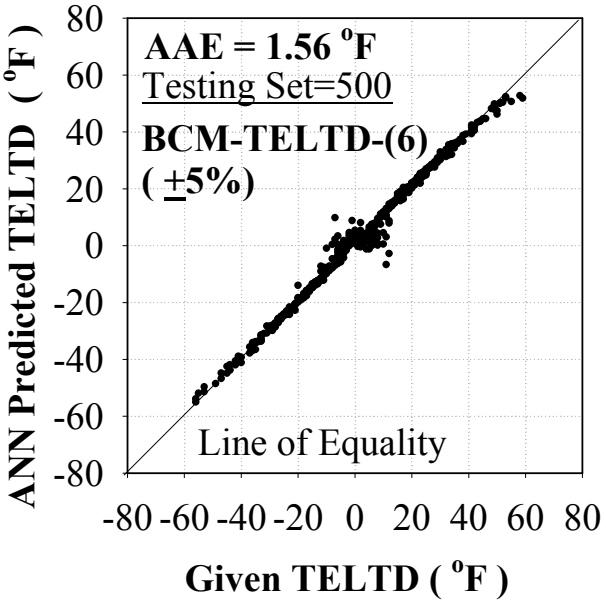

Figure C.13. Prediction performance of the BCM-TELTD-(6) (±5%) model for backcalculating the total effective linear temperature difference, TELTD

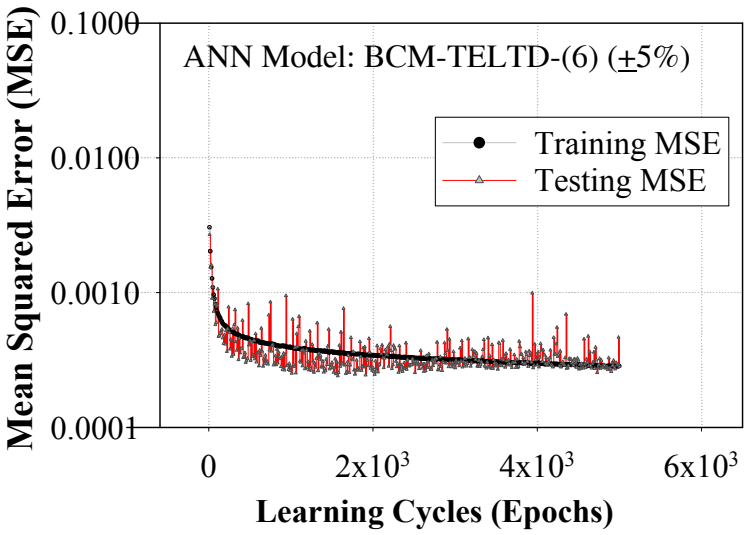

Figure C.14. Training progress curve for the BCM-TELTD-(6) (±5%) model

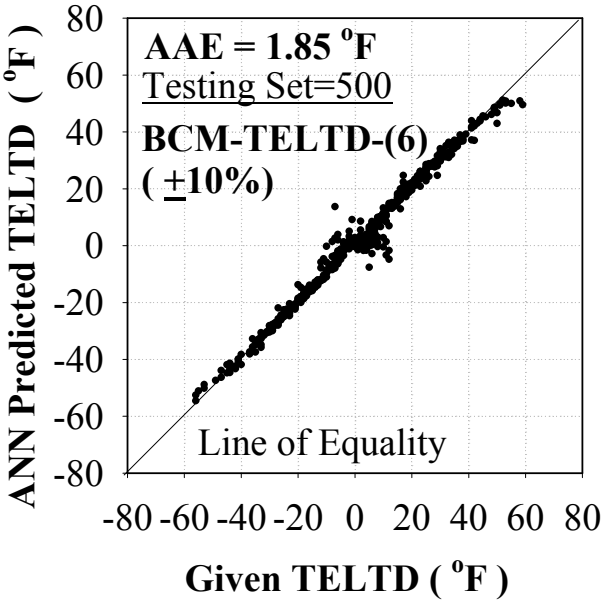

Figure C.15. Prediction performance of the BCM-TELTD-(6) (±10%) model for backcalculating the total effective linear temperature difference, TELTD

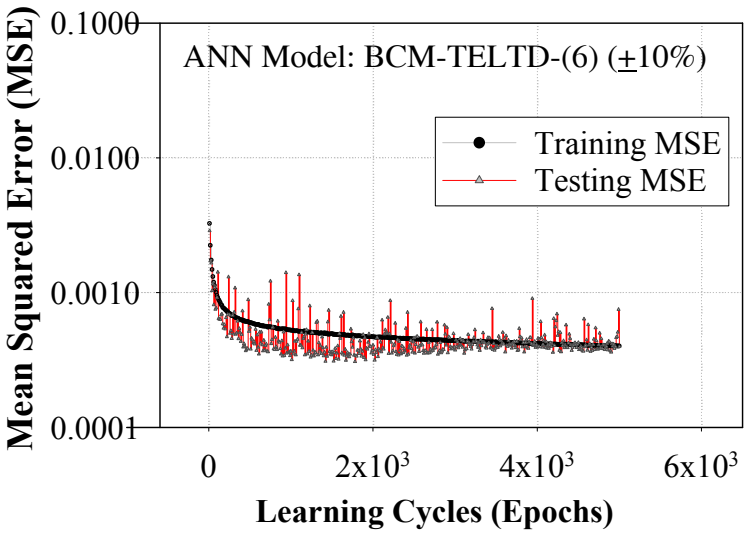

Figure C.16. Training progress curve for the BCM-TELTD-(6) (±10%) model

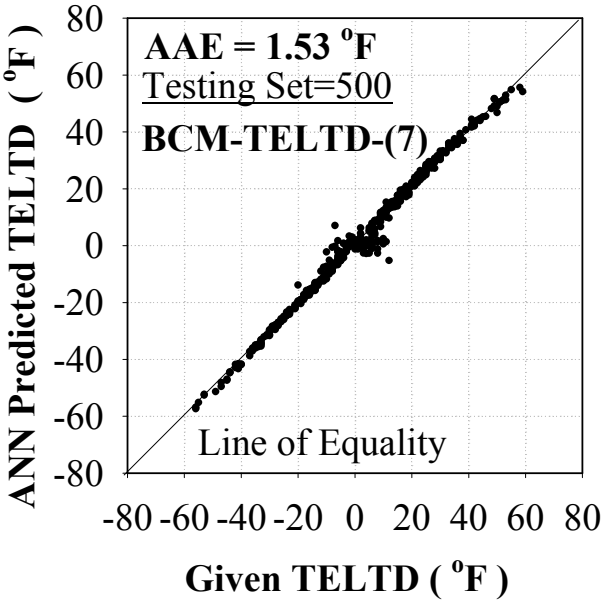

Figure C.17. Prediction performance of the BCM-TELTD-(7) model for backcalculating the total effective linear temperature difference, TELTD

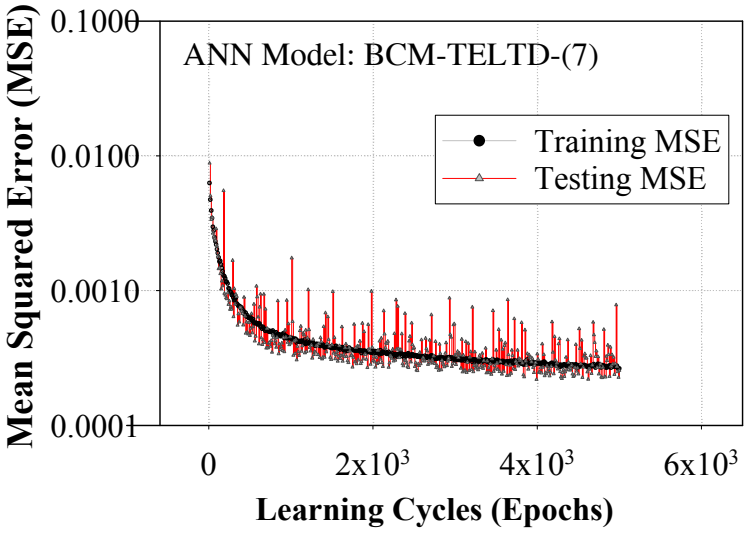

Figure C.18. Training progress curve for the BCM-TELTD-(7) model

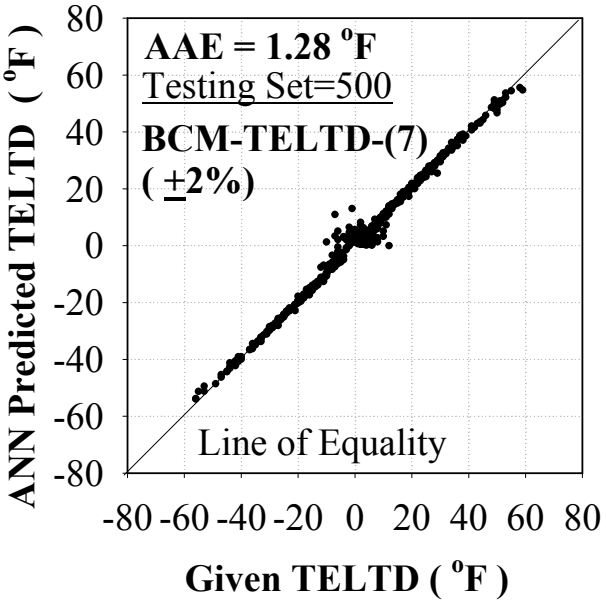

Figure C.19. Prediction performance of the BCM-TELTD-(7) (±2%) model for backcalculating the total effective linear temperature difference, TELTD

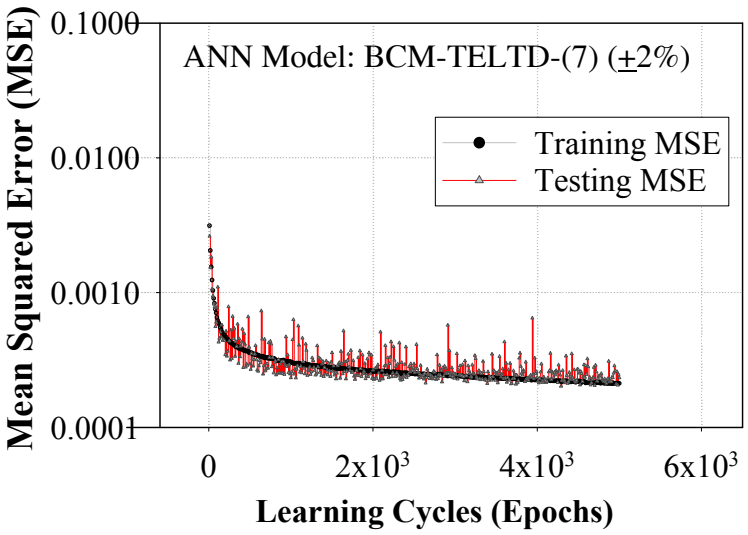

Figure C.20. Training progress curve for the BCM-TELTD-(7) (±2%) model

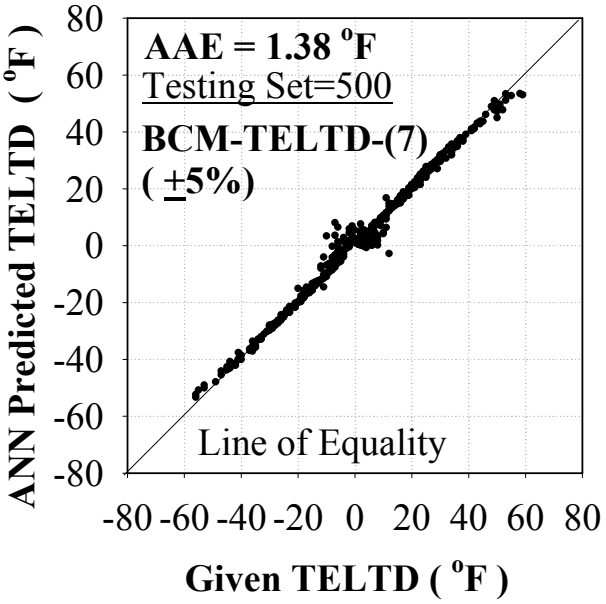

Figure C.21. Prediction performance of the BCM-TELTD-(7) (±5%) model for backcalculating the total effective linear temperature difference, TELTD

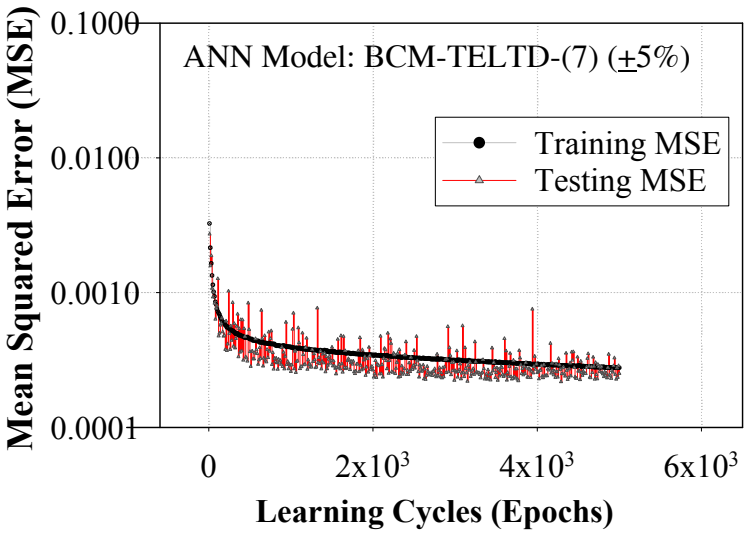

Figure C.22. Training progress curve for the BCM-TELTD-(7) (±5%) model

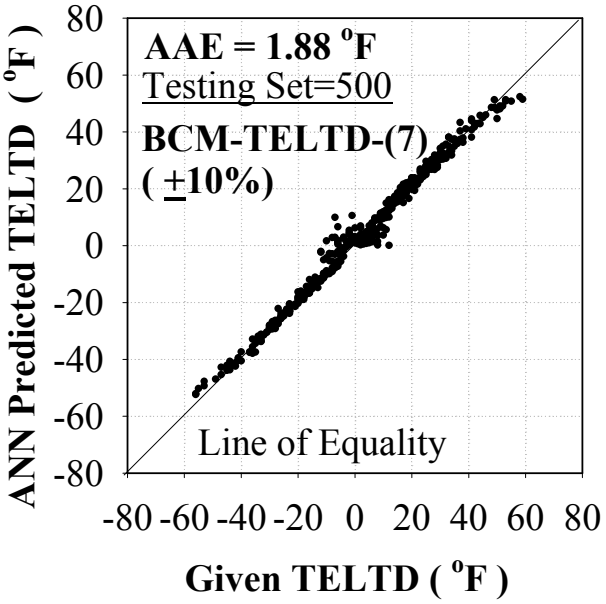

Figure C.23. Prediction performance of the BCM-TELTD-(7) (±10%) model for backcalculating the total effective linear temperature difference, TELTD

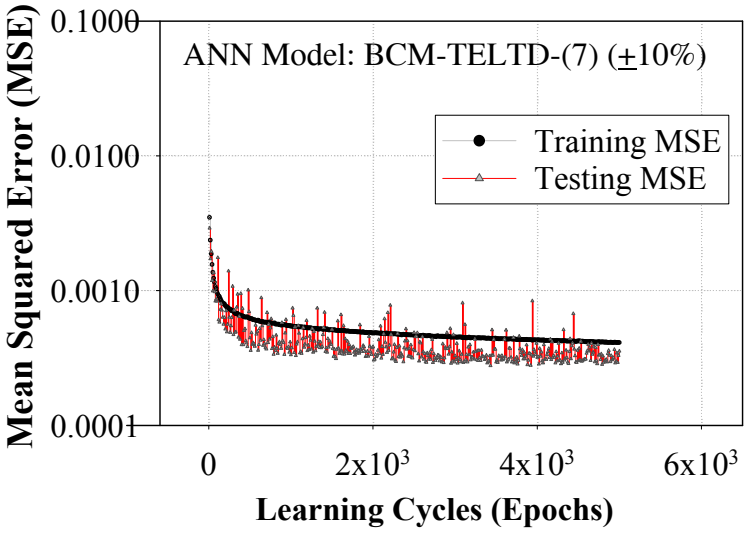

Figure C.24. Training progress curve for the BCM-TELTD-(7) (±10%) model

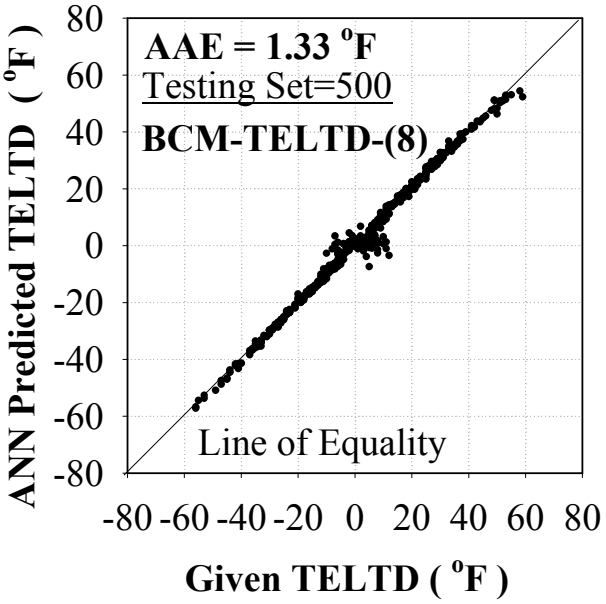

Figure C.25. Prediction performance of the BCM-TELTD-(8) model for backcalculating the total effective linear temperature difference, TELTD

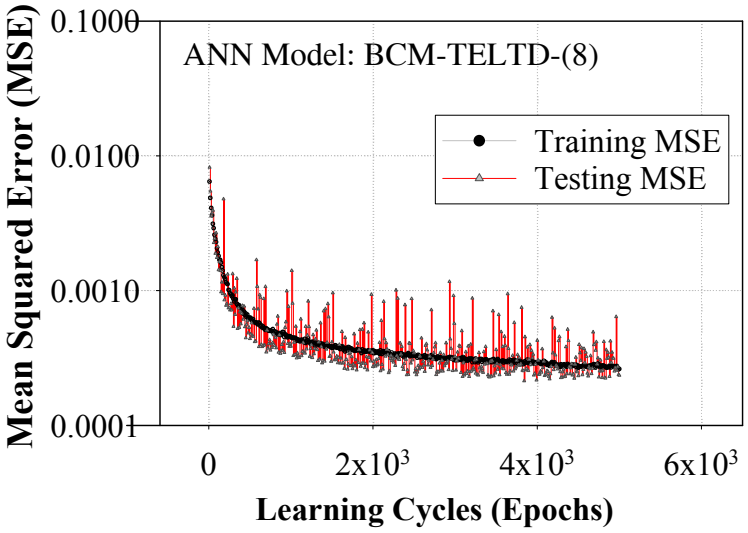

Figure C.26. Training progress curve for the BCM-TELTD-(8) model

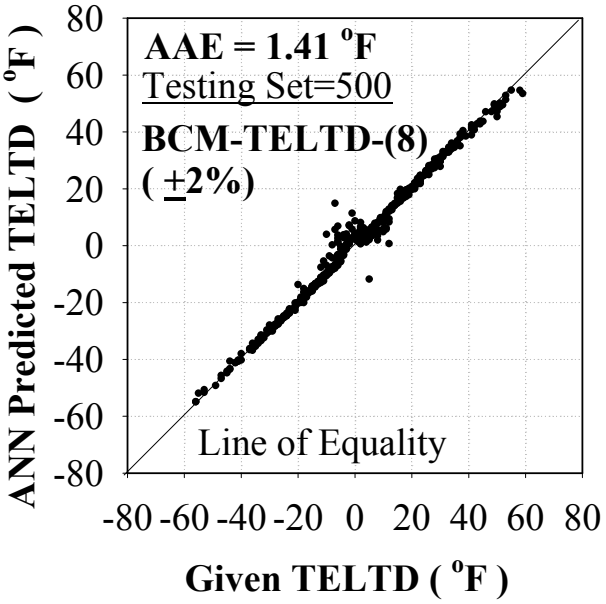

Figure C.27. Prediction performance of the BCM-TELTD-(8) (±2%) model for backcalculating the total effective linear temperature difference, TELTD

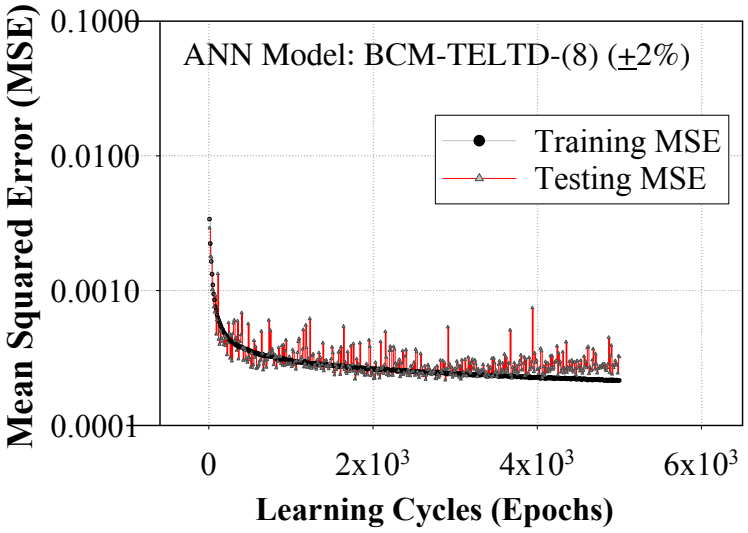

Figure C.28. Training progress curve for the BCM-TELTD-(8) (±2%) model

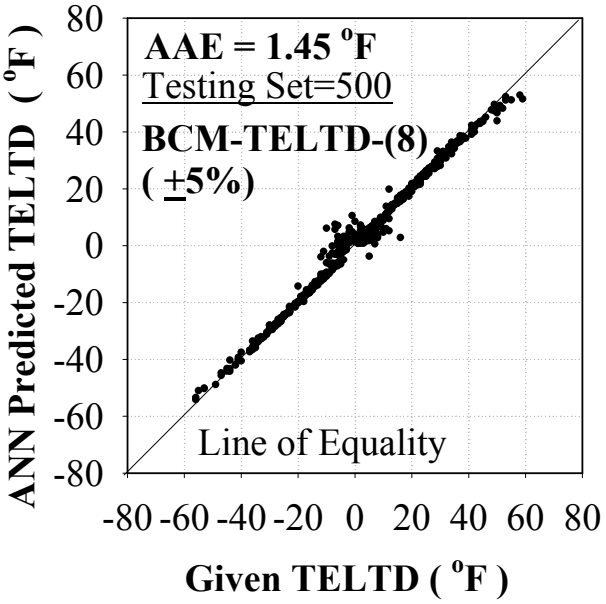

Figure C.29. Prediction performance of the BCM-TELTD-(8) (±5%) model for backcalculating the total effective linear temperature difference, TELTD

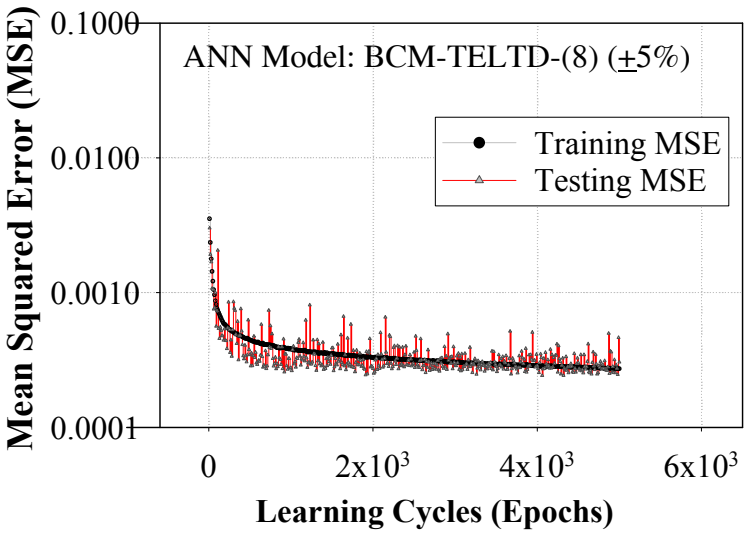

Figure C.30. Training progress curve for the BCM-TELTD-(8) (±5%) model

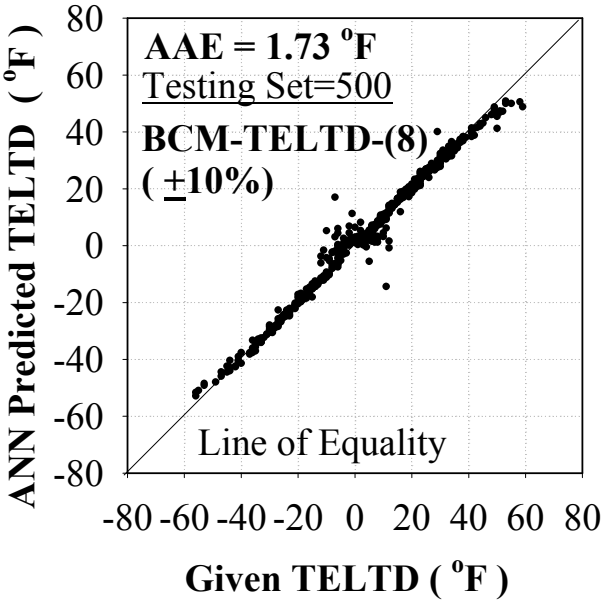

Figure C.31. Prediction performance of the BCM-TELTD-(8) (±10%) model for backcalculating the total effective linear temperature difference, TELTD

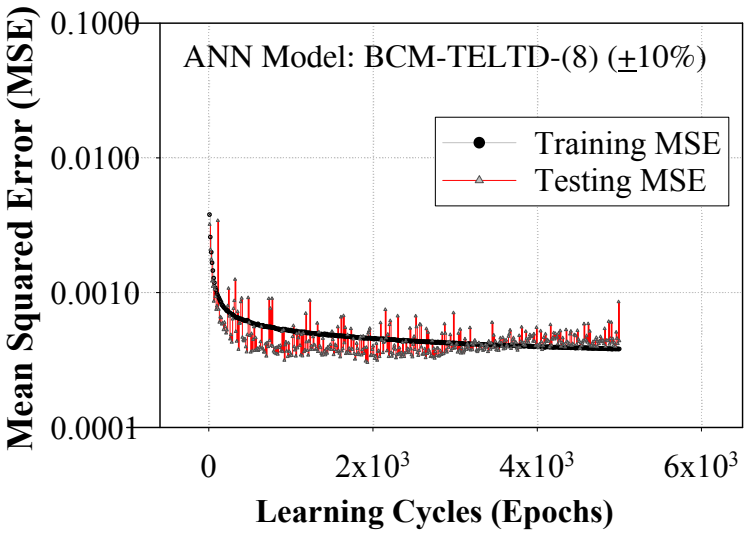

Figure C.32. Training progress curve for the BCM-TELTD-(8) (±10%) model

APPENDIX D. ANN-BASED FORWARD CALCULATION MODELS FOR RADIUS OF RELATIVE STIFFNESS

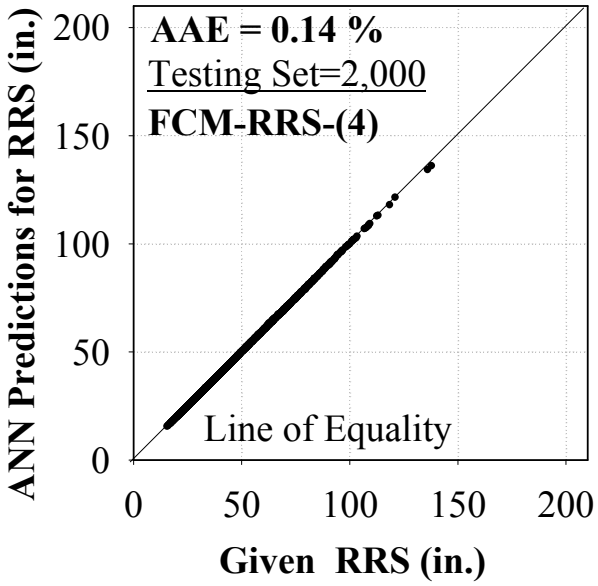

Figure D.1. Prediction performance of the FCM-RRS-(4) model for forward calculating the radius of relative stiffness, RRS

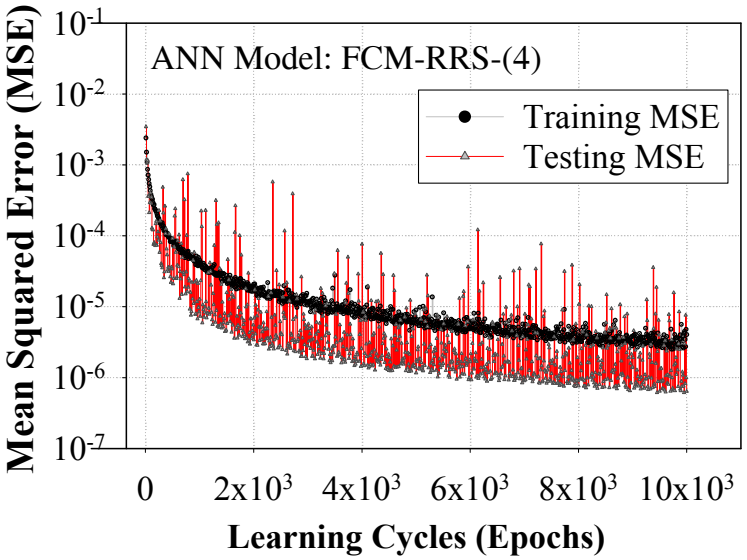

Figure D.2. Training progress curve for the FCM-RRS-(4) model

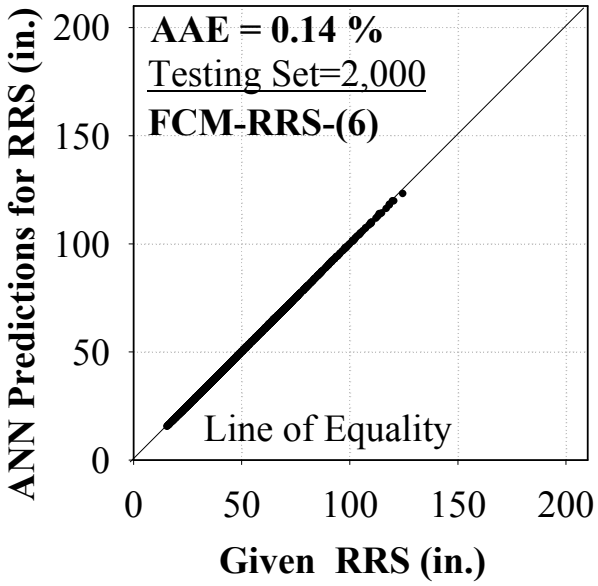

Figure D.3. Prediction performance of the FCM-RRS-(6) model for forward calculating the radius of relative stiffness, RRS

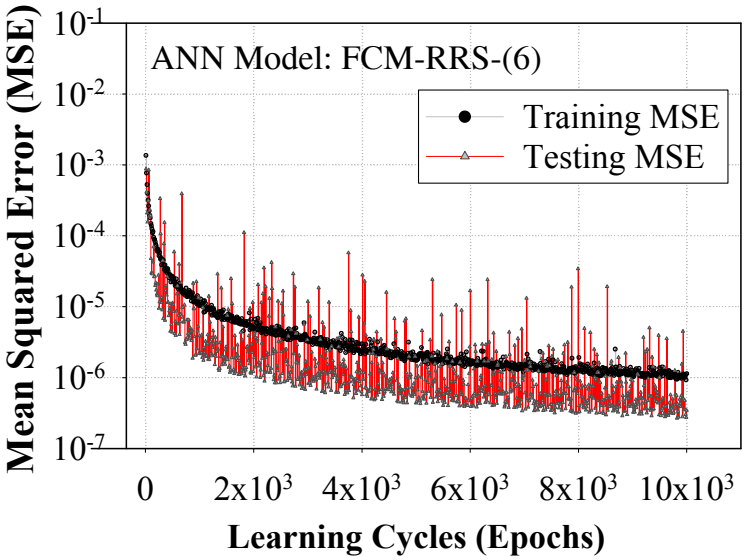

Figure D.4. Training progress curve for the FCM-RRS-(6) model

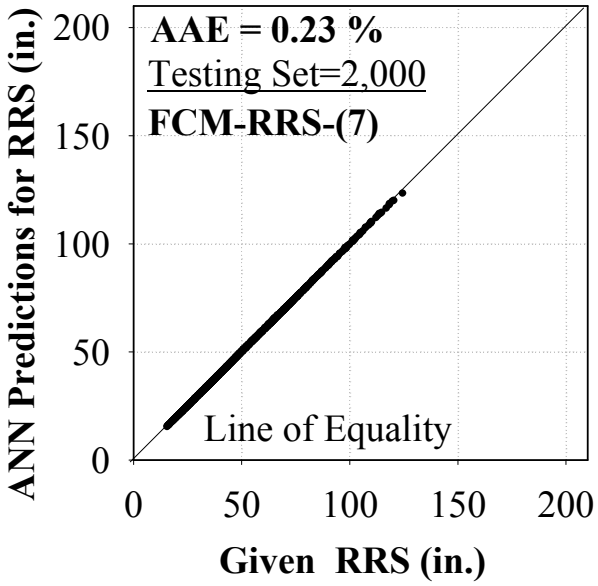

Figure D.5. Prediction performance of the FCM-RRS-(7) model for forward calculating the radius of relative stiffness, RRS

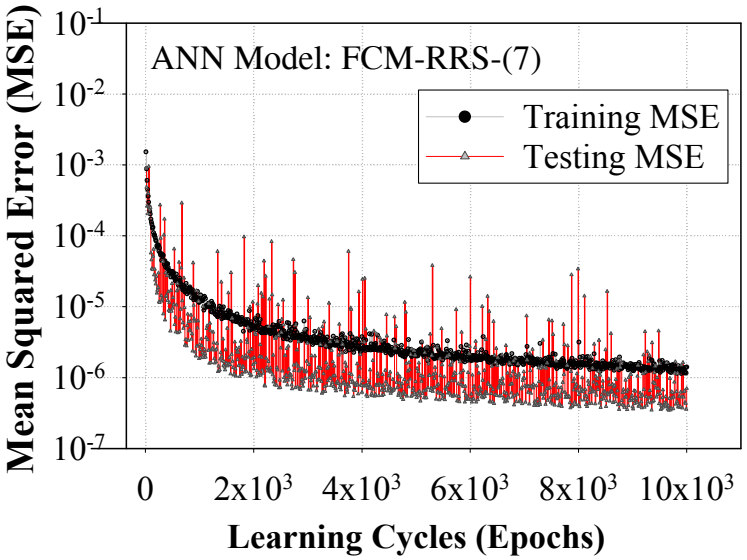

Figure D.6. Training progress curve for the FCM-RRS-(7) model

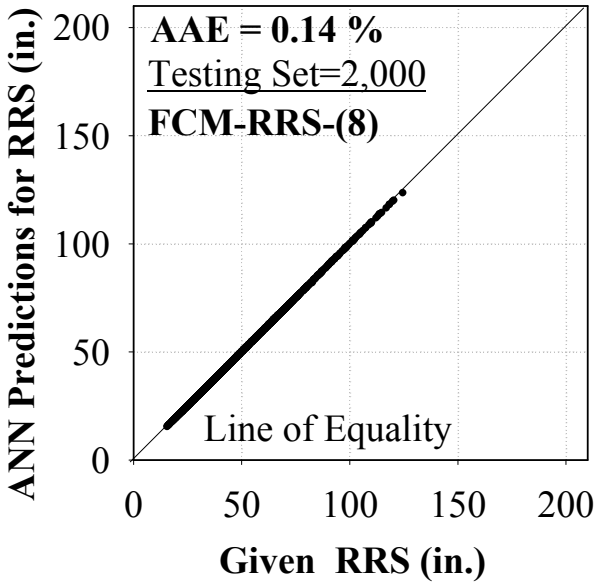

Figure D.7. Prediction performance of the FCM-RRS-(8) model for forward calculating the radius of relative stiffness, RRS

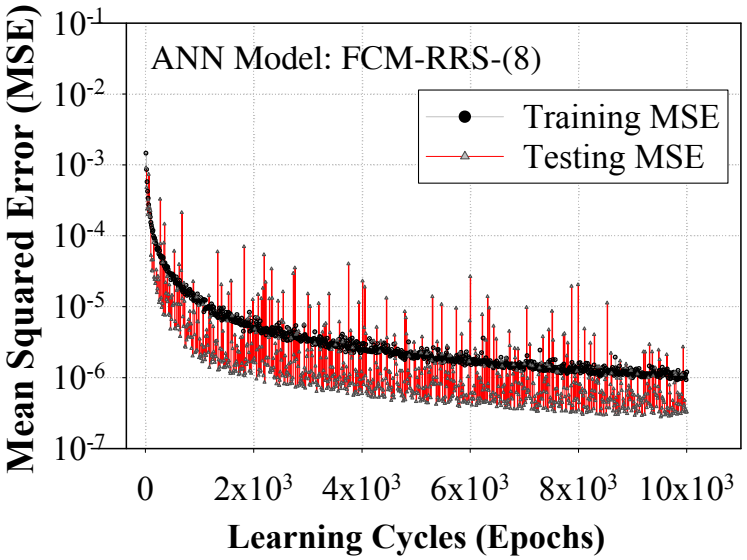

Figure D.8. Training progress curve for the FCM-RRS-(8) model

APPENDIX E. ANN-BASED FORWARD CALCULATION MODELS FOR MAXIMUM TENSILE STRESS AT THE BOTTOM OF THE PCC LAYER

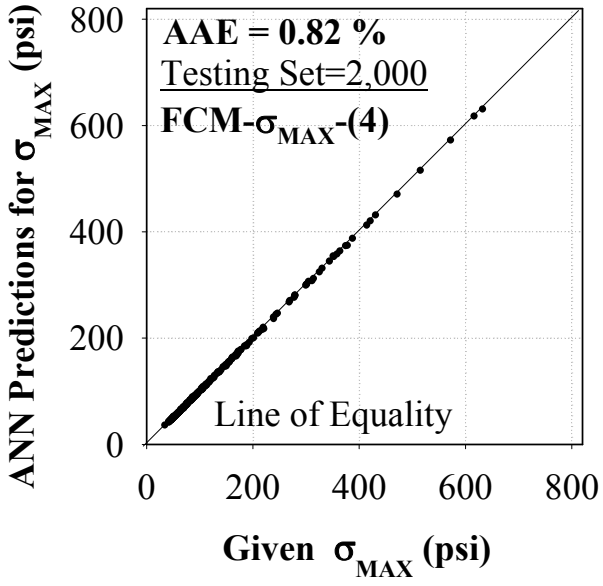

Figure E.1. Prediction performance of the FCM-σ_{MAX}-(4) model for forward calculating the maximum tensile stress at the bottom of the PCC layer, σ_{MAX}

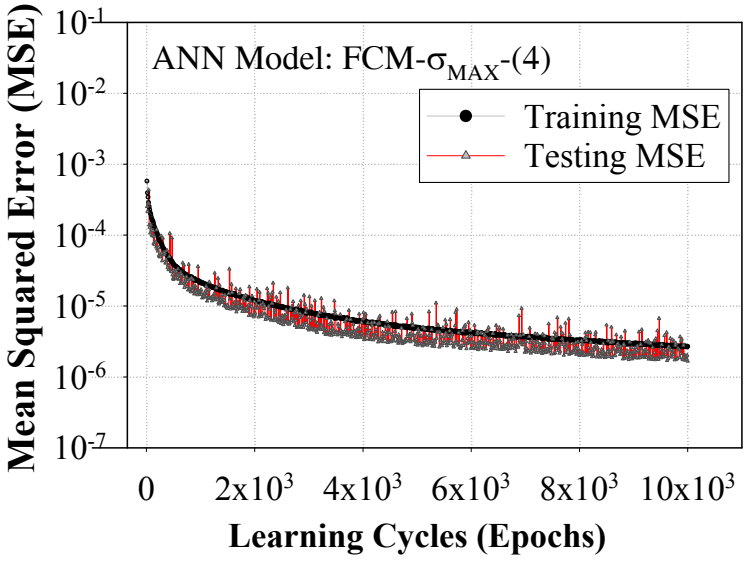

Figure E.2. Training progress curve for the FCM-σ_{MAX} -(4) model

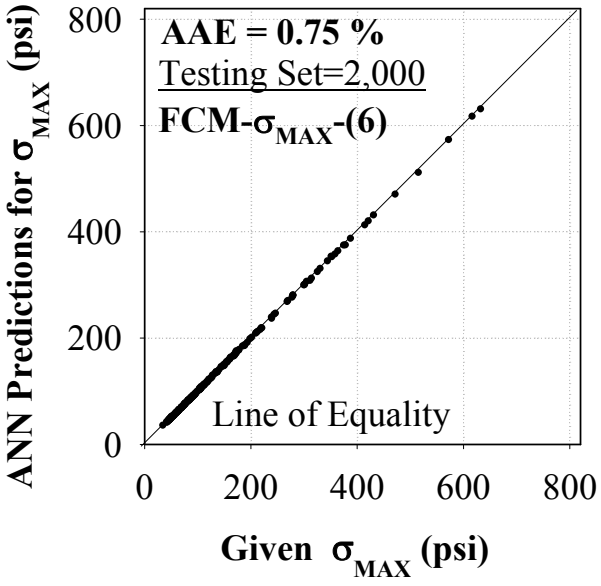

Figure E.3. Prediction performance of the FCM-σ_{MAX}-(6) model for forward calculating the maximum tensile stress at the bottom of the PCC layer, σ_{MAX}

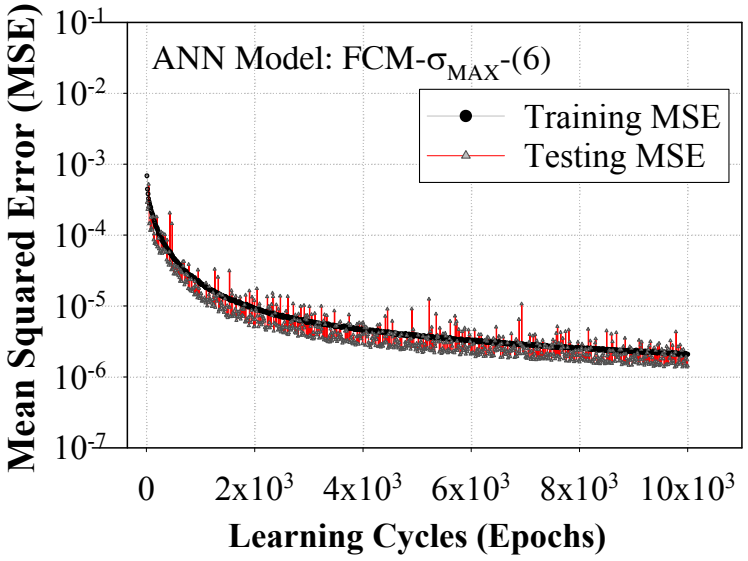

Figure E.4. Training progress curve for the FCM-σ_{MAX} -(6) model

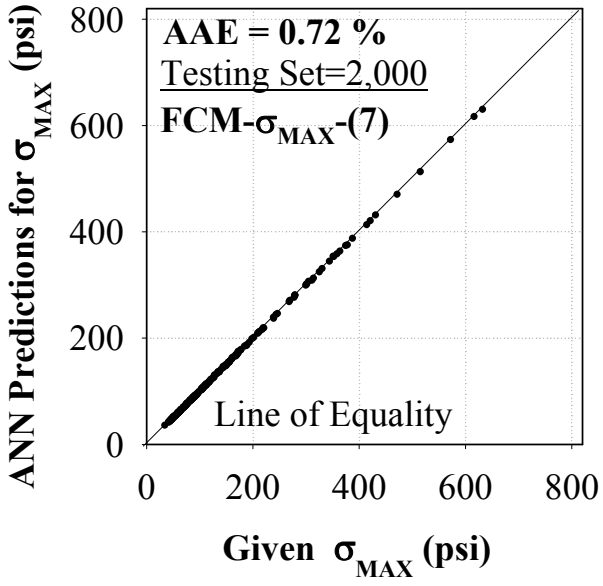

Figure E.5. Prediction performance of the FCM-σ_{MAX}-(7) model for forward calculating the maximum tensile stress at the bottom of the PCC layer, σ_{MAX}

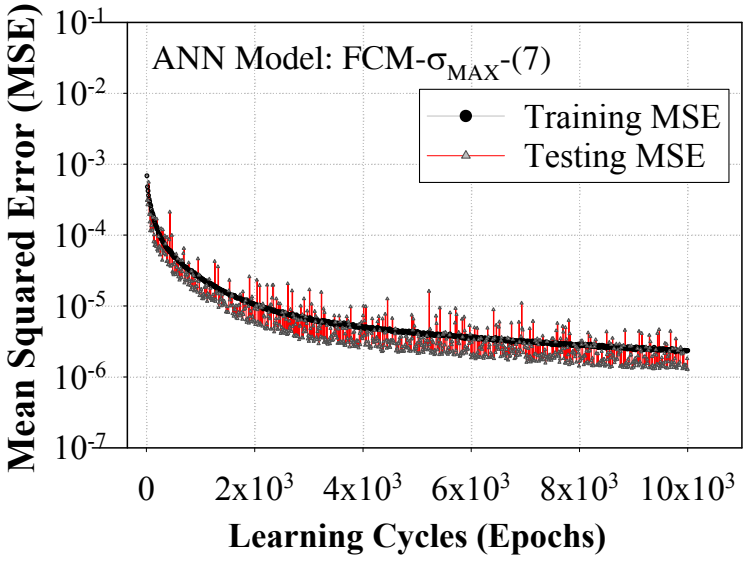

Figure E.6. Training progress curve for the FCM-σ_{MAX} -(7) model

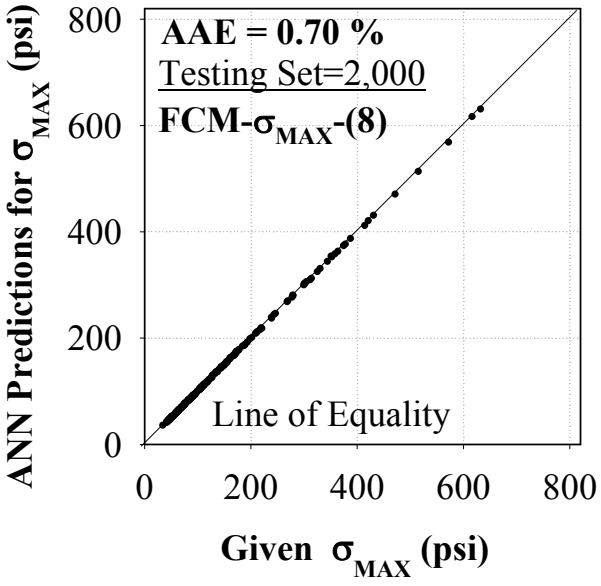

Figure E.7. Prediction performance of the FCM-σ_{MAX}-(8) model for forward calculating the maximum tensile stress at the bottom of the PCC layer, σ_{MAX}

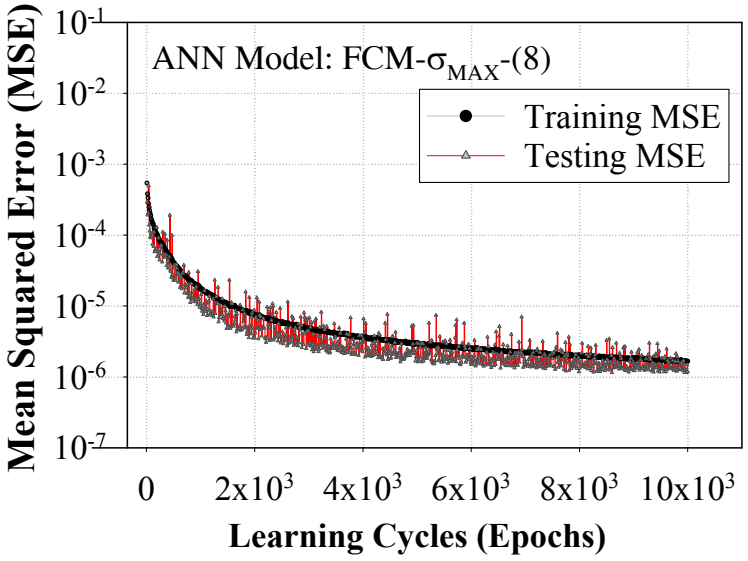

Figure E.8. Training progress curve for the FCM-σ_{MAX} -(8) model